AFML-TR-71-268

AD 739560

INTERACTIVE PROGRAM FOR ANALYSIS AND DESIGN PROBLEMS IN ADVANCED COMPOSITES TECHNOLOGY

T. A. CRUSE

J. L. SWEDLOW

TECHNICAL REPORT AFML-TR-71-268

DECEMBER 1971

Approved for public release; distribution unlimited

AIR FORCE MATERIALS LABORATORY
AIR FORCE SYSTEMS COMMAND
WRIGHT PATTERSON AIR FORCE BASE, OHIO

32-150

300

NOTICE

When Government drawings, specifications, or other data are used for any purpose other than in connection with a definitely related Government procurement operation, the United States Government thereby incurs no responsibility nor any obligation whatsoever; and the fact that the government may have formulated, furnished, or in any way supplied the said drawings, specifications, or other data, is not to be regarded by implication or otherwise as in any manner licensing the holder or any other person or corporation, or conveying any rights or permission to manufacture, use, or sell any patented invention that may in any way be related thereto.

Copies of this report should not be returned unless return is required by security considerations, contractual obligations, or notice on a specific document.

UNCLASSIFIED

Security Classification

DOCUMENT CONTROL DATA - R & D

(Security classification of title, body of abstract and indexing annotation must be entered when the overall report is classified)

1. ORIGINATING ACTIVITY (Corporate author)

Carnegie-Mellon University
Mechanical Engineering Department
Pittsburgh, Pennsylvania 15213

2a. REPORT SECURITY CLASSIFICATION

Unclassified

2b. GROUP

N/A

3. REPORT TITLE

Interactive Program for Analysis and Design Problems in Advanced Composites Technology

4. DESCRIPTIVE NOTES (Type of report and inclusive dates)

Final Report (November 1969 - October 1971)

5. AUTHOR(S) (First name, middle initial, last name)

T. A. Cruse and J. L. Swedlow

6. REPORT DATE

November 1971

7a. TOTAL NO. OF PAGES

296

7b. NO. OF REFS

76

8a. CONTRACT OR GRANT NO.

F33615-70-C-1146

b. PROJECT NO.

6169 CW

c.

d.

9a. ORIGINATOR'S REPORT NUMBER(S)

AFML-TR-71-268

9b. OTHER REPORT NO(S) (Any other numbers that may be assigned this report)

10. DISTRIBUTION STATEMENT

Approved for public release: Distribution unlimited

11. SUPPLEMENTARY NOTES

12. SPONSORING MILITARY ACTIVITY

Advanced Composites Division (AFML/LC)
Air Force Materials Laboratory
Wright-Patterson Air Force Base, Ohio 45433

13. ABSTRACT

The Carnegie-Mellon University team has completed the initial Interactive Program in Advanced Composites Technology. The program has had significant impact as the CMU team, working closely with engineers from industry, has made significant technical progress in several problem areas of current importance. Results on ~~these problems are~~ reported in this Report. During the past year an experimental program in the fracture of advanced fiber composites has been completed. The experimental program has given direction to additional experimental and theoretical work. A synthesis program for designing low weight multifastener joints in composites is proposed, based on extensive analytical background. A number of failed joints have been thoroughly analyzed to evaluate the failure hypothesis used in the synthesis procedure. Finally, the Report includes new solution methods for isotropic and anisotropic (mid-plane symmetric) laminates using the boundary-integral method. The solution method offers significant savings of computer core and time for important problems.

UNCLASSIFIED

Security Classification

14. KEY WORDS	LINK A		LINK B		LINK C	
	ROLE	WT	ROLE	WT	ROLE	WT
Composite Materials						
Education						
Mechanically Fastened Joints						
Fracture Mechanics						
Stress Concentrations						
Numerical Solution Methods						
Anisotropic Elasticity						
Optimization						
Synthesis						

UNCLASSIFIED

Security Classification

AFML-TR-71-268

INTERACTIVE PROGRAM FOR ANALYSIS AND DESIGN PROBLEMS IN ADVANCED COMPOSITES TECHNOLOGY

T. A. CRUSE

J. L. SWEDLOW

DEPARTMENT OF MECHANICAL ENGINEERING
CARNEGIE INSTITUTE OF TECHNOLOGY
CARNEGIE-MELLON UNIVERSITY
PITTSBURGH, PENNSYLVANIA

DECEMBER 1971

FOREWORD

This report describes work performed in the Department of Mechanical Engineering, Carnegie-Mellon University, Pittsburgh, Pennsylvania, 15213, under Air Force Contract F33615-70-C-1146, Project 6169 CW; Subject: "Research for the development of design and analytical techniques for advanced composite structures". This work was accomplished between 1 November 1969 and 31 October 1971. The Program Manager for the Air Force Materials Laboratory was Mr. George E. Husman, AFML/MAC. The research projects in this report were undertaken by several graduate students under the direction of the Principal Investigators, Drs. T. A. Cruse and J. L. Swedlow and it is a pleasure to acknowledge Messrs. H. J. Konish, Jr. (fracture project), J. P. Waszczak (mechanically fastened joints), W. B. Bamford (numerical studies using integral equations) and S. J. Marulis (optimization); it is also a pleasure to acknowledge the work on advanced topics in integral equations performed on a consulting basis by Professor Frank J. Rizzo, University of Kentucky.

Since the emphasis of the program was on interaction with industry it is a pleasure to acknowledge Messrs. C. W. Rogers, P. D. Shockey, M. E. Waddoups, R. B. Pipes and many others in the advanced composites group of Convair Aerospace Division, General Dynamics, Fort Worth, Texas; also the staffs at Boeing/Vertol, Grumman Aerospace, North American Rockwell and Southwest Research Institute.

Portions of the reported work were also supported by NASA Grant NGR-39-002-023 (fracture project) and by General Dynamics P. O. No. 499527 (joint design). The authors would finally like to acknowledge Miss Kathleen Sokol for her careful and selfless devotion to the preparation of this document.

This report was submitted by the Authors on 6 December 1971.

This technical report has been reviewed and is approved,

Robert C. Tomashot
Technical Area Manager
Advanced Composites Division

ABSTRACT

The Carnegie-Mellon University team has completed the initial Interactive Program in Advanced Composites Technology. The program has had significant impact as the CMU team, working closely with engineers from industry, has made significant technical progress in several problem areas of current importance. Results on these problems are reported in this Report. During the past year an experimental program in the fracture of advanced fiber composites has been completed. The experimental program has given direction to additional experimental and theoretical work. A synthesis program for designing low weight multifastener joints in composites is proposed, based on extensive analytical background. A number of failed joints have been thoroughly analyzed to evaluate the failure hypothesis used in the synthesis procedure. Finally, the Report includes new solution methods for isotropic and anisotropic (mid-plane symmetric) laminates using the boundary-integral method. The solution method offers significant savings of computer core and time for important problems.

TABLE OF CONTENTS

CHAPTER		PAGE
I	SUMMARY OF THE INTERACTIVE PROGRAM	1
	1.1 Introduction	1
	1.2 First and Second Year Programs	2
	1.2.1 Phase I	2
	1.2.2 Phase II	3
	1.2.3 Phase III	5
	1.3 Research Projects Completed	6
	1.3.1 Fracture of Advanced Composites	7
	1.3.2 Strength of Mechanically Fastened Joints	7
	1.3.3 Optimization Methods	7
	1.3.4 Boundary-Integral Equation Solution Methods	7
	1.4 Evaluation and Recommendations	8
	1.5 References	11
	1.6 Appendix A: Summary of Educational Material	12
	1.7 Appendix B: Trip Reports	18
	1.8 Appendix C: Research Documents	20
II	FRACTURE OF ADVANCED COMPOSITES	23
	2.1 Stress Analysis of a Cracked Anisotropic Beam	23
	2.1.1 Introduction	23
	2.1.2 Review of Previous Work	23
	2.1.3 Analytical Study	27
	2.1.4 References	31
	2.2 Experimental Investigation of Fracture in an Advanced Fiber Composite	34
	2.2.1 Introduction	34
	2.2.2 Test Procedures; Program	35
	2.2.3 Data Reduction; Results	37
	2.2.4 Discussion	38
	2.2.5 Conclusions	41
	2.2.6 References	42

Preceding page blank

CHAPTER | PAGE

CHAPTER		PAGE
III	STRENGTH OF MECHANICALLY FASTENED JOINTS	54
	3.1 An Investigation of Stress Concentrations Induced in Composite Bolt Bearing Specimens	54
	3.1.1 Introduction	54
	3.1.2 Analysis Method	55
	3.1.3 Strength and Failure Mode Predictions	57
	3.1.4 Future Work	61
	3.1.5 References	62
	3.2 Toward a Design Procedure for Mechanically Fastened Joints Made of Composite Materials	78
	3.2.1 Introduction	78
	3.2.2 Investigation of the Characteristic Crack Length Hypothesis	82
	3.2.3 Review of Past Design Programs Involving Composite Joints	87
	3.2.4 Evaluation of Load Partitioning in Joints	89
	3.2.4.1 Point Strain Matching Technique	89
	3.2.4.2 Displacement Matching Technique	91
	3.2.5 Computer Analysis of Experimentally Failed Composite Joints	93
	3.2.6 Proposed Mechanically Fastened Joint Design Program	103
	3.2.6.1 Outline of Proposed Synthesis Program	103
	3.2.6.2 Discussion of Program Details	104
	3.2.6.2.1 Input Data	104
	3.2.6.2.2 Design Variables	107
	3.2.6.2.3 Design Constraints	109
	3.2.6.2.4 Design Procedures	112
	3.2.7 Areas of Future Work	117
	3.2.8 References	120

CHAPTER		PAGE

IV OPTIMIZATION METHODS 142

4.1 Introduction 142

4.2 Structural Optimization 142

4.2.1 Background 142
4.2.2 Variational Method 143
4.2.3 Non-linear Programming Methods 144

4.3 Torsion of an Elliptic Bar - Variational Example 145

4.4 Bolt Bearing Problem - Non-Linear Programming Example 148

4.5 Discussion 151

4.6 References 153

V BOUNDARY-INTEGRAL EQUATION SOLUTION METHODS 160

5.1 Two Dimensional Isotropic Boundary-Integral Equation Method 160

5.1.1 Introduction 160
5.1.2 Review of the Isotropic Boundary-Integral Equation Method 161
5.1.3 Use of the Isotropic Computer Program 163

5.1.3.1 Dimension Statements 164
5.1.3.2 Definition of Key Parameters; Matrices 165
5.1.3.3 Boundary Conditions 166
5.1.3.4 Input Cards 167
5.1.3.5 Example Problem 167

5.1.4 References 168

5.1.5 Listing for Isotropic Boundary-Integral Equation Computer Program 169

CHAPTER PAGE

5.2 Two Dimensional Anisotropic Boundary-Integral Equation Method 186

5.2.1 Formulation of the Field Equations 186
5.2.2 Fundamental Solution: Point Force Problem 191
5.2.3 Boundary Integral Equation 195
5.2.4 Somigliana's Identity for Interior Strains, Stresses 199
5.2.5 Numerical Solution 201
5.2.6 Usage Guide for ANISOT 205

5.2.6.1 Problem Size Specifications 205
5.2.6.2 Specification of Material Constants 206
5.2.6.3 Use of AXCALC 207
5.2.6.4 Identification of Parameters for ANISOT 208
5.2.6.5 Boundary Conditions 209
5.2.6.6 Input Data for ANISOT 211

5.2.7 References 212
5.2.8 Listing for AXCALC Computer Program 213
5.2.9 Listing for ANISOT Computer Program 220

5.3 Example Solutions for Isotropic and Anisotropic Boundary-Integral Equation Method 237

5.3.1 Tension of an Isotropic Plate 237

5.3.1.1 Circular Cutout 237
5.3.1.2 Elliptical Cutout 238

5.3.2 Tension of an Anisotropic Plate with Circular Cutout 240

5.3.2.1 Orthotropic Material 240
5.3.2.2 Anisotropic Material 241

5.4 Advanced Topics in Anisotropic Integral Equation Solution Methods 256

5.4.1 Introduction 256
5.4.2 Fundamental Three-Dimensional Anisotropic Singularity 257

5.4.2.1 Via John 257
5.4.2.2 Via Fredholm 264

5.4.3 Investigation of the Interlaminar Shear Problem 266
5.4.4 References 273

LIST OF FIGURES

SECTION	FIGURE	TITLE	PAGE
2.1	1	Three-point bend specimen, with global (x,y and r,θ) and material (1,2) coordinate systems shown (insert). The applied load P is modeled as point load. The specimen thickness is denoted by B.	32
	2	A plot of $\overline{G}(a/W,\alpha)$ vs. a/W. The degree of correspondence between the discrete points (obtained numerically) and the continuous curve (obtained from [8]) is a measure of the applicability of an anisotropic continuum analysis [4] to advanced fiber composite materials.	33
2.2	1	Three-point bend specimen geometry, with crack shape shown in inserts, both schematic (left) and actual (right). Fiber direction given by α, crack length by a. Specimen thickness 0.5 in (nom); all dimensions given in inches.	44
	2	Test jig at beginning of loading.	45
	3	Typical trace of load applied to specimen vs. cross-head displacement, showing method used to determine P_S.	46
	4	Failure surfaces for α = 0° specimens of three starter crack lengths (a = 0.6, 0.4, 0.2 in).	47
	5	Failure surfaces for α = 45° specimens of three starter crack lengths (a = 0.6, 0.4, 0.2 in).	48
	6	Failure surfaces for α = 90° specimens of three starter crack lengths (a = 0.6, 0.4, 0.2 in).	49
	7	Failure surfaces for $\alpha = (\pm 45°)_S$ specimens of three starter crack lengths (a = 0.6, 0.4, 0.2 in).	50

SECTION	FIGURE	TITLE	PAGE
2.2	8	Failure surfaces for $\alpha = (0°/\pm45°/90°)_s$ specimens of two starter crack lengths (a = 0.6, 0.4 in).	51
	9	Failed but unbroken specimen ($\alpha = (0°/\pm45°/90°)_s$, a = 0.2 in).	52
	10	Traces of load vs. cross-head displacement for five specimens used in reproducibility tests for a unidirectional laminate (α = 0°, a = 0.4 in).	53
	11	Traces of load vs. cross-head displacement for five specimens used in reproducibility tests for a multidirectional laminate ($\alpha = (0°/\pm45°/90°)_s$, a = 0.4 in).	54
3.1	1	Bolt bearing test specimen	63
	2	Bolt bearing grid representation for e/d-5.0, s/d-10.0 and ℓ/d-20.0.	64
	3a	Isotropic bolt bearing verification: $\sigma_x/\bar{\sigma}$ vs. y.	65
	3b	Isotropic bolt bearing verification: $\sigma_y/\bar{\sigma}$ vs. x.	66
	4	Polar plot of edge stresses for an isotropic test run.	67
	5	Variations about the cosine distribution of normal stress.	68
	6	Bolt bearing test specimen failure modes.	69
	7a	Net tension failure +45° lamina	70
	7b	Net tension failure -45° lamina	71
	7c	Net tension failure 90° lamina	72
	7d	Net tension failure 0° lamina	73

SECTION	FIGURE	TITLE	PAGE
3.1	8	Slug shear-out failure 0° lamina	74
	9	Bearing failure 0° lamina	75
	10	Combination and net tension failure, +45° lamina.	76
3.2	1	Distortional energy contour plots for the 1.0" diameter, anisotropic tension coupon at the experimental failure load.	125
	2a	Distortional energy contour plots for the initial bolt bearing specimen design at the predicted failure load.	126
	2b	Distortional energy contour plots for the revised bolt bearing specimen design at the predicted failure load.	127
	3	Double shear joint configuration.	128
	4	Bolt bearing modeling procedure for joints.	129
	5	Bolt load distribution for Specimens 1 thru 6.	130
	6	Skin stress boundary conditions at the leading edge of a bolt bearing model.	131
	7	Specimen 1: Distortional energy contour plots for the experimental failure load.	132
	8	Specimen 2: Distortional energy contour plots for the experimental failure load.	133
	9	Specimen 3: Distortional energy contour plots for the experimental failure load.	134
	10	Specimen 4: Distortional energy contour plots for the experimental failure load.	135

SECTION	FIGURE	TITLE	PAGE
3.2	11	Specimen 5: Distortional energy contour plots for the experimental failure load.	136
	12	Specimen 6: Distortional energy contour plots for the experimental failure load.	137
	13	The principle of superposition applied to an infinite bolt bearing model.	140
	14	Schematic of a proposed joint design showing the seventeen possible design variables.	141
4	1	Weight vs. load for fixed orientations.	157
	2	Weight vs. load for variable orientations.	158
	3	Summary of weight vs. load results.	159
5.3	1	Local geometry at boundary.	242
	2	Local geometry at boundary.	242
	3	Accuracy of DIPOME - Circular hole.	244
	4	Accuracy of DIPOME - Elliptical cutout.	251
5.4	1	Geometry for interlaminar shear problems.	272
	2	Individual lamina notation.	272

LIST OF TABLES

SECTION	TABLE	TITLE	PAGE
2.2	I	Experimental results.	43
3.1	I	Summary of bolt bearing specimen data.	77
3.2	I	Initial bolt bearing specimen design.	122
	II	Revised bolt bearing specimen design.	122
	III	Description of the six specimens selected for analysis.	123
	IV	Summary of significant data from Figures 7 thru 12.	124
4	I	Coupon weights for fixed orientations.	154
	II	Coupon weights for variable orientations.	155
	III	Coupon weights allowing orientations to be eliminated.	156
5.3	I	Interior stress solutions - DIPOME ($a/b = 1.0$; σ_x).	243
	II	Interior stress solutions - DIPOME ($a/b = 2.0$; σ_x).	245
	III	Interior stress solutions - DIPOME ($a/b = 2.0$; σ_y).	246
	IV	Interior stress solutions - DIPOME ($a/b = 4.5$; σ_x).	247
	V	Interior stress solutions - DIPOME ($a/b = 4.5$; σ_y).	248
	VI	Interior stress solutions - DIPOME ($a/b = 19.5$; σ_x).	249
	VII	Interior stress solutions - DIPOME ($a/b = 19.5$; σ_y).	250
	VIII	Surface hoop stress comparisons ($\alpha = 0°$).	252

SECTION	TABLE	TITLE	PAGE
5.3	IX	Surface hoop stress comparisons ($\alpha = 90°$).	253
	X	Surface hoop stress comparisons ($\alpha = 45°$; 90 Segments).	254
	XI	Surface hoop stress comparisons ($\alpha = 45°$; 20 Segments).	255

LIST OF SYMBOLS AND NOTATION

CHAPTER	SECTION	SYMBOL	DESCRIPTION
II	1	r, θ	Polar coordinates, with the origin at the crack-tip. (See Fig. 1).
		x, y	Cartesian coordinates, with the origin at the crack-tip; these are the global coordinates. (See Fig. 1).
		1, 2	Cartesian coordinates based on the material principal directions (See Fig. 1).
		B	Thickness of the three-point bend specimen.
		S	Span of the three-point bend specimen.
		W	Depth of the three-point bend specimen.
		a	Crack-length.
		α	Angle of rotation between the global and lamina coordinate systems (See Fig. 1).
		$\sigma_{x,y}$	Tensile stresses in the global coordinate system.
		v	Displacement normal to the crack-axis.
		P	Applied load on the three-point bend specimen.
		μ_i	Roots of the characteristic equation.
		a_{ij}	Components of the global compliance matrix.

CHAPTER	SECTION	SYMBOL	DESCRIPTION
II	1	$K_{I,II}$	Stress intensity factors corresponding to symmetric and anti-symmetric loading respectively. A subscript c indicates a critical value of K, i.e., a value at which the crack propagates catastrophically.
	2	K_Q	A candidate value of the critical stress-intensity factor.
		$\bar{K}_Q$	The average value of K_Q for a given laminate, obtained by averaging the K_Q values obtained for several specimens of the laminate.
		G_Q	Strain-energy release rate.
		M_o	Initial slope of the experimental plot of load vs. specimen deflection (See Fig. 12).
		P_S	Load corresponding to the intersection of the secant of slope M_s with the curve of load vs. specimen deflection (See Fig. 12).
		P_Q	Applied load at which crack propagation occurred.
		a	Crack-length (See Fig. 1).
		α	Angle of rotation between the global and lamina coordinate systems (See Fig. 1).

CHAPTER	SECTION	SYMBOL	DESCRIPTION
III	1	e	Specimen edge distance.
		d	Bolt bearing diameter.
		s	Total specimen width.
		ℓ	Total specimen length.
		t	Specimen thickness
		σ_i	i^{th} principal lamina stress.
		σ_{iu}	i^{th} principal ultimate lamina stress.
		DIST	Normalized distortional energy.
	2	F_{TU}	Effective tension strength.
		F_{SU}	Effective shear-out strength.
		F_{BRU}	Effective bearing strength.
		S	Bolt bearing specimen width.
		E	Bolt bearing specimen edge distance.
		t	Bolt bearing specimen thickness.
		D	Bolt bearing specimen diameter.
		L'	Bolt bearing specimen length.
		L	Total joint length.
		N	Number of bolts per column.
		F	Maximum load to be carried per column of bolts

CHAPTER	SECTION	SYMBOL	DESCRIPTION
III	2	Subscripts and Superscripts	
		m	Main plate
		s	Splice plate
		B	Bolt material
		u	Ultimate allowable
		t	Tension
		c	Compression

CHAPTER	SECTION	SYMBOL	DESCRIPTION
IV	2	$W(X_i)$	Weight function of a composite plate.
		X_i	Variables of a composite plate.
		$F_j(X_i)$	Constraint functions on $W(X_i)$.
		λ_j	Lagrange multipliers for the constraint functions.
		P	Objective function for minimization.
	3	M	Applied torsional moment.
		a, b	Semi-major and semi-minor axes of the ellipse.
		τ	Shear stress.
	4	t	Thickness of the bolt bearing specimen.
		S	Width of the bolt bearing specimen.
		E	Distance from the center of the bolt hole to the near edge of the bolt bearing specimen.
		D	Diameter of the bolt hole in the bolt bearing specimen.
		XL	Distance from the bolt hole to the far edge of the bolt bearing specimen.
		P	Load applied to the bolt bearing specimen.
		F^{tu}	Failure stress for the tension mode failure of the bolt bearing specimen.
		F^{su}	Failure stress for the shear out mode failure of the bolt bearing specimen.

CHAPTER	SECTION	SYMBOL	DESCRIPTION
IV	4	F^{bu}	Failure stress for the bearing mode failure of the bolt bearing specimen.
		L	Percentage of 0° plies in the bolt bearing specimen.
		M	Percentage of 90° plies in the bolt bearing specimen.
		N	Percentage of ±45° plies in the bolt bearing specimen.

CHAPTER	SECTION	SYMBOL	DESCRIPTION
V	2		
		$\sigma_x, \sigma_y, \sigma_{xy}$	Stress field.
		$\epsilon_x, \epsilon_y, \gamma_{xy}$	Strain field.
		u_x, u_y	Displacement field.
		β_{ij}	Material compliances.
		E_x, E_y, G_{xy}	Axial, shear moduli.
		$\nu_{xy}, \eta_{xy,y}, \eta_{xy,x}$	Coupling coefficients.
		α_{ij}	Material stiffness.
		F, F_1, F_2	Stress functions.
		z, z_k	Characteristic directions.
		μ	Roots of the characteristic equation.
		i	$\sqrt{-1}$.
		Φ_1, Φ_2	Derivatives of $F_1(z_1)$, $F_2(z_2)$.
		$R[\ ]$	Real part of [ ].
		p_k, q_k	Constants.
		t_x, t_y	Traction components.
		n_x, n_y	Outward normal.
		Φ_{ik}	Stress function.
		δ_{ij}	Kronecker delta.
		A_{jk}, C_{jk}, D_{jk}	Complex, real constants.
		U_{ji}	Fundamental displacement tensor.
		T_{ji}	Fundamental traction tensor.
		P_{ik}, Q_{ik}	Complex constants.
		ϵ_{ij}	Strain field.
		$S_{j\ell i}, D_{j\ell i}$	Tensor kernels for ϵ_{ij}.

CHAPTER	SECTION	SYMBOL	DESCRIPTION
V	1	[illegible]	Cartesian coordinates.
		U_{ij}	Singular influence tensor.
		$P(x)$, $Q(x)$	Boundary points.
		$r(P,Q)$	Distance between $P(x)$, $Q(x)$.
		ν	Poisson's ratio.
		μ	Shear modulus.
		π	Pi.
		δ_{ij}	Kronecker delta.
		u_i	Displacement vector.
		t_i	Traction vector.
		σ_{ij}	Stress tensor.
		n_j	Unit outward normal vector.
		T_{ij}	Singular influences tensor.
		∂R	Surface of the body, R.
		N	Number of boundary segments.
		P_m, Q_n	Discrete boundary points.
		[I]	Identity matrix.
		$[\Delta T]$, $[\Delta U]$	Coefficient matrices.
		{t}	Traction vector.
		{u}	Displacement vector.
		ΔS_{kij}, ΔD_{kij}	Integrals of influence tensors.

CHAPTER	SECTION	SYMBOL	DESCRIPTION
V	3	ϵ_x	x-direction strain.
		$U_x(1)$, $U_x(2)$	x-direction displacement at segment number 1; segment number 2.
		ℓ	Distance between midpoints of adjacent boundary segments, as s own in Fig. 1 and Fig. 2.
		Y*	y-coordinate of last valid data point obtained for interior solution points, before data diverge from the theoretical solution.
		SCF	Stress concentration factor.
		a	Semi-major axis of an ellipse.
		b	Semi-minor axis of an ellipse.
		c	Semi-focal distance.
		σ_x	x-direction stress.
		σ_y	y-direction stress.
	4	C_{ijkl}	Elastic constant tensor.
		U_k	Displacement vector.
		τ_{ij}	Stress tensor.
		e_{ij}	Strain tensor.
		L_{ij}	Second order, linear operator.
		U_{ij}	Singular influence tensor.
		$\underset{\sim}{x}$, $\underset{\sim}{y}$	Spatial points.
		∂R, Γ	Surfaces.
		T_{ij}	Singular influence tensor
		t_i	Traction vector.

CHAPTER	SECTION	SYMBOL	DESCRIPTION
V	4	ε	Radius.
		n_k	Unit outward normal vector.
		π	Pi.
		$\Delta \underset{\sim}{y}$	Laplacian at $\underset{\sim}{y}$.
		$\underset{\sim}{\xi}$	Vector.
		$\Omega_{\underset{\sim}{\xi}}$	Sphere of unit radius $\underset{\sim}{\xi} = 0$.
		$P^{kj}(\underset{\sim}{\xi})$	Inverse of $Q_{ik}(\underset{\sim}{\xi})$.
		$Q_{ik}(\underset{\sim}{\xi})$	Characteristic form of L_{ik}.
		$\underset{\sim}{R}$	Vector, $\underset{\sim}{x} - \underset{\sim}{y}$.
		ψ	Angle between $\underset{\sim}{R}$ and $\underset{\sim}{\xi}$.
		A_{jk}	Tensor.
		ε_{ijk}	Alternating symbol.
		Det Q	Determinant of Q_{ij}.
		λ, μ	Lamé constants.
		α, β	Material constants.
		ψ_i	Angle between $\underset{\sim}{R}$ and x_i; polynomials in $\underset{\sim}{\xi}$, n.
		c	Constant.
		U_1, U_2, U_3	Functions of y, z.
		S_x, S_y, S_z	Surfaces with normals in x, y, z directions.
		ℓ	Length of specimens.
		$\hat{U}_{ij}$, $\hat{T}_{ij}$	Influence tensors, independent of x.
		f_j	Vector function.
		w	Lamina width.
		t	Lamina thickness.

CHAPTER I

SUMMARY OF THE INTERACTIVE PROGRAM

1.1 INTRODUCTION

The Carnegie-Mellon University team of faculty and students has developed a unique program of interaction between the University team, the Air Force Materials Laboratory, and certain aerospace industries, notably General Dynamics, Convair Aerospace Division (Fort Worth). The interactive program has focused on the application of mechanics capabilities of the CMU team to the stress and strength analysis of advanced fiber composite structures. The broad objectives of the program are the following:

1. Creation of new and effective means of communication and interaction between CMU and General Dynamics and other aerospace industries.
2. Involvement of the CMU team in the solution of fundamental engineering problems arising from the application of advanced composites in aerospace structures.
3. Development by the CMU team of new stress analysis capabilities and results, strength criteria, design information and educational material for advanced composites technology.

To accomplish these goals, a two year effort was initiated at CMU under Air Force sponsorship in November, 1969. The two year program has been completed and has successfully met the goals delineated above. The purpose of this Final Report is to summarize the achievements of the Interactive Program. This first Chapter discusses results for all of the objectives. Following Chapters discuss in detail the results for objectives 2 and 3.

The principal investigators for this program originally adopted the position that the second objective would be promoted through extensive contacts with industry, and that student members of the CMU team would be select senior undergraduate and first- and second-year graduate students. This position precluded supporting Ph.D. and faculty research by the program. However, two student members of the CMU team have passed the Ph.D. qualifying exam and are doing their research based on their project experience (Fracture of Composites; Design of Mechanically Fastened Joints). To date, five undergraduate and fifteen graduate students have participated to some extent in the Interactive Program. Faculty other than the Principal Investigators have participated in the educational program to become familiarized with advanced composites technology and to lend particular expertise as needed.

1.2 FIRST AND SECOND YEAR PROGRAMS

1.2.1 Phase I

During each year the Interactive program has been divided into three phases: education, project research, and reporting. The education phase is based on a Fall Semester course, *Mechanics of Fiber Composite Materials*. The purpose of the course is to bring the students "up-to-speed" in advanced composites technology such that they can contribute significantly to the solution of engineering problems. In the second year of the program, Dr. Cruse offered an advanced course, *Two Dimensional Anisotropic Elasticity*, which was based on the analytical solution of membrane problems of composites using the complex variable approach. A summary of the educational program is included in Appendix I, Chapter I. This summary includes course outlines and descriptions, references, and homework problem titles.

The emphasis in the course work is on the identification of state-of-the-art knowledge and on solving meaningful homework problems. An example of this is the use of the "pressure vessel" problem. Students are asked to find the optimal winding angle ($\pm\alpha$) and maximum pressure for a cylindrical pressure vessel, using a fixed material (e.g. graphite-epoxy) and each of the proposed failure criteria. The problem forces the student to exercise lamination theory and allows a comparison of the allowable pressures.

Another important problem area that was used is the stress concentration factors in composite plates subject to in-plane loading. The fact that these factors are always higher than for isotropic materials is emphasized. The discussion leads to other measures of strength such as associated with sharp flaws.

The students make considerable use of the computer and in-house analysis programs such as finite element and boundary-integral methods for boundary value problems and a pattern search program for optimization and synthesis. Through all of the exercises the student develops insight into the fundamental mechanics questions and spends very little time on the nature of the analysis programs.

1.2.2 Phase II

The second phase lasts through the Spring Semester and sometimes, for significant problems, through the summer. The purpose of the second phase is to involve the students in engineering problems in advanced composites technology. The students, with faculty and industry guidance, select problems of interest to the student and industry. The process of problem selection for new members of the team was a major portion of the second half of the Fall Semester course.

In January of each year Dr. Cruse presented the project problems at General Dynamics for evaluation and recommendations. At the same time engineers at General Dynamics were identified who would act as the industrial contact for the student working on a particular project.

A major portion of the budget of the Program was devoted to travel support. The reasoning is that the CMU team, to be effective, must have considerable visibility of the industrial problems in composites technology. Thus, during the second phase the University team made several visits to industrial locations, technical meetings, program reviews, and special Air Force programs. These trips have also served to give the CMU team visibility as a group doing significant work in the area of advanced composites technology. A complete list of trip report titles is presented in Appendix II, Chapter I. This list illustrates the breadth and depth of the CMU team contacts with other teams in the technology area.

In the first year of the program, the CMU team made a group visit to General Dynamics. This trip was for presenting student progress reports on their projects; it also was a chance for the student members of the team to see manufacturing and test programs in progress. In the second year, the new member of the CMU team to pursue project work visited Boeing/Vertol to see their advanced composites manufacturing and test program. However, the rest of the members of the team doing project research were in their second year, and thus a team visit to industry was not made during the second phase of the second year.

The telephone is used heavily during the second phase. By identifying engineers, perhaps at different industrial locations, who had an interest in the student project problem, each student could ask questions and receive advice, data, and evaluation without the necessity of a full visit with the engineer. The CMU team found that continual contact with engineers played a major role in the success of the Interactive Program.

1.2.3 Phase III

The third phase of the program is the reporting phase for each project problem. Each student, upon reaching a major milestone, or when completing his participation in the program, is required to provide a written project report which is typed and filed. Thus, the reporting phase is interweaved throughout the program. A list of the titles of all reports generated and on file is given in Appendix III, Chapter I. The reports contain major homework problem solutions from Phase I work, project proposals and progress reports, tutorial material, and final project reports.

Some of the project reports are significant enough to be published in technical journals [1,2][1] and to be presented at technical meetings [3,4]. In addition other reports have been submitted for presentation to the 13th AIAA/ASME Structures, Structural Dynamics and Materials Conference [5,6], while another has been accepted for the 1972 ASTM

---

[1] References are denoted by brackets [ ] and are found at the end of each major segment of this Report.

meeting on composites [7]. These papers serve to give to CMU team greater visibility in the composites community as well as to report important results.

In addition to the above major reports, the program had a requirement for monthly letter reports, at the request of the Principal Investigators. These reports required monthly student progress reports while the students were doing project research. The monthly report served to force each member of the team to be fully aware of his own and others' progress. In addition the reports kept the industrial team informed of project progress.

At the end of the summer, each year, the CMU team prepared final project reports which were presented at the Air Force Materials Laboratory and at General Dynamics. This final reporting has been the most important facet of Phase III as the CMU team seeks critical review of its programs by the active researchers and engineers at both locations. The final report meetings served as the focal point for examination of progress, but they also provided an opportunity to explore new areas of project work, team emphasis, and industrial support.

1.3 RESEARCH PROJECTS COMPLETED

A sizeable number of project research problems have been solved to date and the titles are listed in Appendix II, Chapter I. Listed below are the major project titles, the responsible investigator, a summary of the project and project reports as found in the SM file in the Mechanical Engineering Department. The following Chapters of this Final Report present in detail the major accomplishments of each project.

1.3.1 Fracture of Advanced Composites (H. J. Konish, Jr.)

This project includes analytical and experimental investigations of the fracture of moderately thick graphite/epoxy specimens. Information to date has been very encouraging in that a considerable amount of linear elastic fracture mechanics theory seems applicable to the material. (SM Reports 31, 41, 53, 64, 74, 80, 81; work in progress).

1.3.2 Strength of Mechanically-Fastened Joints (J. P. Waszczak)

This project has gone from the analysis of single-fastener test coupons to the analysis of joints with many fasteners. Due to the weight penalty associated with these joints, a program has been begun to develop a synthesis procedure for designing multifastener joints. This program has a strong coupling with the engineering team at General Dynamics. (SM Reports 28, 34, 63, 76; work in progress).

1.3.3 Optimization Methods (S. J. Marulis; Ford Motor Co.)

The project was to investigate the use of an in-house, pattern-search optimization method for composite design problems. The design of mechanically-fastened joints was considered, using the in-house program. An effort to couple the optimization program to the available finite element program was unsuccessful but may be completed in the future. The optimization program has been found suitable, if not optimal, for use by Mr. Waszczak in his project research. (Report SM-71; work suspended).

1.3.4 Boundary-Integral Equation Solution Methods (T. A. Cruse, W. H. Bamford, F. J. Rizzo)

Three separate efforts have been completed in this area. The first reported is the development of an isotropic, two dimensional boundary-integral equation method and a subsequent investigation of its

ability to model cutouts under tension. The second reported is the development of a boundary-integral method for fully-anisotropic (mid-plane symmetric) laminates. (Currently, the anisotropic program is being veri-fied on cutout problems and some of these results are report.) The third, completed by Prof. F. J. Rizzo of the University of Kentucky, concerns solutions to Kelvin's problem in anisotropic three dimensional bodies, and the interlaminar shear problem.
(SM Reports 45, 50, 66, 68, 70, 72; work in progress).

1.4 EVALUATION AND RECOMMENDATIONS

It is clear that the goals of the Interactive Program at CMU have been met. The project reports contained in this Final Report give ample evidence of the extent to which the CMU team has become competent in research and application problems in advanced composites technology. There now exists considerable interaction and support between the General Dynamics team and the CMU team. In particular, General Dynamics has provided test specimens for the Fracture Program and a summer contract for the Joint Project.

However, the level of confidence in the CMU team expressed by General Dynamics has come late in the program. Communication and inter-action took place during the first year of the program but the depth of both was not satisfying to either team. One reason for this was that during the first year the CMU team was just coming up to speed in advanced composites technology. However, based on the results of the program re-view at the end of the first year, the support from the General Dynamics team increased rapidly. The other reason for the slow start was the lack of *constant* contact between the CMU team and the General Dynamics team. During the second year, much more contact was made, principally by Dr. Cruse visiting General Dynamics and liberal use of the telephone. Frequent personal contacts are critically important to the success of an interactive program such as ours.

The impact to date on the educational program at CMU has been minor. The two courses cited in Appendix I plus project work (counts as course work) are the extent of highly visible composites activities in the educational program. However, seminars given by General Dynamics and AFML personnel, and by the Principal Investigators have served to make other faculty aware of the questions of materials selection, and composites in particular. During one semester Dr. Cruse taught a section of Senior Design which was concerned with the rationale for materials selection. At the present time Dr. Cruse is involved in an effort to expand the CMU Post-College Professional Education Program. This effort includes a course on fiber composites.

At a harder level to document, instructors in the basic solid mechanics courses in the Mechanical Engineering Department have the specimens and knowledge to demonstrate simple anisotropic effects. It is hoped that more of this information can be meaningfully involved in the undergraduate courses. One of the biggest problems which mitigates against new courses in the undergraduate or graduate program is the financial state of the University. The process of cutting-back is underway and will likely last a few more years.

Finally, the question arises as to the impact the Program has had in developing graduates with a competence in advanced composites, who will use this competence in the aerospace industry. To date this impact has been nearly zero, as most of the students who have done significant project work have yet to graduate. An early graduate with contact with the Interactive Program went to Pratt and Whitney; another graduate went to Ford Motor Company. Several graduate students with other research areas have taken one or both of the courses offered to date. Those in the Program who are still doing project work are commissioned officers in the United States Army. Thus the personnel impact will require more time to develop.

Two years ago, CMU had no active research in the area of advanced composites. In that period the CMU team has developed an effective education – project program that is closely related to fundamental engineering problems in advanced composites technology. Members of the CMU team have presented and published an increasing number of research papers, and have participated in several Air Force review meetings. The depth and breadth of research accomplishments are reported in the remaining Chapters of this Final Report. Other measures of the Program require additional time to mature.

1.5 *REFERENCES*

[1] J. P. Waszczak, T. A. Cruse, "Failure Mode and Strength Predictions of Anisotropic Bolt Bearing Specimens", *J. Comp. Materials* 5, (July 1971).

[2] H. J. Konish, Jr., J. L. Swedlow, T. A. Cruse, "Experimental Investigation of Fracture in an Advanced Fiber Composite", Report SM-74, *J. Comp. Materials* (to appear).

[3] J. P. Waszczak, T. A. Cruse, "Failure Mode and Strength Predictions of Anisotropic Bolt Bearing Specimens", Fifth St. Louis Symposium on Composite Materials (April 1971).

[4] J. P. Waszczak, T. A. Cruse, "Failure Mode and Strength Predictions of Anisotropic Bolt Bearing Specimens", *Proceedings* of the 12th AIAA/ASME Structures, Structural Dynamics and Materials Conference (April 1971).

[5] H. J. Konish, Jr., J. L. Swedlow, T. A. Cruse, "On Fracture in Advanced Fiber Composites", Report SM-80, (Submitted to AIAA/ASME) (October 1971).

[6] T. A. Cruse, "Boundary-Integral Equation Solution Method for Plane Stress Analysis of Composites (Extended Abstract), Report SM-75, (Submitted to AIAA/ASME 13th Structures and Structural Dynamics Meeting) (September 1971).

[7] H. J. Konish, Jr., J. L. Swedlow, T. A. Cruse, "A Proposed Method for Estimating Critical Stress Intensity Factors for Cross-Plied, Mid-Plane Symmetric Composite Laminates", Report SM-81, (Extended abstract submitted to ASTM) (October 1971).

1.6 *APPENDIX I: SUMMARY OF EDUCATIONAL MATERIAL*

I. COURSE: Mechanics of Fiber Composite Materials *(First Semester)*

   A. Course description
   B. References
   C. Course outline

II. Project-type Homework Problems

   A. Develop computer program for calculating [A] matrix
   B. Develop computer program to reduce laminate strains to lamina stresses and strains
   C. Analyze dependence of the [A] mat 'x terms on the fiber orientation
   D. Determine the effect of transverse tension on the inter-laminar shear stress
   E. Determine the optimum winding angle (±) for a pressure vessel
   F. Evaluate the deformation in a helically-wound (+) cylinder
   G. Evaluate the finite element solution for a circular cutout
   H. Evaluate the finite element solution for a composite beam

III. Finite Element Summary

   A. Course notes from a short course for users
   B. Usage guide for in-house finite element computer programs

IV. COURSE: Two Dimensional Anisotropic Elasticity *(Second Semester)*

   A. Course description
   B. Some selected prepared course notes

V. Project-type Homework Problems

   A. Isotropic
      1. General solutions for ring-shaped region
      2. Bolt-bearing solution
      3. Concentrated force in an infinite plate

   B. Anisotropic

      1. Stress concentration at an ellipse
      2. Hoop stress distribution at a circle
      3. Torsion of a prismatic member
      4. Point load in an infinite plate
      5. Bolt-bearing solution
      6. Stress analysis of a cracked, infinite plate

MECHANICS OF FIBER COMPOSITE MATERIALS

Text Material:

T. A. Cruse, *Mechanics of Laminated Fiber Composites* (notes in preparation)

J. E. Ashton et al, *Primer on Composite Materials: Analysis* Technomic (1969)

Course Abstract:

This course deals with the stress and strength analysis of two dimensional anisotropic fiber composite structural materials. These materials have applications in structural reinforcements, pressure vessels, and aerospace structures. Typical materials that can be considered include reinforced concrete, fiberglass, and some of the new, advanced fiber composites such as boron-epoxy and graphite-epoxy. Major topics include the development of the anisotropic stiffness matrix for in-plane and out-of-plane loading of plates and shells, theories of strength and experimental procedures, and stress and displacement analysis of simple plate and shell structures. Students will participate in a number of project problems designed to involve the student in some of the real design problems associated with composite materials. Existing solution techniques such as finite elements, integral equations, and optimization computer programs, as well as analytic solution capabilities will be exercised as appropriate. The student is assumed to have completed the normal undergraduate courses in strength of materials including some introduction to the theory of elasticity.

MECHANICS OF FIBER COMPOSITE MATERIALS

Supplementary Reference Material:

BOOKS:

S. A. Ambartsumyan, *Theory of Anisotropic Plates*, Technomic (1970)

J. E. Ashton, J. M. Whitney, *Theory of Laminated Plates*, Technomic (1970)

G. S. G. Beveridge, R. S. Schechter, *Optimization: Theory and Practice*, McGraw-Hill (1970)

S. W. Tsai, et al (Editors), *Composite Materials Workshop*, Technomic (1968)

L. J. Broutman, R. H. Krock (Editors), *Modern Composite Materials*, Addison Wesley (1967)

__________, *Metal Matrix Composites*, ASTM STP 438 (1968)

__________, *Interfaces in Composites*, ASTM STP 452 (1969)

__________, *Composite Materials: Testing and Design*, ASTM STP 460 (1969)

REPORTS:

T. A. Cruse, J. L. Swedlow, *Interactive Program in Advanced Composites Technology: First Annual Report*, Report SM-46, Carnegie-Mellon University, Pittsburgh, Pennsylvania (1970)

M. S. Howeth, *Design, Materials and Structures*, Report SMD-028, General Dynamics, Fort Worth, Texas (1969).

S. W. Tsai, *Mechanics of Composite Materials*, AFML-TR-66-199

MECHANICS OF FIBER COMPOSITE MATERIALS

COURSE OUTLINE:

I. Review of Two Dimensional elasticity (6 hours)

   A. Stress tensor
   B. Equilibrium
   C. Strain Tensor
   D. Compatibility

II. Linear, anisotropic elasticity (5 hours)

   A. Existence of the strain energy density
   B. Fourth order compliance, stiffness tensors
   C. Transformation equations
      1. Specially orthotropic
      2. Transversely isotropic
      3. Isotropic
   D. Plane stress results

III. Mechanics of a continuous fiber lamina (4 hours)

   A. Manufacturing of fibers, laminae
   B. Rules of mixtures
   C. Summary of micromechanics results
   D. Lamina mechanical properties

IV. Mechanics of Laminates (12 hours)

   A. Manufacturing of laminates
   B. Stiffness, compliance matrices; [A], [B], and [D]
   C. Strength theories
      1. Static theories: Maximum stress, strain; Distortional energy
      2. Energy tensor
      3. Fatigue
      4. Fracture

V. Structural applications and projects (12 hours)

   A. Finite element solution method
   B. Joints and cutouts
   C. Pressure vessels
   D. Stability, vibrations
   E. Limitations on lamination theory

TWO DIMENSIONAL PROBLEMS IN THE THEORY OF ANISOTROPIC ELASTICITY

Recommended Textbooks:

N. I. Muskhelishvili, *Some Basic Problems of the Mathematical Theory of Elasticity*, Noordhoff (1963)

S. G. Lekhnitskii, *Theory of Elasticity of an Anisotropic Elastic Body*, Holden-Day (1963)

Course Abstract:

The first half of the course is devoted to the formulation and solution of the two dimensional, isotropic elastic problem using complex variable methods. Solutions are obtained using the Laurent series expansion for multiply-connected bodies. The second half of the course is devoted to the analysis of anisotropic, two dimensional problems, again using the complex variable method. Example problems and projects are chosen for their relevancy to current engineering problems in anisotropic media, such as advanced fiber composites. Existing numerical solution methods such as finite elements and integral equations are used and compared to the analytic results when possible. The course assumes a knowledge of the basic theorems of analysis of functions of a complex variable as well as the basic theory of elasticity.

TWO DIMENSIONAL PROBLEMS IN THE THEORY OF ANISOTROPIC ELASTICITY

COURSE OUTLINE:

I. Review of complex variable theory (6 hours)

A. Analytic functions
B. Green's theorem
C. Cauchy integral theorems
D. Series

II. Plane theory of isotropic elasticity (18 hours)

A. Equilibrium; stress function
B. Strains; Hooke's law
C. Goursat formula
D. Displacements
E. Tractions
F. Kolosov formula
G. Forces on a contour
H. Single-valued displacements, stresses
I. Laurent series for the stress functions
J. Infinite region with a hole
K. Polar coordinate form of the equations
L. Mapping functions; curvilinear coordinates
M. Transformed field equations
N. Example solutions

III. Plane theory of anisotropic elasticity (15 hours)

A. Hooke's law for various types of anisotropy
B. Stress function
C. Characteristic surfaces for the stress function
D. Roots of the characteristic equation $\ell_4(\mu) = 0$
E. Stresses and displacements
F. Forces on a contour
G. Infinite region with a hole
H. Single-valued stresses and displacements
I. Mapping functions
J. Fourier analysis of the boundary conditions
K. General expansion form of the solution
L. Example solutions

1.7 APPENDIX II: TRIP REPORTS

TRIP REPORT NO.	TITLE	DATE
TR-69-02	Exploration of Possible University-Industry Cooperation in the Area of Advanced Composite Technology (T. A. Cruse)	7/14/69
TR-69-04	Detailed Discussion of Proposed University-Industry Joint Program in Advanced Composite Technology (T. A. Cruse)	8/11-12/69
TR-69-09	Advanced Composites Status Review (T. A. Cruse)	9/30-10/2-69
TR-69-10	University Team Visit to Air Force Materials Laboratory	11/24/69
TR-70-01	Fuselage Program Review (General Dynamics) and Discussion of Project Problems (T. A. Cruse)	1/7-9/70
TR-70-02	Review Meeting, First Edition of Structural Design Guide for Advanced Composite Applications, and Test Methods (R. D. Blevins)	2/11/70
TR-70-03	Discussion of Bolt Bearing Testing Procedures with North American Rockwell/Columbus (J. P. Waszczak)	3/12/70
TR-70-04	Discussion of Test Data, Methods with North American Rockwell/Los Angeles (R. D. Blevins)	3/18/70
TR-70-05	Team Visit to Southwest Research Institute	4/2/70
TR-70-09	Team Visit to General Dynamics/Fort Worth	4/3/70
TR-70-10	Discussion of Consulting Program with Dr. Frank J. Rizzo (T. A. Cruse)	8/19-21/70
TR-70-12a	Project Review Meetings at General Dynamics/Fort Worth and Air Force Materials Laboratory	10/4-6/70

TRIP REPORT NO.	*TITLE*	*DATE*
TR-70-13	Boeing/Vertol: Review of Boron Blade Program (S. J. Marulis; T. A. Cruse)	10/28/70
TR-70-14	NASA/Langley Field; Interactive Program in Composites at CMU (T. A. Cruse, J. L. Swedlow)	12/15/70
TR-71-01	AFML; GD/Ft. Worth: Program Review and New Project Proposals (T. A. Cruse)	1/5-6/71
TR-71-02	GD/Ft. Worth: Program Review Meeting (T. A. Cruse)	4/14/71
TR-71-03	Fifth St. Louis Symposium on Composite Materials	4/6-7/71
	12th AIAA/ASME Structures, Structural Dynamics, and Materials Conference	4/19-21/71
	(T. A. Cruse, J. P. Waszczak)	
TR-71-06	Design Guide Review Meeting; NAR, Los Angeles (T. A. Cruse)	5/24-26/71
TR-71-07	GD/Ft. Worth; Program Review Meeting (T. A. Cruse, J. P. Waszczak, H. J. Konish, Jr.)	6/9-10/71
TR-71-08	Boeing/Vertol: Review of CMU Fracture program (H. J. Konish, Jr.)	6/18/71
TR-71-09	31st National Applied Mechanics Conference (T. A. Cruse)	6/23-25/71
TR-71-10	GD/Ft. Worth: Review of Summer Project (J. P. Waszczak)	7/7-9/71
TR-71-11	GD/Ft. Worth: Review of Summer Project, Boundary-Integral Project (J. P. Waszczak, T. A. Cruse)	8/5/71
TR-71-12	GD/Ft. Worth: Review of Summer Project, (J. P. Waszczak)	8/5-6/71
TR-71 13	5th National Fracture Mechanics Symposium (H. J. Konish, Jr., T. A. Cruse, J. R. Osias)	8/31-9/2/71

1.8 *APPENDIX III: RESEARCH DOCUMENTS*

REPORT NUMBER	*TITLE*	*DATE*
SM-22	Anisotropic Stress Strain Program Layer Usage Guide (H. J. Konish, Jr.)	January 1970
SM-23	Project Problems for Air Force Contract F33615-70-C-1146 (T. A. Cruse)	January 1970
SM-24	Summary of the Direct Potential Method (T. A. Cruse)	January 1970
SM-25	Interactive Program in Advanced Composites Technology (T. A. Cruse)	February 1970
SM-27	Symmetric Laminate Constitutive Equation Program-EMAT Usage Guide (J. P. Waszczak)	February 1970
SM-28	Bolt Bearing Specimen Co-ordinate Transformation Program - Usage Guide TRANS (J. P. Waszczak)	April 1970
SM-29	Certain Aspects of Design with Advanced Fibrous Composites (R. D. Blevins)	April 1970
SM-31	Stress Analysis of a Cracked Advanced Composite Beam (H. J. Konish, Jr.)	April 1970
SM-32	An Investigation of Fracture in Advanced Composites (W. H. Bamford)	April 1970
SM-34	An Investigation of Stress Concentrations Induced in Anisotropic Plates Loaded by Means of a Single Fastener Hole (J. P. Waszczak)	May 1970
SM-38	Integral Equation Methods in Potential Theory (T. A. Cruse)	August 1970
SM-41	Stress Analysis of a Cracked Anisotropic Beam (H. J. Konish, J. L. Swedlow)	September 1970
SM-42	An Investigation of Stress Concentrations Induced in Anisotropic Plates Loaded by Means of a Single Fastener Hole (J. P. Waszczak, T. A. Cruse)	September 1970
SM-45	The Use of Singular Integral Equations with Application to Problems of Composite Materials (F. J. Rizzo)	October 1970

REPORT NUMBER	*TITLE*	*DATE*
SM-49	Report on the Relation Between the Stiffness Matrix and the Angle of Rotation of a Lamina (J. Kolter)	November 1970
SM-50	Numerical Solution Accuracy for the Infinite Plate with a Cutout — Progress Report (W. Bamford)	December 1970
SM-52	Failure Mode and Strength Predictions of Anisotropic Bolt Bearing Specimens (J. P. Waszczak; T. A. Cruse)	September 1970
SM-53	A Proposed Experimental Investigation of Fracture Phenomena in Advanced Fiber Composite Materials (H. J. Konish, Jr.)	February 1971
SM-63	Loaded Circular Hole in an Anisotropic Plate (J. P. Waszczak)	May 1971
SM-64	Stress Analysis of the Crack-Tip Region in a Cracked Anisotropic Plate (H. J. Konish, Jr.)	May 1971
SM-65	Numerical Calculation of the Characteristic Directions for a Generally Anisotropic Plate - MULTMU Usage Guide (H. J. Konish, Jr.)	June 1971
SM-68	Solution to Kelvin's Problem for Planar Anisotropy (W. Bamford)	June 1971
SM-70	USER'S DOCUMENT: Two Dimensional Boundary-Integral Equation Program (T. A. Cruse)	June 1971
SM-71	Optimization of Advanced Composite Plates (S. Marulis)	June 1971
SM-72	Two Dimensional Anisotropic Boundary-Integral Equation Method (W. H. Bamford, T. A. Cruse)	August 1971

REPORT NUMBER	*TITLE*	*DATE*
SM-74	Experimental Investigation of Fracture in an Advanced Fiber Composite (H. J. Konish, J. L. Swedlow, T. A. Cruse)	September 1971
SM-76	Toward a Design Procedure for Mechanically Fastened Joints Made of Composite Materials (J. P. Waszczak)	September 1971
SM-77	Review of: Structural Design Guide for Advanced Composite Applications, 2nd Edition, Appendix A: Theoretical Methods (T. A. Cruse)	May 1971
SM-80	On Fracture in Advanced Fiber Composites (H. J. Konish, Jr., J. L. Swedlow, T. A. Cruse)	October 1971
SM-81	A Proposed Method for Estimating Critical Stress Intensity Factors for Cross-Plied, Mid-Plane Symmetric Composite Laminates, (Abstract) (H. J. Konish, Jr., J. L. Swedlow, T. A. Cruse)	October 1971

CHAPTER II

FRACTURE OF ADVANCED COMPOSITES

2.1 *STRESS ANALYSIS OF A CRACKED ANISOTROPIC BEAM*

2.1.1 *Introduction*

The high specific strength and specific stiffness of advanced fiber composite materials have made them very attractive to the aerospace industry. The fact that they are both anisotropic and inhomogeneous, however, has somewhat retarded their use, as the design and analysis procedures developed for metals are not strictly applicable; thus, it is necessary to adapt old procedures, or develop new ones, which can deal with the more complex composite materials.

The project discussed in this chapter deals with one such effort. The specific problem under consideration is the effect of a crack in a unidirectional advanced fiber composite material. Although this problem is one of great significance in aerospace structures, it has not yet been extensively treated. An analytic solution has been derived for the elastic stresses and strains induced by a crack in a loaded anisotropic plate [1]. The solution does assume material homogeneity, but this is a good approximation for advanced fiber composite materials on a macroscopic scale. However, relatively little has been done to follow up the analytic work.

2.1.2 *Review of Previous Work*

The most extensive investigation of fracture of composites in the literature is that done by Professor E. M. Wu of Washington University, St. Louis. He considers the problem of a central crack, aligned with the fibers of a unidirectional composite material, which are, in turn, aligned with the edges of a plate subjected to general edge loadings.

Wu demonstrates that linear-elastic fracture mechanics are applicable to this problem [2]. His analysis yields results of the form

$$\sigma = K_I F\sqrt{2\pi r} \tag{1}$$

$$K_I = \sqrt{a}\ G \tag{2}$$

where F is a function of the external loading and G is a function of specimen geometry, material constants, and external loading. These results are similar in form to the results obtained from the analysis of an isotropic problem.

Wu verified his analysis experimentally [2,3]. His experimental work, (done with fiberglass plates), does demonstrate the applicability of a linear elastic fracture mechanics analysis to his particular problem. It further shows that the critical stress intensity factors K_{Ic} (corresponding to symmetric loading on the plate) and K_{IIc} (corresponding to skew-symmetric loading on the plate) are material constants. Under combined external loading, the following empirical relationship is observed to be valid at incipient unstable crack propagation:

$$K_I/K_{Ic} + (K_{II}/K_{IIc})^2 = 1 \tag{3}$$

This result is not, however, particularly surprising in view of [1], where it is analytically shown that any arbitrary two-dimensional fracture problem in an anisotropic material may be decomposed into two independent problems, one symmetric and one skew-symmetric. Thus, only the form of (3) may be considered as original; its existence is predicted by analysis.

Wu has also investigated the problem of an external loading of combined compression and shear [4]. This loading will lead to crack propagation by the second, or "sliding" mode. Three possible subcases are considered analytically: Relative displacement of the crack surfaces, over a portion of the crack surfaces, and over none of the crack surfaces.

This analysis was verified by an experimental program carried out on fiberglass. The results show that, for ratios of compressive load to shear load greater than approximately 0.4, failure does not occur by unstable crack propagation; the crack velocity remains quasi-stable until the specimen fails from propagation of the crack completely through it. If the ratio of compressive load to shear load is increased, internal buckling of the fibers and separation of the fibers from the matrix is observed; at most, the crack will propagate some small distance at an angle of 45° from its initial direction, then diffuse and die out. The specimen buckles thereafter with no additional crack propagation. Wu thus concludes that fracture mechanics is only applicable to this problem when the ratio of compressive stress to shear stress is less than 0.4. The second subcase of the analysis gives the best agreement between analysis and experiment when fracture mechanics are applicable. The quasi-stable crack propagation found to occur experimentally when the ratio of compressive load to shear load is approximately 0.4 seems to be well-described by the first subcase of the analysis. The third subcase of the analysis is believed to be applicable when the compressive load is sufficiently large to prevent crack extension; however, buckling, rather than crack propagation, becomes the dominant mode of failure before this load is reached, so the presence of the crack not significant in the failure of the specimen.

Wu notes that stable crack propagation occurs in an intermittent manner in fiberglass [2]; he postulates that this is caused by the crack crossing the reinforcing fibers. This hypothesis is investigated both analytically and experimentally [5].

The analysis is based on the assumption that crack growth is primarily caused by the component of tensile stress perpendicular to the direction of crack growth, as the intermittent stable crack propagation is most frequently observed under skew-symmetric loading. It indicates that the crack does not necessarily propagate in a direction collinear with itself, but rather at an angle where the combination of the size of a sub-critical flaw and the maximum tensile stress reaches some critical value, causing the flaw to grow. Under skew-symmetric loading, the maximum tensile stress is not perpendicular to the crack direction, and, assuming that flaws of any given size are uniformly distributed in the material, the crack will propagate at some angle to its initial direction. Since the initial direction of the crack is collinear with the fibers, the propagating crack must cross fibers. The direction of crack growth is thus a function of the direction of the shear loading.

It is noteworthy that Wu finds the Griffith energy criterion to be applicable to composite materials only when the crack propagates across fibers. Although Wu offers no explanation for this anomaly, it may be due to the fact that, for this particular geometry, the crack propagates only through resin unless it crosses fibers. Thus, the crack would "sense" a brittle, high-strength material, for which the Griffith criterion is applicable, only when it crosses fibers.

Wu's specimen is also analyzed for symmetric loading by Bowie and Freese [6]. They use a modified mapping-boundary collocation technique to derive the stress intensity factor numerically. Of particular interest is the result of Bowie and Freesc that, when the strength of the material in a direction transverse to the crack is much larger than the strength of the material collinear with the crack, the stress intensity factor is not longer the same for both the isotropic and anisotropic cases, as predicted by Sih, Paris, and Irwin [1]. However, Bowie and Freese do note that, when the strength of the material in the direction collinear with the crack is greater than or equal to the strength of the material in a direction transverse to the crack, the two stress-intensity factors agree to within five per cent.

2.1.3 *Analytical Study*

The efforts described above comprise the significant work now available in open literature on macroscopic analysis of fracture in anisotropic materials. Both of them consider only cracks which are aligned with the fibers of the composite material, and must therefore be considered incomplete, as no provision has been made for cracks with arbitrary orientation to the material axes. The purpose of the project described in this section is to investigate the behavior of a crack in an anisotropic material where the crack is not, in general, collinear with one of the material axes (though these cases are considered). Information is also sought on the behavior of the stress-intensity factor as the orientation of the crack with respect to the material axes and the specimen geometry are varied. Finally, it is desired to obtain verification of either Bowie and Freese [6], or Sih, Paris, and Irwin [1] concerning the differences, if any, between the isotropic and anisotropic stress intensity factors.

In pursuit of these objectives, a series of anisotropic three-point bend specimens with edge cracks of different lengths (Fig. 1) has been studied analytically to determine the stress and deformation response in the vicinity of the crack-tip. Material properties were chosen such that the specimen represents uni-directional boron/epoxy. The orientation of the material axes relative to the crack-axis is completely arbitrary.

The analysis was performed using a linear elastic, plane stress, finite element technique. Two element grids were used, one representing the entire beam and the other representing a small region of the beam surrounding the crack-tip. The latter grid is used to provide more detailed information in the region of the crack-tip than can be obtained from the relatively coarse grid of the entire beam and still remain in the core of the computer. Details of the numerical studies are contained in [7].

Load is applied to the beam by specifying the transverse displacement of the point on the upper edge of the beam in line with the crack-axis. Appropriate nodal displacements from the grid of the full beam are then applied to the grid of the crack-tip region as boundary conditions. From the analysis of the grid of the crack-tip region, stresses and displacements are determined as functions of position.

The stresses and deformations are represented in the form given by Sih, Paris, and Irwin [1]:

$$\sigma_x = \frac{K_I}{\sqrt{2\pi r}} \operatorname{Re}\left[\frac{\mu_1\mu_2}{\mu_1-\mu_2}\left(\frac{\mu_2}{\sqrt{\cos\theta + \mu_2\sin\theta}} - \frac{\mu_1}{\sqrt{\cos\theta + \mu_1\sin\theta}}\right)\right] \tag{4}$$

$$\sigma_y = \frac{K_I}{\sqrt{2\pi r}} \text{ Re } [\frac{1}{\mu_1 - \mu_2} (\frac{\mu_1}{\sqrt{\cos\theta + \mu_2 \sin\theta}} - \frac{\mu_2}{\sqrt{\cos\theta + \mu_1 \sin}})] \quad (5)$$

$$v = K_I \sqrt{\frac{2r}{\pi}} \text{ Re } [\frac{1}{\mu_1 - \mu_2} (\mu_1 q_2 \sqrt{\cos\theta + \mu_2 \sin\theta} - \mu_2 q_1 \sqrt{\cos\theta + \mu_2 \sin\theta})] \quad (6)$$

where K_I is the stress intensity factor for an isotropic specimen of the same geometry as that being analyzed; r and θ are the coordinates shown in Figure 1. The μ_1 are the roots of the characteristic equation

$$a_{11}\mu^4 - 2a_{16}\mu^3 + (2a_{16} + a_{66})\mu^2 - 2a_{26}\mu + a_{22} = 0 \quad (7)$$

where a_{ij} are the material compliances as given by

$$\epsilon_i = a_{ij}\sigma_j \quad (8)$$

The q_j are defined as

$$q_j = a_{12}\mu_j + a_{22}/\mu_j - a_{26} \quad (9)$$

Using the equations (4-9), the stress intensity factor K_I can be obtained in various ways from both the stresses and the displacements found in the analysis of the crack-tip region. It is hypothesized that the stress intensity factor is a separable function of the load on the beam and the specimen geometry, i.e.,

$$K_I = f(\text{load}) \quad g(\text{geometry}) \quad (10)$$

Since the analysis is linear elastic,

$$f(\text{load}) = P/B \quad (11)$$

The effect of the specimen geometry is a function of the crack-length, the effects of finite specimen boundaries, and possibly the material anisotropy. It is further hypothesized that

$$g(\text{geometry}) = \sqrt{a}\, G(a/W,\alpha) \quad (12)$$

where the function G contains the effects of the finite boundaries of the specimen and any effect of the material anisotropy. Thus, combining equations (10-12)

$$K_I = (P\sqrt{a}\,/B)\ G\ (a/W,\alpha)$$

or (13)

$$G\ (a/W,\alpha) = K_I B/P\sqrt{a}$$

The function $G(a/W,\alpha)$ has been obtained analytically for three values of α and five values of a/W, using values of K_I obtained from both stress and displacement data. Each $G(a/W,\alpha)$ was then normalized on the value G $(0.2,\alpha)$ for corresponding methods of determining K_I. The resulting value, denoted as $\bar{G}$ $(a/W,\alpha)$ is shown plotted as function of a/W in Figure 2. On the same graph is shown a curve representing $\bar{G}$ (a/W) for an isotropic specimen, as obtained from [8]. The data points show satisfactory agreement with the curve, in view of the numerical noise introduced by two finite element grids which are not entirely compatible. Thus, $\bar{G}$ $(a/W,\alpha)$ is identical with $\bar{G}(a/W)$. This, in turn, implies that the anisotropic stress intensity factor is the isotropic stress intensity factor.

Although the stress intensity factor in equations (4-6) is the isotropic stress intensity factor, stress and deformation are functions of material constants. Thus, fracture in advanced fiber composite materials cannot be ascribed solely to any combination of the stress intensity factors. To some extent, therefore, the applicability of fracture mechanics to composite materials is questionable. Exactly what importance a crack has in composite materials, and what role the material properties play in describing it, are questions which were investigated experimentally and are reported in Section 2.2.

2.1.4 References

[1] G. C. Sih, P. C. Paris, and G. R. Irwin, "On Cracks in Rectilinearly Anisotropic Bodies", *International Journal of Fracture Mechanics, I,* (September 1965) 189-203.

[2] E. M. Wu, "Application of Fracture Mechanics to Orthotropic Plates", *Department of Theoretical and Applied Mechanics, University of Illinois,* Urbana, Illinois (June 1963).

[3] E. M. Wu and R. C. Reuter, "Crack-Extension in Fiberglass-reinforced Plastics", *Department of Theoretical and Applied Mechanics, University of Illinois,* Urbana, Illinois (February 1965).

[4] E. M. Wu, "A Fracture Criterion for Orthotropic Plates Under the Influence of Compression and Shear", *Department of Theoretical and Applied Mechanics, University of Illinois,* Urbana, Illinois (September 1965).

[5] E. M. Wu, "Discontinuous Mode of Crack Extension in Unidirectional Composites", *Department of Theoretical and Applied Mechanics, University of Illinois,* Urbana, Illinois (February 1968).

[6] O. L. Bowie and C. E. Freese, Unpublished Results, Army Materials and Mechanics Research Agency, Watertown, Massachusetts (1970).

[7] H. J. Konish, Jr. and J. L. Swedlow, "Stress Analysis of a Cracked Anisotropic Beam", Report SM-41, *Department of Mechanical Engineering, Carnegie-Mellon University,* Pittsburgh, Pennsylvania (September 1970).

[8] J. E. Srawley and W. F. Brown, Jr., *Plane Strain Crack Toughness Testing of High Strength Metallic Materials, ASTM STP 410,* American Society for Testing and Materials, Philadelphia, Pennsylvania (1967) 13.

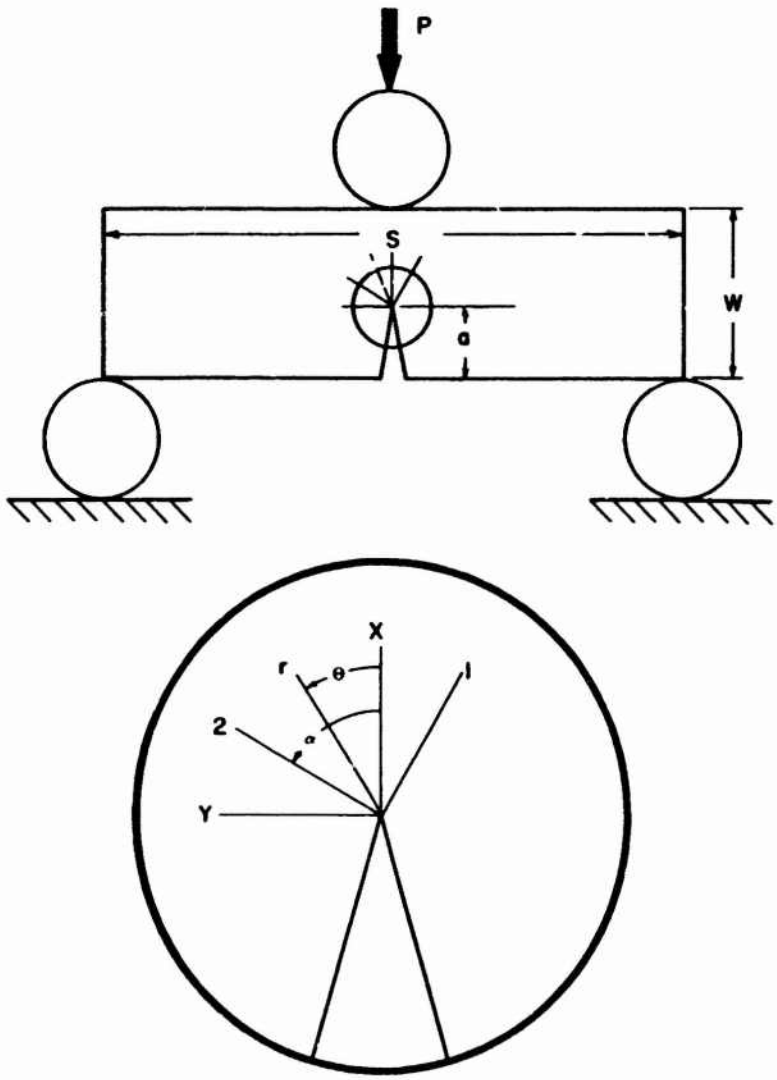

Figure 1: Three-point bend fracture specimen, with global (x,y and r,θ) and material (1,2) coordinate systems shown (insert). The applied load P is modelled as point load. The specimen thickness is denoted by B.

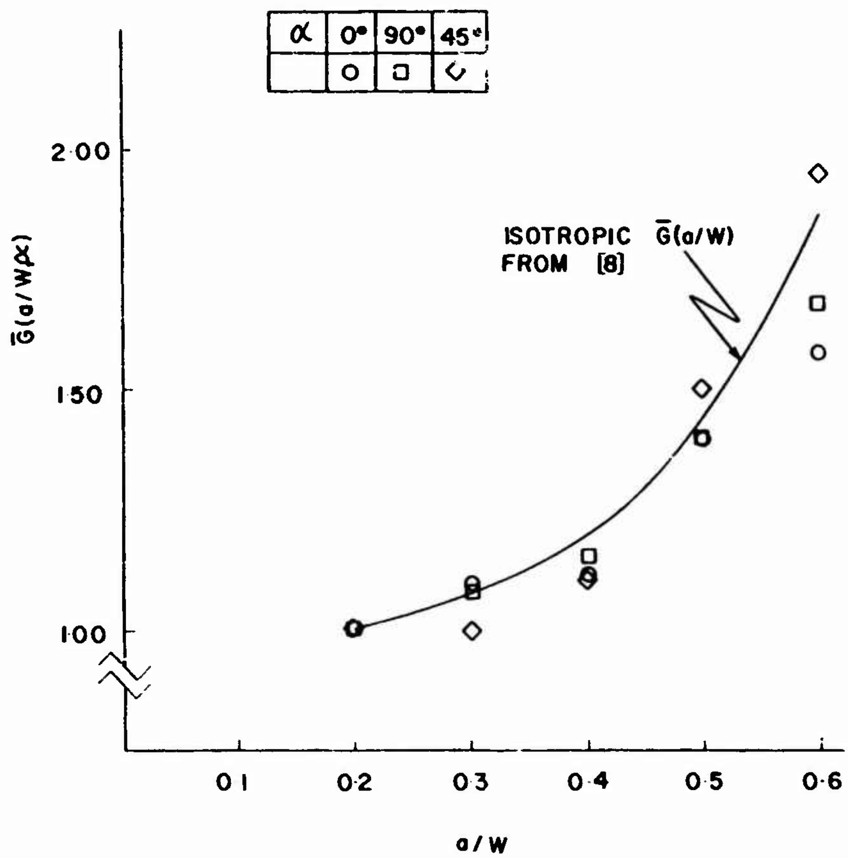

Figure 2: A plot of $\bar{G}(a/W,\alpha)$ vs. a/W. The degree of correspondence between the discrete points (obtained numerically) and the continuous curve (obtained from [8]) is a measure of the applicab.lity of an anisotropic continuum analysis [4] to advanced fiber composite materials.

2.2 *EXPERIMENTAL INVESTIGATION OF FRACTURE IN AN ADVANCED FIBER COMPOSITE*

2.2.1 *Introduction*

Linear elastic fracture mechanics (LEFM) is now accepted as the rationale for characterizing crack toughness of materials that are ostensibly homogeneous and isotropic, the outstanding examples being a wide range of metallic alloys. The basic experience that supports this approach is that presence of a macro crack dominates the response of a structure to remote loading. With the advent of advanced fiber composites, however, there arises the question of the degree of homogeneity of the structure surrounding the crack that is necessary for LEFM to be applicable. In particular, there is concern over whether heterogeneity and anisotropy will preclude practical use of LEFM in composites.

Vigorous discussion of this issue is important and widespread, but the interchanges so far have tended to be theoretical and even speculative. In an effort to supply some physically based information, a pilot series of experiments has been performed, to answer two specific questions:

1. If a cracked, composite specimen is loaded to failure, is the path of crack prolongation determined by the geometry of the initial crack and the loading, or by material orientation?

2. Can LEFM, suitably modified to account for material anisotropy, be usefully applied to composites?

The data now in hand, although limited, indicates that a crack in a composite is at least influential in determining failure patterns and, in many cases, the crack is dominant; furthermore that LEFM provides useful procedures for evaluating crack toughness of composites.

This section gives a brief review of the test procedures, methods of data reduction, and experimental results. Observations made during the course of the tests are reported, and failure surfaces are shown. Analytical work stimulated by these results is underway and will be reported subsequently.

2.2.2 *Test Procedures; Program*

It was obvious from the objective of the test program that the test procedures should follow those developed within the framework of conventional fracture mechanics. There is, in fact, a wealth of literature on this subject including an ASTM Tentative Method [1] and extensive interpretation of it (see, e.g., [2,3]). Departures from the specifications in [1] were minimal and were dictated either by the special nature of the material under test or by simple practicality.

The three-point bend specimen prescribed in [1] was chosen largely to bypass problems associated with gripping the test piece. (See Figure 1.) In the extensive data base that now exists for metals testing, results for this configuration compare well to those for other geometries so that, among other matters, there was no reason to expect that the bearing load opposite the crack front should influence unduly the processes of crack prolongation. In fact, the data reduction scheme in [1] accounts for such details of specimen geometry and load arrangement.

The specimen proportions shown in Figure 1 follow the recommendations in [1] except that the crack front was not sharpened under fatigue loading. Instead, the notch was produced by a sawcut followed by a final lengthening and sharpening using an ultrasonic cutter.

As shown in Figure 2, each specimen was centered on two parallel rollers (1 in dia) whose centerlines were 4 in apart. A third parallel roller was then located directly above the crack, and the specimen was loaded vertically downward. Testing was performed in an Instron machine of 10,000 lb capacity, and cross-head motion was set at 10^{-2} in/min to minimize dynamic effects. Load and cross-head motion were monitored during each test and then cross-plotted to give the basic data for later reduction. While the requirement of [1] is to record crack-mouth opening by means of a special clip gauge, both the basic linearity of material response and the rigidity of the test machine, relative to the specimen, seemed to make this degree of fidelity to [1] unnecessary for the pilot test series.

The program involved twenty-three specimens, thus allowing for two reproducibility tests, and for the testing of both uni- and multi-directional laminates having a range of starter crack lengths. The material used was a NARMCO graphite-epoxy with Morganite II fibers in 5206 resin.

Reproducibility was evaluated by testing two sets of five specimens, each set of the same lay-up and geometry. The first set was a uni-directional laminate ($\alpha = 0°$) and had an initial crack length of 0.4 in. The second set was multi-directional ($\alpha = (0°/\pm45°/90°)_s$) and had the same starter crack length. Single tests were run for $\alpha = 0°, 45°, 90°$; $(\pm45°)_s$; and $(0°/\pm45°/90°)_s$. Starter crack lengths were 0.2, 0.4, and 0.6 in, the shortest of which was less than the requirements in [1]. Such specimens were included to permit evidence of material dominance to develop.

2.2.3 *Data Reduction; Results*

A typical load-cross-head displacement trace is reproduced in Figure 3. There is an initial region of increasing slope during which slack in the load train is taken up, and bearing surfaces under the loading rollers develop. This is followed by a linear region in which the specimen deforms elastically. A third region of decreasing slope then begins as a result both of nonlinear load-displacement behavior and of damage initiation. Finally the load peaks and falls off as the test piece breaks in two.

In order to differentiate the nonlinear effects from those ascribable to damage, the Tentative Method prescribes the following data reduction scheme.[1] The slope M_o of the linear portion of the curve is identified, and a line of slope 5% less than M_o is drawn as shown in Figure 3. This line intersects the curve at a load termed P_S. If P_S is the greatest load withstood by the specimen to that point in the test, P_S is set equal to P_Q. If any load maximum precedes P_S, then P_Q is equated to that maximum value. In either case, the experience in metals testing has shown P_Q to correspond reasonably well to the point of failure initiation. In the absence of a suitable data base for composites, this procedure was used to find P_Q; the data obtained is thus surely consistent and probably conservative. Together with specimen geometry, P_Q is then used to compute K_Q, the critical stress intensity or candidate fracture

[1]It should be borne in mind that the present discussion is but an abstract of a most explicitly defined procedure; the interested reader is urged to consult [1] for complete details.

toughness.[2] See [2,3].

For each laminate, the K_Q values were averaged to give $\overline{K}_Q$ which, in turn, was used to find a critical strain energy release rate G_Q — see [3,4]. The results are shown in Table I. Also of interest are the failure surfaces, depicted in Figures 4-8; a specimen that did not part fully is shown in Figure 9.

2.2.4 Discussion

At the outset, two questions were posed regarding the utility of LEFM in characterizing fracture of composites. The first concerns paths of crack prolongation; the answer may be inferred from inspection of the failure surface. The second involves use of LEFM as a data reduction scheme; the answer to this question comes from physical measurements.

The appearance of the failure surfaces suggests that, in the main, the crack and loading dominate fracture. In Figure 4 (specimens for which $\alpha = 0°$), the path of crack growth is observed to be roughly coplanar with the starter crack. Note that in the case of the longest crack ($a = 0.6$ in), where a longitudinal secondary crack formed, the path is generally forward, Indeed, the crack seems to have made a series of sharp turns to regain its coplanar path.

It is not surprising, on the other hand, to see that, in the $\alpha = 45°$ specimens, the crack grew along a plane containing no fibers. This is clear in Figure 5 and, although fracture occurred as the result

[2]In metals testing, certain additional steps are taken to establish the validity of an individual test result. Since these steps necessitate use of the yield stress, they cannot be followed in this work. Thus only *candidate* values of fracture toughness, or K_Q, are reported. The data cannot be presumed to give K_{Ic} for these materials because compliance with the strict requirements of [1] are definitionally impossible.

of crack propagation (in the matrix), the mode is a mixture of opening and sliding [3]. More sophisticated instrumentation would have permitted articulation of the relative presence of each mode, but such instrumentation was not used in this program.

Forward crack growth is evident for the $\alpha = 90°$ specimens as depicted in Figure 6. Growth again was along a plane containing no fibers which, in this case, is coplanar with the starter crack.

During testing the uni-directional specimens described above emitted popping noises prior to failure. Because the fracture process also involved matrix breaking of one sort or another, the two phenomena are believed to be related. Even in the $\alpha = 0°$ specimens, the crack appears at the outset to have operated on virtually independent fiber bundles as they pulled out from the matrix. The resulting failure surfaces are very rough for the early stages of growth but then become more nearly uniform. The noise levels for the remaining specimens were much lower, and their failure surfaces are less suggestive of matrix cracking.

Figure 7 is instructive in that it shows for the $\alpha = (\pm 45°)_s$ test pieces an increasing crack dominances as the starter crack is made longer. For a = 0.2 in, the crack path almost immediately turns 45° from its initial orientation, there being but a slight indication of forward growth. A greater tendency toward coplanar growth is apparent when a = 0.4 in, and crack dominance is manifest when a = 0.6 in. Crack growth is not possible on a plane containing no fibers — there being none by virtue of the lay-up — and some zig-zagging is apparent. This group of specimens thus shows a transition from some material dominance where the starter crack is shorter than required by the Tentative Method to a fracture pattern fully dominated by the starter crack, as the length of the starter crack occurs.

Crack dominance is also clear in Figure 8, which shows failure surfaces for $\alpha = (0°/\pm45°/90°)_s$. In these specimens, the crack moved in its own plane but apparently grew further in the interior of the test piece than on its surface. An indication of this behavior, not uncommon in metals testing, is shown in Figure 9.

The use of K_Q to characterize behavior of these specimens appears, on the whole, to be warranted. The reproducibility tests on the $\alpha = 0°$ specimens[3] and the $\alpha = (0°/\pm45°/90°)_s$ specimens were satisfactory. Load-displacement traces are shown in Figures 10 and 11, and the average K_Q values found are

$$\alpha = 0° \quad : \quad K_Q = 28.8 \times 10^3 \text{ lb/in}^2\sqrt{\text{in}} \quad {}^{+0.4\%}_{-5.5\%}$$

$$\alpha = (0°/\pm45°/90°)_s \quad : \quad K_Q = 21.7 \times 10^3 \text{ lb/in}^2\sqrt{\text{in}} \quad {}^{+1.7\%}_{-3.2\%}$$

The scatter is not unlike that found in metals testing. For three laminates, the data are fairly consistent with values obtained independently by Halpin [5] ($25\text{-}28 \times 10^3$ lb/in$^2\sqrt{\text{in}}$, $\alpha = (0°/\pm45°/90°)_s$) and by Weiss [6] ($31 \times 10^3$ lb/in$^2\sqrt{\text{in}}$, $\alpha = 0°$; 19×10^3 lb/in$^2\sqrt{\text{in}}$, $\alpha = (\pm45°)_s$) using other specimen geometries (shape and thickness) and load arrangements.

Inspection of Table I will show further that the K_Q values for various starter crack sizes are within a reasonable range of the average $\overline{K}_Q$ for each laminate. It should also be noted that the majority of largest deviations occur for subsize starter cracks, and none of these is serious.

---

[3]One exception occurred for the $\alpha = 0°$ specimen set; because it was the first specimen of the entire series tested, it is presumably due to lack of experience with the test procedure, rather than material variation.

2.2.5 *Conclusions*

This pilot test series has been successful, for it has answered the questions posed at the outset. The failure mechanism of the specimen tested is crack dominated in most cases, and the procedures of LEFM can be applied even where the overt failure mechanism is not so obviously dominated by the starter crack.

There remains, however, a variety of questions about cracks in an advanced fiber composite material. Some concern the effects of specimen geometry and load arrangement, and can be answered only by further testing. Such work is needed, first, to define and delineate more fully the respective influence of cracks and material. Further, the entire matter of fracture in composites needs for its resolution an extensive data base similar to that which has evolved for metals. The building of this kind of experience is important not only to determine what constitutes meaningful laboratory work, but also to provide guidance in treating service situations. Experimentally determined K_Q values for given laminates might also be relat to the properties of individual laminae within other laminates. Ultimately, the designer should be in a position to use fracture toughness as he would other material properties.

It would now appear that efforts to address these questions are warranted, for the present test series indicates that, when suitably modified to account for anisotropy, linear elastic fracture mechanics may usefully be applied to advanced fiber composite materials.

2.2.6 References

[1] Tentative Method of Test E 399 for Plane-Strain Fracture Toughness of Metallic Material, *1971 Annual Book of ASTM Standards*, Part 31, American Society for Testing and Materials, Philadelphia (1971).

[2] J. E. Srawley and W. F. Brown, Jr., *Plane Strain Crack Toughness Testing of High Strength Metallic Materials*, ASTM STP 410, American Society for Testing and Materials, Philadelphia (1967).

[3] *Fracture Toughness Testing and its Applications*, ASTM STP 381, American Society for Testing and Materials, Philadelphia (1965). (n.b. p. 52 et seq.)

[4] G. C. Sih, P. C. Paris, and G. R. Irwin, "On Cracks in Rectilinearly Anisotropic Bodies", *International Journal of Fracture Mechanics* 1 (1965) 189-203.

[5] J. C. Halpin, U. S. Air Force Materials Laboratory, private communication, 1971.

[6] O. E. Weiss, Convair Aerospace Division, General Dynamics Corporation, Fort Worth, private communication, 1971.

TABLE I

EXPERIMENTAL RESULTS

fiber orientation angle, α	K_Q, $lb/in^2\sqrt{in} \times 10^3$ a = 0.2 in	a = 0.4 in	a = 0.6 in	$\bar{K}_Q$, $lb/in^2\sqrt{in} \times 10^3$	G_Q, in lb/in^2
0°	— [1]	28.8	36.3	32.6 +11% -11%	117.
90°	1.66	1.46	— [2]	1.56 +6.3% -6.3%	0.943
45°	0.690 [3]	2.22	2.39	2.30 +3.9% -3.8%	— [4]
$(\pm 45°)_s$	18.5	18.5	16.3	17.7 +4.8% -9.4%	45.0
$(0°/\pm 45°/90°)_s$	23.5	21.7	20.5	21.9 +7.3% -8.6%	55.1

Notes:

1. Specimen was crushed before crack propagation occurred.
2. Instrumentation failure.
3. This value omitted when calculating $\bar{K}_Q$.
4. No G_Q available because the crack propagated in a mixed mode, which could not be directly uncoupled.

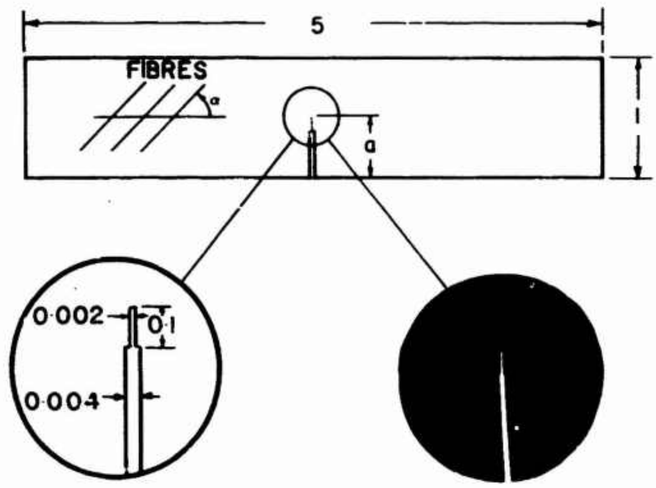

Figure 1: Three-point bend specimen geometry, with crack shape shown in inserts, both schematic (left) and actual (right). Fiber direction given by α, crack length by a. Specimen thickness 0.5 in (nom); all dimensions given in inches.

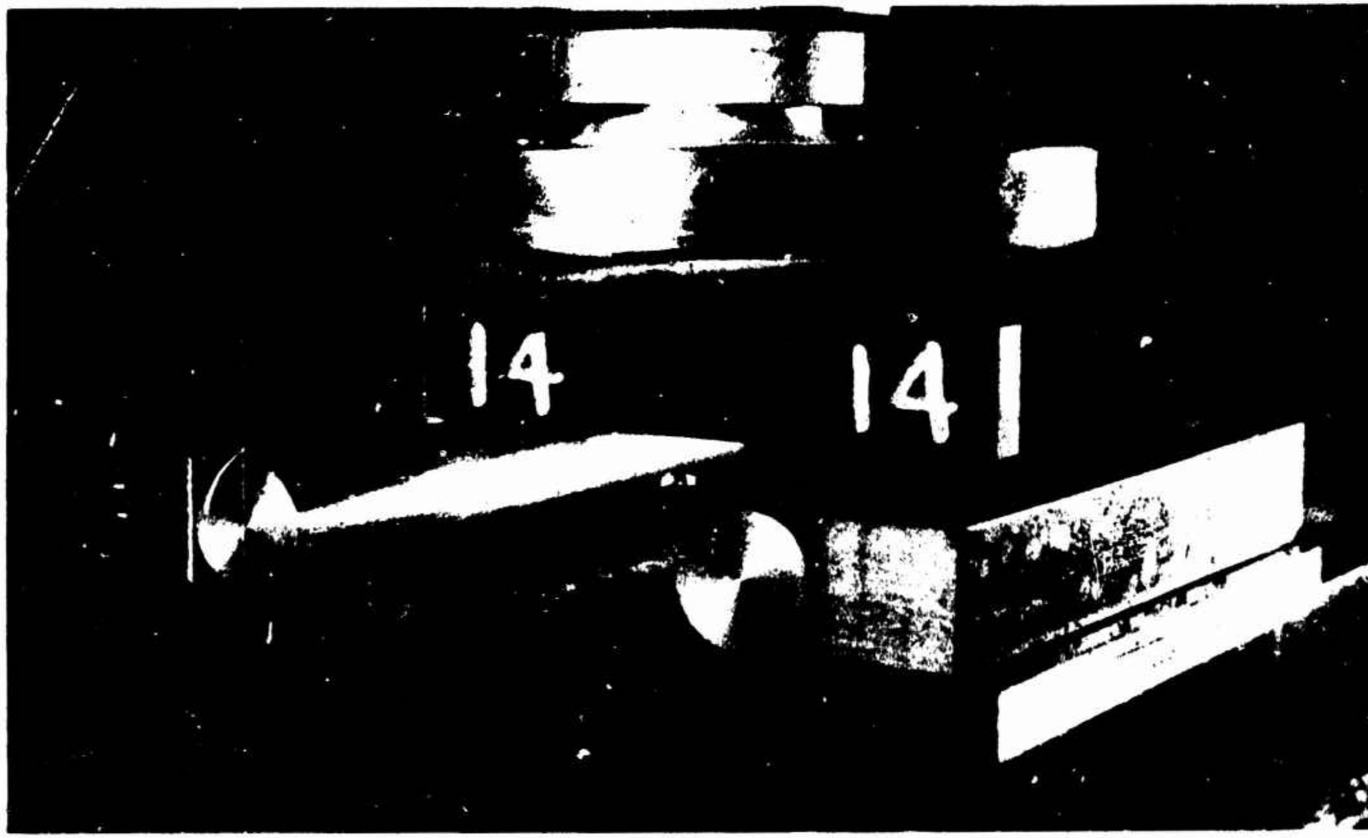

Figure 2: Test jig at beginning of loading.

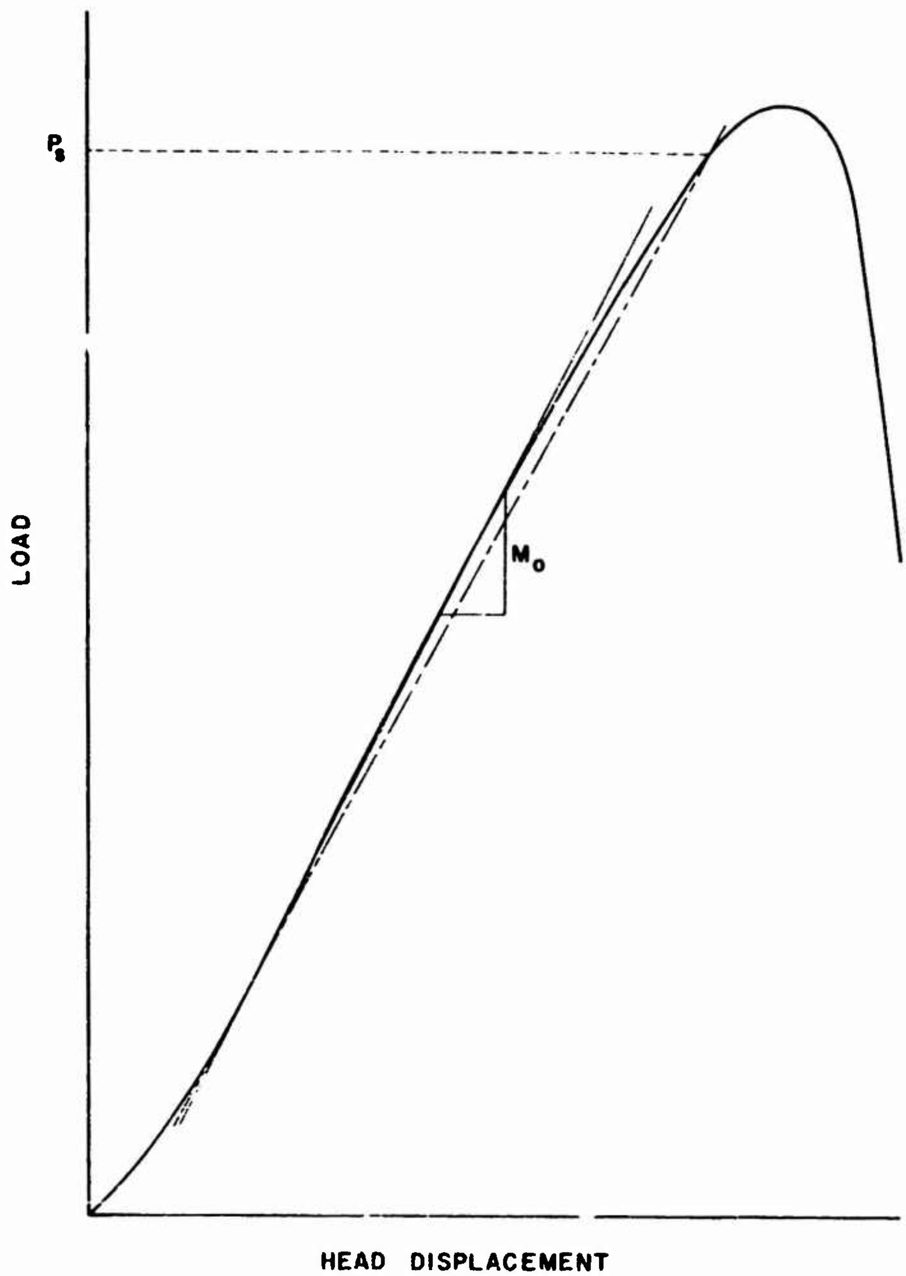

Figure 3: Typical trace of load applied to specimen vs. cross-head displacement, showing method used to determine P_S.

Figure 4: Failure surfaces for $\alpha = 0°$ specimens of three starter crack lengths ($a = 0.6, 0.4, 0.2$ in).

Figure 5: Failure surfaces for $\alpha = 45°$ specimens of three starter crack lengths (a = 0.6, 0.4, 0.2 in).

Figure 6: Failure surfaces for α = 90° specimens of three starter crack lengths (a = 0.6, 0.4, 0.2 in).

Figure 7: Failure surfaces for $\alpha = (\pm 45°)_s$ specimens of three starter crack lengths (a = 0.6, 0.4, 0.2 in).

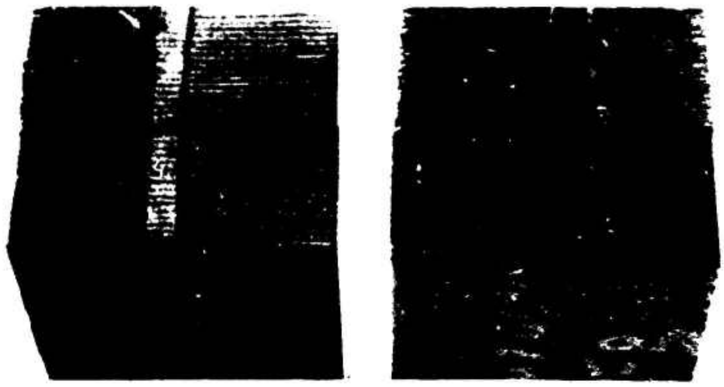

Figure 8: Failure surfaces for $\alpha = (0°/\pm45°/90°)_S$ specimens of two starter crack lengths (a = 0.6, 0.4 in).

Figure 9: Failed but unbroken specimen ($\alpha = (0°/\pm45°/90°)_S$, a = 0.2 in).

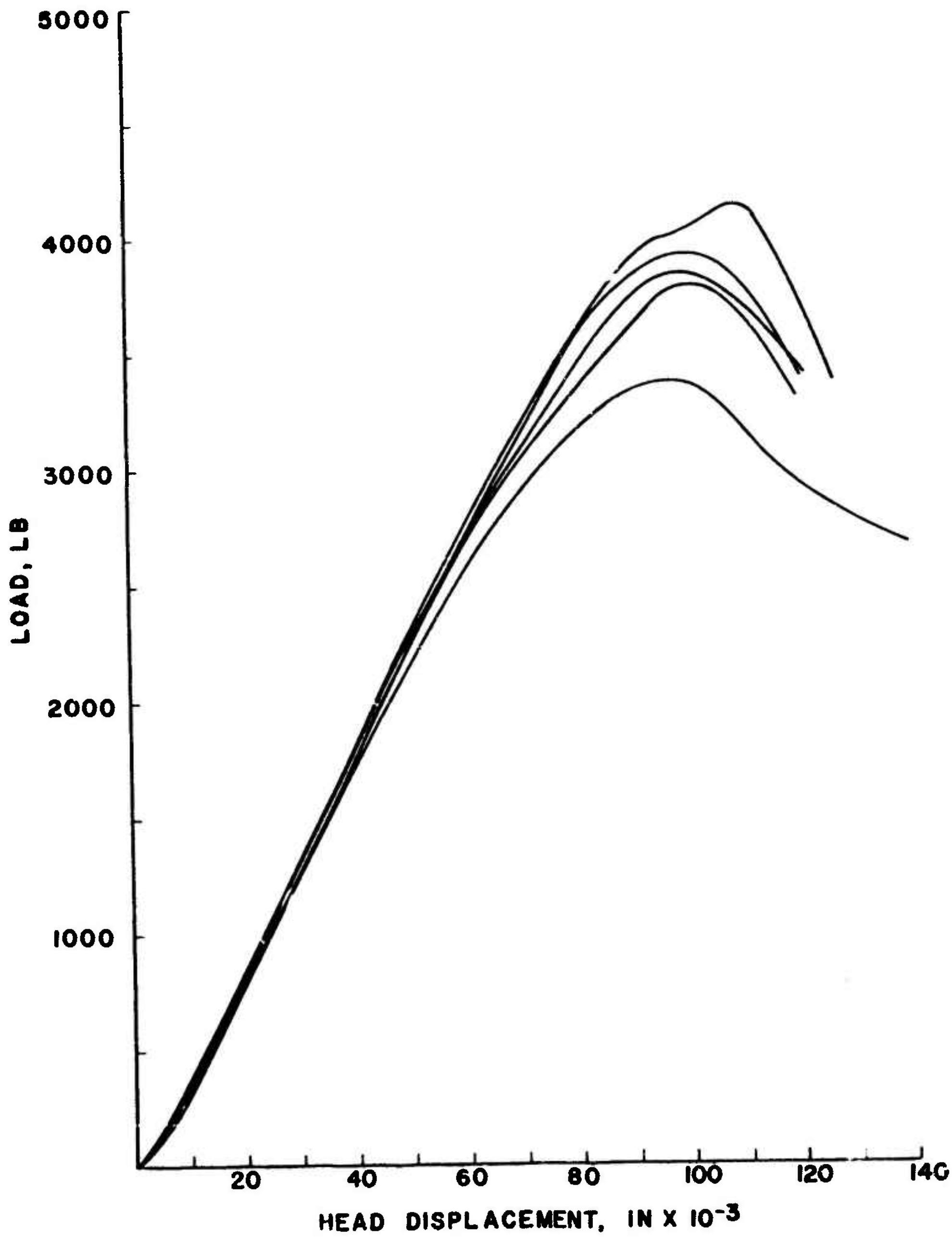

Figure 10: Traces of load vs. cross-head displacement for five specimens used in reproducibility tests for a uni-directional laminate ($\alpha = 0°$, $a = 0.4$ in).

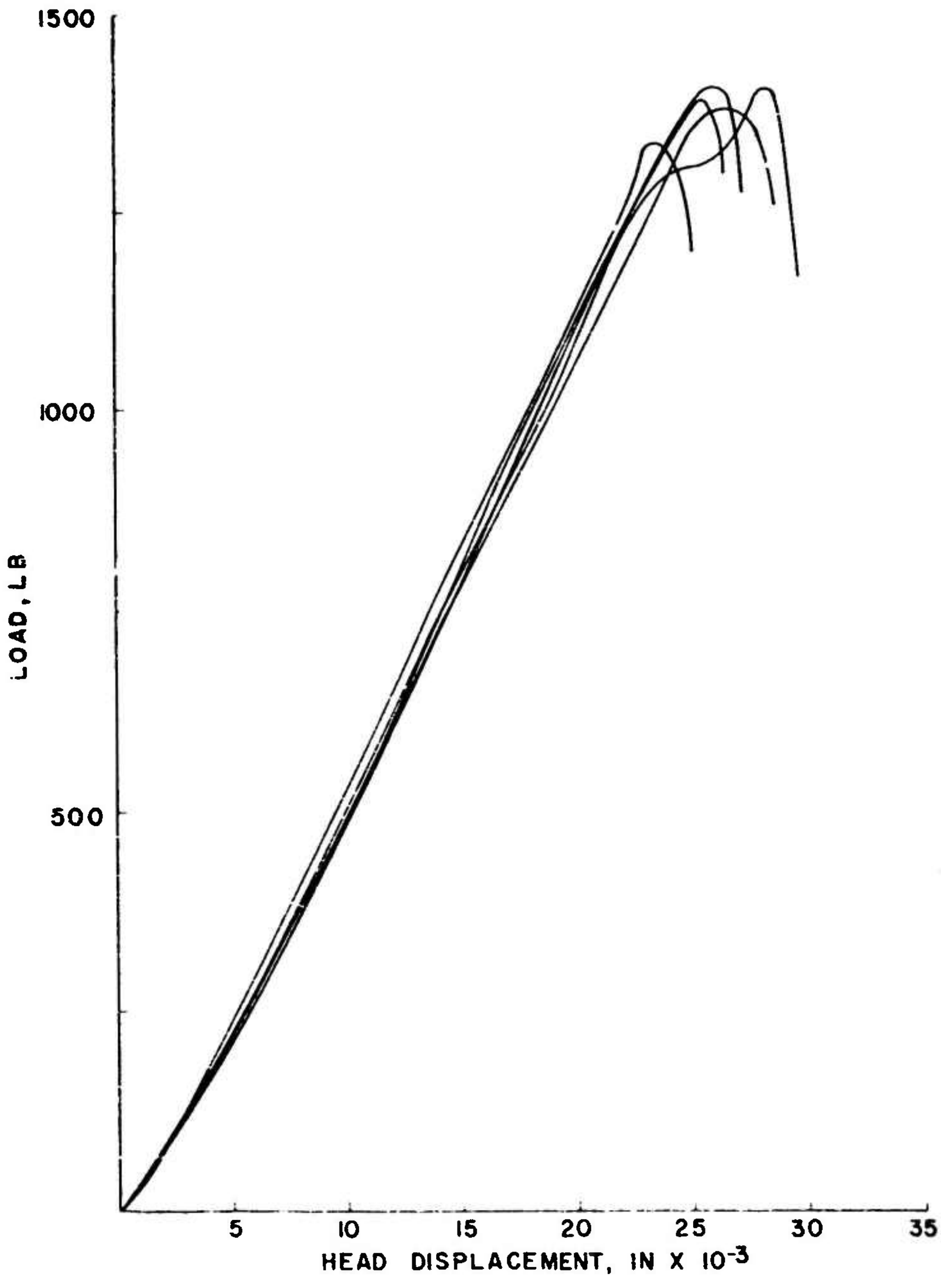

Figure 11: Traces of load vs. cross-head displacement for five specimens used in reproducibility tests for a multi-directional laminate ($\alpha = (0°/\pm45°/90°)_s$, a = 0.4 in).

CHAPTER III

STRENGTH OF MECHANICALLY FASTENED JOINTS

3.1 AN INVESTIGATION OF STRESS CONCENTRATIONS INDUCED IN COMPOSITE BOLT BEARING SPECIMENS

3.1.1 Introduction

This study is concerned with materials which consist of parallel, high strength fibers supported in a relatively ductile matrix material. The fibers act as load carriers while the matrix serves principally as a load transfer medium. In particular, it is concerned with advanced fibers, such as boron or graphite, in an epoxy matrix.

Because of their superior specific strength and specific stiffness, advanced fiber composite materials have a vast potential in the aerospace industry. Lamina, which are single layers of parallel fibers surrounded by the matrix material, are stacked at various orientations relative to one another to form a laminate. This procedure enables the designer to achieve desired strength and stiffness properties and to increase the structural efficiency of a given amount of material.

The strength and stiffness properties, however, are highly directional; panels fabricated out of layers of unidirectional composite tape are anisotropic. The designer therefore has the difficulty of including the effects of this anisotropy in his calculations.

One particular problem area in a structure made of composite materials is the bolted joint. The bolted joint in a composite material has a significantly lower efficiency than the same joint in metals. Furthermore, the composite joint may fail in unique modes not found in metal joints.

This study, therefore, investigates the stress concentrations induced in anisotropic plates loaded by means of a single fastener hole. The study is an attempt to further understand the failure characteristics of such bolted joints. The development of a prediction capability for both the failure mode and ultimate load is the major goal of the early part of this work. Such a capability would allow synthesis rather than analysis to be used in the future design of fastener joints. An implied goal in this study is an evaluation of the three proposed anisotropic failure criterion; maximum stress, maximum strain, and distortional energy.

3.1.2 Analysis Method

A constant strain, finite element computer program using triangular elements was modified to handle anisotropic composite materials using lamination theory as presented in [1]. The experimental work done on bolt bearing specimens, from which this study draws heavily, only considered cross-plied laminates which were mid-plane symmetric. As a result, this numerical study is also limited to this class of laminates. It is important to remember that the use of lamination theory ignores interlaminar shear; consequently, it is expected that the degree of error in the results will vary with specimen anisotropy.

The design of a finite element grid representation to simulate the bolt bearing test specimen was subject to two major considerations First, the grid had to be sufficiently detailed around the bolt hole to pick up the large stress gradients which are induced in this area. Secondly, the number of elements and nodes was restricted by the storage capacity of the computer. Taking advantage of the two lines of specimen symmetry shown in Figure 1 only one-fourth of the specimen was included in the finite element simulation. Figure 2 shows a computer plot of the specimen section for e/d = 5.0, s/d = 10.0, and ℓ/d = 20.0. The grid representation used contains 480 elements and 279 nodes. The conditions of specimen symmetry are met by forcing the x-displacement of the vertical line of symmetry and the y-displacement of the horizontal line of symmetry to be zero in each computer run. A computer subroutine was also developed which transforms the co-ordinates of the grid shown in Figure 2 to any desired specimen geometry, i.e., e/d, s/d, ℓ/d.

To check whether or not the grid was sufficiently detailed around the hole an isotropic test case and several anisotropic test cases were run. A uniform tension stress was applied to the ends of each specimen. Comparison with the isotropic results presented in [2] (See Figures 3a and 3b) and the anisotropic results of [3] indicated that further refinement of the finite element mesh around the hole was not necessary. The observation that the computed finite element values of stress are higher than the exact values agrees well with the results illustrated in [4].

A cosine distribution of normal stress acting over the upper half of the hole surface was used to simulate the resulting stress distribution caused by the bolt. The interaction was, therefore, assumed to be frictionless. Bickley [5] shows this to be an excellant approximation for isotropic bolt bearing specimens. A finite element analysis of the bolt-specimen interaction in certain composite laminates was performed at General Dynamics [6]. The cosine distribution of normal stress was again shown to be a realistic approximation of the interaction stresses.

Further confidence was gained in both the cosine distribution and the grid mesh by running an isotropic bolt bearing test problem and observing the qualitative agreement of the computed stress field around the hole surface (See Figure 4) with work by Coker and Filon [7]. The specimen used in their study had significantly larger values of e/d and s/d and thus a quantitative comparison was not possible.

Finally, two other normal distributions of stress, which were significantly different from the cosine distribution (See Figure 5), were used as the bolt-specimen interface stress boundary condition for one of the composite material specimen runs.

The net force in the load direction in each case was equivalent. It was observed that significant variance about the cosine distribution resulted in insignificant alterations of the calculated stress fields for the specimen considered.

3.1.3 Strength and Failure Mode Predictions

The selection of specimen geometries for this investigation was made from data which has been published by General Dynamics [8,9] and Grumman Aerospace [10]. Included were two net-tension failure specimens, two shear-out failure specimens, one bearing failure specimen and one specimen which exhibited failures in a transition region between a net tension and combination failure mode. See Figure 6 for illustrations of these various failure modes.

Performing a strength analysis on a laminated composite material may be based on the strengths of its individual lamina. The strength of a single orthotropic lamina can, in theory, first be determined experimentally, producing an ultimate strength envelope for that material. This three dimensional surface (in terms of principal lamina stresses) could then be used to analytically predict the ultimate strength of the total laminate. The state-of-the-art has yet to reach this level of sophistication. The present three dimensional ultimate strength envelope is constructed using only five points on the stress axes due to the, as yet, unsolved problems encountered in off-axis testing.

The Hill failure criterion is a widely accepted representation of this three dimensional envelope; it has been found in this study to be the only reliable means of predicting bolt bearing specimen failure modes. As shown in [11] lamina failure is predicted to occur when the following set of principal stress ratios (normalized on their respective ultimate stresses) add to a number, DIST, greater than or equal to one.

$$\mathrm{DIST} = \left(\frac{\sigma_1}{\sigma_{1_u}}\right)^2 + \left(\frac{\sigma_2}{\sigma_{2_u}}\right)^2 + \left(\frac{\tau_{12}}{\tau_{12_u}}\right)^2 - \left(\frac{\sigma_{2_u}}{\sigma_{1_u}}\right)\left(\frac{\sigma_1}{\sigma_{1_u}}\right)\left(\frac{\sigma_2}{\sigma_{2_u}}\right) \qquad (1)$$

Figures 7 through 10 are plots of DIST for typical net tension, shear-out, bearing, and combination failure modes respectively.[1] An initial application of the experimental failure load was used as the applied load for each computer run. The resulting contour plots were sufficient to predict the failure modes in all but the shear-out cases. For these specimens it was sometimes necessary to consider the ratios of lamina principal stresses to their respective ultimate stresses to differentiate between a plug type shear-out mode and a bending, tear-out mode.

---

[1]Figures 7a through 7d represent DIST contour plots of four laminae which compose a net tension failure specimen. A single plot of the major load carrying lamina for each of the other three failure modes is included to illustrate the contour patterns for these various modes.

Prediction of failure load was also made on the basis of the Hill criterion. The values of DIST in the first row of circumferential elements around the hole were considered for each lamina. A successive failure analysis similar to that discussed in [12] was used to predict ultimate load. As soon as an element in any given lamina achieved a value of DIST equal to 1.0 that lamina was assumed to have failed and was locally removed from the laminate. The load was then redistributed among the remaining laminae and all values of DIST were recalculated. If all recalculated values of DIST were less than 1.0 more load was applied until another lamina reached failure. This process was repeated until total laminate failure occurred.

The predictions of failure load based on equation (1) were always conservative. The degree of conservatism varied with failure mode, but more importantly it appeared to be a function of specimen anisotropy. To date only 0°/90°/±45° specimens have been considered. The predicted failure loads for the net tension specimens improve greatly as the percentage of ±45° lamina decreases (See Table 1). For example, for a 100% (±45°) laminate the predicted failure load is about one-half the experimental failure load. For a (±45°/90°) laminate which contains 62.5% (±45°) lamina the predicted failure load is about nine-tenths the experimental failure load. This same type of behavior was reported by Grumman Aerospace [13] in a study they performed on laminate tension data.

The Hill criterion was the only criterion of the three which was conservative in predicting failure load for each specimen investigated. Both the maximum strain failure criterion and the maximum stress failure criterion overpredicted at least one specimen ultimate load. That is, even when the experimentally determined failure load was applied the ratio of principal strains (or stresses) to their respective ultimate strains (or stresses) did not exceed 1.0 as is required by these two criterion respectively.

Investigation of experimentally failed specimens exhibit excellant agreement with predicted failure behavior. For example, specimens which failed according to a slug type shear-out mode exhibited relatively smooth, clear fracture surfaces. The high values of DIST for the shear-out failure mode pictured in Figure 8 are a result of very high principal shear stress ratios in these regions, which would lend to rather smooth shear fracture surfaces. On the other hand, specimens which failed by a bending, tear-out failure mode (which is also considered a shear-out failure mode by some investigators) exhibited a very coarse, jagged fracture surface. This behavior is again expected from the computed stress ratios. Along lines at ±45° in a (0°/90°/±45°) specimen, where the values of DIST are high, the largest stress ratios act in the first principal direction. These are the stresses which are trying to break fibers in tension. As a result, as the triangular section is being torn away from the specimen, fibers along these failure lines at ±45° are being broken in tension; resulting in a very coarse, jagged fracture surface.

Another interesting feature of the experimentally failed specimens was the presence of a highly localized region of laminate destruction at the bolt-specimen interface. It was observed that a bearing failure of variable magnitude had occurred in conjunction with almost every other type of experimental failure mode. This behavior was again predictable as is shown in Figures 7c, 7d, 8, 9 and 10.

3.1.4 Future Work

Three important areas in this analysis where simplifications have been made will be investigated in the future.

1) The effects of interlaminar shear on the stress field near the hole.
2) The significant variation in material properties and ultimate allowables reported in the literature.
3) The non-linear stress-strain response of the composite materials.

The need for reliable off-axis failure data is also critical to the complete understanding of the failure of a composite structure under complicated loading. It is felt that continued investigation of the simple bolt bearing problem will yield further clues as to the mechanisms of failure due to stress concentrations.

It was also felt at the completion of this project that a similar failure analysis could be performed on more complex mechanically fastened joints made of composite materials. Such an investigation has been performed by this investigator and is reported in the next section.

3.1.5 References

[1] J. E. Ashton, J. C. Halpin, and P. H. Petit, *Primer on Composite Materials: Analysis*, Technomic Publishing Company, Stanford, Connecticut (1969).

[2] S. Timoshenko and J. N. Goodier, *Theory of Elasticity*, Second Edition, McGraw-Hill Book Company, 80 (1951).

[3] S. G. Lekhnitskii, *Theory of Elasticity for Anisotropic Elastic Body*, Holden-Day, Inc., 170 (1963).

[4] O. C. Zienkiewicz, *The Finite Element Method*, McGraw-Hill Publishing Company, 38 (1967).

[5] W. Bickley, "The Distribution of Stress Round a Circular Hole in a Plate", Phil. Trans. Roy., Soc., A. (London), 227, 383 (1928).

[6] Advanced Composite Technology, Fuselage Program - Phase I, Second Quarterly Progress Report, General Dynamics, 164-172, (1 November 1969).

[7] E. G. Coker and L. N. G. Filon, *Photo-Elasticity*, Cambridge, 524-530 (1957).

[8] Advanced Composite Technology, Fuselage Program - Phase I, Second Quarterly Progress Report, General Dynamics, 90-110, (1 November 1969).

[9] Advanced Composite Technology, Fuselage Program - Phase I, Third Quarterly Progress Report, General Dynamics, 107-122, (1 February 1970).

[10] Advanced Composite Wing Structures Boron-Epoxy Design Data - Volume II, Grumman Aerospace Corporation, 187-191, (November 1969).

[11] J. E. Ashton, J. C. Halpin, and P. H. Petit, *Primer on Composite Materials: Analysis*, Technomic Publishing Company, Stanford, Connecticut, 26 (1969).

[12] Investigation of Joints in Advanced Fibrous Composites for Aircraft Structures, Air Force Flight Dynamics Laboratory, 13, (June 1969).

[13] Advanced Composite Wing Structures Boron-Epoxy Design Data - Volume II, Grumman Aerospace Corporation, (November 1969).

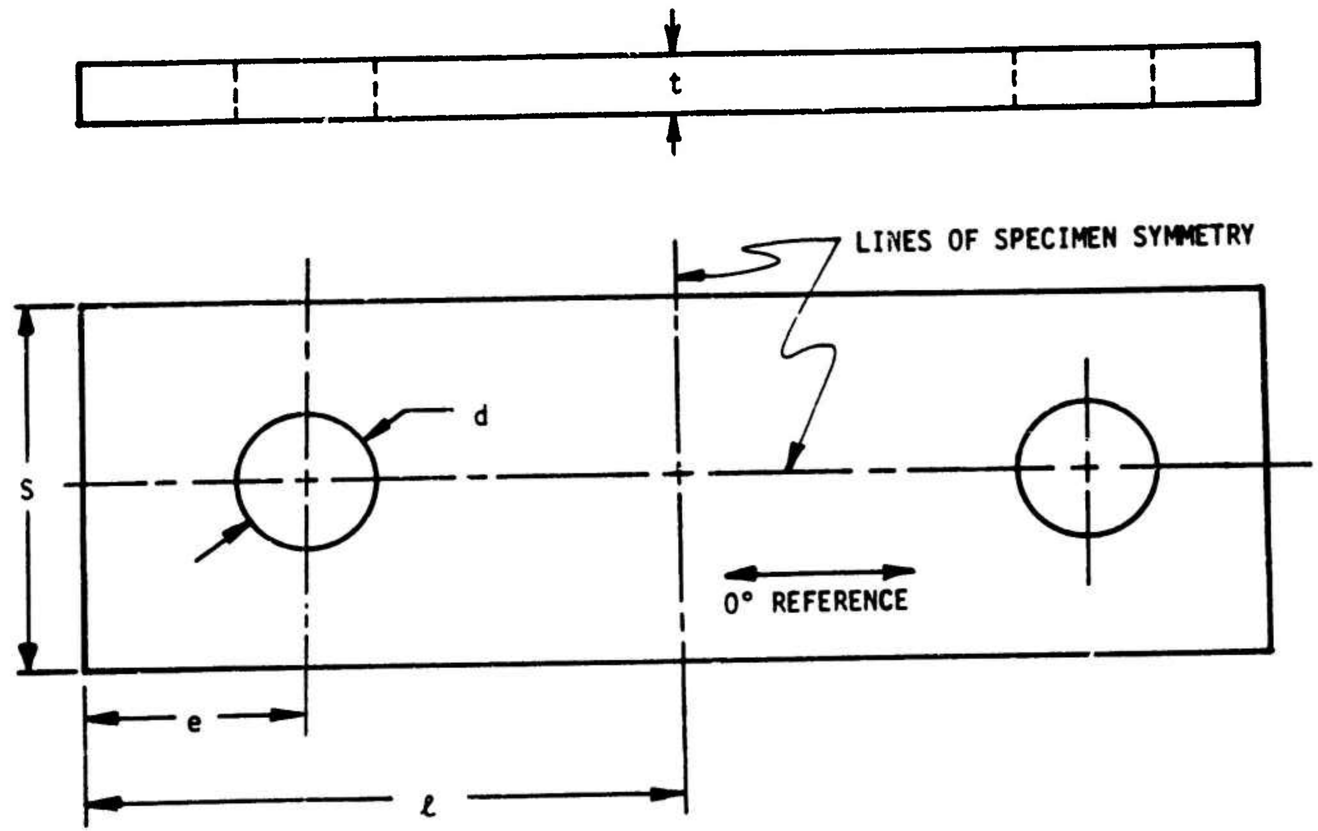

FIGURE 1: BOLT BEARING TEST SPECIMEN

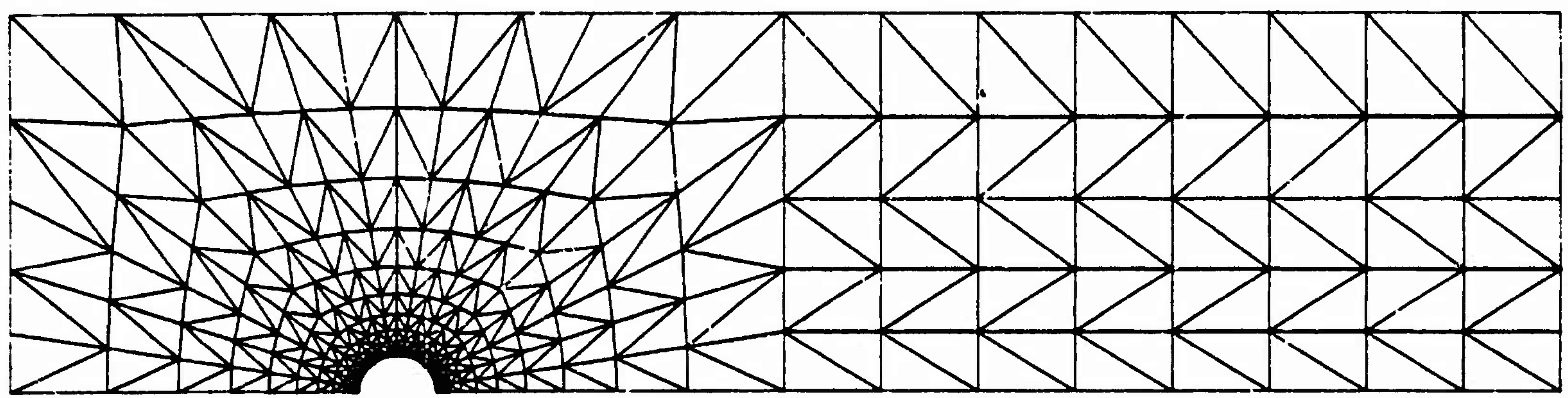

480 ELEMENTS
279 NODES

FIGURE 2: BOLT BEARING GRID REPRESENTATION FOR E/D=5.0, S/D=10.0 & L/D=20.0

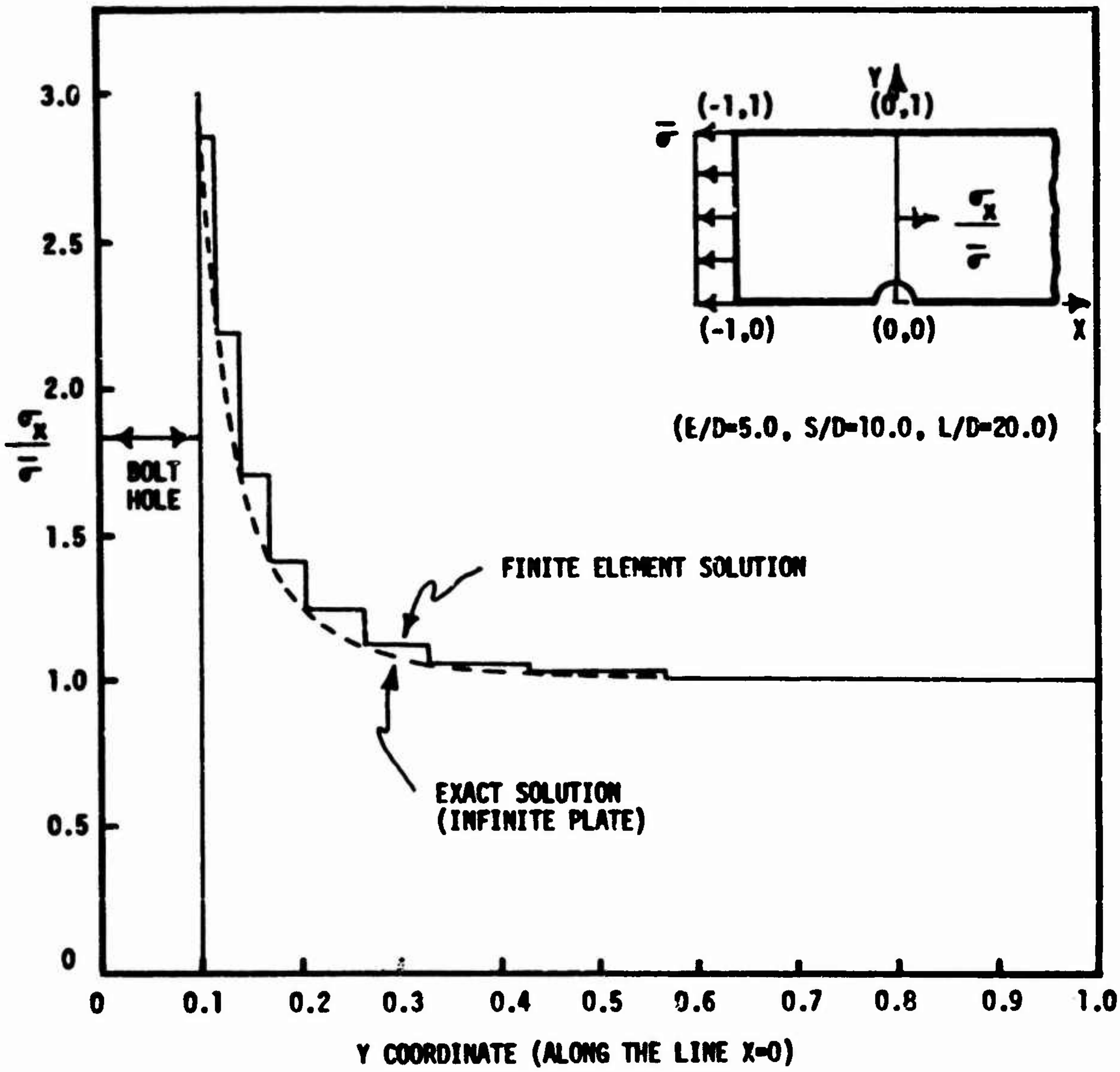

FIGURE 3a: ISOTROPIC BOLT BEARING VERIFICATION: $\sigma_x/\bar{\sigma}$ vs Y

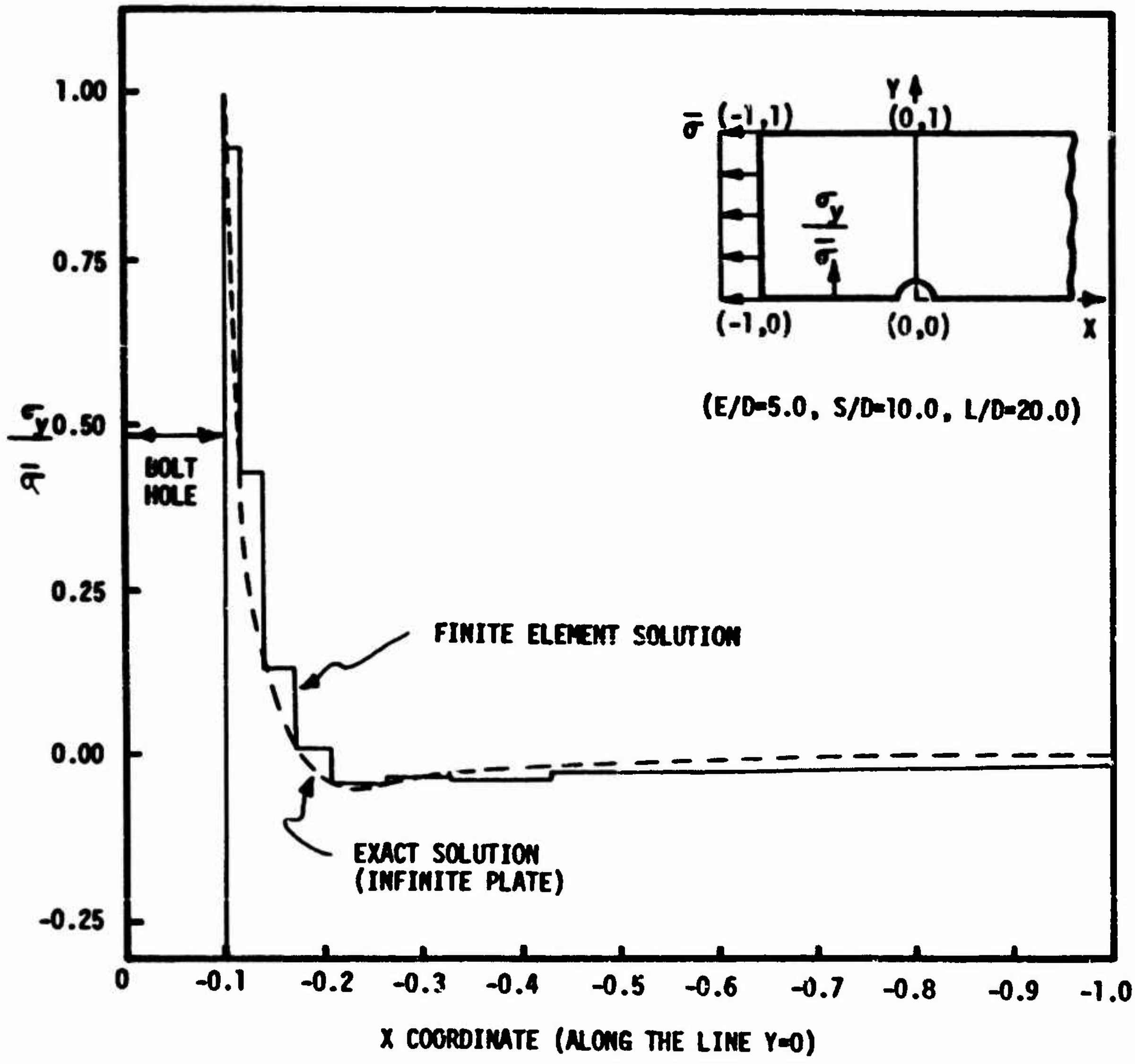

FIGURE 3b: ISOTROPIC BOLT BEARING VERIFICATION: $\sigma_y/\bar{\sigma}$ vs X

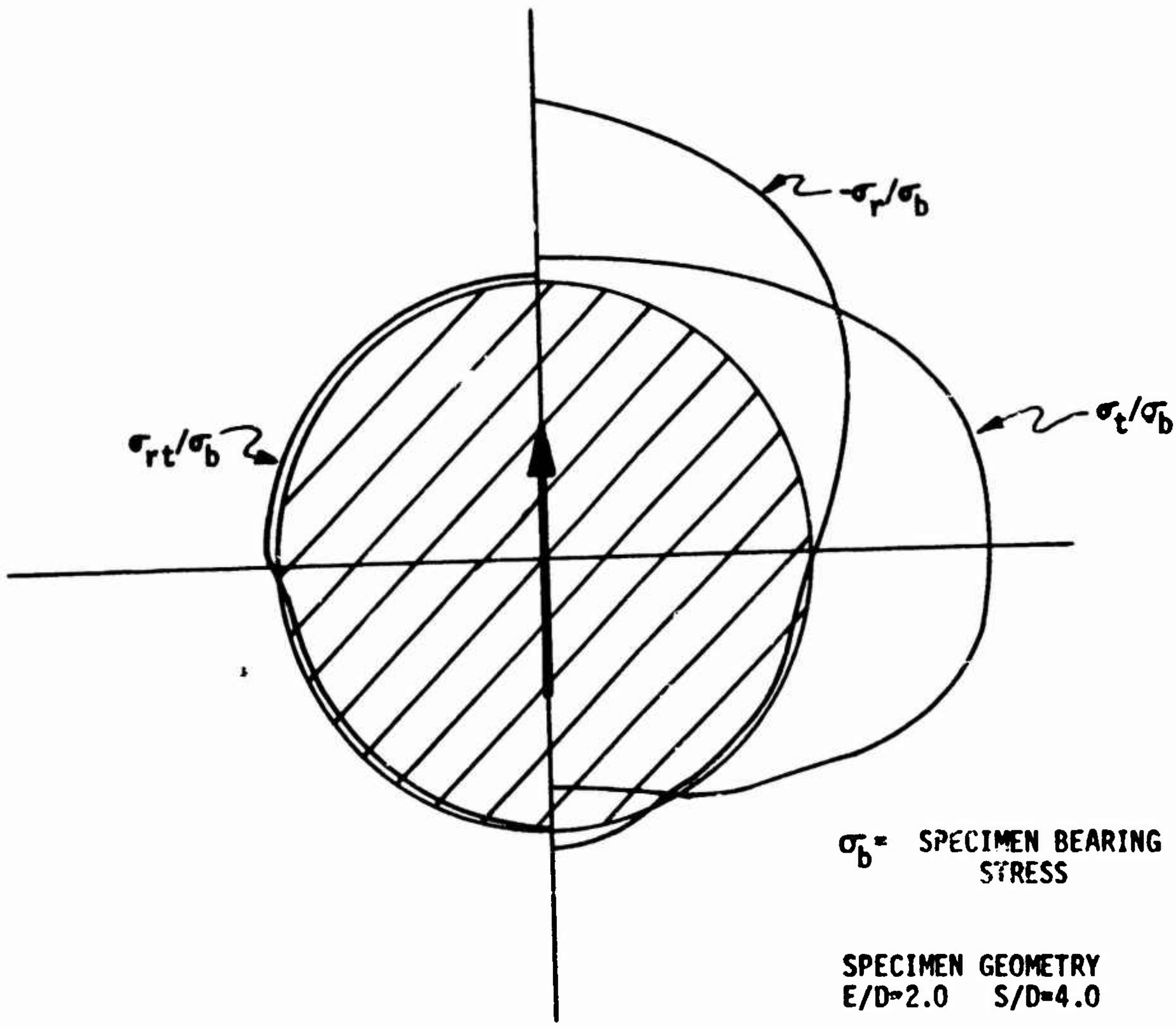

FIGURE 4: POLAR PLOT OF EDGE STRESSES FOR AN ISOTROPIC TEST RUN

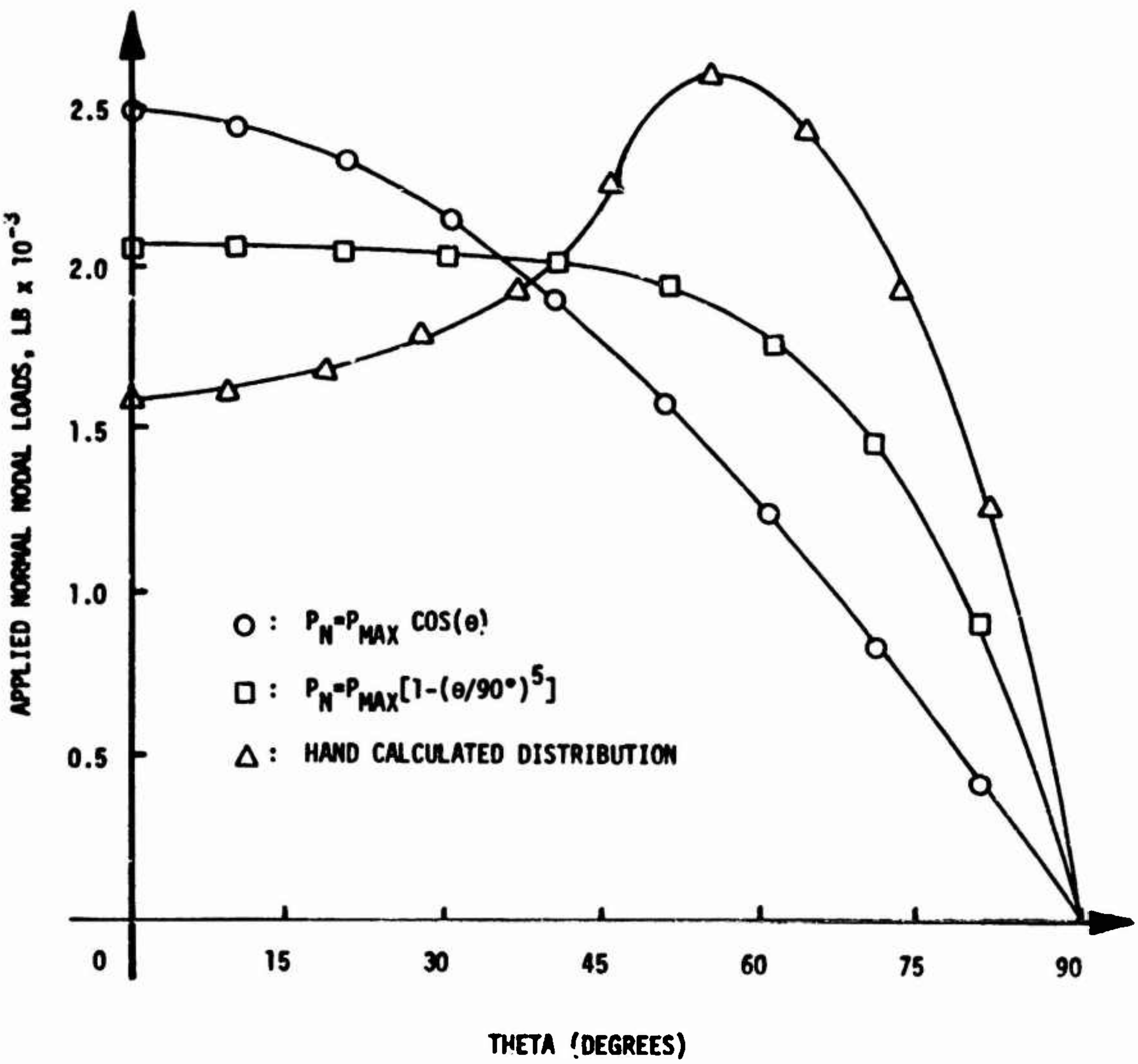

FIGURE 5: VARIATIONS ABOUT THE COSINE DISTRIBUTION OF NORMAL STRESS

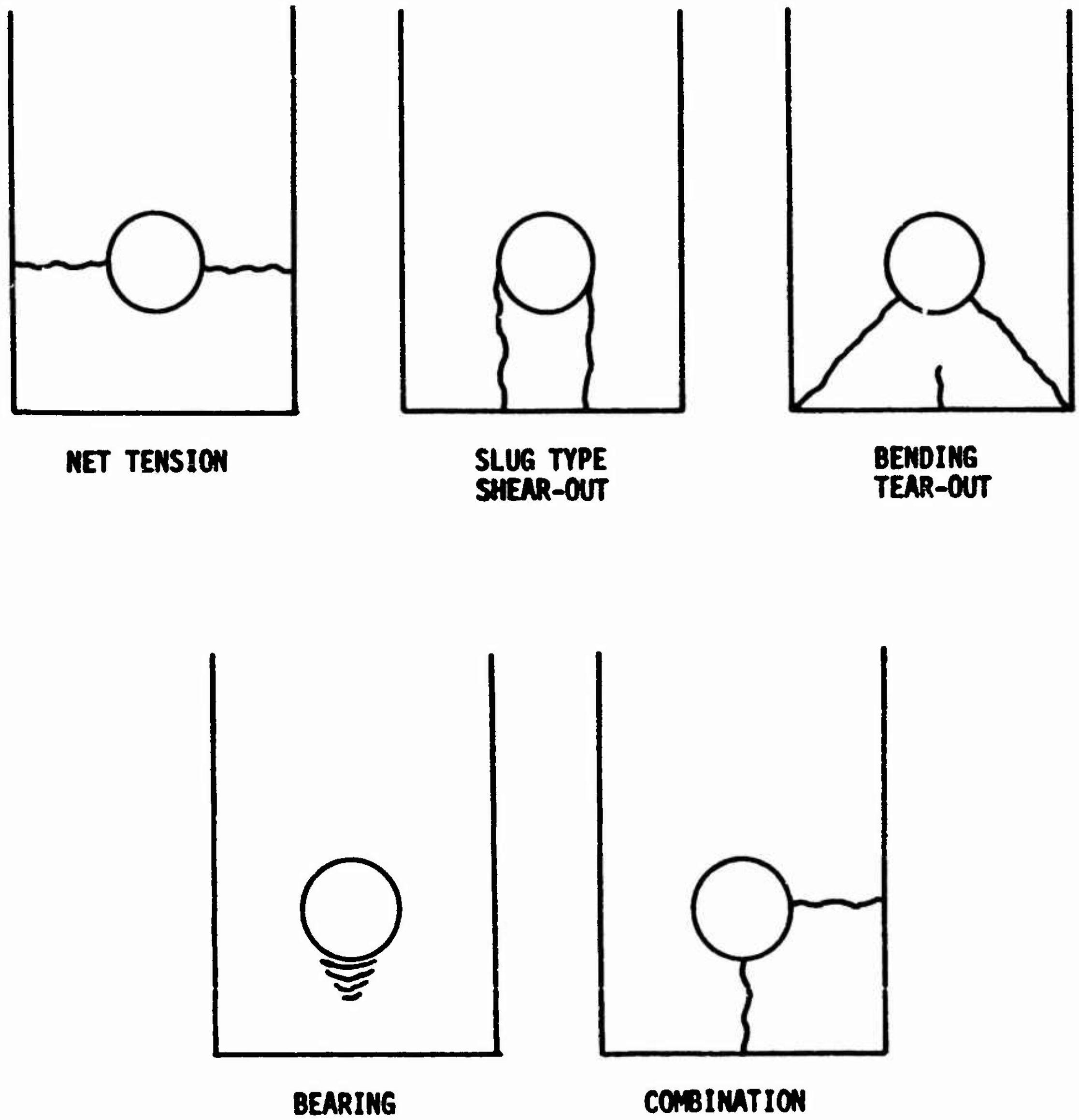

FIGURE 6: BOLT BEARING TEST SPECIMEN FAILURE MODES

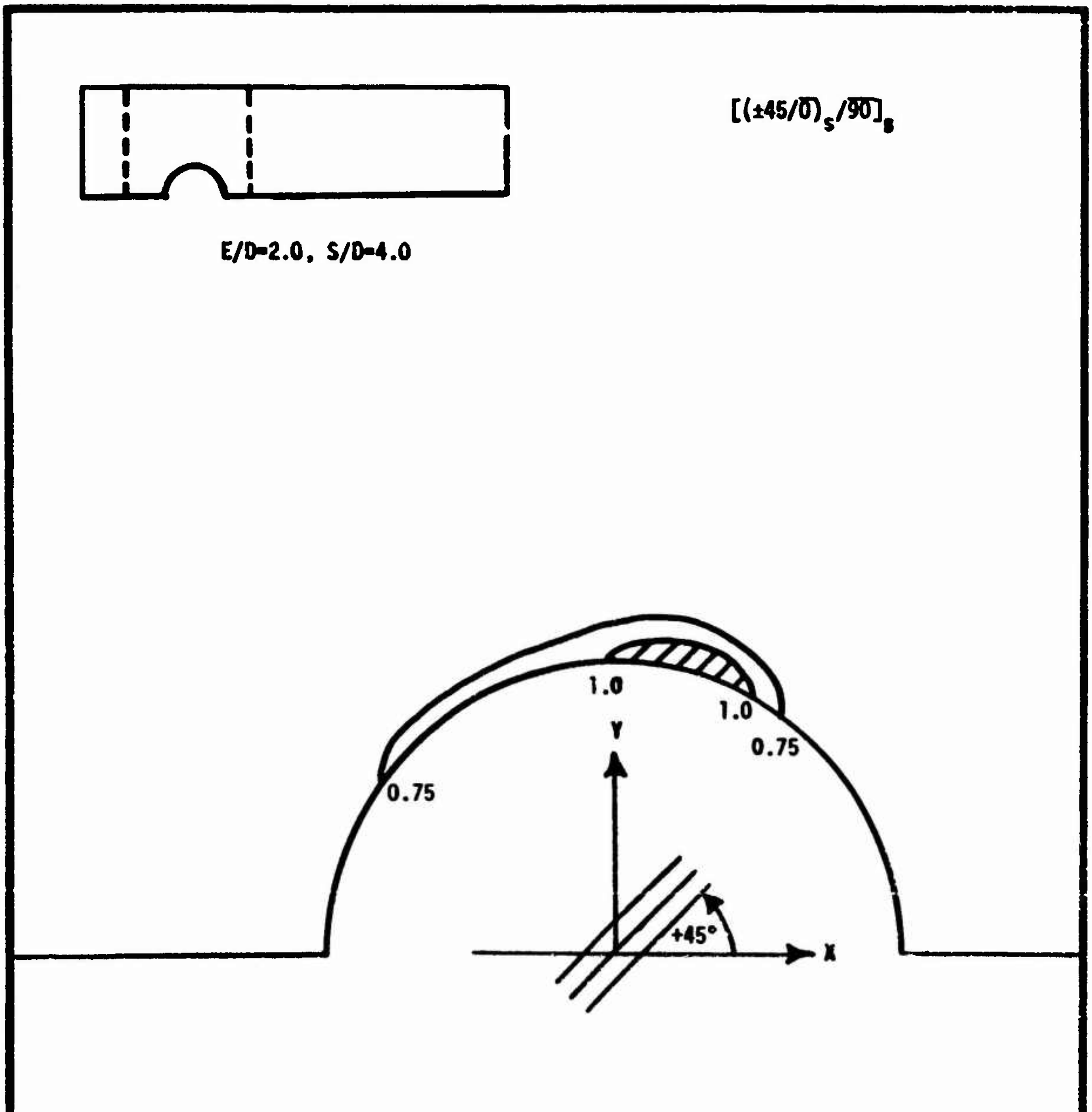

FIGURE 7a: NET TENSION FAILURE +45° LAMINA

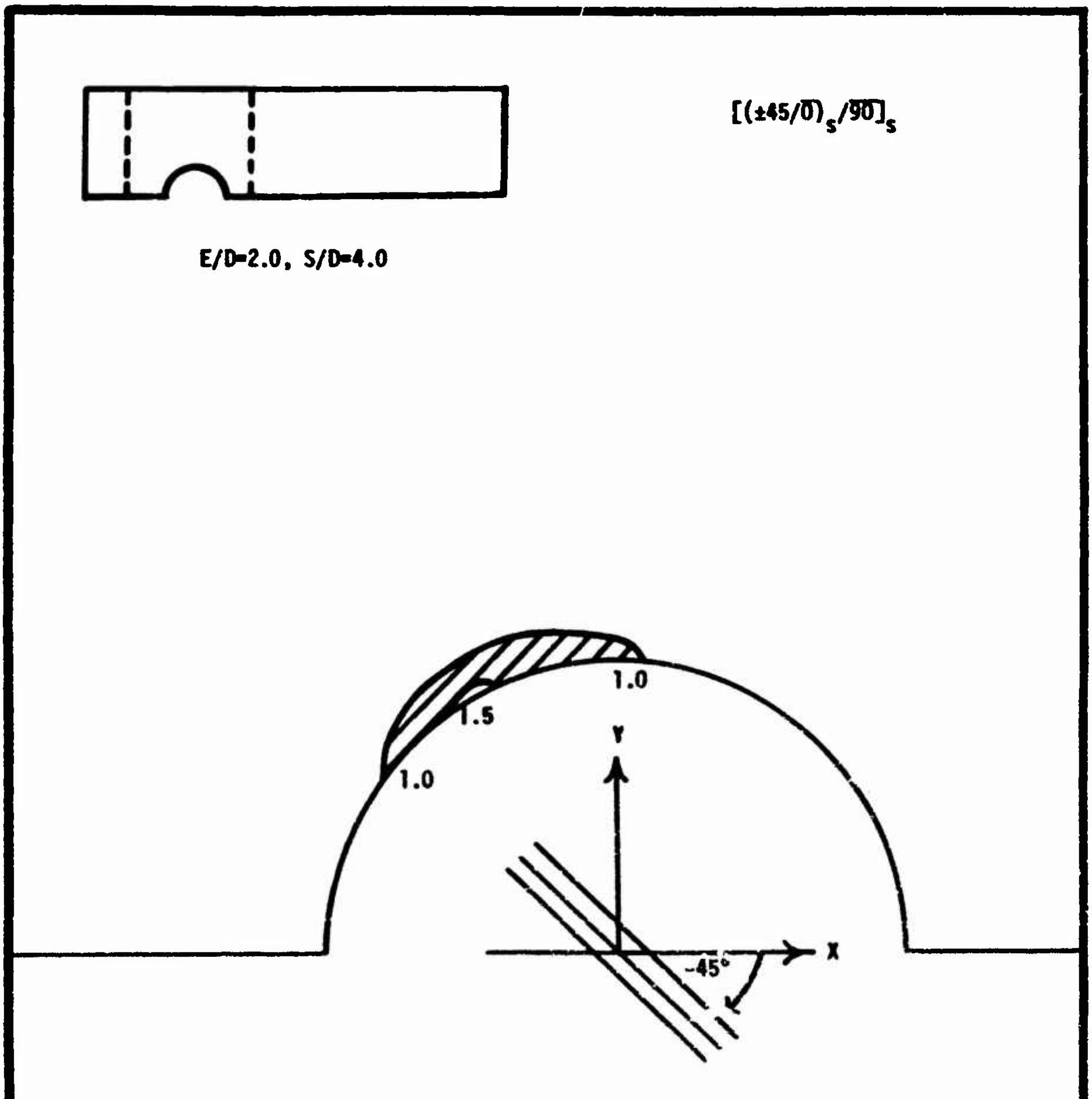

FIGURE 7b: NET TENSION FAILURE -45° LAMINA

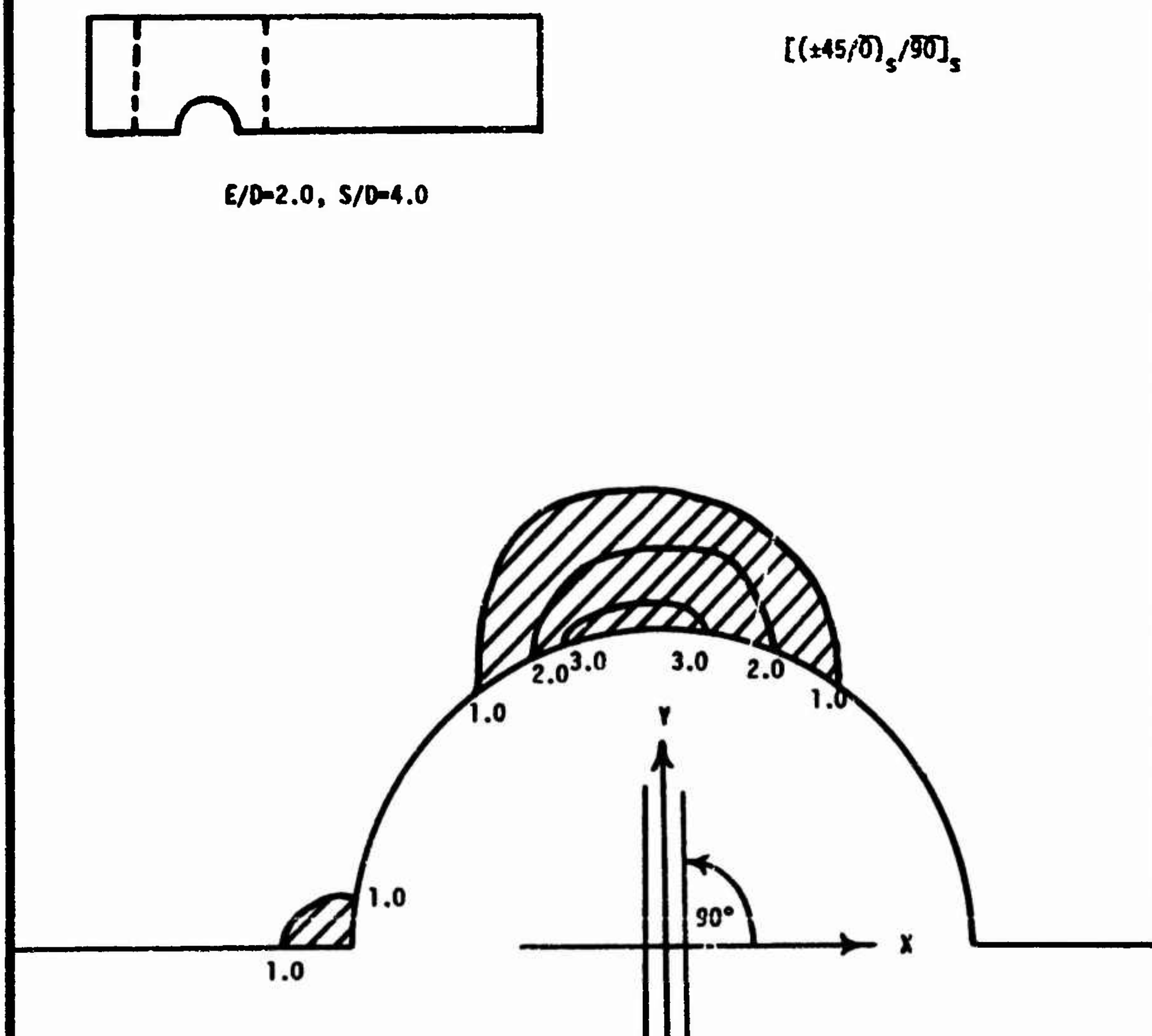

FIGURE 7c: NET TENSION FAILURE 90° LAMINA

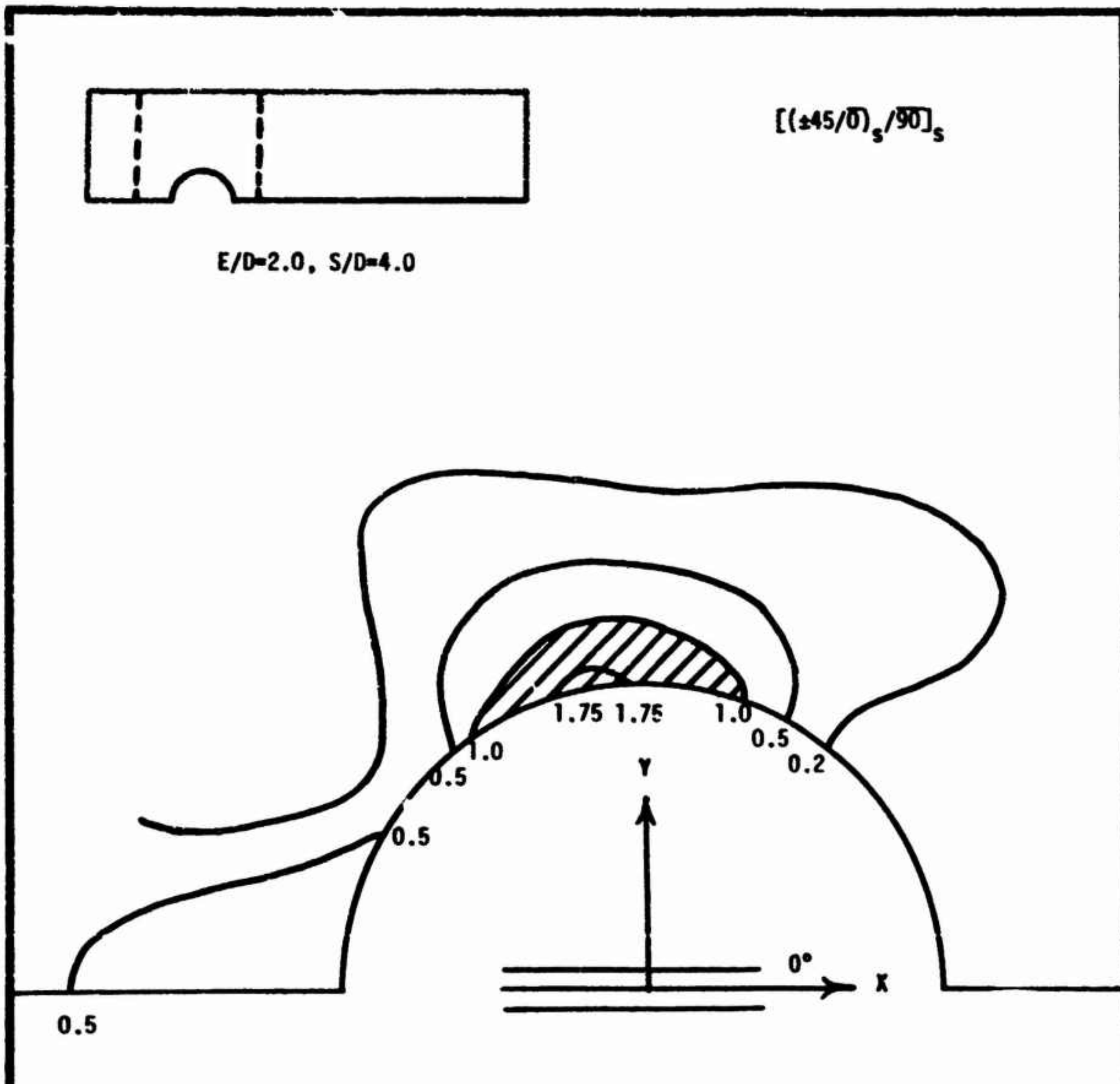

FIGURE 7d: NET TENSION FAILURE 0° LAMINA

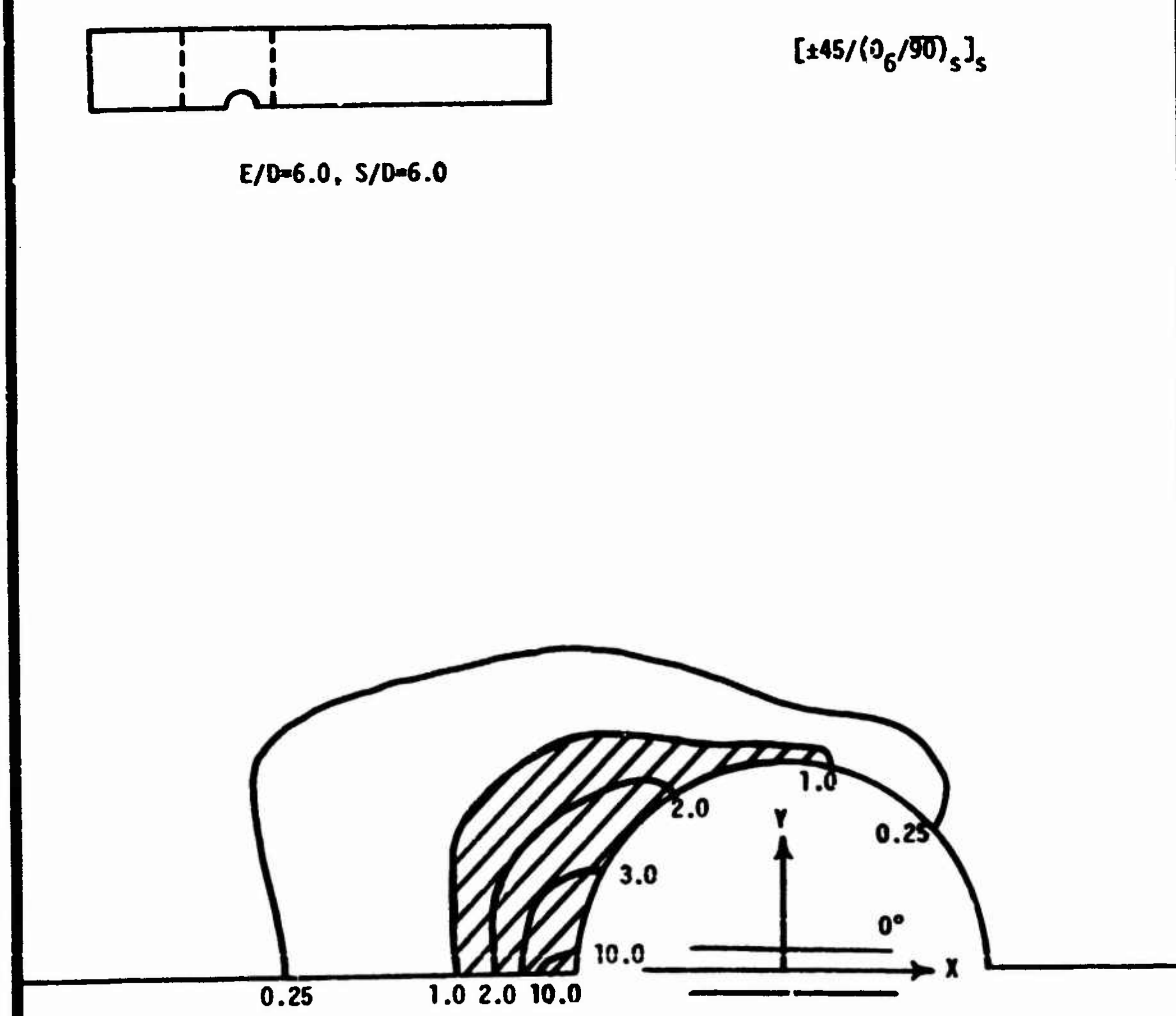

FIGURE 8: SLUG SHEAR-OUT FAILURE 0° LAMINA

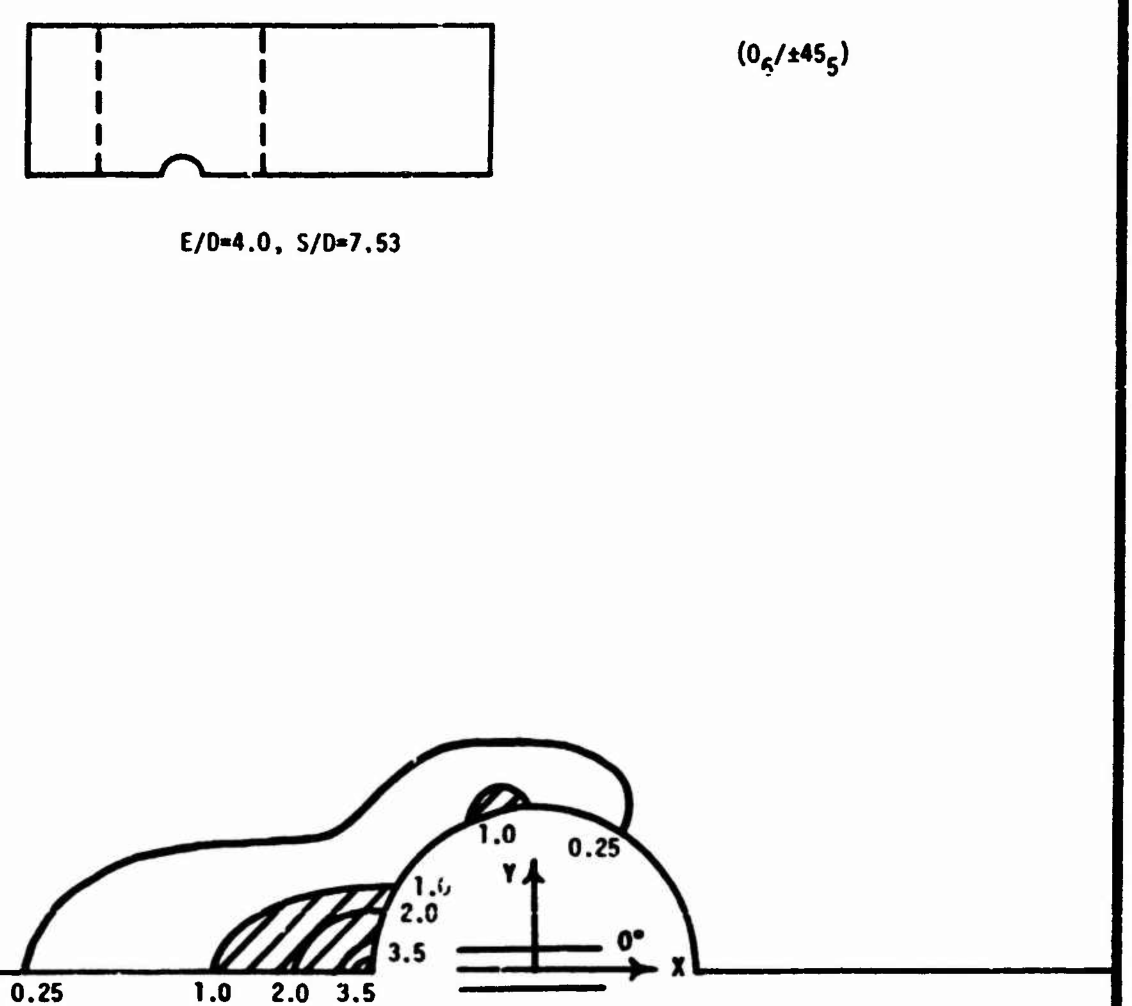

FIGURE 9: BEARING FAILURE 0° LAMINA

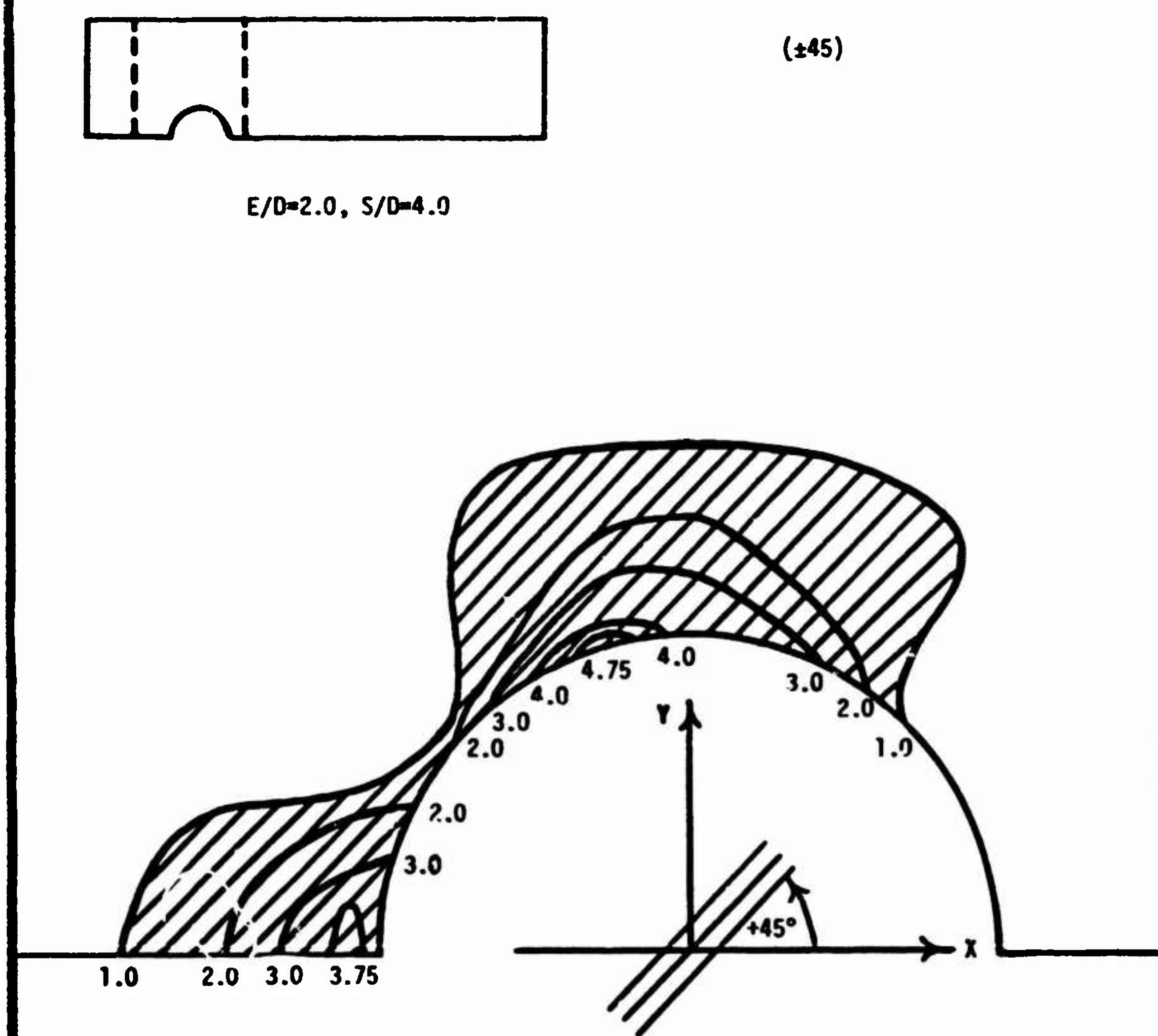

FIGURE 10: COMBINATION AND NET TENSION FAILURE +45° LAMINA

TABLE 1

SUMMARY OF BOLT BEARING SPECIMEN DATA

Failure Mode	Laminate	Material	% ±45°	% 0°	% 90°	$\frac{e}{d} : \frac{s}{d}$	Predicted Failure Load / Experimental Failure Load		
							DIST	Maximum Stress	Maximum Strain
T,T,C	(±45)	G/E	100	-0-	-0-	2:4	0.47	0.47	0.62
T	$[(\pm45/\bar{0})_s/\overline{90}]_s$	B/E	72.7	18.2	9.1	2:4	0.76	0.58	0.49
T	$(\pm45_5/90_6)$	B/E	62.5	-0-	37.5	3:4	0.93	0.94	1.00
S	$[\pm45/(0_6/\overline{90})_s]_s$	B/E	13.3	80.0	6.7	6:6	0.58	0.61	1.89
S	$(0_6/\pm45_5)$	B/E	62.5	37.5	-0-	2.5:7.53	0.98	1.10	0.95
B	$(0_6/\pm45_5)$	B/E	62.5	37.5	-0-	4:7.53	∿0.65	0.58	0.49

Nomenclature:

T	Tension	G/E	Graphite-Epoxy
C	Combination	B/E	Boron-Epoxy
S	Shear-Out		
B	Bearing		

3.2 *TOWARD A DESIGN PROCEDURE FOR MECHANICALLY FASTENED JOINTS MADE OF COMPOSITE MATERIALS*

3.2.1 *Introduction*

Currently much emphasis is being directed toward replacing metal components in weight sensitive structures, such as aircraft, with composite materials, due to their superior specific strength and specific stiffness properties. The potential weight savings which could result from such practices, however, have not, as yet, been realized.

Significant weight savings can be achieved throughout the bulk of a replacement component by tailoring the composite material to efficiently carry the loads which are known to occur in the existing metal component. The weight savings which result, however, are usually eliminated due to the inefficient joint[2] designs which are proposed by the designer to fasten the replacement component to the remainder of the existing structure. The measure of efficiency used here is simply load carried per pound of material. Thus, if a given load is to be carried by a structural member, the load carrying efficiency of that member increases as its weight is decreased.

In the design of metal joints only three failure modes need be considered; net tension, shear-out, and bearing. For a given metal the values of F_{TU}, F_{SU}, and F_{BRU} can be experimentally determined and used to specify the joint parameters S, E, and t respectively, given the bolt diameter. Thus, the design of metal joints is based on a very limited amount of experimental data.

---

[2]The term joint will imply a mechanically fastened joint throughout the report.

Consider the complications which would arise if a similar empirical design procedure were used for joints made of composite materials. First of all, several additional failure modes are exhibited by composite joints which do not occur in metal joints, due to the anisotropy of composite materials. Thus, for a given laminate the amount of data required for design purposes would be about doubled. The major problem, however, is that the feasibility of obtaining effective stress allowables which can be related to geometric parameters for splitting, shear-out, or bending tear-out failure modes in composite materials has yet to be determined.

Secondly, consider the problems associated with the selection of joint lamination. The designer is using a material which may be tailored to satisfy certain design constraints which are application dependent. The number of possible lay up patterns which could be considered during a single design are innumerable. Thus, the amount of data acquisition which would be necessary to support an empirical design procedure in composite joints is prohibitive.

As a result, the designer is presently forced to select a laminate for which some data does exist. Since laminate effective stresses for the various failure modes are unknown, an overly conservative design must be proposed by the designer based on his interpretation of the available data. An overly conservative design, unfortunately, implies that additional material has been used wherever necessary to compensate for a lack of confidence in predicting various failure modes. Such practices, of course, lead to inefficient designs.

There is one other important difference between metal joints and composite joints which should be mentioned. It can be deduced, using the results from [1], that the stress concentration factor which results in an anisotropic joint is greater than that which occurs in a geometrically similar isotropic joint. This is, of course, a disadvantage associated with using composite materials in joints. It is, however, more than compensated for by the materials specific strength and specific stiffness properties.

To recover the potential weight savings of designing with composite materials new design procedures must be proposed which will result in optimum joint designs with respect to total joint weight. It is the purpose of the reported study to investigate such improved design procedures.

A first attempt at such design procedures is proposed and is discussed in detail in Section 3.2.6. The procedures are sufficiently general that they may be used in conjunction with most available optimization routines. The results are being programmed by this investigator using an in-house pattern search optimization routine. Given valid input data, the program is designed to output that joint design in design space which has the minimum total joint weight while satisfying all the imposed design constraints. The results will, of course, only be as accurate as the assumptions on which the analysis is based. As a result, further investigations regarding the accuracy of these assumptions is warranted and will be performed by this investigator.

As mentioned above, three failure modes have been observed in metal joints: net tensic shear-out, and bearing. Each of these modes exhibits ductile fracture behavior. In composite joints not only are there additional modes of failure to consider but fracture behavior ranges from ductile to brittle, depending on the failure mode being considered.

Finite element stress analyses of bearing and shear-out failures in composite materials [2] have shown that large regions of laminate destruction, on the order of a hole diameter in size, occur prior to actual laminate failure. It was also found that highly localized regions of laminate failure, about two orders of magnitude smaller than those required for bearing and shear-out failures, were present when net tension failures occurred. It is apparent, therefore, that these various failure mechanisms must be understood before a truly optimum joint design can be achieved, since a single failure criterion is not applicable to all the possible modes of failure in composite materials.

A recent study [3] has postulated the existence of a small but finite region of intense energy which supposedly governs failure in composite tension coupons. If stress concentrations induce such regions of intense energy in composite tension coupons a similar phenomenon should occur in composite bolt bearing specimens. The results reported in [2], therefore, tend to support such a theory.

To further understand the phenomenon, a finite element study was performed for several composite tension coupons and is reported in Section 3.2.2. Again, very small, highly localized regions of laminate destruction were observed prior to actual failure. As a logical extension to the tension coupon experimental study [3] four geometrically similar bolt bearing specimens were designed, Section 3.2.2, to fail in net tension using a quasi-isotropic boron-epoxy material. These specimens are presently being fabricated and will be tested at General Dynamics, Fort Worth. If a characteristic crack length hypothesis is indeed valid, significant differences in applied failure stresses for these specimens should be observed. These differences should be predictable from the theory presented in [3].

The design procedures outlined and discussed in Section 3.2.6 are only intended to represent an initial attempt at moving toward the desired design procedures for joints made from composite materials. In Section 3.2.7 those areas which require further investigation are indicated.

3.2.2 Investigation of the Characteristic Crack Length Hypothesis

Past experience with predicting net tension failure in anisotropic bolt bearing specimens using the distortional energy failure criterion[3] [2] has shown that a small but finite region of material at the hole surface is always "past the point of failure" before laminate failure occurs. These regions were originally considered to result from an inherent conservatism of the finite element solution technique. A recent sutdy performed at General Dynamics [3] has postulated the existence of a region of intense energy in composite tension coupons which seems to govern failure. The finite element results [2] in retrospect appear to support such a theory.

In the study performed at GD a series of graphite/epoxy tension coupons were designed and tested to failure. The specimens were identical in overall size and lamination but the sizes of the circular cutouts varied. If a similar series of metal specimens were tested it would be possible to predict the failure loads of all the specimens from the experimental failure load of a single specimen, using scaling factors which are only geometry dependent. In the case of the graphite/epoxy coupons a simple scaling of failure loads was not possible. It was found, however, that the observed failure behavior could be explained via fracture mechanics if the existence of a region of intense energy or a characteristic crack length was hypothesized. For a given laminate the size of the region was assumed constant.

---

[3] It is well known that the Hill failure criterion is not a distortional stress energy. However, because of the close similarity with the isotropic failure criterion of distortional energy, the phrase "distortional energy failure criterion" will denote the Hill failure criterion as used in Section 3.1.

As previously mentioned highly localized regions of predicted laminate failure have been observed via finite elements in composite bolt bearing specimens. An investigation to determine whether or not similar regions could be observed via finite elements in composite tension coupons has since been completed. Two specimens were selected from [3] for analysis. The failure loads predicted by the theory [3] for these two specimens were used as applied loads for the computer runs. Using the most recent graphite/epoxy material constants and ultimate allowables it was found that for a tension coupon containing a 1.0 inch diameter hole the region of localized failure measured 50 mils. Likewise, for a specimen containing a 0.2 inch diameter hole the region measured 31 mils. The characteristic crack length proposed for the laminate used in the actual specimens was approximately 40 mils and agrees quite well with the finite element results. Distortional energy contour plots for the various laminae in the 1.0 inch diameter specimen are shown in Figure 1. Localized lamina failure is predicted to occur when the value of the normalized distortional energy exceeds 1.0 [2].

There are several reasons to suspect that the values of the distortional energies near the hole are not entirely accurate. Finite element size differences in the two specimens at the hole surface, the effects of interlaminar shear at the circular boundaries, and uncertainties regarding the cross term in the distortional energy failure criterion probably account for a large percentage of any possible error. The fact that a small region of material appears to be "past the point of failure" in both specimens before laminate failure occurs, however, is the significant result rather than the actual sizes of these regions.

If a region of intense energy actually governs failure in composite tension coupons it should also govern failure in bolt bearing specimens made of the same material. Thus, four geometrically similar bolt bearing specimens were sized using a quasi-isotropic graphite/epoxy laminate to see if differences in experimental failure loads could be observed and explained using the characteristic crack length hypothesis. The equations presented in [4] were used to size the initial design, Table 1. The ultimate load predicted by the equations for a net tension failure was slightly less than that necessary for a bearing failure and only about two thirds that necessary for a shear-out failure. A computer analysis of the proposed specimen configuration indicated that a net tension failure would occur at precisely the load predicted by the equations. The resulting distortional energy plots for the initial design are shown in Figure 2a.

Note, however, that the results reported in [2] indicate that before a bearing failure may occur in a bolt bearing specimen a large region of material directly ahead of the bolt must exhibit normalized distortional energies greater than 1.0. Thus, the computer analysis predicts a net tension failure to occur well ahead of any possible bearing failures, Figure 2a. This, however, disagrees with the behavior predicted by the equations.

At the request of Mr. J. R. Eisenmann the specimen was resized to eliminate even the remotest possibility of premature bearing failures since such failures would give no information regarding the possible presence of a characteristic crack length. In the revised design (Table 2) the specimen width has been decreased and the edge distance increased. The equations now predict a net tension failure to occur well ahead of both bearing and shear-out failures. A computer analysis of the revised design again indicated that a net tension failure would occur (See Figure 2b). The failure load predicted by the computer analysis, however, was 58% greater than the failure load predicted by the equations. Both the equations and the finite element analysis agree that a net tension failure will occur well ahead of both bearing and shear-out failures. The two methods disagree significantly, however, on the predicted failure loads.

These differences in predicted failure loads indicate clearly that basing bolt bearing specimen failure predictions on the equations presented in [4] is very dangerous. The equations are empirical in origin and only apply to a limited range of specimen geometries. The revised design is obviously outside the region of applicability.

3.2.3 Review of Past Design Programs Involving Composite Joints

Two programs involving the design and testing of joints made of composite materials were recently completed at General Dynamics, Fort Worth. In the original program [5] specimens were sized to fail in net tension at the innermost row of bolts. The maximum load to be carried by a joint was first specified. An estimate as to bolt load partitioning was next made based on the designers understanding of load distributions in isotropic joints. The laminate to be used was selected and the joint dimensions were then scaled from existing single- and double-fastener coupon data.

During testing, eight of the nine specimen designs failed in a splitting mode rather than the desired net tension mode. Thus the techniques used in sizing these joints proved to be unsatisfactory.

In the second joints program [6] only one joint was designed and tested. The maximum load to be carried by the joint was again specified. The designer assumed that each bolt in the joint would carry an equal percentage of the total joint load at failure. The longitudinal strains in the splice plate and main plate were set equal at two locations in the joint; midway between the first two rows and last two rows of bolts. The specimen was sized at these two locations to fail in net tension at the innermost row of bolts. A linear taper in both geometry and lamina thicknesses was then employed. The resulting joint design was built and tested. It failed in net tension at the innermost row of bolts as desired.

The major criticism of the latter design procedure is that it ignores the interaction between bolt load partitioning and joint geometry. The design procedures proposed by this investigator include such interaction relationships. The following section, Section 3.2.4 describes the proposed load partitioning analysis in detail. In Section 3.2.5 the analysis technique is used to predict bolt load distributions for six specimens selected from [5] and [6]. The results are used as input data for finite element analyses of the various specimens. A joint failure criterion is then proposed which, when applied to the finite element results, successfully predicts failure modes and conservatively predicts failure loads for each of the specimens.

3.2.4 Evaluation of Load Partitioning in Joints

To design a joint one must first understand the way in which changes in joint geometry affect bolt load partitioning. Two methods for predicting bolt load distributions in a given joint are proposed here. The first will be referred to as the point strain matching technique, and the second, as the displacement matching technique.

In both techniques only a single column of bolts will be considered. Larger joints may be constructed from identical columns of bolts connected to one another along their common sides. When stress analyses are performed for such joints curves presented in [7] will be used to correct for the effects induced by the adjacent columns. Both techniques assume that all bolts act as rigid pins and that the effects of plate bending are negligible.

3.2.4.1 Point Strain Matching Technique

In the point strain matching technique the average longitudinal strain in the main plate, ε_m, is equated to the average longitudinal strain in the splice plates, ε_s, midway between each set of adjacent bolts in a given column. Referring to Figure 3 we may write

$$\varepsilon_m\,(i,\ i+1) = \left(F - \sum_{k=1}^{i} P_k\right) / \left(E_{xm} A_m\right) \tag{1}$$

and

$$\varepsilon_s\,(i,\ i+1) = \frac{1}{2} \sum_{k=1}^{i} P_k \;/\; \left(E_{xs} A_s\right) \tag{2}$$

The notation (i, i + 1) implies evaluation at the midpoint between the bolts labeled i and (i + 1). Note that equations (1) and (2) are written for joints loaded in double shear. The equations may be used, however, for joints which are loaded in single shear if one half the total cross sectional area of the single shear splice plate at the various midpoints is substituted for A_s.

The assumption is now made that

$$\varepsilon_m(i, i + 1) = \varepsilon_s(i, i + 1) \tag{3}$$

Substituting equations (1) and (2) into (3) and rearranging we have:

$$\sum_{k=1}^{i} P_k = \frac{F}{1 + \frac{1}{2}\left(\frac{E_m(x)\ A_m(x)}{E_s(x)\ A_s(x)}\right)_{i,\ i+1}} \tag{4}$$

Equation (4) may be evaluated for i = 1, N - 1, where N is the total number of bolts per column. Thus, equation (4) represents a total of (N - 1) equations in N unknowns, namely P_1 thru P_N. One other equation can be written which relates the individual bolt loads. It is, of course, the overall joint equilibrium equation.

$$F = \sum_{k=1}^{N} P_k \tag{5}$$

For a given specimen the modulus and cross sectional area of both the main plate and splice plates are known at every point along the specimen. Therefore, equations (4) and (5) can be used to solve directly for P_1 thru P_N.

3.2.4.2 Displacement Matching Technique

In the displacement matching technique the change in length of a section of main plate between two adjacent bolts is equated to the change in length of the section of splice plates between the same two bolts. That is

$$\Delta\ell_m \ (i \rightarrow i+1) = \Delta\ell_s \ (i \rightarrow i+1) \tag{6}$$

Equations (1) and (2) may be rewritten as follows:

$$d\ell_m = \frac{(F - \sum_{k=1}^{i} P_k)\ dx}{E_m(x)\ A_m(x)} \tag{7}$$

$$d\ell_s = \frac{(\frac{1}{2} \sum_{k=1}^{i} P_k)\ dx}{E_s(x)\ A_s(x)} \tag{8}$$

These equations require that the modulus and cross sectional area of both the main plate and splice plates be expressed as functions of x. Integrating (7) and (8) with respect to x from x_i to x_{i+1} and substituting into (6) it follows that

$$\sum_{k=1}^{i} P_k = \frac{M}{M + S/2} \times F \tag{9}$$

where

$$M = \int_{x_i}^{x_{i+1}} \frac{dx}{E_m(x)A_m(x)} \quad \text{and} \quad S = \int_{x_i}^{x_{i+1}} \frac{dx}{E_s(x)A_s(x)} \tag{10}$$

As before from equilibrium we have

$$F = \sum_{k=1}^{N} P_k \tag{11}$$

Equations (9) and (11) represent N equations in N unknowns which may be solved directly for P_1 thru P_N.

The point strain matching technique is used in Section 3.2.5 to calculate load distributions for the specimens analyzed. The load distribution for one of the specimens was calculated a second time using the displacement matching technique. A comparison of the results is shown in Section 3.2.5. The differences in load distributions are seen to be negligible.

The displacement matching technique is based on a more realistic assumption regarding physical joint behavior than is the point strain matching technique. Thus the reader may prefer to use the displacement matching equations in the proposed joint synthesis procedure discussed in Section 3.2.6. Further investigation regarding possible differences in the predicted behavior of the two techniques is warranted.

3.2.5 Computer Analysis of Experimentally Failed Composite Joints

The purpose of the analysis phase was to establish a proposed joint failure criterion which could be automated and included in the final optimization program. The proposed criterion should be able to predict both joint failure location and failure mode. It should also be conservative in predicting failure loads and as simple operationally as possible.

Six joints designed and tested at General Dynamics were selected from [5] and [6] and were analyzed via finite elements. Table 3 describes these various joints in detail.

Analyzing a complete joint in a single finite element run with any degree of accuracy was impossible due to computer storage limitations. It was, in fact, only possible to analyze one hole at a time to achieve suitable accuracy.

Thus, the following analysis procedure was used. Each of the joints analyzed consisted of a number of identical columns of bolts as illustrated in Figure 4a. It was assumed that each column could be analyzed separately and that each carried an equal share of the total joint load which was present at failure. The joint geometries of six specimens selected for investigation were such that if the joints were made of an isotropic material the effects of adjacent columns of bolts would be negligible [7]. The equations from [1] indicate that the stress concentration factors which result in anisotropic tension coupons are always greater than the stress concentration factors which result in geometrically similar isotropic tension coupons. It is reasonable to assume that the same holds true for bolt bearing specimens. Thus the assumption was made that the effects of adjacent columns of bolts were negligible in the actual composite joints since for the same applied loads a greater stress concentration factor implies a more rapid stress field decay.

To determine the effects of adjacent columns of bolts on the column of interest in the synthesis routine the graphical results from [7] will be used due to a lack of similar information for composite materials. Thus, conservative designs with respect to specimen width will result. Excessive conservatism implies a wasting of material and unwanted weight. Thus the degree of conservatism which results from using the correction factors from [7] will be investigated in the future.

The point strain matching technique was used to determine the bolt load distribution for each of the six joints. The resulting distributions are shown in Figure 5. The displacement matching technique was only applied to one specimen, specimen 6, for reasons of comparison with the point strain matching technique. The displacement matching results are included in Figure 5 and are denoted by the dashed lines. The differences between the two sets of results are seen to be negligible.

As mentioned above it was necessary to isolate single bolt holes for analysis to achieve suitable finite element accuracy. The holes which were selected for analysis were modeled as single fastener coupons as shown in Figure 4b. Each hole in specimen 6 was analyzed while only the first and last holes were analyzed for specimens 1 thru 5.

The stress boundary conditions for the resulting single fastener coupons were determined from the bolt load distribution results in the following manner. Consider the i^{th} hole in the column of bolts illustrated in Figure 4c. The load carried by the i^{th} bolt is P_{Bi}. From equilibrium considerations we require that a skin load, P_{si}, of magnitude

$$P_{si} = \sum_{k=i+1}^{N} P_{Bk} \tag{12}$$

be carried by the leading edge of the i^{th} coupon. The skin load was applied to the leading edge of the coupon as a uniform stress in the computer analyses. In the actual specimens, however, the material surrounding a given bolt hole does not see a uniform skin stress in the vicinity of the preceding loaded hole unless the holes are separated by a sufficient amount of material. Compare the actual stress distribution at the leading edge of the imaginary coupon, Figure 6a, with the uniform stress distribution imposed at that boundary in the finite element analysis, Figure 6b. The amount of load which must flow around the bolt hole in Figure 6b is significantly greater than that in Figure 6a. Thus the resulting stress concentration factor in the computer analysis will be greater than that which occurs in the actual specimen.

Corrections were made to the computed stress concentrations using [8] in an attempt to account for the error induced through the use of the uniform skin stress boundary condition. Distortional energy contour plots for the six specimens analyzed are shown in Figures 7 thru 12. It has been found by this investigator [2] that such plots are extremely convenient for data presentation. In regions of high distortional energies the principal stress ratios which are dominant have been indicated. Table 4 summarizes the important information contained in these figures.

Figures 7 thru 11 are for the five specimens selected from the original testing program at General Dynamics [5]. The first four specimens failed experimentally in splitting modes which appear to originate, upon examination of the specimens, at the last row of bolts. The fifth specimen, Figure 11, failed experimentally in net tension at the first row of bolts. Figure 12 represents the single specimen tested in the second General Dynamics program [6]. It also failed in net tension at the first row of bolts. The experimental failure behavior of these specimens, in conjunction with the stress analysis results illustrated in the figures, was used in the development of the proposed joint failure criterion. A description of how the criterion evolved is presented below.

Consider for the moment Figures 7 thru 10. The stress patterns are identical; the values only differ slightly. The discussion which follows for Figure 7 is also valid for Figures 8 thru 10. A region of very high distortional energies occurs in the 0° laminae directly ahead of the last row of bolts in the specimen. The $\sigma_2/\sigma_{2_{ut}}$ stress ratios are dominant in the region, which implies local matrix failure (splitting). The maximum value of $\sigma_1/\sigma_{1_{uc}}$ in the region is 0.49. Results from [2] indicate that once the 0° laminae split (i.e., $\sigma_2/\sigma_{2_{ut}} > 1.0$) a value of $\sigma_1/\sigma_{1_{uc}} \geq 0.65$ is necessary to cause a bearing failure to occur. Thus, even though the 0° laminae have split, Figure 7, the values of $\sigma_1/\sigma_{1_{uc}}$ are not large enough to cause a bearing failure to occur.

It has been assumed here that matrix failure does not significantly degrade the laminate since the percentage of hoop load carried by the 0° laminae directly ahead of the bolt was small. However, in specimens where a large percentage of the hoop load is carried by the matrix prior to failure a similar assumption is not possible. Consider a specimen consisting of almost all 0° laminae and only a few ±45° laminae. Matrix failures in the 0° laminae would result in significant load transfer from the 0° laminae to the ±45° laminae. Even if laminate failure did not occur as a result of the load transfer the laminate would be significantly damaged. It is apparent, therefore, that a successive failure analysis must be included in the final design procedure to account for such load redistribution.

High distortional energies also result in the 0° laminae at $\theta = 90°$, Figure 7, at both the first and last row of bolts due to large values of $\sigma_1/\sigma_{1_{ut}}$ in these regions. The maximum distortional energy value at the last row of bolts, 2.0, is greater than the maximum value at the first row, 1.5. The same is true of the maximum values of $\sigma_1/\sigma_{1_{ut}}$ in these two regions. If the 0° laminae were to fail, the ±45° laminae would not be able to carry the additional load transferred to them from the 0° laminae; as a result, laminate failure would occur. Thus a net tension failure at the last row of bolts is the most probable failure mode indicated from the results so far.

The assumption that matrix failure does not significantly degrade the laminate is valid throughout specimen 1. The regions of high distortional energies which result from large $\sigma_2/\sigma_{2_{ut}}$ ratios are therefore eliminated from consideration. The only remaining region of interest is the one in the +45° laminae which occurs at the last row of bolts where the fibers are tangent to the hole. Both the maximum distortional energy value and maximum $\sigma_1/\sigma_{1_{ut}}$ value in this region are greater than the corresponding values which indicated a net tension failure at the same hole. Once the +45° fibers break in tension the remainder of the laminate cannot carry the existing load and laminate of failure also occurs. Thus a splitting mode is favored over the net tension mode previously indicated for specimen 1. Since all the possible regions of failure initiation have been examined a splitting mode is predicted by the analysis. The actual specimen did indeed fail in a splitting mode. The predicted failure load is conservative. If P_F is the actual experimental failure load for specimen 1 the distortional energy failure criterion predicts failure to occur at $P_F/\sqrt{2.5}$ or 0.64 P_F. The maximum stress failure criterion predicts failure to occur at $P_F/1.5$ or 0.67 P_F. Analyses of specimens 2 thru 4 yield very similar results.

Following the same procedure it can be deduced that a bearing failure does not occur in specimen 5, Figure 11. Both the distortional energy and maximum stress failure criteria conservatively predict a net tension failure to occur at the first row of bolts, which again agrees with the experimental failure mode.

Predicting failure for specimen 6 is slightly more complicated. The finite element results, Figure 12, indicate that $\sigma_1/\sigma_{1_{uc}}$ reaches 0.65 at the last row of bolts in the 0° laminae prior to matrix failure, $\sigma_2/\sigma_{2_{ut}} = 1.0$. A bearing failure is predicted to occur in such a case at that load where either $\sigma_2/\sigma_{2_{ut}}$ reaches 1.0 or $\sigma_1/\sigma_{1_{uc}}$ reaches 1.0, whichever occurs first. The assumption is made at bearing failure initiation that the bolt causing the bearing failure to occur is unable to carry any additional load during subsequent specimen loading. The additional applied load is distributed among the remaining bolts in the column in proportion to the loads which they carried at bearing failure initiation. Figure 12 is the finite element representation of the state of stress present in specimen 6 when the experimental failure load was applied. Notice that $\sigma_2/\sigma_{2_{ut}}$ = 1.0 and $\sigma_1/\sigma_{1_{uc}}$ = 0.80 in the 0° laminae directly ahead of the last row of bolts. The material ahead of the last row of bolts has failed in bearing and load redistribution, as described above, has taken place. A load distribution plot for specimen 6 is illustrated in Figure 12. Note that the revised load distribution plot is much more uniform than that of Figure 5(f).

Observe that regions of high distortional energies do not occur in the vicinity θ = +45° at any of the bolt holes except at the last row of bolts in the -45° laminae. Matrix failure is on the verge of occurring here. Net tension failures, however, are indicated at various locations along the specimen which would occur prior to matrix failure in the -45° laminae. A splitting mode is, therefore, definitely not indicated by the distortional energy plots.

Regions of high distortional energies in the 0° laminae at θ = 90° are present at the first and third through sixth rows of bolts. The maximum distortional energy value, 1.2, occurs at the fifth row. The largest value of $\sigma_1/\sigma_{1_{ut}}$ in these four regions of interest is 1.03, which also occurs at the fifth row. Thus, both the distortional energy and maximum stress failure criteria predict a net tension failure to occur in specimen 6 at the fifth row of bolts at 0.97 P_F, where P_F is the actual experimental failure load for the specimen. The predicted failure load is again conservative but only by about 3% as opposed to about 35% for specimens 1 thru 5. The predicted failure mode was again correct but the location was not.

The analysis of specimen 6 shows that the design was a good one, in that each hole was close to failure when the joint failed experimentally. Notice also that the various bolts were fairly equally loaded when joint failure occurred. Some designers feel that such a bolt load distribution is necessary if a joint is to carry load efficiently. The validity of such a statement can only be determined by further analytical and experimental investigation.

Thus a joint failure criterion has been proposed which has successfully satisfied the requirements imposed on it at the beginning of Section 3.2.5. The criterion was able to predict both failure location and failure mode in all but Specimen 6 where it incorrectly predicted failure location. More importantly it was able to conservatively predict failure loads for each specimen. It was found that the maximum stress failure criterion agreed with the distortional energy failure criterion to within just a few percent in predicting failure loads. It was also found that failure was always initiated at locations around hole surfaces where fibers were being broken in tension and were tangent to the hole surface.

Therefore, to make the failure criterion as operationally simple as possible we need only check for fiber failures where the fibers run tangent to the hole surface. A successive failure analysis must be performed at these locations to insure against premature failures induced by matrix failures in other laminae. The successive failure analysis should also be performed in regions where fibers are perpendicular to the hole surface since matrix failures in these laminae may also induce premature laminate failures.

3.2.6 Proposed Mechanically Fastened Joint Design Program

The preceding sections explain the procedures one would go through if a given joint were to be analyzed. A method is now proposed by which a joint may be designed to meet certain design constraints while attempting to minimize total joint weight.

An outline of the proposed mechanically fastened joint synthesis program is presented below to give a general understanding of the procedures involved in arriving at an optimum joint design with respect to total joint weight. The various procedures are then discussed in detail.

3.2.6.1 Outline of Proposed Synthesis Program

(A) Specify the known input data.

(B) Determine the design variables and their range of allowable values.

(C) Specify the necessary design constraint equations which will insure that joint failure does not occur until the design ultimate load is reached. The design ultimate load will be included as part of the input data.

(D) Specify an initial design.

(E) Calculate the various bolt loads for the current proposed geometry using the bolt load partitioning results, Section 3.2.4.

(F) Perform a stress analysis of the proposed design to determine the average laminate stresses at various critical points along each of the circular boundaries. A closed form solution to the problem illustrated in Figure 13a, based on the theory presented in [9], will be used to perform the required stress analyses. Corrections will be made to account for the effects of finite specimen size from [10].

(G) Transform these average laminate stresses to lamina stresses.

(H) Determine whether any of the lamina stresses exceed the design constraints imposed in (C).

(I) Assign penalty functions to the weight function for each design constraint which is not satisfied and calculate the total weight for the proposed joint design.

(J) Select a new design by moving in design space along a path which tends to decrease the total weight function.

(K) Repeat (E) thru (J) until a suitable optimum design is achieved.

(L) If desired, a detailed stress analysis may be performed for the proposed optimum design using finite elements, Section 3.2.5. A final check may be necessary since the stress analyses performed in (F) are based on isotropic correction factors.

3.2.6.2 Discussion of Program Details

3.2.6.2.1 Input Data

The following information will be read into computer program as input data. It may be desirable in later work to include one or more of these parameters as program variables. The diameters of the bolts used in a given joint will all be the same, $\underline{D}$[4]. The actual size

---

[4]Underlined symbols and phrases denote input information.

will be dictated by joint application as well as by standard size limitations. Given an effective shear allowable for the bolt material, F_{SU}^{B}, and the maximum load to be carried by the joint per column of fasteners, F, one may determine a safe number of bolts, N, to be used in a given column since it appears from the analysis of specimen 6 that a fairly uniform load distribution is desirable.

Selection of the splice plate material will be application dependent. The material will probably be either a high strength steel or titanium. In either case the values of F_{TU}^{S}, F_{SU}^{S}, and F_{BRU}^{S} must be input so that constraint relationships may be later defined to insure against splice plate failures in net tension, shear-out and bearing respectively. In the load partitioning calculations the splice plate modulus, E_S, is also required.

Similarly a decision must be made as to whether boron/epoxy or graphite/epoxy will be used as the main plate material. The material properties and ultimate allowables must be input for the material system selected.

The leading edge distance of the main plate must be defined since values of F_{SU} are not tabulated for composite laminates. Such information would be very valuable to the current effort since excessively large edge distances result in low joint efficiencies. A value of E/D = 4.0 will be used for the leading edge of the composite main plate. A value of E/D may be calculated for the for the leading edge of the splice plate from the value of $F_{SU}{}^{S}$ and the maximum bolt load carried by the last row of bolts, which will be determined using the bolt load partitioning analysis.

In summary the required input data is:

D	Bolt diameters
$F_{SU}{}^{B}$	Effective shear strength of bolt material
F	Maximum load to be carried per column of bolts
N	Number of bolts per column
$F_{TU}{}^{S}$	Effective tension strength of splice plate material
$F_{SU}{}^{S}$	Effective shear-out strength of splice plate material
$F_{BRU}{}^{S}$	Effective bearing strength of splice plate material
E_S	Splice plate modulus
E_{11}, E_{22}, G_{12}, ν_{12}	Composite material lamina properties
σ_{1ut}, σ_{2ut}, σ_{1uc}, σ_{2uc}, ε_{1ut}, ε_{2ut}, ε_{1uc}, ε_{2uc}, τ_{12u}, γ_{12u}	Lamina ultimate allowables (Main plate)

3.2.6.2.2 Design Variables

In this section seventeen parameters are defined which can be used in conjunction with the input data to completely define a given joint. If restrictions are not imposed on the design once the input data is determined, the seventeen parameters would represent seventeen design variables. If restrictions are imposed the number of design variables would be less than seventeen.

At the beginning of the program, just after the input data is read in, flags will be used to indicate which of the seventeen parameters are to be predefined. The values of these predefined parameters will then be read in as additional input data. The remaining parameters will represent the design variables.

In some cases the design variables have been restricted to a certain range of allowable values. Optimization routines require a well defined design space within which they may search for local minima. Therefore, where limits have not been specified for design variables it is up to the programmer to do so.

The program has been restricted to the $(0/\pm\alpha/\pm\beta/90)$ class of laminates; α and β being design variables. The values of α and β are restricted to the range 15° to 75°. It may be desirable later to restrict the possible values of α and β to integer values, but for the present work integer optimization procedures will not be used. It will also be required that at least one ply of each of the four lamina orientations be present in each proposed design. In this manner we are assured that fiber failures will accompany laminate failure regardless of failure mode. A design where α and β are set equal, $(0/\pm\alpha/90)$, is also acceptable since fiber failures still must accompany all possible laminate failure modes. The total thicknesses of the various lamina orientations are assumed to be, at most, linear functions of x, the position along the joint. More complicated lay up patterns will not be included in the present study.

Consider the joint design shown in Figure 14. The seventeen possible design variables are indicated on the figure. As previously mentioned the values of $(E/D)_m$ and $(E/D)_s$ will be specified by the program. If a joint is being designed which will consist of a number of identical columns of bolts the widths of the main plate and splice plates must be equal and constant along their lengths. The designer must input such information as described above.

In summary the seventeen possible design paramters are as follows:

Parameters	*Description*	*Range*
α, β	Lamina orientations	$15° \rightarrow 75°$
$W_s(0)$, $W_s(L)$	Width of splice plate at x=0, L	$3D \rightarrow$
$t_s(0)$, $t_s(L)$	Thickness of splice plate at x=0, L	$\rightarrow$
$W_m(0)$, $W_m(L)$	Width of main plate at x=0, L	$3D \rightarrow$
L	Joint length	$[2(N-1)+4]D \rightarrow$
$t_0(0)$, $t_0(L)$	Thickness of 0° laminae at x=0, L	1 ply
$t_{90}(0)$, $t_{90}(L)$	Thickness of 90° laminae at x=0, L	1 ply $\rightarrow$
$t_{\pm\alpha}(0)$, $t_{\pm\alpha}(L)$	Thickness of ±α° laminae at x=0, L	1 ply $\rightarrow$
$t_{\pm\beta}(0)$, $t_{\pm\beta}(L)$	Thickness of ±β° laminae at x=0, L	1 ply $\rightarrow$

The lower limits on the widths and length measurements are based on a minimum separation of free surfaces of one diameter. These values may be changed by the programmer if desired. The upper and lower limits which have not been specified must be provided by the programmer.

3.2.6.2.3 Design Constraints

Once a design is proposed it must be loaded to design ultimate. The joint failure criterion, Section 3.2.5, must then be applied to determine whether or not the proposed design can indeed carry the design ultimate load, as required. In order to automate the process of examining the joint for possible failure at the i^{th} critical location an equality constraint, F(i), must be defined. For the in-house pattern search optimization routine, the equation must be written in such a form that $F(i) \leq 0$ if failure is not indicated. If failure is predicted to occur, then $F(i) > 0$. As previously mentioned a penalty function is added to the weight function when $F(i) > 0$. To minimize the total weight of the joint the design must move in design space in a direction which tends to reduce the penalty functions.

Consider the possible failures which could occur at each hole along the joint. They are:

(1) Bolt failure in shear.

(2) Splice plate failures in bearing, shear-out, or net tension.

(3) Main plate failures in bearing, shear-out, net tension, splitting, bending tear-out, or combination modes.

An inequality constraint equation must be written for each of the possible failure initiation sites.

To test for bolt failure in shear we calculate the maximum shear stress, TAU, acting on the bolt cross sectional area.

$$TAU = P_B / (\pi R^2) \tag{13}$$

P_B represents the bolt load acting at the hole of interest. The magnitude of P_B is determined via the bolt load partitioning analysis, Section 3.2.4.

To insure against a bolt failure in shear we require that $TAU \leq F_{SU}{}^{B}$. Stating this in the form of a valid inequality constraint we have:

$$F(1) = P_B / (\pi R^2) - F_{SU}{}^{B} \tag{14}$$

Similarly, to insure against splice plate failures at a given hole in bearing, net tension or shear-out we have respectively:

$$F(2) = P_B / Dt - F_{BRU}{}^{S} \tag{15}$$

$$F(3) = (P_B + P_S) / t(S - D) - F_{TU}{}^{S} \tag{16}$$

$$F(4) = P_B / 2tE - F_{SU}{}^{S} \tag{17}$$

The skin load, P_S, is calculated from equation (12). The values of t, E, and S for a given bolt bearing model are determined as was shown in Figure 4.

Now consider the possible composite main plate failures. Once a stress analysis is performed, checks for possible failure initiation must be made at four locations (possibly only three if

α equals β) around each hole as discussed in Section 3.2.5. Bearing failures may or may not be considered desirable. If they are, the load redistribution procedures discussed in Section 3.2.5 can be built into the computer logic. To simplify the following discussion assume that bearing failures are undesirable.

Thus, if at $\theta = 0°$, a matrix failure occurs in the 0° laminae ($\sigma_2/\sigma_{2_{ut}} \geq 1.0$) a bearing failure would be predicted to occur when $\sigma_1/\sigma_{1_{uc}} = 0.65$. If matrix failures do not occur during loading then $\sigma_1/\sigma_{1_{uc}} \geq 1.0$ would be necessary for a bearing failure to occur. Since the likelihood of a bearing failure is only dependent on the stresses at $\theta = 0°$ in the 0° laminae, an inequality constraint equation may be written at that location of the form

$$F(5) = \begin{cases} \sigma_1/\sigma_{1_{uc}} - 1.0 & \text{if} \quad \sigma_2/\sigma_{2_{ut}} < 1.0 \\ \sigma_1/\sigma_{1_{uc}} - 0.65 & \text{if} \quad \sigma_2/\sigma_{2_{ut}} \geq 1.0 \end{cases} \tag{18}$$

It was postulated in Section 3.2.5 that all failure modes, except bearing, have one thing in common. They all seem to occur at locations where fibers are tangent to a hole surface. In a $(0/\pm\alpha/\pm\beta/90)$ laminate fibers are tangent to the hole surface at $\theta = 90°$, $(90 - \alpha)°$, $(90 - \beta)°$, and 0° in the 0°, $+\alpha°$, $+\beta°$, and 90° laminae respectively. If, at ultimate load, matrix failures have occurred at any of these hole locations load redistribution among the various laminae must be considered. The stresses in the remaining laminae would be recalculated. A check would then be made in the laminae which are tangent to the hole surface to see whether or not the fibers have failed in tension. The inequality constraint used for this purpose is:

$$F(6) = \sigma_1/\sigma_{1_{ut}} - 1.0 \tag{19}$$

Equation (19) must be applied four times per hole; to the 0° fibers at $\theta = 90°$, the 90° fibers at $\theta = 0°$, the $+\alpha°$ fibers at $\theta = (90 - \alpha)°$, and the $+\beta°$ fibers at $\theta = (90 - \beta)°$. Thus, a total of nine inequality constraints must be satisfied at each and every hole.

In the past, designers have designed for net tension failures at the innermost row of bolts. An equality constraint of the form

$$\sigma_1/\sigma_{1_{ut}} - 1.0 = 0 \tag{20}$$

could be imposed on the stress field in the 0° laminae at the innermost row of holes to force the design to fail there in net tension. Such a restriction is not justified, however. When an optimum design is arrived at using the nine inequality constraint equations per hole, one of the nine equations will, in the process, be automatically forced to zero. This will specify joint failure mode and location. Net tension failures at the innermost row of bolts may not result when minimum weight designs are required.

3.2.6.2.4 Design Procedures

In order to begin the design process an initial design must be selected. The initial design must, of course, be in the design space which is defined by the upper and lower limits placed on the design variables.

If the designer has a design in mind he may use it to activate the program. Otherwise, the program will specify an initial design. The in-house pattern search routine uses a random number generator for the purpose of specifying initial values for the design variables. It may be desirable to use several random starting points, if run times are not excessively long, to check for possible local minimum in the design space.

Once an initial design is proposed the bolt load partitioning results would be used to calculate the bolt load distribution for the geometry and lamination selected. To perform such calculations the main plate and splice plate cross sectional areas as well as the main plate modulus must be defined as functions of x. Referring back to Figure 14 it can be shown that

$$A_m(x) = [(t_m(L)-t_m(0))\ (x/L) + t_m(0)]\ [(W_m(L)-W_m(0))\ (x/L) + W_m(0)] \quad (21)$$

$$A_s(x) = [(t_s(L)-t_s(0))\ (x/L) + t_s(0)]\ [(W_s(L)-W_s(0))\ (x/L) + W_s(0)] \quad (22)$$

It has been found by this investigator that a quadratic polynomial in x can be used to represent the modulus of the main plate to within a few percent when linear variations in lamina thicknesses are employed.

Thus, the modulus of the main plate may be determined at several locations along the joint using lamination theory and a second order curve of the form

$$E_m(x) = Ax^2 + Bx + C \tag{23}$$

may be fit to the resulting modulus values. The values of A, B, and C will be determined automatically by an internal curve fitting subroutine for the proposed design.

The only remaining unknowns which are needed to calculate the bolt load distribution are the coordinate locations of the N bolts. Since L, the joint length, and $(E/D)_m$, the leading edge distance of the composite main plate, are known, we may express the N bolt locations as:

$$X(I) = \frac{I-1}{N-1}\left[L - \left(\frac{E}{D}\right)_m\right] \quad \text{where } I = 1, N \tag{24}$$

The bolt loads could then be calculated using equations (4) and (5) or equations (9) and (11).

The next step in the design procedure is to perform a row by row stress analysis of the proposed design. The column of bolts is broken down into individual bolt bearing specimens as shown in Figure 4. The value of P_{si} would be calculated using equation (12). Thus, each bolt bearing model is acted on by a bolt load, P_{Bi}, and a skin stress, $\sigma_{si} = P_{si}/St$. Since a finite element solution of each bolt bearing specimen is too costly the following procedures will be followed.

The problem of an infinite plate containing a circular cutout which is loaded as shown in Figure 13a will be solved. This investigator's solution [11] to the problem illustrated in Figure 13b will be added to the solution of the problem illustrated in Figure 13c, which is presented in [12]. Corrections to the stress concentration factors induced at $\theta = 90°$ and $\theta = 0°$ will be made to account for the effects of finite specimen size using the results presented in [13] and [14]. Corrections to the average laminate stresses along the circular boundary from $\theta = 0°$ to $\theta = 90°$ can then be estimated.

The corrected average laminate stresses would be transformed to lamina stresses and checks would then be made to see if the design constraints discussed in Section 3.2.6.2.3 were satisfied. Penalty functions would be assigned to the weight function for each of the constraint equations which was not satisfied and the total joint weight would then be calculated. The optimization procedure would determine a preferred path and select a new design along that path which would have a lower total joint weight while more closely satisfying all the imposed design constraints.

The entire process, beginning with the calculation of bolt loads for the new design would be repeated until the design constraints were all satisfied and a local minimum weight were achieved.

Since the design procedure uses isotropic correction factors to account for finite specimen size there is, of course, some doubt concerning the actual failure behavior of the proposed optimum design. Therefore, it may be desirable to perform a complete stress analysis for the proposed optimum design to see how closely the predicted failure behavior would agree with the desired failure behavior. The analysis method described in Section 3.2.5 would be used if the final check were to be made.

3.2.7 Areas of Future Work

Several important questions have been raised regarding the solution technique thus far which deserve mention and in most cases warrant further investigation. The first involves the basically different failure mechanisms which can occur in a given joint made of composite materials. Net tension failures appear to behave as brittle failures once a very small but finite region of localized laminate destruction occurs. Bearing failures and shear-out failures, on the other hand, do not occur unless extensive laminate damage has resulted during loading. Thus bearing and shear-out failures behave in a relatively ductile manner. Additional analytical and experimental work must be done to understand the various failure mechanisms which occur in composite joints before truly optimum designs can be achieved. The results of the proposed geometrically similar bolt bearing specimen testing program should bring us closer to such an understanding.

In metals, effective bearing strengths, F_{BRU}, and effective shear-out strengths, F_{SU}, have been experimentally determined and are used in the design process to specify such parameters as leading edge distances. Similar information is generally not available for composites due to the number of possible laminates which could be used for design purposes. Such "material properties" would be invaluable, however, in the design of composite joints and deserve further investigation.

Similarly, a lack of data concerning the effects of finite size on stress concentrations induced at circular cut-outs in composite plates has forced us to predict these effects from available isotropic data. Making corrections from isotropic data results in a conservative design and is, therefore, partially satisfactory. The need for correction factors could be eliminated, however, if the in-house two dimensional anisotropic integral equation program developed by Dr. T. A. Cruse could be built into the optimization program in such a way as to not result in excessive computer run times. One other technique would be to derive the necessary correction factors for various laminates using the integral equation program and use such data in place of the isotropic correction factors which are now being used. Both possibilities are presently being investigated.

The following questions will also be considered:

(1) Are uniform bolt load distributions and net tension failures at the innermost row of bolts requirements for optimum joint designs?

(2) Is it advantageous to use the displacement matching technique rather than the strain matching technique to predict bolt load distributions?

(3) How should load redistribution in a joint be handled once a bearing failure occurs either in the main plate or splice plates?

(4) Is the uncertainty regarding the cross term in the distortional energy failure criterion, as discussed in [15], a major problem to be considered? A preliminary investigation performed during

the contract period has shown that in certain cases the cross term may be the most important term in the energy relationship. These questions will be pursued as part of this investigator's doctoral thesis during the current academic year.

3.2.8 *References*

[1] S. G. Lekhnitskii, *Theory of Elasticity of an Anisotropic Elastic Body*, Holden-Day, Inc., 170 (1963).

[2] J. P. Waszczak, T. A. Cruse, "Failure Mode and Strength Predictions of Anisotropic Bolt Bearing Specimens", *Journal of Composite Materials*, 421 (July 1971).

[3] M. E. Waddoups, J. R. Eisenmann, and B. E. Kaminski, "Macroscopic Fracture Mechanics of Advanced Composite Materials", Convair Aerospace Division of General Dynamics, FZM-5670, (February 1971).

[4] Advanced Composite Wing Structures, Boron-Epoxy Design Data-Volume II, Grummon Aerospace Corporation, 180-186, TR-AC-SM-ST-8085, (November 1969).

[5] Advanced Development of Boron Composite Wing Structural Components, Convair Aerospace Division of General Dynamics, AFML-TR-70-261, 66 (December 1970).

[6] R. H. Roberts, Personal communication, Convair Aerospace Division of General Dynamics, Drawing Number FW7[illegible]06048, (June 1971).

[7] R. E. Peterson, *Stress Concentration Design Factors*, John Wiley and Sons, Inc., 92 (1966).

[8] R. E. Peterson, *Stress Concentration Design Factors*, John Wiley and Sons, Inc., 91 & 94, (1966).

[9] S. G. Lekhnitskii, *Theory of Elasticity of an Anisotropic Elastic Body*, Holden-Day, Inc., (1963).

[10] R. E. Peterson, *Stress Concentration Design Factors*, John Wiley and Sons, Inc., (1966).

[11] J. P. Waszczak, "Stress Analysis of a Loaded Circular Hole in an Anisotropic Plate," Report SM-63, Department of Mechanical Engineering, Carnegie Institute of Technology, Carnegie-Mellon University, Pittsburgh, Pennsylvania (May 1971).

[12] S. G. Lekhnitskii, *Theory of Elasticity of an Anisotropic Elastic Body*, Holden-Day, Inc., 170 (1963).

[13] R. E. Peterson, *Stress Concentration Design Factors*, John Wiley and Sons, Inc., 84 & 99 (1966).

[14] S. Timoshenko, J. N. Goodier, *Theory of Elasticity*, Second Edition, McGraw-Hill Book Company, 62 & 123 (1951).

[15] S. W. Tsai, E. M. Wu, "A General Theory of Strength for Anisotropic Materials", *Journal of Composite Materials*, 58 (January 1971).

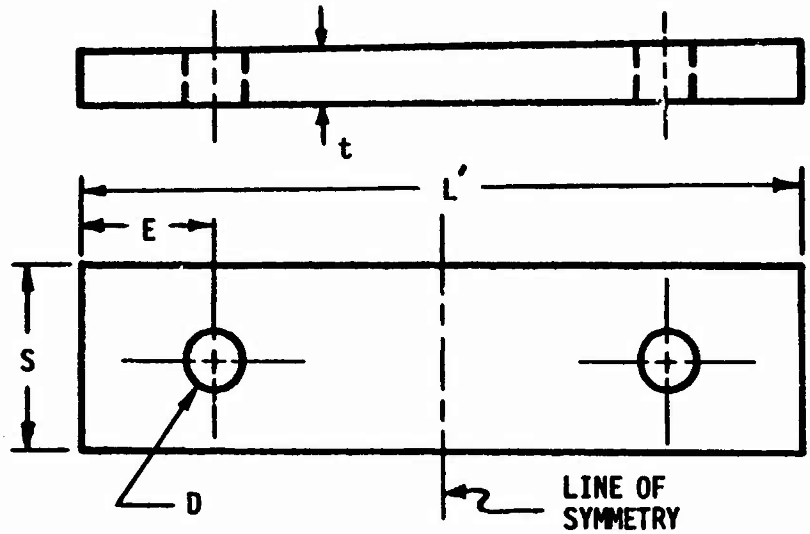

B/E

(0/±45/90)

Table 1. Initial Bolt Bearing Specimen Design

Spec. No.	D	E	S	L'	t	No. Plies	Predicted Failure Loads(lb) Equations(4)	Finite Elements
1	0.125	0.31	0.53	1.875	0.08	16	647	647
2	0.250	0.62	1.06	3.750	0.16	32	2,587	2,587
3	0.375	0.93	1.59	5.625	0.24	48	5,820	5,820
4	0.500	1.24	2.12	7.500	0.32	64	10,350	10,350

Table 2. Revised Bolt Bearing Specimen Design

Spec. No.	D	E	S	L'	t	No. Plies	Predicted Failure Loads(lb) Equations(4)	Finite Elements
1	0.125	0.50	0.375	2.25	0.08	16	400	625
2	0.250	1.00	0.750	4.50	0.16	32	1,600	2,500
3	0.375	1.50	1.125	6.75	0.24	48	3,600	5,620
4	0.500	2.00	1.500	9.00	0.32	64	6,400	10,000

Table 3. Description of the Six Specimens Selected for Analysis

Spec. No.	Lamination	Splice Plate Material	Loading	Rows of Bolts	Bolts per Row	Failure Mode	Ultimate Load(lb)
1	B/E,$0_4/\pm45$	D6-AC Steel	SS	6	4	SP	94,200
2	B/E,$0_4/\pm45$	D6-AC Steel	SS	5	4	SP	115,500
3	B/E,$0_4/\pm45$	6-4 Ti	SS	5	4	SP	110,400
4	B/E,$0_4/\pm45$	D6-AC Steel	SS	4	4	SP	125,400
5	B/E,$0_2/\pm45$	D6-AC Steel	DS	4	4	T	189,000
6	G/E,$0/\pm45$[1]	6-4 Ti	SS	6	2	T	74,800

Nomenclature:

SS Single Shear

DS Double Shear

B/E Boron-Epoxy

G/E Graphite-Epoxy

SP Splitting

T Tension

Notes:

(1) Lamina thicknesses vary linearly along the specimen length from $0_2/\pm45$ at the first row of bolts to $0_2/\pm45_3$ at the last row of bolts.

Table 4. Summary of Significant Data from Figures 7 thru 12

Spec. No.	Row No.	Bearing, $\theta=0°$ 0° Lamina			Tension, $\theta=90°$ 0° Lamina		Splitting, $\theta=\pm45°$ +45° Lamina		-45° Lamina	
		$\frac{\sigma_1}{\sigma_{1uc}}$	$\frac{\sigma_2}{\sigma_{2ut}}$	DIST	$\frac{\sigma_1}{\sigma_{1ut}}$	DIST	$\frac{\sigma_1}{\sigma_{1ut}}$	DIST	$\frac{\sigma_2}{\sigma_{2ut}}$	DIST
1	First	0.07	C*	0.02	1.05	1.50	0.21	0.10	0.83	1.10
	Last	0.49	2.50	5.80	1.33	2.00	1.50	2.50	1.65	3.20
2	First	0.10	0.04	0.01	0.91	1.00	0.42	0.25	0.80	0.75
	Last	0.50	2.30	5.10	1.11	1.41	1.30	2.10	1.55	2.60
3	First	0.07	0.05	0.01	0.83	0.90	0.63	0.47	0.79	0.71
	Last	0.47	2.50	6.00	1.34	1.45	1.43	2.50	1.73	3.00
4	First	0.13	0.29	0.11	0.85	0.85	0.58	0.40	0.69	0.55
	Last	0.52	2.80	7.95	1.07	1.51	1.55	2.70	1.90	3.75
5	First	0.30	0.56	0.42	1.29	2.00	0.79	0.90	0.92	0.90
	Last	0.60	2.00	4.00	1.02	1.41	1.15	1.65	1.21	1.88
6	First	0.17	0.04	0.03	0.90	0.95	0.57	0.44	0.75	1.12
	Fifth	0.37	0.26	0.21	1.03	1.20	0.63	0.60	0.83	1.15
	Sixth	0.80	1.00	1.90	0.80	1.00	0.63	0.65	0.95	0.95

*C Compressive stress

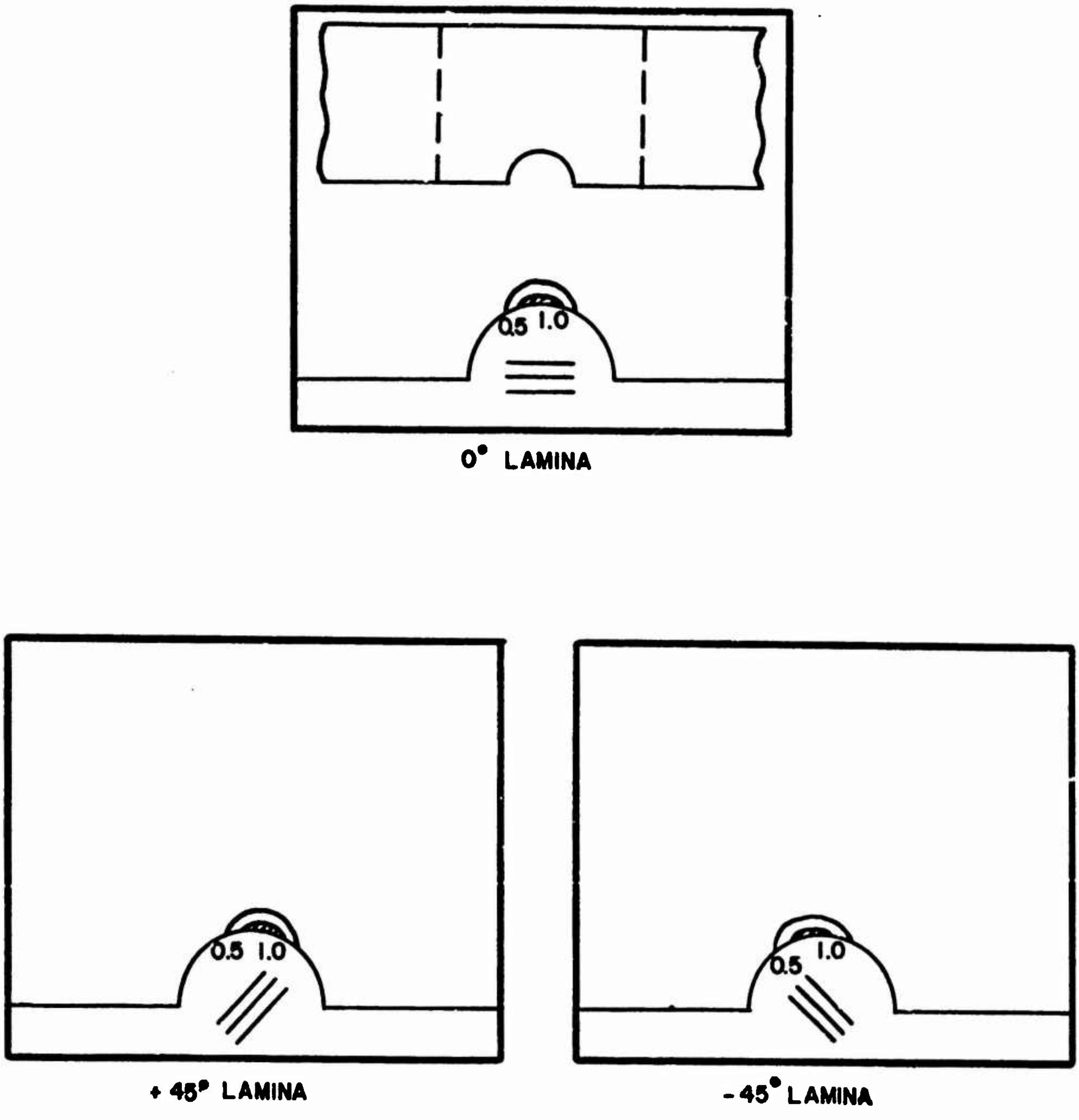

Figure 1. Distortional Energy Contour Plots for the 1.0" Diameter, Anisotropic Tension Coupon at the Experimental Failure Load.

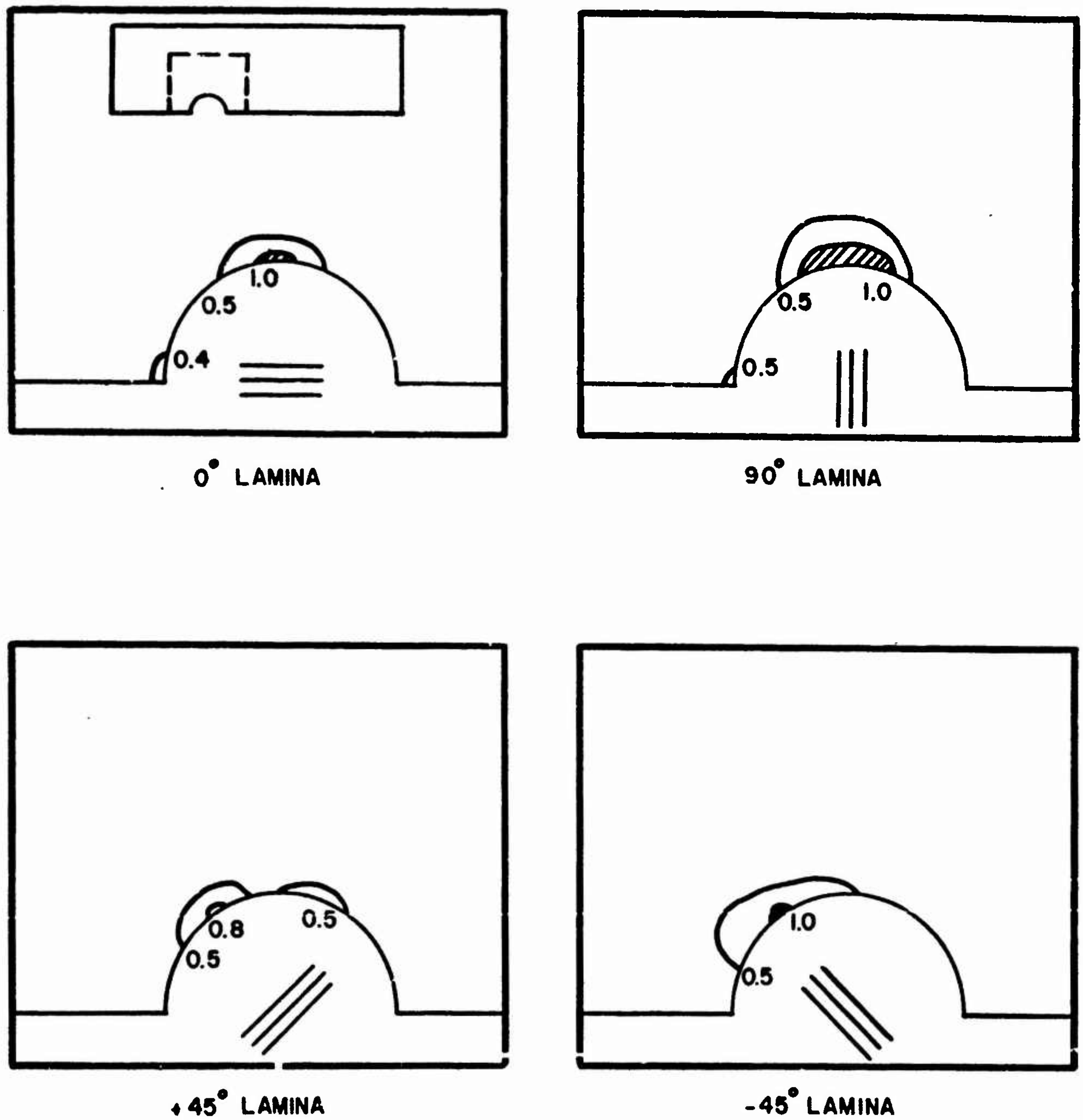

Figure 2a. Distortional Energy Contour Plots for the Initial Bolt Bearing Speciman Design at the Predicted Failure Load.

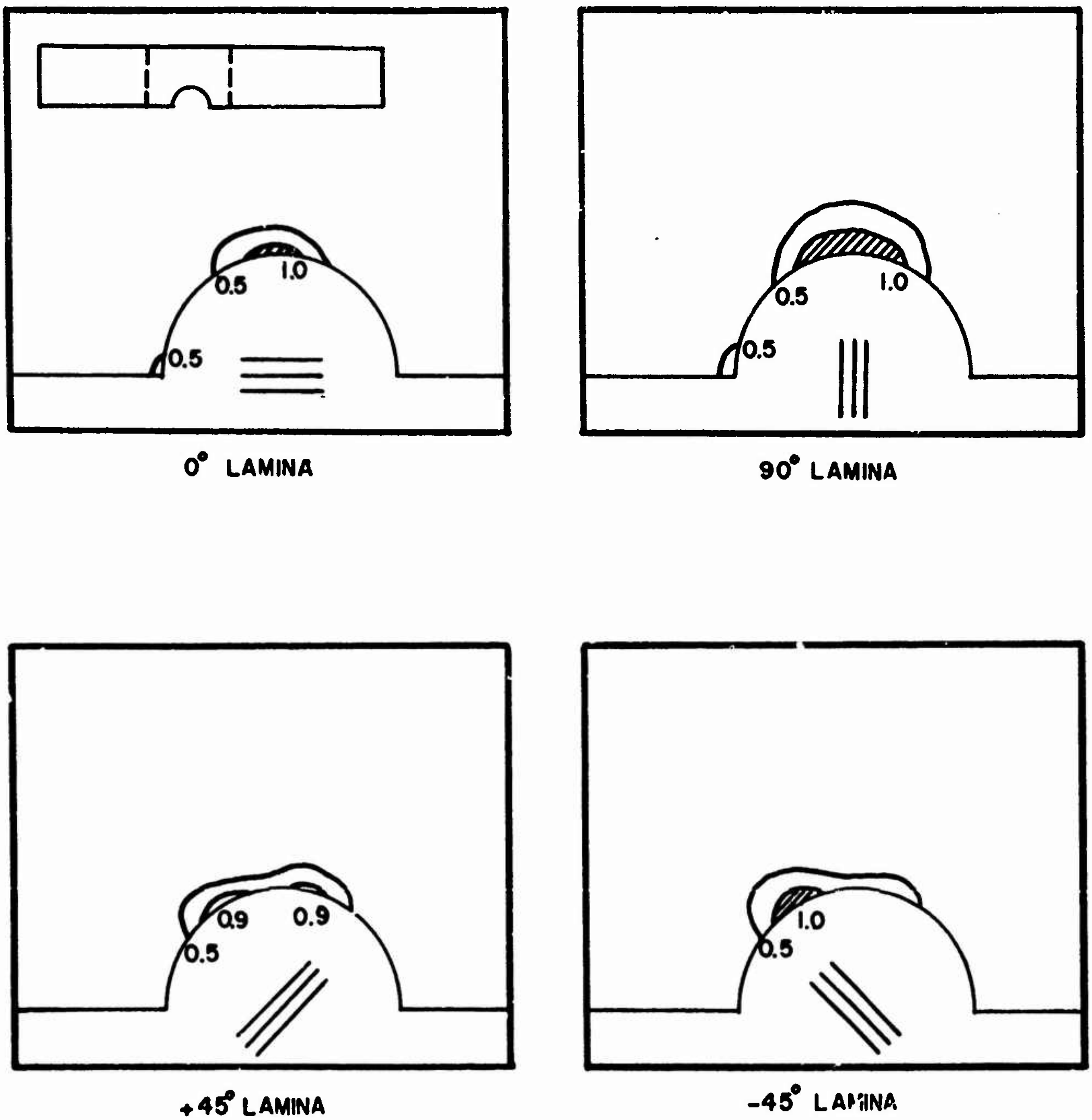

Figure 2b. Distortional Energy Contour Plots for the Revised Bolt Bearing Specimen Design at the Predicted Failure Load.

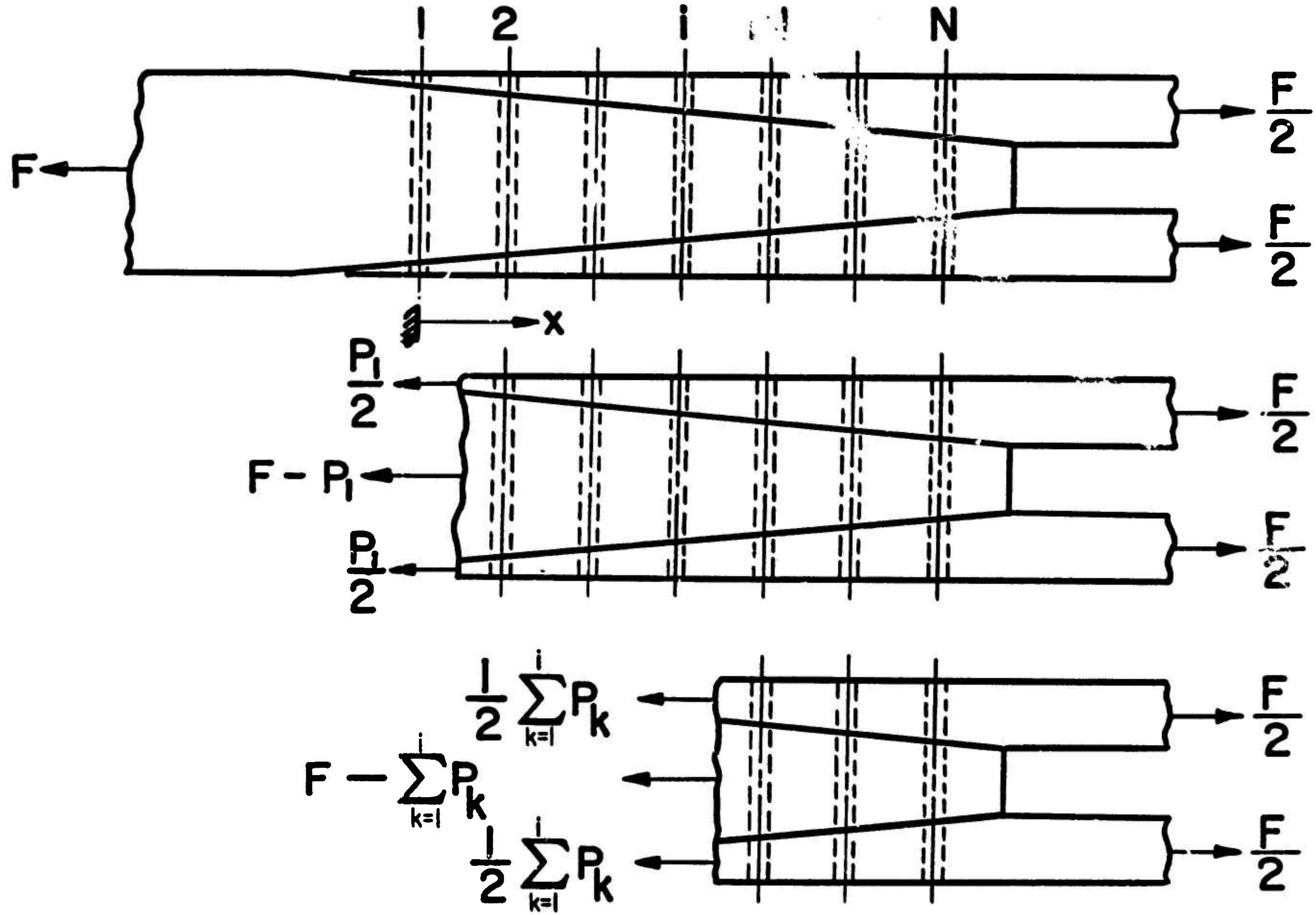

Figure 3. Double Shear Joint Configuration.

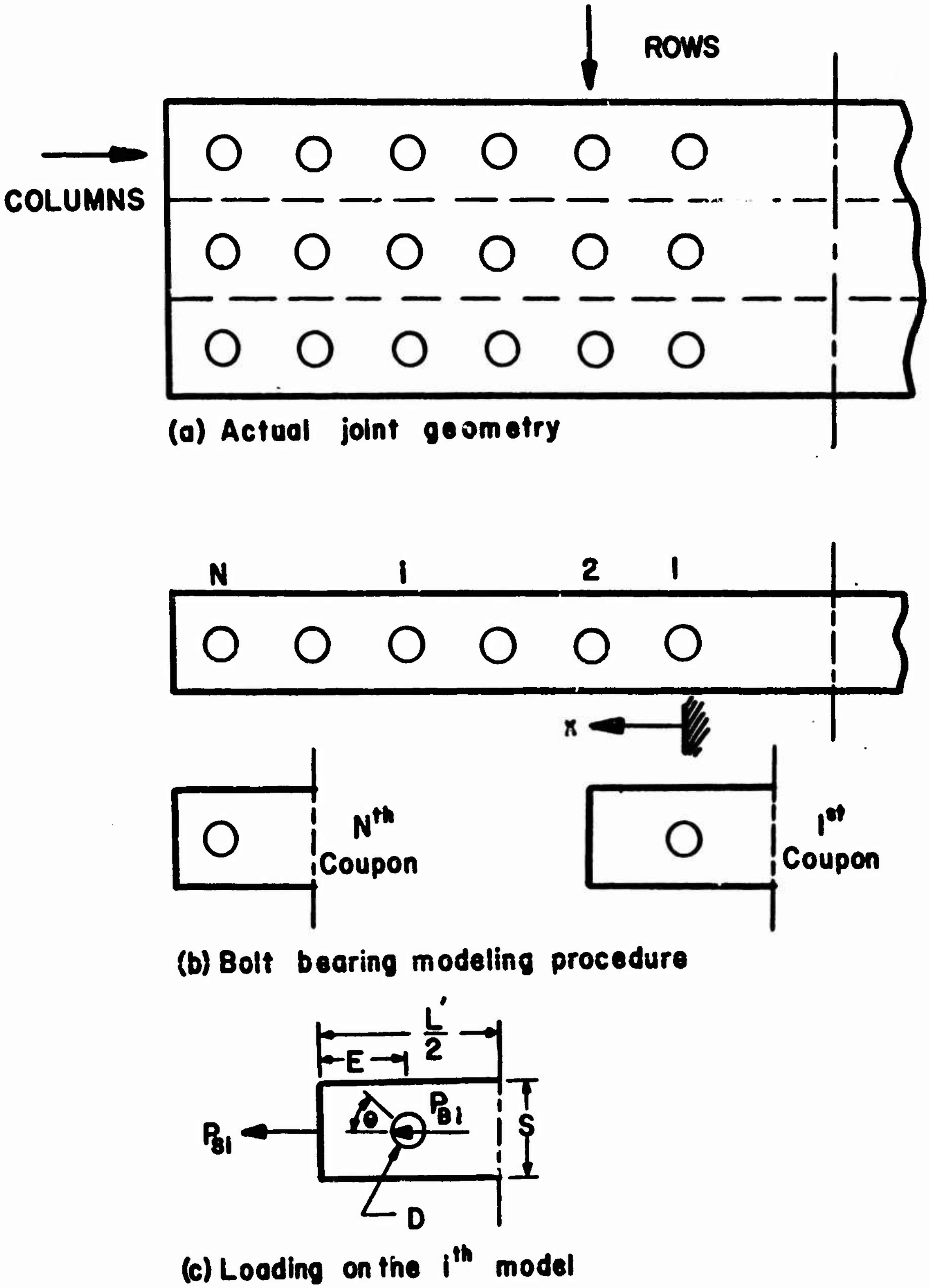

Figure 4. Bolt Bearing Modeling Procedure for Joints.

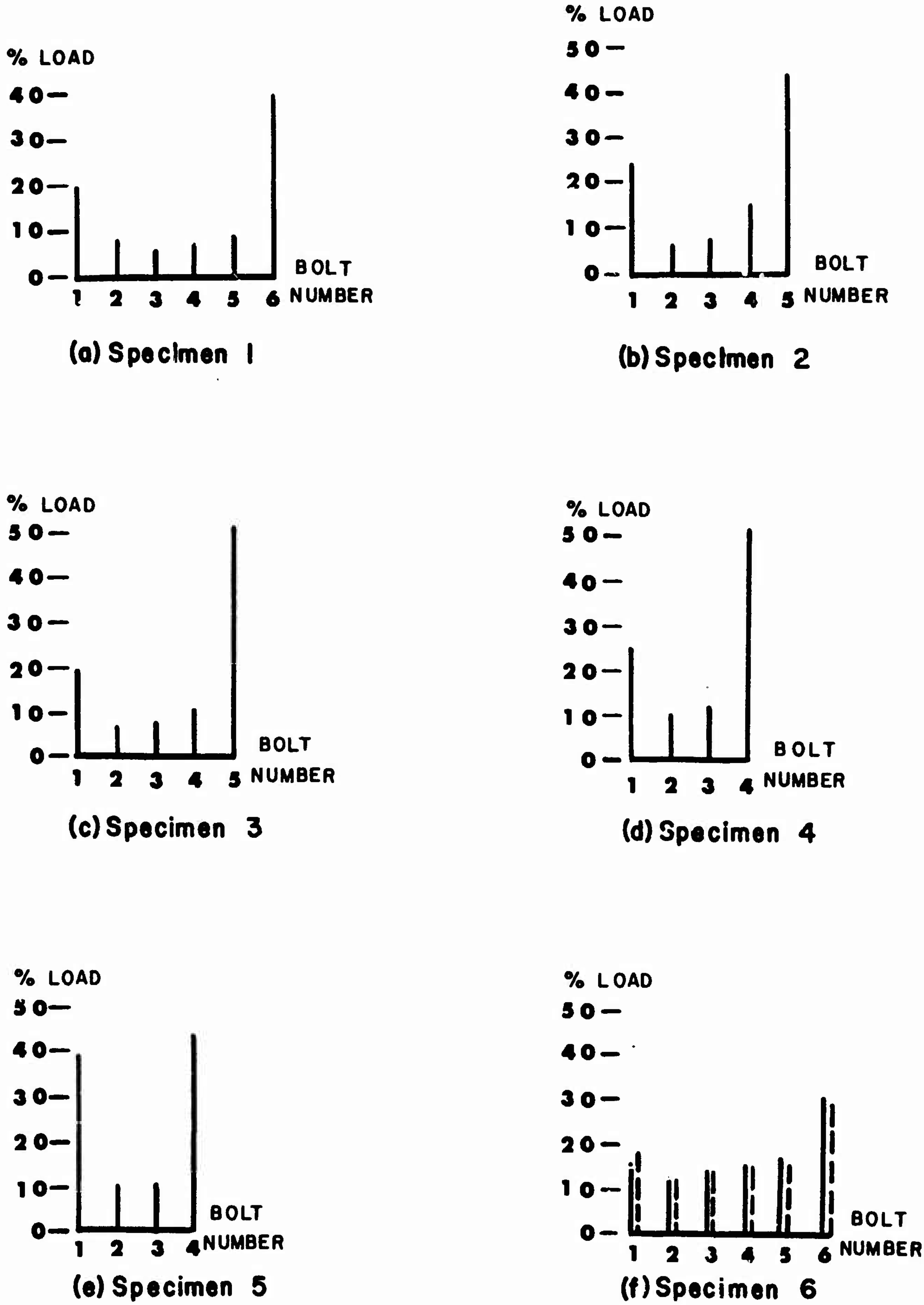

Figure 5. Bolt Load Distributions for Specimens 1 thru 6.

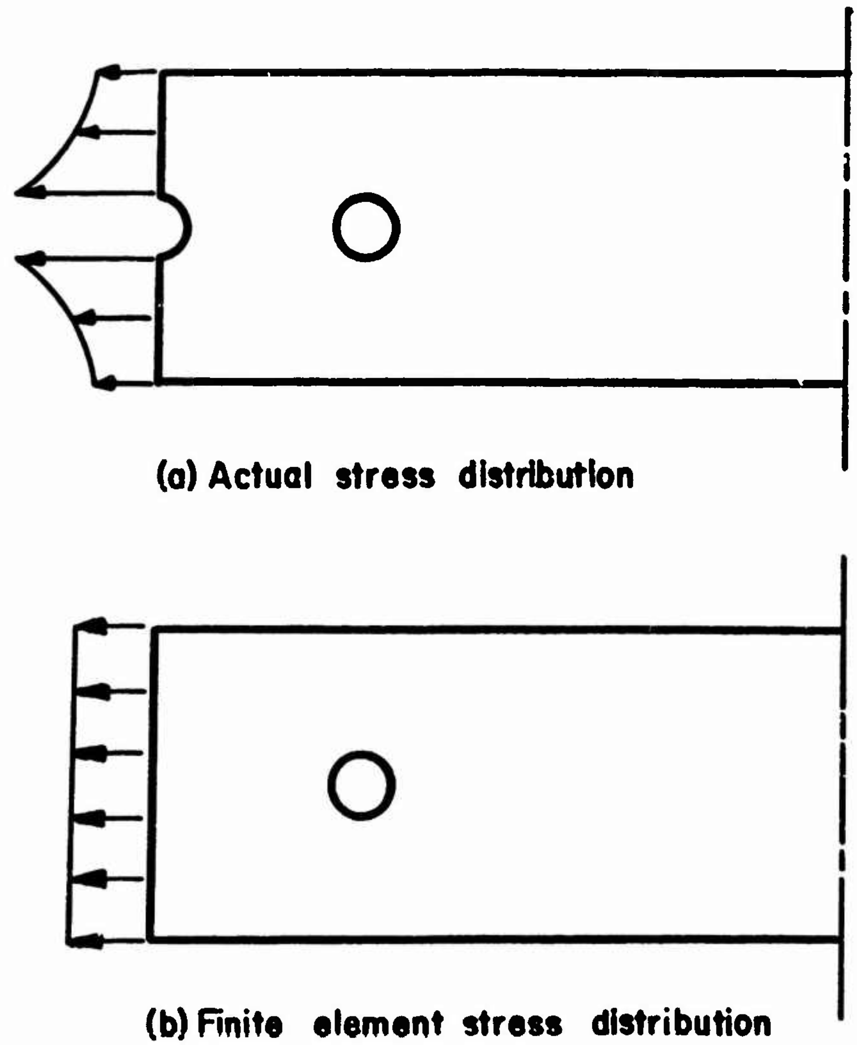

Figure 6. Skin Stress Boundary Conditions at the Leading Edge of a Bolt Bearing Model.

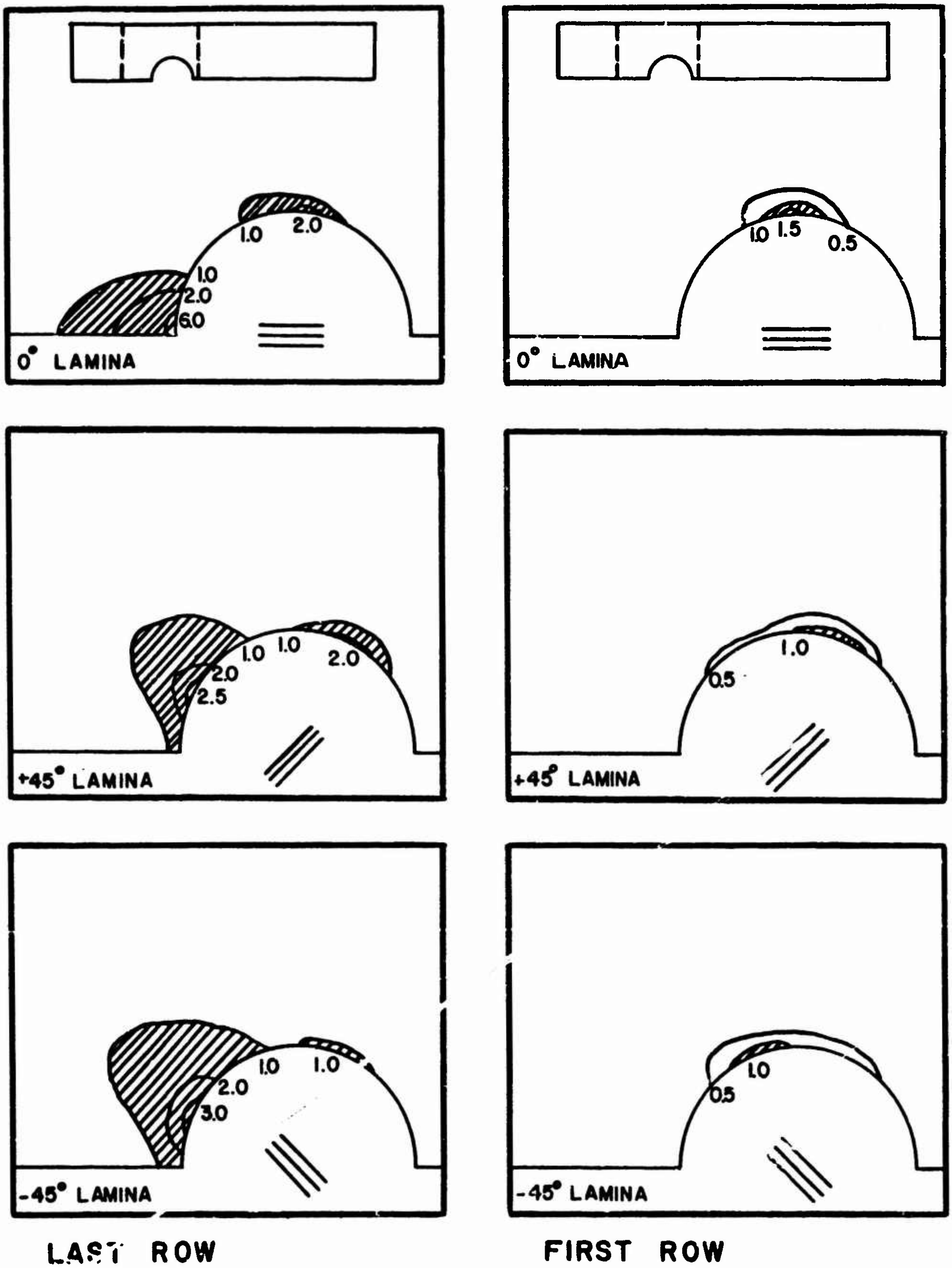

Figure 7. Specimen 1: Distortional Energy Contour Plots for the Experimental Failure Load.

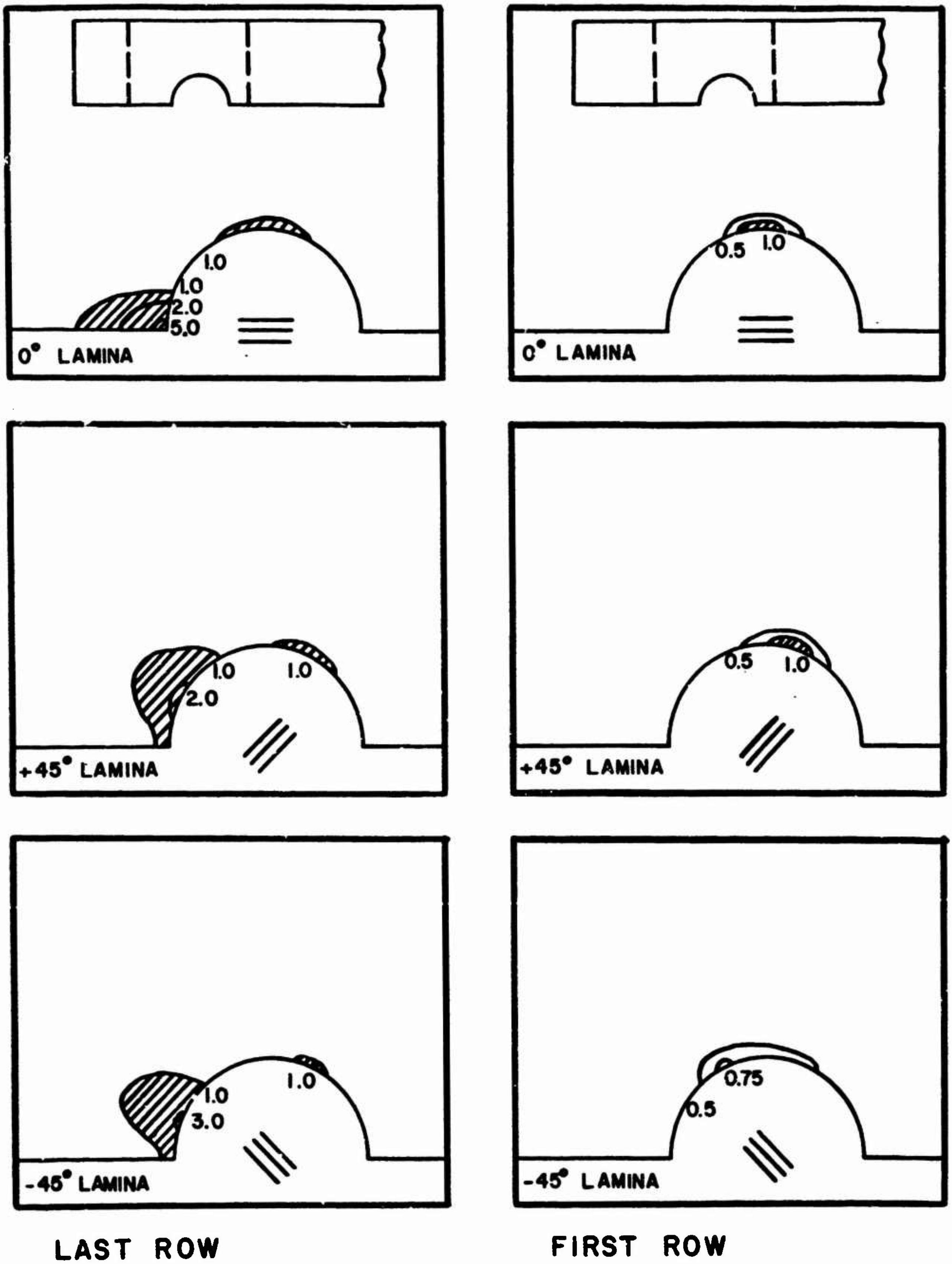

Figure 8. Specimen 2: Distortional Energy Contour Plots for the Experimental Failure Load.

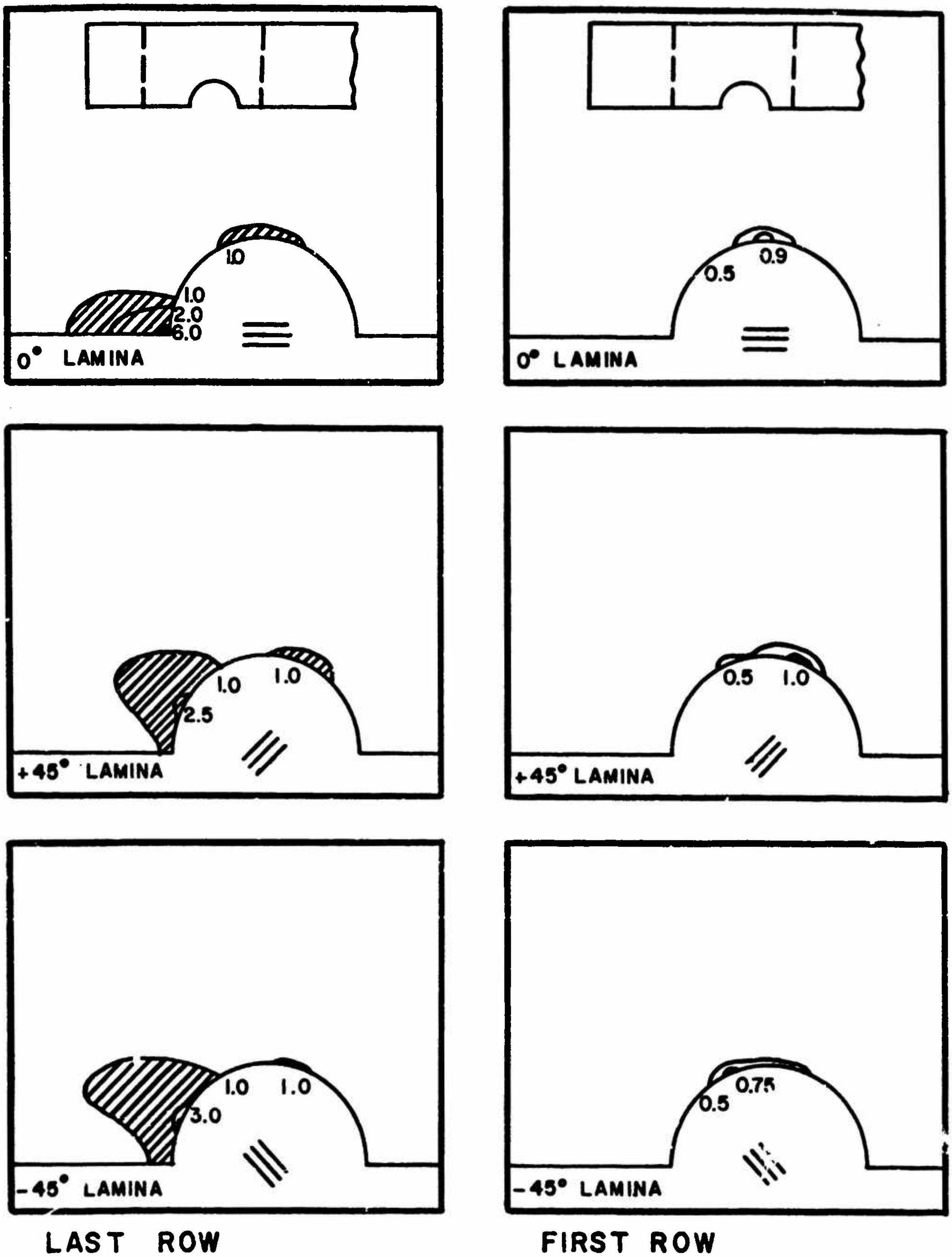

Figure 9. Specimen 3: Distortional Energy Contour Plots for the Experimental Failure Load.

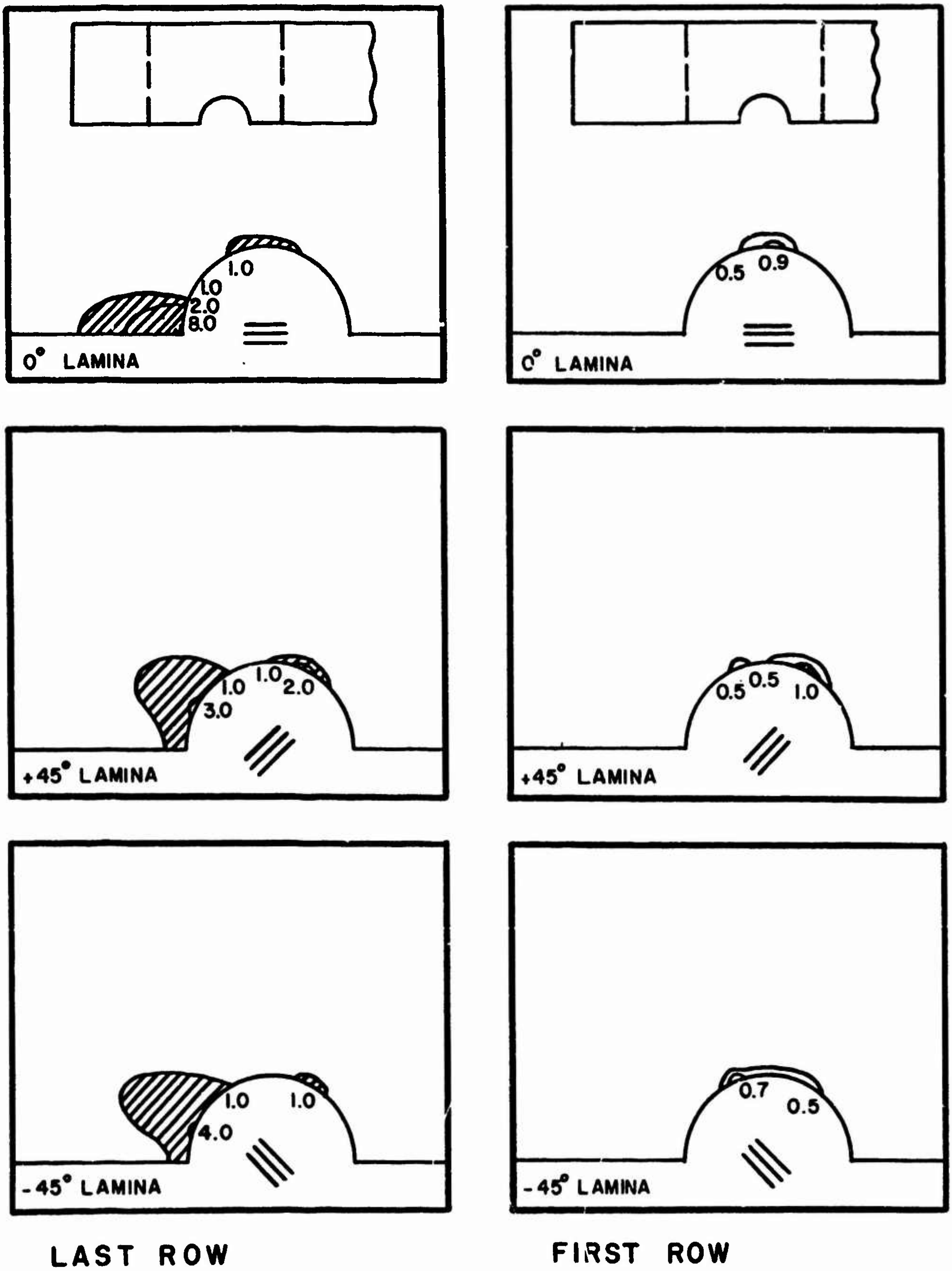

Figure 10. Specimen 4: Distortional Energy Contour Plots for the Experimental Failure Load.

Figure 11. Specimen 5: Distortional Energy Contour Plots for the Experimental Failure Load.

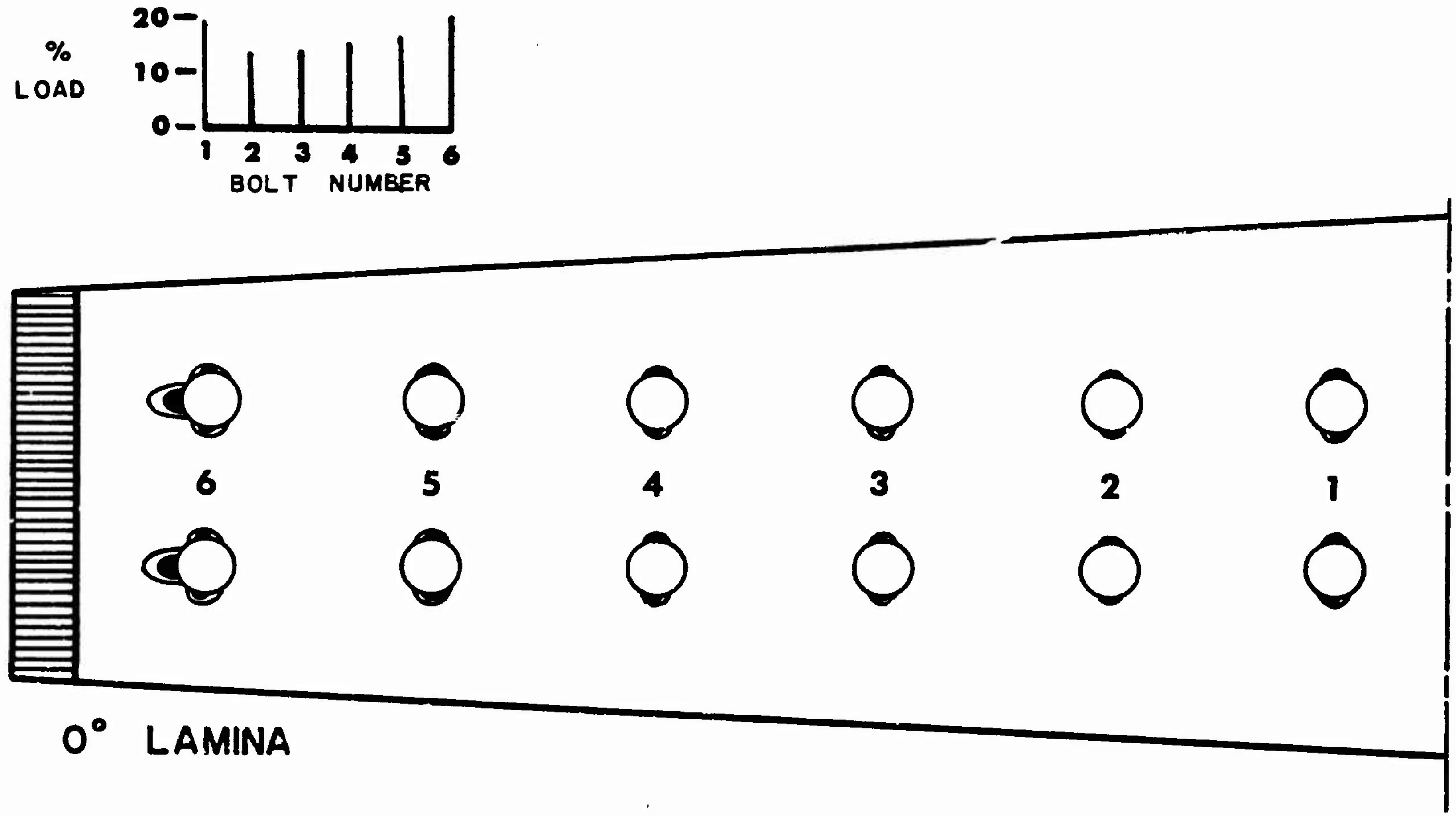

Figure 12a. Specimen 6: Distortional Energy Contour Plots for the Experimental Failure Load.

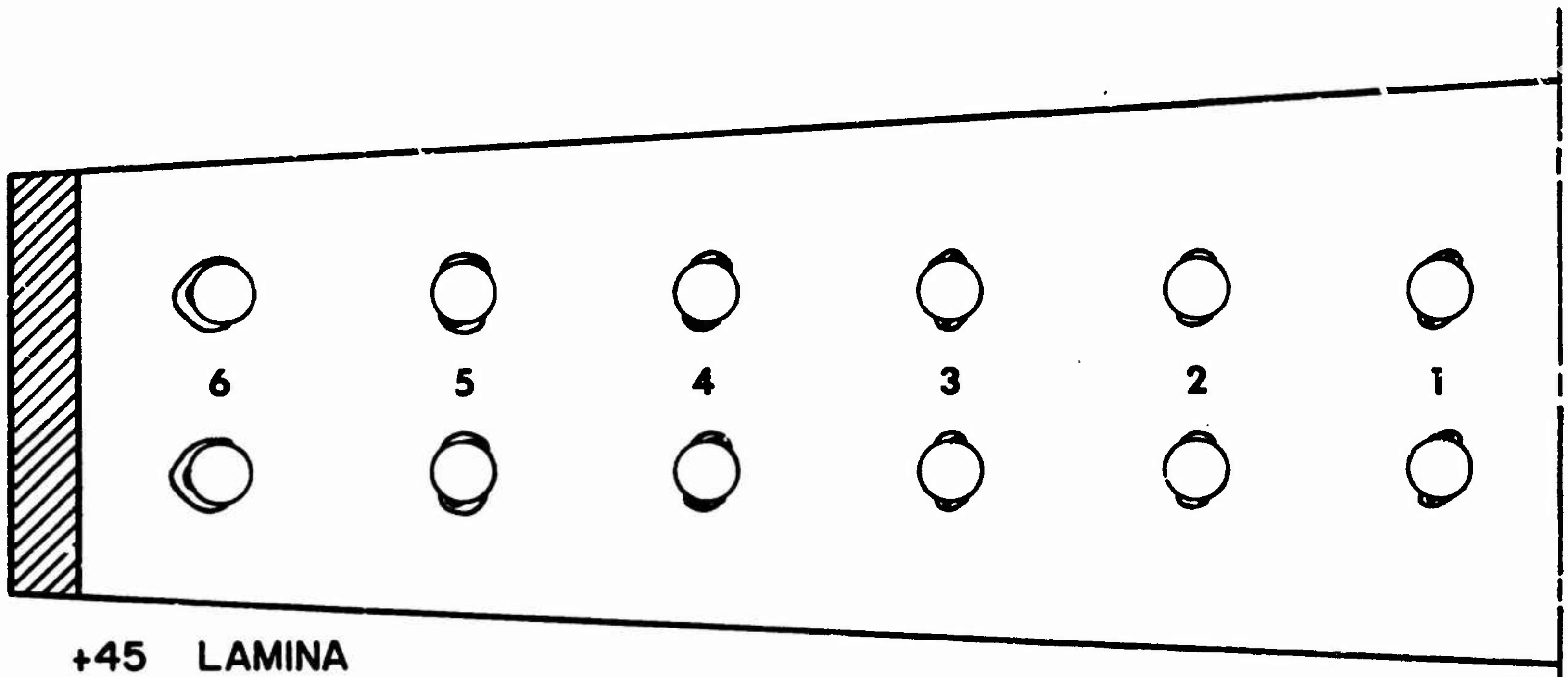

Figure 12b. Specimen 6: Distortional Energy Contour Plots for the Experimental Failure Load.

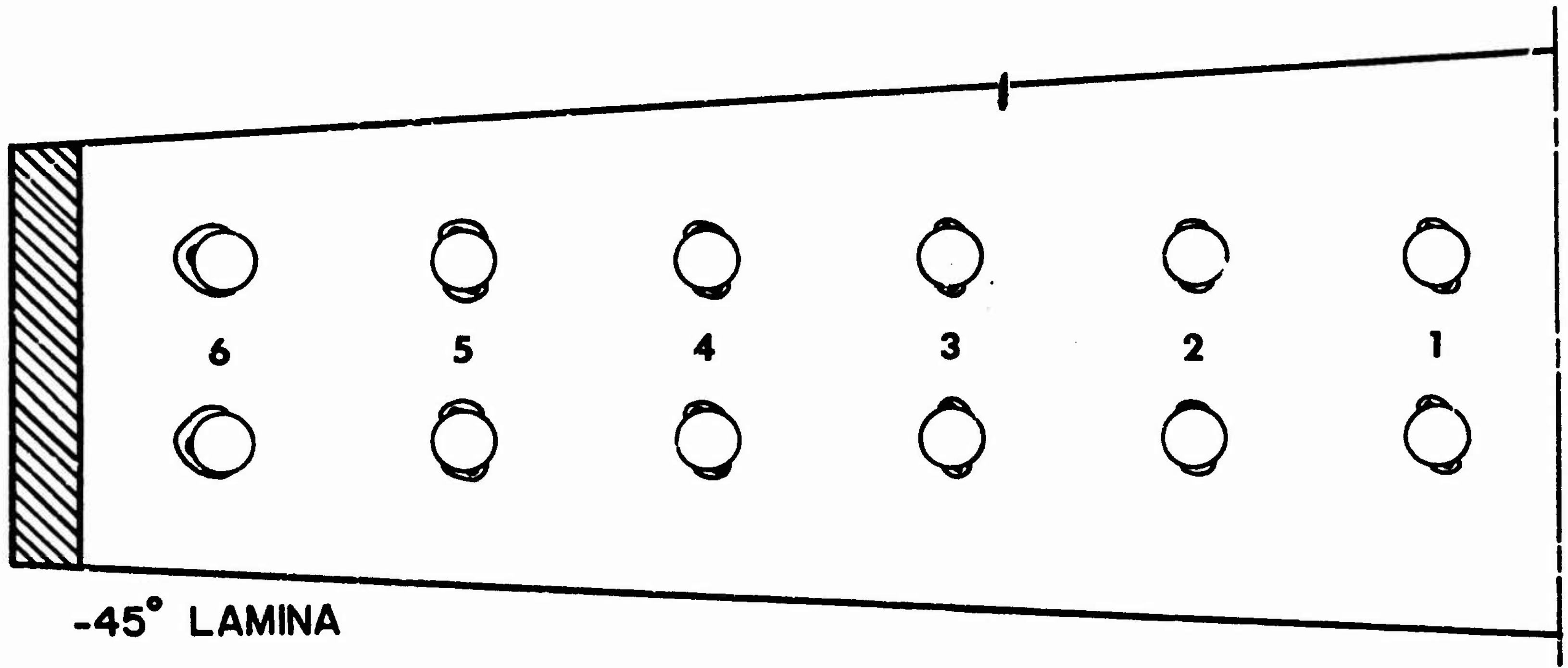

Figure 12c. Specimen 6: Distortional Energy Contour Plots for the Experimental Failure Load.

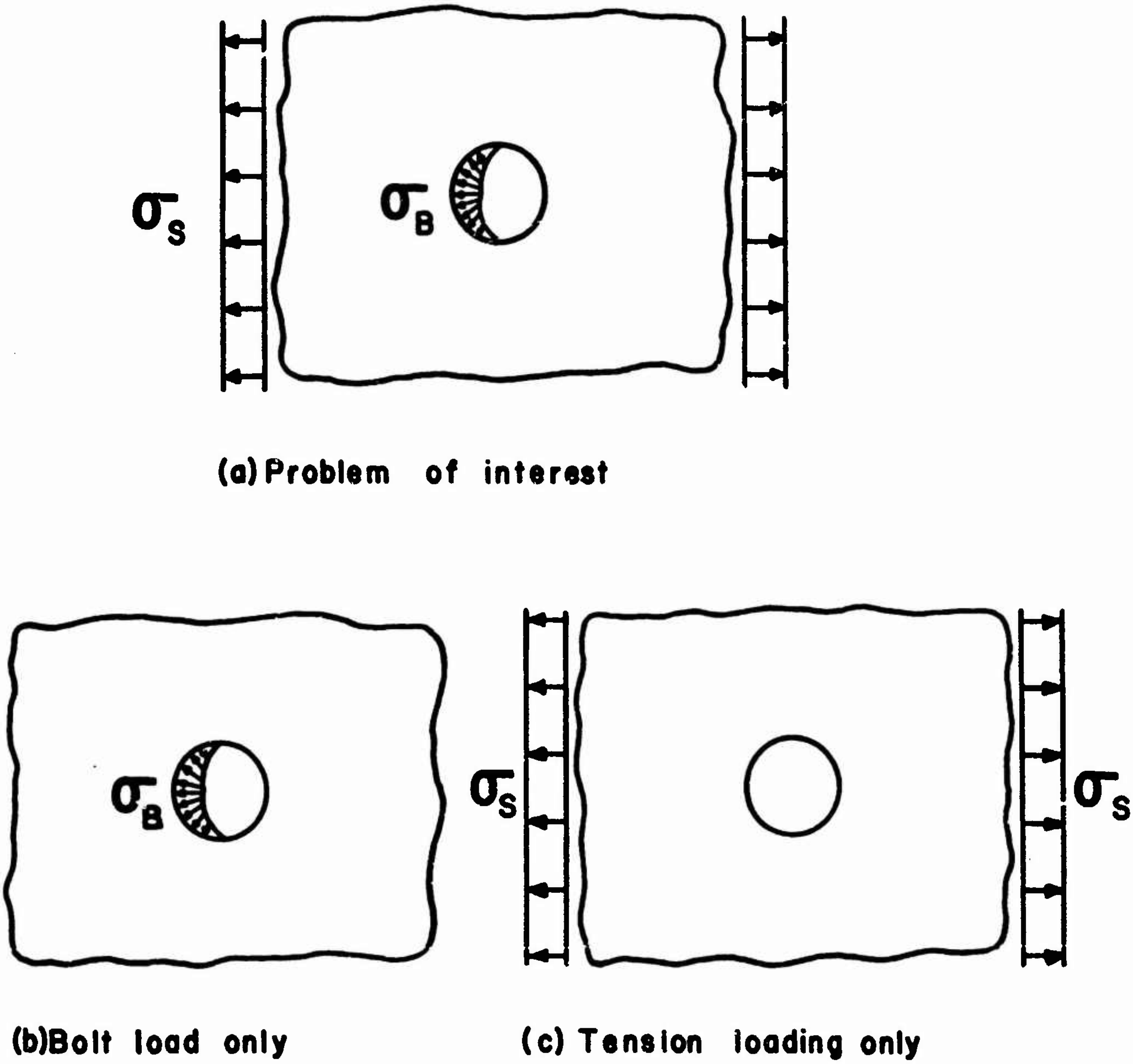

Figure 13. The Principle of Superposition Applied to an Infinite Bolt Bearing Model.

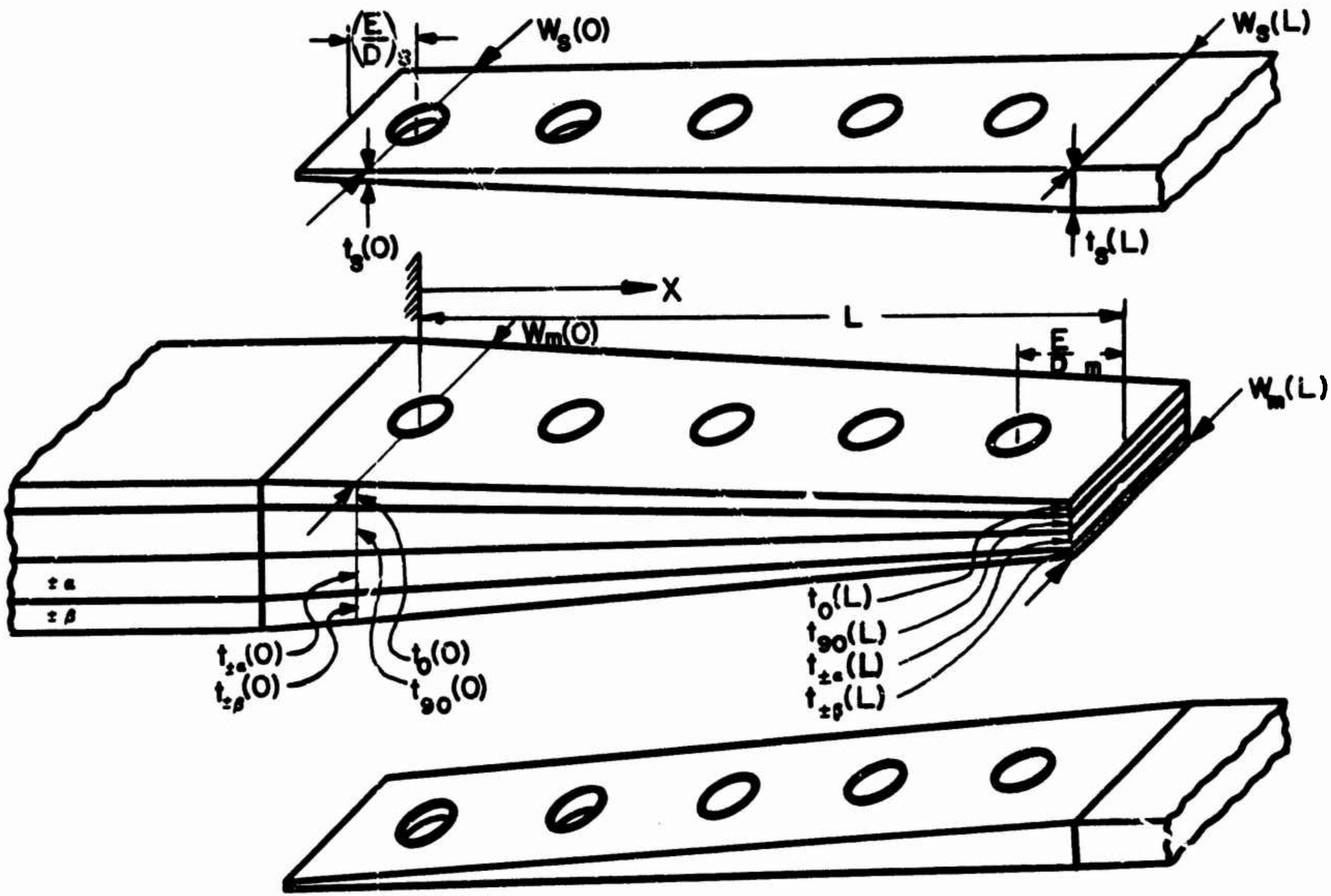

Figure 14. Schematic of a Proposed Joint Design Showing the Seventeen Possible Design Variables.

CHAPTER IV

OPTIMIZATION METHODS

4.1 *INTRODUCTION*

A computer program for optimization using non-linear programming by pattern search (OPTIM), written by Martin Schussel [1] was used for this study. Some time was spent studying this program and a sample problem was run (torsion of an elliptic bar). The time spent in finding the predicted result of this problem yielded much insight into optimization techniques and the OPTIM program itself.

The bolt-bearing problem was analyzed, using OPTIM, which included variation of the ply orientations. This study involved a problem with six variables and four constraints. For a given load, the minimum weight dimensions and orientations were found. The results of this study are discussed in some detail.

4.2 *STRUCTURAL OPTIMIZATION*

4.2.1 *Background*

The structural optimization project consisted of finding the minimum weight design of a structure for which certain limitations were posed. The limitations or constraints can be of the following form:

a) Geometric
- Maximum overall dimensions of the structure
- Maximum thickness, cross-section, length, width, etc. of an internal member
- Maximum deflection of a member
- Maximum rates of deflection

b) Mechanical - Yield criterion

- Failure modes
- Fatigue properties
- Natural frequencies
- Buckling loads

If the structure can be analytically solved for an internal stress state as a function of the external loads (given) and the dimensions of the piece (to be used as variables) then the problem becomes a mathematical one: Find the extreme values of a non-linear function of several variables, subject to one or several non-linear constraints. The function is usually the weight of the structure and the variables are its dimensions. The constraints can be in the form of equalities or inequalities. The equality constraints would generally concern a total dimension which is not fixed but is the sum of a number of internal dimensions. Inequality constraints are far more common, they usually insure that yield stresses, buckling loads, etc. are not exceeded.

4.2.2 Variational Method

There are several methods of mathematically solving the problem, but non-linear programming is the only reliable one. Graphical methods have a very limited use as they can only be used in two-dimensional problems. Transformation into a series of linear problems by use of Taylor series expansions is tedious and inaccurate. The use of penalty functions transforms the problem into an unconstrained minimization. Lagrange multipliers are an example; the formulation of the problem with Lagrange multipliers is as follows:

Assume we want to minimize a weight function $W(X_i)$ where X_i $(i = 1,...,N)$ are the variables. The constraints to be satisfied are

are $F_j(X_i) = 0$ ($j = 1,\ldots,M$). The Lagrange multipliers (λ_j) are added and we form an unconstrained objective function (P) to be minimized.

$$P = W(X_i) + \lambda_j F_j (X_i)$$

Now setting the derivatives to zero will find the extrema:

$$\frac{\partial P}{\partial X_i} = 0 \qquad i = 1,\ldots,N$$

$$\frac{\partial P}{\partial \lambda_j} = 0 \qquad j = 1,\ldots,M$$

The problem now requires the solution of N + M simultaneous non-linear algebraic equations in N + M unknowns. Solutions are difficult to find and are not unique, so this method is useless for large, complicated problems.

4.2.3 Non-linear Programming Methods

By far the most useful methods for solving non-linear optimization problems are searching techniques. There are many methods of search mentioned in the literature (pattern search, directed search, Fibonacci search, steepest ascent search), but basically they all consist of searching the domain of the variables until no further improvement can be found in the objective function.

Included in the Appendix of [2] are the listing and instructions for a pattern search optimization program (OPTIM) by Martin Schussel, Carnegie-Mellon University 1968. The program works in the following way: An objective function is defined:

$$P = COST + \Sigma\, A(K)\ (\ F(K)\ )^2$$

where COST = weight function

A(K) = penalty functions

F(K) = constraints

COST and F(K) which are functions of the variables (X(I)) are defined by the user of the program in a subroutine called CALC.

The program increases and decreases the variables and recalculates COST and F(K) until the improvement in the objective function is smaller percentagewise than 10^{-5}.

The program is best suited to handle inequality constraints (less than or equal) which it handles in the following way: If the constraint becomes negative during the search it is neglected, but if it becomes positive it is multiplied by a penalty (some large number A(K)). When the objective function is minimized the constraints will either approach zero or remain negative.

The application of optimization to design of structures using advanced fiber composite materials adds another facet to the problem. The orientations of the plies become variables as well as the dimensions. In some cases, the problem can be handled similarly to the above procedure with the orientations merely being additional variables. However, analytical equations for composite materials are difficult to derive and are usually not solvable in closed form. The bolt bearing problem was solved using empirical equations which relate the failure loads to the dimensions of the piece and ply orientations.

4.3 TORSION OF AN ELLIPTIC BAR — VARIATIONAL EXAMPLE

The problem is to find the values of the major and minor axes of an elliptic bar for minimum weight for a given applied torsional moment M. The weight is proportional to the cross sectional area

$$A = \pi ab \tag{1}$$

We want to minimize A, subject to the constraint that the allowable shear stress is not exceeded at any point. The maximum stress is at $y = b$, $x = 0$ and is given by

$$\tau_{max} = \frac{2M}{\pi a b^2} \tag{2}$$

If τ_y is the yield stress, the constraint equation becomes

$$\frac{2M}{\pi a b^2} - \tau_y \leq 0$$
$$\text{or } 2M - \pi a b^2 \tau_y \leq 0 \tag{3}$$

The solution was then sought using Lagrange multipliers. The results were incorrect since two more constraints must be added. The first one is due to the fact that the stress formula is only correct if a is larger than b.

$$b \leq a$$
$$b - a \leq 0 \tag{4}$$

We must also insure that b and a are positive for the answers to make sense. If we insure that b is positive, the first constraint allows a to be positive, thus the last necessary constraint is

$$b \geq 0 \tag{5}$$

We can now change the problem into an unconstrained minimization problem by the use of Lagrange multipliers and slack variables. The solution is to find an extreme value of a function F by variational methods where F is given by

$$F = \pi ab + \lambda_1 \left(\pi ab^2 - \frac{2M}{\tau_y} - \gamma^2\right)$$
$$\lambda_2 (a-b-\beta^2) + \lambda_3 (b - \delta^2) \tag{6}$$

where λ_1, λ_2, λ_3 are the Lagrange multipliers, and γ, β, δ are the slack variables used in inequality constraints. The derivatives of (6) with respect to each variable yields the following set of equations

$$
\begin{aligned}
\frac{\partial F}{\partial a} &= 0 = \pi b + \lambda_1 \pi b^2 + \lambda_2 \\
\frac{\partial F}{\partial b} &= 0 = \pi a + \lambda_1 2\pi ab - \lambda_2 + \lambda_3 \\
\frac{\partial F}{\partial \lambda_1} &= 0 = \pi ab^2 - \frac{2M}{\tau_y} - \gamma^2 \\
\frac{\partial F}{\partial \lambda_2} &= 0 = a - b - \beta^2 \\
\frac{\partial F}{\partial \lambda_3} &= 0 = b - \delta^2 \\
\frac{\partial F}{\partial \gamma} &= 0 = -2\gamma\lambda_1 \\
\frac{\partial F}{\partial \beta} &= 0 = -2\beta\lambda_2 \\
\frac{\partial F}{\partial \delta} &= 0 = -2\delta\lambda_3
\end{aligned}
\tag{7}
$$

Since $\beta=0$, (4) gives $a=b$ (circular section); Eqn (3) gives $\pi ab^2 = \frac{2M}{\tau_y}$ for $\gamma=0$. Since $a=b$, we have $\pi a^3 = \frac{2M}{\tau_y}$ and thus

$$
a = [2M/\pi\tau_y]^{1/3} \tag{8}
$$

The problem was also solved using the optimization computer program (OPTIM). First the problem was attempted using only the first constraint and a minimum was found with b about twice the size of a. This violated the condition that a be greater than or equal to b for the stress equation to apply. Next all three constraints were used and the minimum was found to agree with the analytical result (8). Thus we conclude that inclusion of *all* constraint relations is absolutely essential for success.

4.4 *BOLT BEARING PROBLEM – NON-LINEAR PROGRAMMING EXAMPLE*

The problem consists of finding the minimum weight of plates loaded by bolted joints. The specimen appears as shown below:

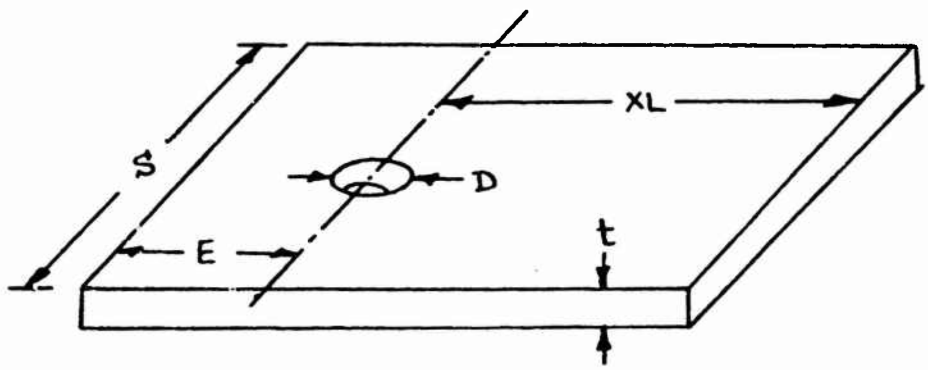

XL is a constant

D is chosen as .375 in.

The weight of the specimen is:

$$W = \rho(XL + E)S\ t \tag{9}$$

The weight of the material which would be in the hole is included since it must be wasted. Empirical equations [3] for the three failure modes found in experiments are as follows:

Tension

$$P \leq .69\ t(S-D)F^{tu} \tag{10}$$

where P = applied load and P cannot exceed the expression on the right. The symbol F^{tu} is defined as:

$$F^{tu} = \frac{157L + \left(\dfrac{20.7N^2}{3M + N}\right)}{1+.0538\left[4\dfrac{M}{L} - \left(\dfrac{M}{L}\right)^2\right]} \qquad \text{for } \frac{M}{L} \leq 2$$

$$F^{tu} = 129L + 27N - \frac{N(10N + 162L)}{3M + N} \qquad \text{for } \frac{M}{L} > 2 \tag{11}$$

where $L = \%\ 0°$ plies

$M = \%\ 90°$ plies

$N = \%\ \pm 45°$ plies

The constraint for this failure mode is $F(1) = P - .69\ t(S-D)F^{tu}$. If this quantity stays negative then P is below failure load. If it is near zero, failure in this mode is impending. The problem was treated from two different viewpoints.

First the orientation percentages L, M, and N were held constant and the dimensions for minimum weight of the specimen were found. The answer in this case yields the optimum dimensions for the orientations chosen.

The second way of treating the problem was to leave the orientations as variable. This way, both the dimensions and the orientations were optimized. The results showed a 20-30% improvement over the fixed orientations case. The orientations chosen were those of an experimental specimen which failed at P = 1020 lb. The program gave a weight reduction for failure at the same load and with the same orientations.

The problem also included equations for failure in two other modes-shear out and bearing. These were the second and third constraints. The failure mode in a given problem is found by checking which of the three constraints is closest to zero. The constraints are

Shear Out

$$P \leq 2tEF^{su} \qquad (12)$$

$$F(2) = P - 2tEF^{su}$$

where

$F^{su} = 40N \qquad N \geq .23$

$F^{su} = 9.2 \qquad N < .23$

Bearing

$$P \le \frac{Dt}{4} (1 + .45 \frac{D}{t}) F^{bu}$$

$$F(3) = P - \frac{Dt}{4} (1 + .45 \frac{D}{t}) F^{bu} \qquad (13)$$

where

$$F^{bu} = L F^{L} + (M + N)F^{M}$$

$$\text{if } L \ge .25 \qquad F^{L} = 600, \; F^{M} = 30$$

$$L \le .25 \qquad F^{L} = 450, \; F^{M} = 80$$

The results of the program for fixed orientations are shown in Table I.

Choose L = 18.2% (0° plies)

M = 9.1% (90° plies)

N = 72.7% (±45° plies)

The orientations in Table I were chosen because test data was available for a failed specimen. The specimen failed at 1000 lbs. and had the dimensions shown below:

P	THK	EDGE	SIDE	COST
1000	.056	.50	1.0	.044

The optimum dimensions for P = 1000 give COST = .039 (10% wieght reduction).

Table II contains the results of the analysis for the case of using the orientations as variables. Surprisingly, the optimum orientations do not change for different loads.

The orientations were allowed to vary between .10 and .80 in the above procedure.

The results in Table III were found for variable orientations with the possibility of eliminating certain plies. There is some doubt of the applicability of the equations for less than 10% of any of the plies, but it is informative to see what will happen in this case.

The results for all three cases are plotted together for comparison in Fig 3.

4.5 DISCUSSION

The OPTIM program has proven to be very effective in dealing with problems for which analytical equations can be derived. The elliptic bar and bolt bearing problems treated above are examples.

The bolt-bearing problem is unusual for composite materials in that analytical equations are available which allow us to optimize both the dimensions and the lamina orientations. The equations are empirical and therefore introduce doubt as to their accuracy. There also may be ranges of dimensions or orientation percentages in which they are not applicable.

Table I shows optimum dimensions for varying load with the ply orientations fixed. The case of P = 1000 lb. shows a 10% weight reduction over the experimental specimen. The values of the constraints show this to be a simultaneous failure in tension and shear out. The cases of P (applied load) between 3000 lbs. and 15,000 lbs. show failure in all three modes simultaneously. There is no apparent pattern in the variation of optimum dimensions with load. The weight is seen to vary non-linearly with load as can be inferred from Fig 1.

If we allow the orientation percents to vary between 10% and 80% the optimum laminate will be found with respect to both dimensions and orientations. OPTIM found values of five of the six variables which were optimum for all loads considered. Only the total thickness changed and it varied linearly with load. This situation forced the weight to vary linearly with load also as seen in Fig 2. For each load, the specimen exhibited failure in tension and shear out simultaneously with bearing failure not being a factor. The orientations chosen for each load were L = 73%, M = 17%, N = 10%. The fact that N was brought to the minimum of its range led to the results in Table 3 where N was allowed to vary between 0% and 80%. The results are similar to those in Table 2 except that N goes to zero with L and M increasing proportionately. As noted, the equations may not apply for N less than 10%, but the results indicate that the ±45° laminae are of little benefit in the bolt bearing specimen. The thickness and weight vary linearly with load as in the previous case. All three cases are plotted in Fig 3. The variable orientation case shows an improvement on the fixed case of between 30% and 100%, with the case for N = 0 about 15% better still.

The results show a useful and convenient relationship for design. The designer is given the optimum orientations and side and edge distances and he merely chooses his thickness to suit the load which must be carried. The empirical nature of the equations suggests that experiments should be run to verify the derived results before putting them into use as a design criterion.

4.6 *REFERENCES*

[1] M. D. Schussel, "Optimization by Pattern Search Program Description and Usage Instructions", prepared for GE-580, Department of Mechanical Engineering, Carnegie-Mellon University (1968).

[2] S. J. Marulis, "Optimization of Advanced Composite Plates", Report SM-71, Department of Mechanical Engineering, Carnegie-Mellon University, Pittsburgh, Pennsylvania (June 1971).

[3] Advanced Composite Wing Structures, Boron-Epoxy Design Data — Volume II, Grumman Aerospace Corporation, 180-186, TR-AC-SM-ST-8085 (November 1969).

Table 1: Coupon Weights for Fixed Orientations

P (LOAD)	THICKNESS	EDGE DIST.	SIDE DIST.	F(1) TENSION FAILURE	F(2) SHEAR OUT FAILURE	F(3) BEARING FAILURE	COST (WEIGHT)
1000	.014	1.31	3.42	-.0061	-.0093	-1485.	.039
3000	.048	1.07	2.87	-.0024	-.00073	-.144	.115
7500	.374	3.45	1.18	-.037	-.028	-.169	.342
10,000	.559	.31	1.09	-.0[illegible]1	-.20	-.210	.473
15,000	.916	.28	1.03	-.069	-.58	-.484	.729

Table 2: Coupon Weights for Variable Orientations

P (LOAD)	THICK NESS	EDGE DIST.	SIDE DIST.	F(1) TENSION FAILURE	F(2) SHEAR OUT FAILURE	F(3) BEARING FAILURE	L %0°	M %90°	N %±45°	COST (WEIGHT)
1000	.016	3.32	1.52	-.0098	-.0068	-6602.	.72	.18	.10	.025
3000	.050	3.34	1.49	-.0013	-.019	-6207.	.74	.16	.10	.075
5000	.082	3.29	1.53	-.013	-.028	-5547.	.73	.17	.10	.124
7500	.125	3.31	1.51	-.0023	-.010	-4808.	.73	.17	.10	.186
10,000	.167	3.30	1.49	-.061	-.018	-5685.	.72	.18	.10	.251
15,000	.243	3.35	1.50	-.0033	-.071	-2350.	.74	.16	.10	.373

Table 3: Coupon Weights Allowing Orientations to be Eliminated

P (LOAD)	THICKNESS	EDGE DIST.	SIDE DIST.	F(1) TENSION FAILURE	F(2) SHEAR OUT FAILURE	F(3) BEARING FAILURE	L %0°	M %90°	N %±45°	COST (WEIGHT)
1000	.015	3.60	1.32	-.00084	.000	-7060	.77	.23	.00	.0207
3000	.049	3.34	1.23	-.0024	-.0011	-6846	.80	.20	.00	.0607
5000	.072	3.78	1.39	-.042	-.011	-5841	.79	.21	.00	.1014
7500	.109	3.71	1.32	-.039	-.0019	-5143	.80	.20	.00	.1506
10,000	.143	3.82	1.41	-.016	-.018	-4196	.80	.20	.00	.2008
15,000	.217	3.73	1.34	-.056	-.0021	-6032	.80	.20	.00	.3073

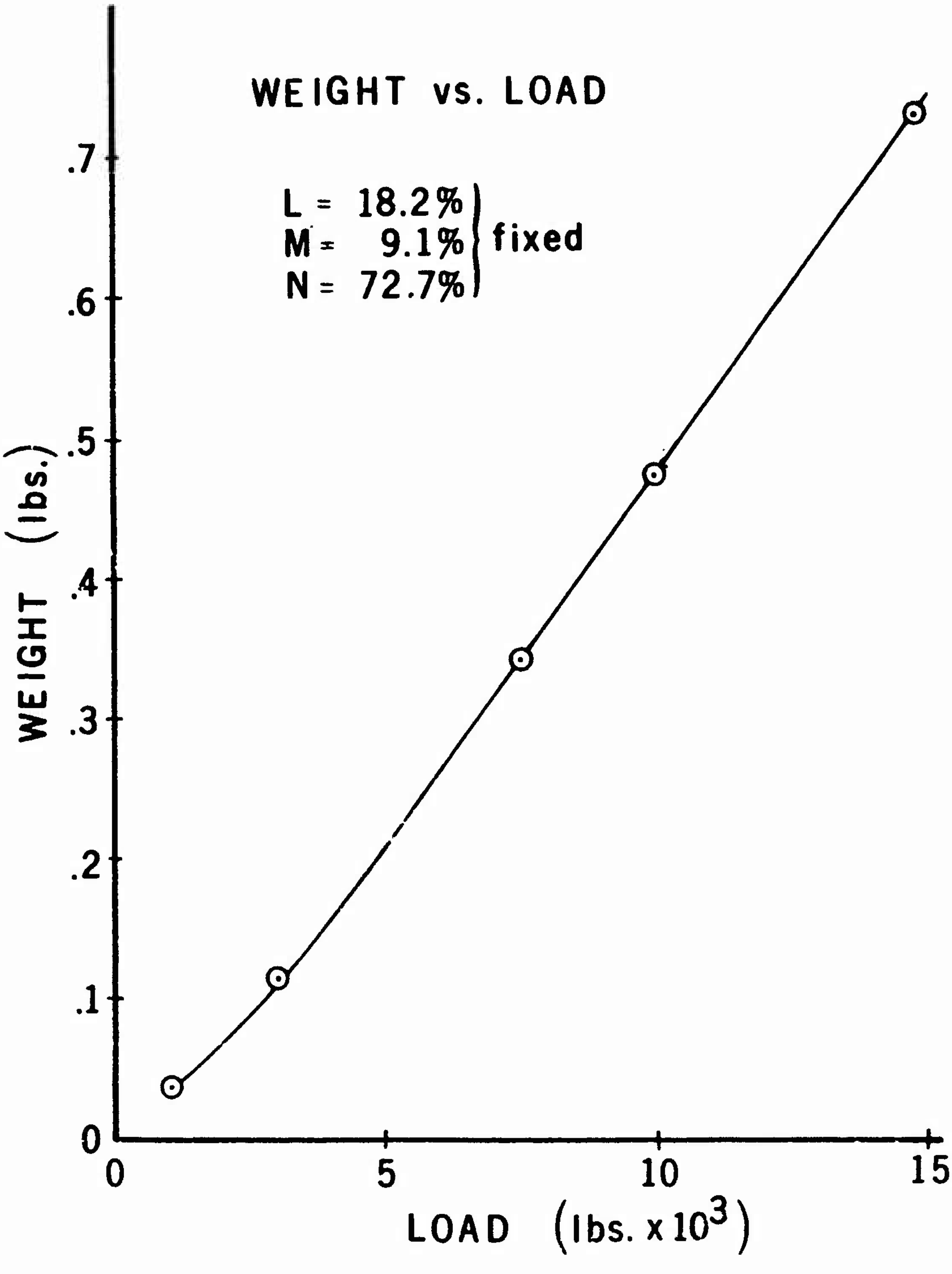

FIGURE 1: WEIGHT VS. LOAD FOR FIXED ORIENTATIONS

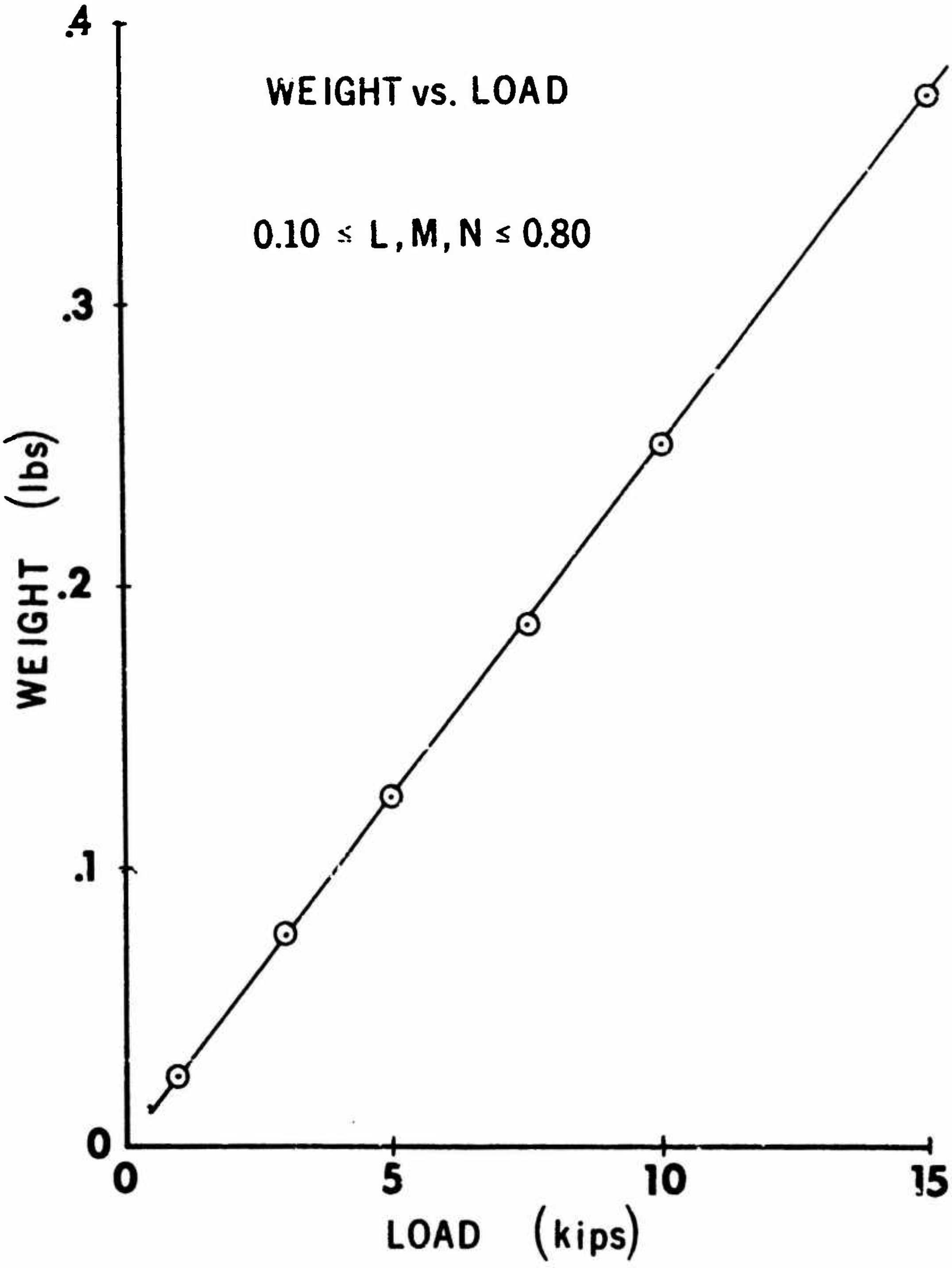

FIGURE 2: WEIGHT VS. LOAD FOR VARIABLE ORIENTATIONS

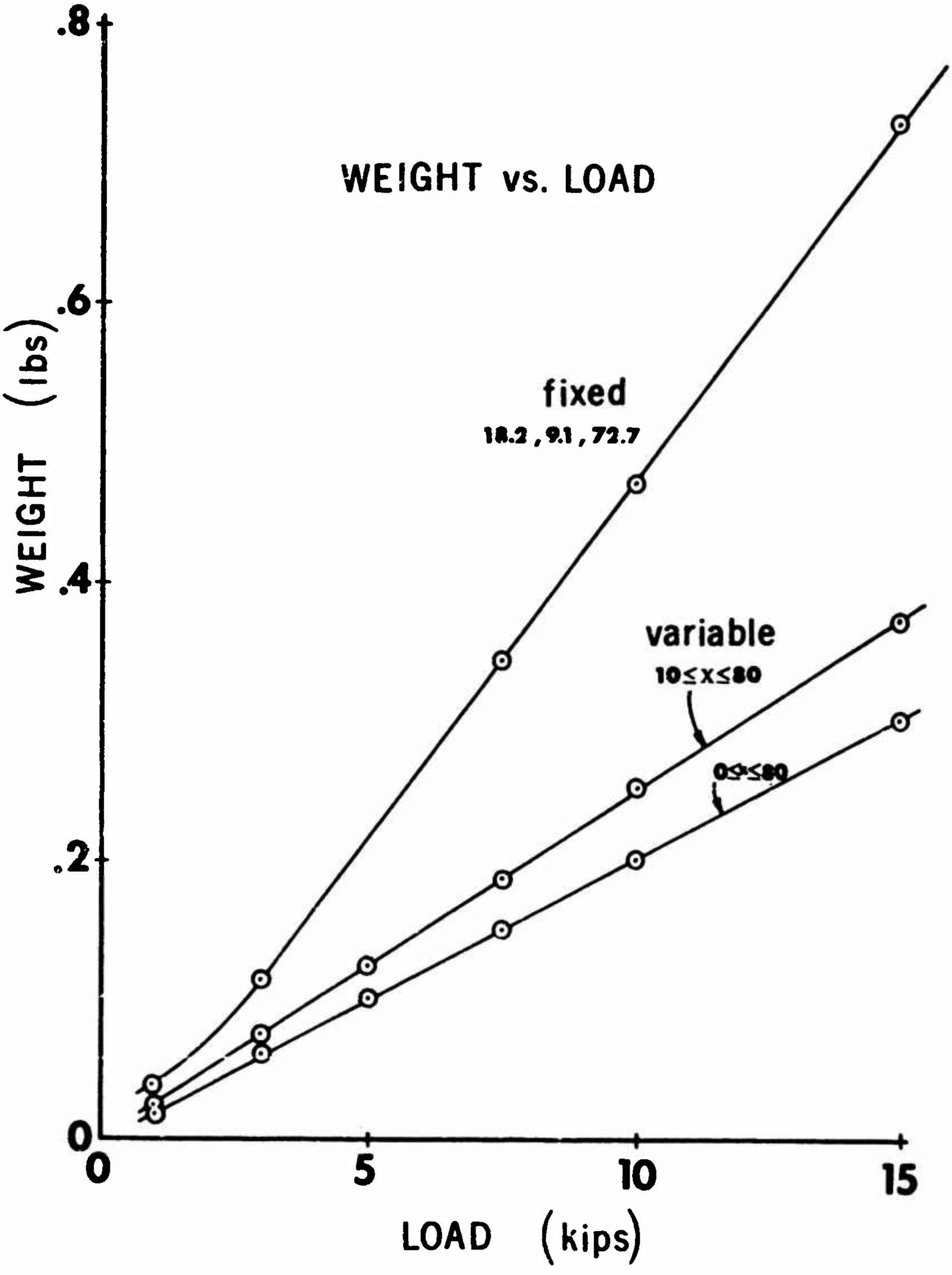

FIGURE 3: SUMMARY OF WEIGHT VS. LOAD RESULTS

CHAPTER V

BOUNDARY-INTEGRAL EQUATION SOLUTION METHODS

5.1 *TWO DIMENSIONAL ISOTROPIC BOUNDARY-INTEGRAL EQUATION METHOD*

5.1.1 *Introduction*

The boundary-integral equation method is a new tool for the solution of many problems in solid mechanics. The method has significant advantages over the finite element method. Numerical approximations are not made over the field but over the surface, thereby increasing accuracy. The dimension of the problem is reduced by one, allowing many problems too large for today's computers to be solved. Both of these features permit the analyst to obtain highly refined data in the vicinity of stress concentrations such as near cracks and notches.

Important to the user of the boundary-integral equation (BIE) method, is the ease of data preparation and the rapidity of solution. The BIE method utilizes a numerical solution of a boundary constraint equation. This equation relates all of the surface displacements to all of the surface tractions. The analyst specifies how he wishes to subdivide the surface and specifies the boundary data; all well-posed problems are acceptable including mixed-mixed problems. The geometry is completely general and may be multiply-connected. Once the surface solution is found the stresses may be generated at *any* points that the analyst desires on the interior of the region.

The BIE method has been widely adapted to many problems in solid mechanics, as can be seen by the literature [1-8]. The purpose for presenting it in this report is twofold. First, the tool is being developed by the CMU team for two dimensional, anisotropic problems for use in several on-going research efforts. Second, it is desirable to make the method available to the widest possible group of users. Listings of both the isotropic and anisotropic computer programs are therefore contained in this Chapter.

5.1.2 Review of the Isotropic Boundary-Integral Equation Method

Two elements are required for the development of the boundary constraint equation of the BIE method. The first is a reciprocal relation between two solution states (Betti's reciprocal work theorem); the second is a fundamental solution or influence function (Kelvin's problem of a point load in an infinite body). The development herein follows that used in classical potential theory (see, for example, [9-13]).

The solution to Kelvin's problem consists of displacement vectors in each of the x_j directions due to concentrated loads applied in the x_i directions. These solutions are denoted by the displacement tensor U_{ij}; the appropriate forms can be found in the literature [1-10]. In two dimensional, isotropic, elastostatics this tensor is

$$U_{ij}(P,Q) = -[\ell n(1/r(P,Q))\ (3-4\nu)\delta_{ij} + r_{,i}r_{,j}]/8\pi\mu(1-\nu) \tag{1}$$

In (1) the distance between the point of load application $P(x)$ and the field point $Q(x)$ is denoted $r(P,Q)$; μ and ν are the shear modulus and Poisson's ratio. The derivative of $r(P,Q)$ in the x_i direction is denoted

$$r_{,i} = \frac{\partial r}{\partial x_i|_Q} = \frac{x_i|_Q - x_i|_P}{r(P,Q)} \tag{2}$$

It is easily shown that (1) satisfies Navier's equation of equilibrium

$$(1/1-2\nu)u_{i,ij} + u_{j,ii} \tag{3}$$

A second tensor is required for the use of the reciprocal work theorem: the tractions corresponding to the U_{ij} on the physical surface ∂R of the body. These tractions, T_{ij}, are obtained by using Hooke's law and the definition of the traction vector

$$t_i = \sigma_{ij}n_j = \mu[(2\nu/1-2\nu)u_{k,k}\delta_{ij} + u_{i,j} + u_{j,i}]\, n_j \tag{4}$$

Utilizing (1) and (4) the traction tensor T_{ij} is found

$$T_{ij} = \{\partial r/\partial n[(1-2\nu)\delta_{ij}+2r_{,i}r_{,j}]+(1-2\nu)(n_i r_{,j}-n_j r_{,i})\}/4\pi(1-\nu)r(P,Q) \tag{5}$$

After some amount of manipulation of the reciprocal work theorem and letting P,Q be boundary points (P *not at a corner*) the following boundary constraint equation can be found

$$u_i(P)/2 + \int_{\partial R} u_j(Q)T_{ij}(P,Q)dS(Q) = \int_{\partial R} t_j(Q)U_{ij}(P,Q)dS(Q) \tag{6}$$

In (6) u_i, t_i are the displacements and tractions on the physical surface ∂R for the problem to be solved.

The numerical solution to (6) is obtained by discretizing the boundary and boundary data in some suitable fashion. Presently the displacements, u_i, and tractions, t_i, are taken as piecewise constant over each of N boundary segments. Work is well underway to use linear variations. The boundary segments are assumed to be flat in the programs used by this investigator. This allows for a completely general computer program for arbitrary surface shapes. When the approximations are made (6) becomes

$$u_i(Pm)/2 + \sum_{n=1}^{N} u_j(Qn)\int_{\partial Rn} T_{ij}(Pm,Q)dS(Q) = \sum_{n=1}^{N} t_j(Qn)\int_{\partial Rn} U_{ij}(Pm,Q)dS(Q) \tag{7}$$

Eq. (7) can be written in matrix form as

$$(1/2[I] + [\Delta T])\ \{u\} = [\Delta U]\ \{t\} \tag{8}$$

where [I] is the identity matrix; $[\Delta T]$ and $[\Delta U]$ are coefficient matrices from the integrations in (7): These integrals are calculated analytically in the program by specifying the coordinates of the ends of the boundary segments.

When the boundary data for a well-posed problem are specified then 2N quantities in (8) are known and 2N quantities are unknown. Standard reduction schemes are employed to solve for the unknowns. After the entirety of the surface data is formed the interior stresses at any selected points are found by the quadrature relation

$$\sigma_{ij}(p) = \sum_{n=1}^{N} u_k(Qn)\ \Delta S_{kij}(p,Qn) - \sum_{n=1}^{N} t_k(Qn)\ \Delta D_{kij}(p,Qn) \tag{9}$$

The tensors ΔS_{kij} and ΔD_{kij} are calculated as indicated in [7]. A procedure for calculating the stress tensor at the surface is accomplished using surface displacements and tractions as discussed in [8].

5.1.3 Use of the Isotropic Computer Program

The isotropic version of the program is limited to linear, isotropic, homogeneous, elastic problems with known material constants μ (or G, shear modulus), defined as FMU in the program, and ν, defined as POISN, or PR, in the program. The user has available four operating modes for the program:

Boundary Solution: This capability is the first step always for each problem as it solves (8) for all unknown boundary data in terms of specified boundary conditions and geometry. The entire set of boundary data may be output on punched cards (see next section).

Interior Solution: Upon completion of the boundary solution the analyst may request stress solutions, using (9), at as many interior points he desires by specifying their number and location.

Boundary Solution: The boundary stress solution is based on the same finite difference result discussed in the Appendix of [8]. The solution is obtained at a specified boundary segment from the known or calculated surface tractions and the calculated tangential derivative of displacements. The means for calculating the tangential derivative is discussed in greater detail in the next section.

Restart: By reading the entire set of boundary data the program may solve directly for interior or boundary stresses.

5.1.3.1 Dimension Statements

The current version of the program (See Section 5.1.5) admits up to two degrees of symmetry of geometry and boundary conditions. The program is limited to a total of 80 boundary segments (320 with symmetry). To increase the size of the program change the following cards,

COMMON / ARRAY1 / ···

COMMON / ARRAY2 / ···

in the various routines; also the following sequence numbered cards should be changed

10060	20035
10065	
10075	50005
15050	
15200	

The program is limited to 200 interior solution points, COMMON / ARRAY3 / ···, and to 50 surface points, COMMON / ARRAY4 / .

An 1108 assembler language routine for calculating time is attached for 1108 users. Other users must supply a similar subroutine to obtain a time-breakdown chart for each solution; if not available, insert a *dummy* subroutine, SUBROUTINE TIME (T).

5.1.3.2 Definition of Key Parameters, Matrices

The key parameters are described in cards 15060 - 15115, in SETUP. These parameters govern geometry (NSEG, NSYM, NNOD), execution options (IPUNCH, ISTRS, IBDY), and particular stress solutions (NPT, NBDYP). The first card read is a TITLE card followed by the control numbers, read by cards 15120 and 15125.

The temporary array NODE (I,J) stores the two node numbers associated with each segment number and is read by card 15130. The temporary array XYZM (I,J) reads in the x_1, x_2 coordinates of each of the nodes by card 15135.[1] The material constants FMU, POISN are then read by card 15140.

At this time the program merges the geometric information to form the permanent geometric array XYZ (Segment Number, Node Number, Coordinate Number). If NPT $\neq$ 0, the coordinates of the interior stress points are read in by card 15225. If NBDYP $\neq$ 0, three segment numbers are read by card 15240. The three numbers in NBDY (I,J) have the following meanings:

NBDY (Segment No., 1) = Segment number for which stress calculations is to be done.

---

[1] Only the geometry for the basic symmetric part is read in. If NSYM $\neq$ 0, the program assumes one degree of symmetry (y=0 axis), or two degrees of symmetry (y=0 axis, then x=0 axis) according to NSYM.

NBDY (Segment No., 2) = Segment number for the "rear" point in calculating $\Delta U/\Delta S$.

NBDY (Segment No., 3) = Segment number for the "forward" point in calculating $\Delta U/\Delta S$.

NOTE: The sequence of numbers in NODE and NBDY is the "rear" number, then the "forward" number. The positive - s direction is *always* taken such that the material is always on the left.

5.1.3.3 Boundary Conditions

The current version of the program uses a NAMELIST read (Fortran IV) statement. The procedure is to precede and close the block of boundary data with control cards in the following way

```
-$ BDYCON
     DATA
-$ END
```

See standard references for formats for the data block.

NOTE: When NSYM = 1,0 the solutions admit a rigid body motion in the unconstrained direction(s) (x,y). A displacement freedom is fixed by letting LDC for that freedom be set to "2".

All boundary conditions are *initialized to zero* and LDC is initialized to "1". All x-direction data is stored, then y-direction data is stored:

$$\left\{ \begin{array}{ll} \{t_x\} & 1,\ \text{NSEG} \\ \{t_y\} & \text{NSEG} + 1,\ 2 * \text{NSEG} \end{array} \right\} = \{\text{TCON}\}$$

etc. LDC = 1, means traction boundary conditions for the given segment and direction. LDC = 2 means displacement boundary condition for given segment and direction.

5.1.3.4 *Input Cards:*

Information	*No. Cards*
Title	1
Control parameters	1
NODE (NSEG,2)	1 + (NSEG/12)
XYZM (NNOD,2)	1 + (NNOD/8
FMU, POISN	1
Boundary Conditions	?
PITN (NPT,2)	1 + (NPT/8)
NBDY (NBDYP,3)	1 + (NBDYP/8)

5.1.3.5 *Example Problem*

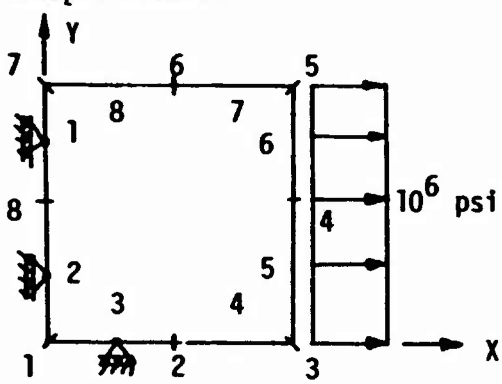

NSEG = 8
NNOD = 8
NSYM = 0
IPUNCH = 0
ISTRS = 1 (Plane Stress)
IBDY = 0
NPT = 3
NBDYP = 3

<u>Column 1</u>

NODE: --1--2--2--3--3--4--4--5--5--6--6--7--7--8--8--1

XYZM: -0000-2000-0000-1000-0000-0000-1000-0000-2000-0000-2000-1000-
-2000-2000-1000-2000

FMU, POISN: ---.1153846E+08----.30000

PTIN: -0500-1000-1000-1000-0750-0750

NBDY: --7--7--8--7--6--7--6--5--6

NAMELIST:

-TCON(5) = 1.0E+6, TCON(6) = 1.0E+6,

-LDC(1) = 2, LDC(2) = 2, LDC(11) = 2,

5.1.4 References

[1] F. J. Rizzo, An Integral Approach to Boundary Value Problems of Classical Elastostatics, *Quarterly of Applied Mathematics* 25, (1967) 83-95.

[2] T. A. Cruse and F. J. Rizzo, A Direct Formulation and Numerical Solution of the General Transient Elastodynamic Problem - I, *Journal of Mathematical Analysis and Applications* 22, (1968) 244-259.

[3] T. A. Cruse, A Direct Formulation and Numerical Solution of the General Transient Elastodynamic Problem - II, *Journal of Mathematical Analysis and Applications* 22, (1968) 341-355.

[4] T. A. Cruse, Numerical Solutions in Three Dimensional Elastostatics, *International Journal of Solids Structures* 5, (1969) 1259-1274.

[5] T. A. Cruse and W. Van Buren, Three Dimensional Elastic Stress Analysis of a Fracture Specimen with an Edge Crack, *International Journal of Fracture Mechanics* 6 (1970).

[6] T. A. Cruse and J. L. Swedlow, A Direct Method for Solving Three-Dimensional Problems of Elasto-Plastic Flow, Report SM-43, Department of Mechanical Engineering, Carnegie-Mellon University (1970).

[7] F. J. Rizzo and D. J. Shippy, A Formulation and Solution Procedure for the General Non-Homogeneous Elastic Inclusion Problem, *International Journal of Solids Structures* 4, (1968) 1161-1179.

[8] F. J. Rizzo and D. J. Shippy, A Method for Stress Determination in Plane Anistropic Elastic Bodies, *Journal of Composite Materials*, 4, (1970) 36-61.

[9] W. V. Lovitt, *Linear Integral Equations*, Dover (1950).

[10] O. D. Kellogg, *Foundations of Potential Theory*, Dover (1953).

[11] V. D. Kupradze, *Potential Methods in the Theory of Elasticity*, D. Davey & Co. (1965).

[12] S. G. Mikhlin, *Multidimensional Singular Integrals and Integral Equations*, Pergamon Press (1965).

[13] C. E. Pearson, *Theoretical Elasticity*, Ch. VI, Harvard University Press (1959).

5.1.5 *Listing for Isotropic Boundary-Integral Equation Computer Program*

```
C
C  MAIN PROGRAM -- INITIALIZES DATA - CALLS SUBROUTINES
C
      COMMON / ARRAY1 / XYZ(100,2,2), UCON(200), TCON(200), LOC(200)
      COMMON / ARRAY2 / BVAL(200)
      COMMON / MATCON / FMU, PISN, PI, P1, P2, P3, P4, P5
      COMMON / CONTR1 / NSEG, NSYM, NTOTAL, NSIZE, NPT, NBDYP
      COMMON / CONTR2 / TITL(16), IPUNCH, ISTRS, IBDY
      COMMON / TIMERS / T (10)
C
C  THE DIMENSIONS OF THE FOLLOWING ARRAYS ARE PROBLEM DEPENDENT
C
      DIMENSION C(160,160)
      DOUBLE PRECISION RHS(160)
      PI = 3.14159265
   05 CONTINUE
      DO 10 I = 1,200
      UCON(I) = 0.
      TCON(I) = 0.
   10 BVAL(I) = 0.
      CALL TIME ( T(1) )
      DO 20 I = 2,10
   20 T(I) = 0.
      CALL SETUP
      IF (IBDY.NE.0) GO TO 30
      CALL BVSOLU (C, RHS)
   30 CALL INSOLU (C)
      CALL BDYSTR (C)
C
C  CALCULATE TIME CHART
C
      T(2) = (T(2)-T(1))*10**(-3)
      T(4) = (T(4)-T(3))*10**(-3)
      T(6) = (T(6)-T(5))*10**(-3)
      T(8) = (T(8)-T(7))*10**(-3)
      T(10) = (T(10)-T(9))*10**(-3)
      WRITE (6,2000)  TITL
      WRITE (6,2100)
      WRITE (6,2200) T(2), T(4), T(6), T(8), T(10)
      GO TO 05
      STOP
 1000 FORMAT ( 16A5)
 2000 FORMAT (1H1, 16A5)
 2100 FORMAT ( 21H TIME BREAKDOWN CHART //)
 2200 FORMAT ( 5X 15HTIME FOR SETUP   F12.7, 2X 7HSECONDS //
     1         5X 15HTIME FOR DELINT  F12.7, 2X 7HSECONDS //
     2         5X 15HTIME FOR SOLVER  F12.7, 2X 7HSECONDS //
     3         5X 15HTIME FOR INSOLU  F12.7, 2X 7HSECONDS //
     4         5X 15HTIME FOR BDYSOL  F12.7, 2X 7HSECONDS)
      END
```

```
      SUBROUTINE SETUP
      COMMON / ARRAY1 / XYZ(100,2,2), UCON(200), TCON(200), LOC(200)
      COMMON / ARRAY2 / BVAL(200)
      COMMON / ARRAY3 / PTIN(100,2)
      COMMON / ARRAY4 / NBDY(50,3)
      COMMON / MATCON / FMU, POISN, PI, P1, P2, P3, P4, P5
      COMMON / TIMERS / TIM( 6)
      COMMON / CONTR1 / NSEG, NSYM, NTOTAL, NSIZE, NPT, NBDYP
      COMMON / CONTR2 / TITL(16), IPUNCH, ISTRS, IBDY
      NAMELIST / BDYCON / UCON, TCON, LOC
      DIMENSION NODE(100,2), XYZM(100,2)
      EQUIVALENCE (NODE, LOC), (XYZM, UCON)
C
C  NSEG = NUMBER OF SEGMENTS ON THE BOUNDARY
C  NSYM = NUMBER OF DEGREES OF SYMMETRY STARTING WITH Y, THEN X
C  NNOD = NUMBER OF BOUNDARY NODES CONNECTING BOUNDARY SEGMENTS
C  IPUNCH = 1 -- THE BOUNDARY SOLUTION WILL BE PUNCHED OUT
C  ISTRS = 0, PLSTRN --  ISTRS = 1, PLSTRS
C  IF IBDY.EQ.0  ---  BOUNDARY DATA STORED IN COMMON
C  IF IBDY.NE.0  ---  BOUNDARY DATA READ IN FROM CARDS ADDED TO END
C                     OF THE DATA DECK
C  NPT = NUMBER OF INTERIOR SOLUTION POINTS FOR STRESS SOLUTION
C  NBDYP = NUMBER OF BOUNDARY POINTS FOR STRESS SOLUTION
C
      READ (5,1000) TITL
      READ (5,1100) NSEG, NSYM, NNOD, IPUNCH, ISTRS, IBDY, NPT, NBDYP
      READ (5,1200) ((NODE(I,J),J=1,2),I=1,NSEG)
      READ (5,1300) ((XYZM(I,J),J=1,2),I=1,NNOD)
      READ (5,1400) FMU, POISN
      WRITE (6,2000) TITL
      WRITE (6,2100) NSEG, NSYM, NNOD, IPUNCH, ISTRS, IBDY, NPT, NBDYP
      WRITE (6,2200) ((NODE(I,J),J=1,2),I=1,NSEG)
      WRITE (6,2300) ((XYZM(I,J),J=1,2),I=1,NNOD)
      WRITE (6,2400) FMU, POISN
      NSIZE = 2 * NSEG
      DO 10 I = 1,NSEG
      DO 10 J = 1,2
      DO 10 K = 1,2
      N = NODE(I,J)
   10 XYZ(I,J,K) = XYZM(N,K)
      DO 20 I = 1,200
      UCON(I) = 0.
   20 LOC(I) = 1
      READ (5,BDYCON)
      IF (NPT.EQ.0) GO TO 30
      READ  (5,1500) ((PTIN(I,J),J=1,2),I=1,NPT)
      WRITE (6,2500) ((PTIN(I,J),J=1,2),I=1,NPT)
   30 IF (NBDYP.EQ.0) GO TO 40
      READ  (5,1600) ((NBDY(I,J),J=1,3),I=1,NBDYP)
      WRITE (6,2600) ((NBDY(I,J),J=1,3),I=1,NBDYP)
   40 CONTINUE
      NFAC = 2**NSYM
      IF (NSYM.EQ.0) NFAC = 1
      NTOTAL = NSEG * NFAC
C
C   CALCULATE NEEDED MATERIAL CONSTANTS
C
```

```
      IF (ISTRS.EQ.1) POISN = POISN/ (1.+POISN)
      P1 = 1./(8.*PI*FMU*(1.-POISN))
      P2 = 3.-4.*POISN
      P3 = 1./(4.*PI*(1.-POISN))
      P4 = 1.-2.*POISN
      CALL TIME ( TIM(2) )
      RETURN
 1000 FORMAT (16A5)
 1100 FORMAT (10I5)
C
C   ****** CAUTION*****   FORMATS PROBLEM DEPENDENT   ***** CAUTION ******
C
 1200 FORMAT (24I3)
 1300 FORMAT (16F5.3)
 1400 FORMAT (E15.7, F10.5)
 1500 FORMAT (16F5.3)
 1600 FORMAT (24I3)
 2000 FORMAT (1H1, 10X, 16A5)
 2100 FORMAT (// 10I5)
 2200 FORMAT (// 8(3X 2I3))
 2300 FORMAT (// 4(3X 2F10.6))
 2400 FORMAT (// 5X E15.7, F10.5)
 2500 FORMAT (// 4(3X 2F10.6))
 2600 FORMAT (// 6(3X 3I3))
      END
```

```
      SUBROUTINE BVSOLU (C, RHS)
      COMMON / ARRAY1 / XYZ(100,2,2), UCON(200), TCON(200), LOC(200)
      COMMON / ARRAY2 / BVAL(200)
      COMMON / MATCON / FMU, POISN, PI, P1, P2, P3, P4, P5
      COMMON / CONTR1 / NSEG, NSYM, NTOTAL, NSIZE, NPT, NBDYP
      COMMON / CONTR2 / TITL(16), IPUNCH, ISTRS, IBDY
      COMMON / TIMERS / TIM (10)
      DIMENSION A(200), PXYZ(2), C(NSIZE,NSIZE)
      EQUIVALENCE (A, UCON)
      DOUBLE PRECISION RHS(NSIZE)
      NMAX = 2 * NSEG
      WRITE (6,2000) TITL
      IF (ISTRS.EQ.0) WRITE (6,2050)
      IF (ISTRS.EQ.1) WRITE (6,2060)
      WRITE (6,2100)
C
C  WRITE THE STARTING BOUNDARY CONDITIONS
C
      DO 10 I = 1,NSEG
      J = I + NSEG
      DO 15 N = 1,2
   15 PXYZ(N) = (XYZ(I,1,N) + XYZ(I,2,N))/2.
   10 WRITE (6,2200) I, UCON(I), UCON(J), TCON(I), TCON(J),
     1                    LOC(I), LOC(J), PXYZ(1), PXYZ(2)
      DO 20 I = 1,NMAX
      RHS(I) = 0.0D0
      IF (LOC(I).EQ.1) GO TO 30
      BVAL(I) = FMU * UCON(I)
      GO TO 20
   30 BVAL(I) = TCON(I)
   20 CONTINUE
C
C  CALCULATE DELU, DELT, RHS
C
      CALL TIME ( TIM(3) )
      CALL DELTNT (C, RHS)
      CALL TIME ( TIM(4) )
      WRITE (6,3000) ((C(I,J),J=1,NSIZE),I=1,NSIZE)
C
C  WRITE RIGHT HAND SIDE VECTOR
C
      WRITE (6,2300) TITL
      DO 40 I = 1,NSEG
      J = I + NSEG
   40 WRITE (6,2400) I, RHS(I), RHS(J)
C
C  SOLVE SYSTEM OF EQUATIONS
C
      CALL TIME ( TIM(5) )
      CALL SOLVER (NMAX, RHS, A, C)
      CALL TIME ( TIM(6) )
C
C  FILL IN UCON, TCON  --- PRINT RESULTS
C
      DO 60 I = 1,NMAX
      IF (LOC(I).EQ.1) GO TO 60
      TCON(I) = FMU * A(I)
```

```
      UCON(I) = (1./FMU) * BVAL(I)                                   2D*20285
      GO TO 50                                                       2D*20290
   60 TCON(I) = BVAL(I)                                              2D*20295
      UCON(I) = A(I)                                                 2D*20300
   50 CONTINUE                                                       2D*20305
      WRITE (6,2000) TITL                                            2D*20310
      IF (ISTRS.EQ.0) WRITE (6,2050)                                 2D*20315
      IF (ISTRS.EQ.1) WRITE (6,2060)                                 2D*20320
      WRITE (6,2100)                                                 2D*20325
      DO 70 I = 1,NSEG                                               2D*20330
      J = I + NSEG                                                   2D*20335
      DO 80 N = 1,2                                                  2D*20340
   80 PXYZ(N) = (XYZ(I,1,N) + XYZ(I,2,N))/2.                         2D*20345
   70 WRITE (6,2200) I, UCON(I), UCON(J), TCON(I), TCON(J),          2D*20350
     1                 LDC(I), LDC(J), PXYZ(1), PXYZ(2)              2D*20355
      IF (IPUNCH.EQ.0) RETURN                                        2D*20360
      DO 120 I = 1,NSEG                                              2D*20365
      J = I + NSEG                                                   2D*20370
  120 WRITE (7,2500) I, UCON(I), UCON(J)                             2D*20375
      DO 130 I = 1,NSEG                                              2D*20380
      J = I + NSEG                                                   2D*20385
  130 WRITE (7,2500) I , TCON(I), TCON(J)                            2D*20390
      RETURN                                                         2D*20395
 2000 FORMAT (1H1, 15A5 // 10X 19HBOUNDARY CONDITIONS)               2D*20400
 2050 FORMAT ( / 4( 18H PLANE STRAIN **** ) )                        2D*20405
 2060 FORMAT ( / 4( 18H PLANE STRESS **** ) )                        2D*20410
 2100 FORMAT (// 4X 4H SEG 7X 2HU1 10X 2HU2 10X 2HT1 10X 2HT2 8X 4HLDC1 2D*20415
     1  6X 4HLDC2 8X 2HX1 10X 2HX2 //)                               2D*20420
 2200 FORMAT (2X I5, 2F12.8, 2F12.0, 6X I1, 11X I1, 2F12.6)          2D*20425
 2300 FORMAT (1H1, 16A5 // 10X 22HRIGHT HAND SIDE VECTOR //)         2D*20430
 2400 FORMAT (5X, I5, 2E15.8)                                        2D*20435
 2500 FORMAT ( I10, 2E30.10)                                         2D*20440
 3000 FORMAT (/// ( 2(8F12.6 /) //) )                                2D*20445
      END                                                            2D*20450
```

```
      SUBROUTINE DELINT (G, RHS)
      COMMON / ARRAY1 / XYZ(100,2,2), UCON(200), TCON(200), LOC(200)
      COMMON / ARRAY2 / BVAL(200)
      COMMON / MATCON / EMU, POISN, P0, P1, P2, P3, P4, P5
      COMMON / CONTR1 / NSEG, NSYM, NTOTAL, NSIZE, NPT, NBDYP
      COMMON / CONTR2 / TITL(16), IPUNCH, ISTRS, IBDY
      DIMENSION A(2), E1(2), E2(2), P(2), X(2,2), R1(2), R2(2)
      DIMENSION ISYM(2),U(2,2),T(2,2),G(NSIZE,NSIZE)
      DOUBLE PRECISION RHS(NSIZE), XI1, XI2, XI3, XI4, XI5
      DO 10 I = 1,NSIZE
      DO 10 J = 1,NSIZE
   10 G(I,J) = 0.
      DO 20 M = 1,NTOTAL
      IFLG = 0
      JFLG = 0
      M1 = (M-1)/NSEG
      M2 = M - M1*NSEG
      M3 = M2 + NSEG
C     IF (LOC(M2).EQ.1.AND.ABS(BVAL(M2)).LT.1.0.AND.
C    1    LOC(M3).EQ.1.AND.ABS(BVAL(M3)).LT.1.0) IFLG = 1
C     IF (LOC(M2).EQ.2.AND.ABS(BVAL(M2)).LT.1.0E-08.AND.
C    1    LOC(M3).EQ.2.AND.ABS(BVAL(M3)).LT.1.0E-08) JFLG = 1
C
C  COMPUTE SYMMETRY COEFFICIENTS USING Y, THEN X
C
      IFLAG = 1
      DO 16 K = 1,2
      J = 3 - K
      I = (M-1)/(NSEG*((2**J)/2))
      ISYM(K) = (-1)**I
      IF (I.EQ.0) ISYM(K) = 1
   16 IFLAG = IFLAG * ISYM(K)
      DO 30 J = 1,2
      IF (IFLAG.GT.0) GO TO 25
      X(1,J) = XYZ(M2,2,J) * ISYM(J)
      X(2,J) = XYZ(M2,1,J) * ISYM(J)
      GO TO 35
   25 X(1,J) = XYZ(M2,1,J) * ISYM(J)
      X(2,J) = XYZ(M2,2,J) * ISYM(J)
   35 CONTINUE
C
C   DEFINE DIRECTION OF THE LINE SEGMENT  E2 = A(J) / AMAG
C
   30 A(J) = X(2,J) - X(1,J)
      AMAG = SQRT (A(1)**2 + A(2)**2)
      DO 33 I = 1,2
      E2(I) = A(I)/AMAG
      J = 3 - I
   33 E1(J) = E2(I) * (-1)**(J+1)
C
C   CALCULATE THE ANGLES T1 AND T2 AND THE DISTANCE D
C
      DO 20 N = 1,NSEG
      DO 15 J = 1,2
      P(J) = (XYZ(N,1,J) + XYZ(N,2,J))/2.
      R1(J) = X(1,J) - P(J)
      R2(J) = X(2,J) - P(J)
```

```
      DO 15 I = 1,2
      U(I,J) = 0.
   15 T(I,J) = 0.
      CALL DOTPRD (R1, E1, D)
      CALL DOTPRD (R1, E2, R12)
      CALL DOTPRD (R2, E2, R22)
      CALL DOTPRD (R1, R1, R1MAG)
      CALL DOTPRD (R2, R2, R2MAG)
      R1MAG = SQRT (R1MAG)
      R2MAG = SQRT (R2MAG)
      RA = ABS(R12)
      RB = ABS(R22)
      RMAG = AMAX1 (RA, RB)
      IF (ABS(D /RMAG).LT.1.0E-03) GO TO 40
      SIGD = D / ABS(D)
      T1 = ATAN(R12/D) - (1.-SIGD)*PI/2.
      T2 = ATAN(R22/D) - (1.-SIGD)*PI/2.
      ST1 = R12 / R1MAG
      ST2 = R22 / R2MAG
      CT1 = D / R1MAG
      CT2 = D / R2MAG
      TN1 = R12 / D
      TN2 = R22 / D
C
C  DIAGNOSTIC PRINT --- OCCURS ONLY IN THE CASE OF SERIOUS DATA ERROR
C
      IF ( (CT1/CT2) .GT. 0.) GOTO 500
      WRITE (6,2000) M, N, X, P, R1, R2, E1, E2, T1, T2, CT1, CT2, D
  500 CONTINUE
      XL1 = ALOG(D/CT1)
      XL2 = ALOG(D/CT2)
C
C  CALCULATE DELU INTEGRAL FOR D.NE.0
C
      IF (IFLG.EQ.1) GO TO 45
      XI1 = D*(TN2*XL2-TN2+T2-TN1*XL1+TN1-T1)
      XI2 = D*(T2-T1)
      XI3 = D*(XL2-XL1)
      XI4 = D*(TN2-TN1-T2+T1)
      DO 50 IX =  1,2
      DO 50 JX = IX,2
      DEL = 0.
      IF (IX.EQ.JX) DEL = 1.
      UXY = P1*(P2*DEL*XI1-E1(IX)*E1(JX)*XI2-(E1(IX)*E2(JX)+E1(JX)*E2(IX
     1        ))*XI3-E2(IX)*E2(JX)*XI4)
      U(IX,JX) = UXY * ISYM(JX)
      IF (IX.EQ.JX) GO TO 50
      U(JX,IX) = UXY * ISYM(IX)
   50 CONTINUE
C
C  CALCULATE DELT INTEGRAL FOR D.NE.0
C
   45 IF (JFLG.EQ.1) GO TO 75
      XI1 = T2-T1
      XI2 = T2+ST2*CT2-T1-ST1*CT1
      XI3 = ST2**2-ST1**2
      XI4 = T2-ST2*CT2-T1+ST1*CT1
      XI5 = ALOG(CT1/CT2)
```

```
      DO 60 IX =  1,2
      DO 60 JX = IX,2
      TXY = 0.
      IF (IX.EQ.JX.AND.M.EQ.N) GO TO 60
      DEL = 0.
      IF (IX.EQ.JX) DEL = 1.
      TXY = P3*(P4*DEL*XI1+E1(IX)*E1(JX)*XI2+(E1(IX)*E2(JX)+E2(IX)*
     1     E1(JX))*XI3+E2(IX)*E2(JX)*XI4)
      T(IX,JX) = TXY * ISYM(JX)
      IF (IX.EQ.JX) GO TO 60
      TSTAR = -P3*P4*(E2(IX)*E1(JX)-E1(IX)*E2(JX))*XI5
      T(IX,JX) = (TXY+TSTAR)*ISYM(JX)
      T(JX,IX) = (TXY-TSTAR)*ISYM(IX)
   60 CONTINUE
      GO TO 75
   40 CONTINUE
      XI1 = R22*(ALOG(RB)-1.)-R12*(ALOG(RA)-1.)
      XI2 = R22 - R12
      XI3 = ALOG(RB) - ALOG(RA)
C
C  CALCULATE DELU FOR D.EQ.0
      IF (IFLG.EQ.1) GO TO 65
      DO 70 IX =  1,2
      DO 70 JX = IX,2
      DEL = 0.
      IF (IX.EQ.JX) DEL = 1.
      UXY = P1*(P2*DEL*XI1-E2(IX)*E2(JX)*XI2)
      U(IX,JX) = UXY * ISYM(JX)
      IF (IX.EQ.JX) GO TO 70
      U(JX,IX) = UXY * ISYM(IX)
   70 CONTINUE
C
C  CALCULATE DELT INTEGRAL FOR D.EQ.0
   65 IF (JFLG.EQ.1) GO TO 75
      DO 80 IX =  1,2
      DO 80 JX = IX,2
      IF (IX.EQ.JX) GO TO 80
      TXY = -P3*P4*(E2(IX)*E1(JX)-E1(IX)*E2(JX))*XI3
      T(IX,JX) = TXY * ISYM(JX)
      T(JX,IX) =-TXY * ISYM(IX)
   80 CONTINUE
   75 DO 85 IX = 1,2
      DO 85 JX = 1,2
      N4 = N  + (IX-1)*NSEG
      M4 = M2 + (JX-1)*NSEG
      IF (IX.EQ.JX.AND.M.EQ.N) T(IX,JX) = -0.50
      IF (LOC(M4).EQ.1) GO TO 90
      TRANS = U(IX,JX)
      U(IX,JX) = -(1./FMU) * T(IX,JX)
      T(IX,JX) = -FMU * TRANS
   90 RHS(N4) = RHS(N4) + U(IX,JX) * BVAL(M4)
   85 G(N4,M4) = G(N4,M4) + T(IX,JX)
   20 CONTINUE
      RETURN
 2000 FORMAT (// 5X 2I5 / (2F10.5 /))
      END
```

```
      SUBROUTINE INSOLU( C )
      COMMON / ARRAY1 / XYZ(100,2,2), UCON(200), TCON(200), LDC(200)
      COMMON / ARRAY3 / PTIN(100,2)
      COMMON / MATCON / FMU, POISN, PI, P1, P2, P3, P4, P5
      COMMON / TIMERS / TIM (10)
      COMMON / CONTR1 / NSEG, NSYM, NTOTAL, NSIZE, NPT, NBDYP
      COMMON / CONTR2 / TITL(16), IPUNCH, ISTRS, IBDY
      DIMENSION C(100,3), A(4), PXYZ(3)
      IF (IBDY.NE.0) GO TO 100
  110 IF (NPT.EQ.0) RETURN
      CALL TIME ( TIM(7) )
      WRITE (6,2000) TITL
      IF (ISTRS.EQ.0) WRITE (6,2050)
      IF (ISTRS.EQ.1) WRITE (6,2060)
C
C  CALL FOR CALCULATION OF DELD AND DELS
C
      WRITE (6,2100)
      A(4) = 0.
      CALL DELSD (C)
      DO 10 NP = 1,NPT
      DO 20  I = 1,3
   20 A(I) = C(NP,I)
      IF (ISTRS.EQ.1) GO TO 30
      A(4) = POISN * (A(1) + A(3))
   30 CONTINUE
      THETA = (A(1) + A(3) + A(4))/3.
      TAUOCT = SQRT(2.*(A(1)**2+A(3)**2+A(4)**2-A(1)*A(3)-A(3)*A(4)-
     1          A(1)*A(4)+3.*A(2)**2))/3.
      WRITE (6,2200) NP,(A(K),K=1,4),THETA,TAUOCT,PTIN(NP,1),PTIN(NP,2)
   10 CONTINUE
      CALL TIME ( TIM(8) )
      RETURN
  100 WRITE (6,2000) TITL
      DO 120 I = 1,NSEG
      J = I + NSEG
  120 READ (5,1100) N, UCON(I), UCON(J)
      DO 130 I = 1,NSEG
      J = I + NSEG
  130 READ (5,1100) N, TCON(I), TCON(J)
      WRITE (6,2300)
      DO 140 I = 1,NSEG
      J = I + NSEG
      DO 150 N = 1,2
  150 PXYZ(N) = (XYZ(I,1,N) + XYZ(I,2,N))/2.
  140 WRITE (6,2400) I, UCON(I), UCON(J), TCON(I), TCON(J),
     1                   LDC(I), LDC(J), PXYZ(1), PXYZ(2)
      GO TO 110
 1100 FORMAT (I10, 2E30.10)
 2000 FORMAT (1H1, 10X, 16A5)
 2050 FORMAT ( / 4( 18H PLANE STRAIN **** ) )
 2060 FORMAT ( / 4( 18H PLANE STRESS **** ) )
 2100 FORMAT (6HOPOINT, 2X 10H SIGMA(XX) 2X 10H SIGMA(XY) 2X
     1      10H SIGMA(YY) 2X 10H SIGMA(ZZ) 4X 6H THETA 6X 7H TAUOCT
     2      5X 2H X 6X 2H Y)
 2200 FORMAT (2X I3, 2X 6F12.2, 2F8.4)
 2300 FORMAT (// 4X 4H SEG 7X 2HU1 10X 2HU2 10X 2HT1 10X 2HT2 8X 4HLDC1
```

```
    1  6X 4HLDC2 8X 2HX1 10X 2HX2 //)                                   2D*30285
 2400 FORMAT (2X I5, 2F12.8, 2F12.0, 6X I1, 11X I1, 2F12.6)             2D*30290
      END                                                               2D*30295
```

```
      SUBROUTINE DELSD (G)
      COMMON / ARRAY1 / XYZ(100,2,2), UCON(200), TCON(200), LOC(200)
      COMMON / ARRAY3 / PTIN(100,2)
      COMMON / MATCON / FMU, PR, PI, C1, C2, C3, C4
      COMMON / CONTR1 / NSEG, NSYM, NTOTAL, NSIZE, NPT, NBDYP
      COMMON / CONTR2 / TITL(16), IPUNCH, ISTRS, IBDY
      DIMENSION A(2), E1(2), E2(2), P(2), X(2,2), R1(2), R2(2)
      DIMENSION ISYM(2), G(100,3)
      DO 10 I = 1,100
      DO 10 J = 1,3
   10 G(I,J) = 0.
      DO 20 M = 1,NTOTAL
      M1 = (M-1)/NSEG
      M2 = M - M1*NSEG
C
C  COMPUTE SYMMETRY COEFFICIENTS USING Y, THEN X
      IFLAG = 1
      DO 16 K = 1,2
      J = 3 - K
      I = (M-1)/(NSEG*((2**J)/2))
      ISYM(K) = (-1)**I
      IF (I.EQ.0) ISYM(K) = 1
   16 IFLAG = IFLAG * ISYM(K)
      DO 32 J = 1,2
      IF (IFLAG.GT.0) GO TO 23
      X(1,J) = XYZ(M2,2,J) * ISYM(J)
      X(2,J) = XYZ(M2,1,J) * ISYM(J)
      GO TO 35
   23 X(1,J) = XYZ(M2,1,J) * ISYM(J)
      X(2,J) = XYZ(M2,2,J) * ISYM(J)
   35 CONTINUE
C
C  DEFINE DIRECTION OF THE LINE SEGMENT E2 = A(J)/AMAG
C
   32 A(J) = X(2,J) - X(1,J)
      AMAG = SQRT (A(1)**2 + A(2)**2)
      DO 33 I = 1,2
      E2(I) = A(I)/AMAG
      J = 3 - I
   33 E1(J) = E2(I) * (-1)**(J+1)
C
C  CALCULATE THE ANGLES T1 AND T2 AND THE DISTANCE D
C
      DO 20 N = 1,NPT
      DO 15 J = 1,2
      P(J) = PTIN(N,J)
      R2(J) = X(2,J) - P(J)
      R1(J) = X(1,J) - P(J)
   15 CONTINUE
      D1 = 0.
      D2 = 0.
      DO 17 J=1,2
      D1 = D1 + R1(J)*R1(J)
   17 D2 = D2 + R2(J)*R2(J)
      D1 = SQRT(D1)
      D2 = SQRT(D2)
      CALL DOTPRD (R1, E1, D)
```

```
      CALL DOTPRD (R1, E2, R12)
      CALL DOTPRD (R2, E2, R22)
      CALL DOTPRD (R1, R1, R1MAG)
      CALL DOTPRD (R2, R2, R2MAG)
      R1MAG = SQRT (R1MAG)
      R2MAG = SQRT (R2MAG)
      RA = ABS(R12)
      RB = ABS(R22)
      RMAG = AMAX1(RA,RB)
      IF (ABS(D /RMAG).LT.1.0E-03) GO TO 40
      SIGD = D / ABS(D)
      T1 = ATAN(R12/D ) - (1.-SIGD)*PI/2.
      T2 = ATAN(R22/D ) - (1.-SIGD)*PI/2.
      S1 = R12 / R1MAG
      S2 = R22 / R2MAG
      C1 = D / R1MAG
      C2 = D / R2MAG
      XL1 = ALOG(D1)
      XL2 = ALOG(D2)
   40 L = 0
      DO 25 I = 1,2
      DO 25 J = I,2
      L = L + 1
      DO 25 K = 1,2
      DELIK = 0.
      DELKJ = 0.
      DELIJ = 0.
      IF (I.EQ.K) DELIK = 1.
      IF (K.EQ.J) DELKJ = 1.
      IF (I.EQ.J) DELIJ = 1.
      IF (ABS(D/RMAG).LT.1.0E-03) GO TO 30
      DD1 = T2 - T1
      DD2 = XL2 - XL1
      DD3 = T2-T1+S2*C2-S1*C1
      DD4 = S2**2-S1**2
      DD5 = T2-T1-S2*C2+S1*C1
      DD6 = 2.*DD2-S2**2+S1**2
      DS1 = DD3/D
      DS2 = DD4/D
      DS3 = DD5/D
      DS4 = DD1/D
      DS5 = 3.*DS1 + 2.*(S2*C2**3-S1*C1**3)/D
      DS6 = 2.*(C1**4-C2**4)/D
      DS7 = 4.*DS1 - DS5
      DS8 = 2.*(S2**4-S1**4)/D
      AIJK = DELIK*E1(J)+DELKJ*E1(I)-DELIJ*E1(K)
      BIJK = DELIK*E2(J)+DELKJ*E2(I)-DELIJ*E2(K)
      CIJK = E1(I)*E1(J)*E1(K)
      FIJK = E2(I)*E2(J)*E2(K)
      DIJK = E1(I)*E2(J)*E1(K)+E2(I)*E1(J)*E1(K)+E1(I)*E1(J)*E2(K)
      EIJK = E1(I)*E2(J)*E2(K)+E2(I)*E1(J)*E2(K)+E2(I)*E2(J)*E1(K)
      GIJK = C4*DELIJ*E1(K)+E1(I)*E1(J)*E1(K)+PR*(DELIK*E1(J)+DELKJ*
     1       E1(I))
      HIJK = C4*DELIJ*E2(K)+E1(I)*E2(J)*E1(K)+E2(I)*E1(J)*E1(K)+
     1          PR*(DELIK*E2(J)+DELKJ*E2(I)+2.*E1(I)*E1(J)*E2(K)-
     2          E1(I)*E2(J)*E1(K)-E2(I)*E1(J)*E1(K))
      OIJK = C4*E2(I)*E2(J)*E1(K)+PR*(E1(I)*E2(J)*E2(K)+E2(I)*E1(J)*
     1          E2(K))
```

```
      PIJK = C4*(DELIK*E1(J)+DELKJ*E1(I))-DELIJ*E1(K)*(1.-4.*PR)
      DD = C3*(C4*(AIJK*DD1+BIJK*DD2)+CIJK*DD3+DIJK*DD4+EIJK*DD5
     1         +FIJK*DD6)*ISYM(K)
      DS = 2.*FMU*C3*(GIJK*DS1+HIJK*DS2+OIJK*DS3+PIJK*DS4-CIJK*DS5
     1         -DIJK*DS6-EIJK*DS7-FIJK*DS8)*ISYM(K)
      GO TO 24
   30 CONTINUE
      BIJK = DELIK*E2(J)+DELKJ*E2(I)-DELIJ*E2(K)
      QIJK = C4*(2.*E1(K)*E2(I)*E2(J)+E1(J)*DELIK+E1(I)*DELKJ)+
     1         2.*PR*(E1(I)*E2(J)*E2(K)+E2(I)*E1(J)*E2(K))-DELIJ*E1(K)
      S1 = R12/RA
      S2 = R22/RB
C
C   FOLLOWING IDIOT CARDS REQUIRED FOR 1108 FORTRAN
C
      ARG1 = RB
      ARG2 = RA
      DD2 = S2*ALOG(ARG1) - S1*ALOG(ARG2)
      DD6 = DD2
      DS9 = 1./RA-1./RB
      DD = C3*(C4*BIJK*DD2+2.*E2(I)*E2(J)*E2(K)*DD6)*ISYM(K)
      DS = 2.*FMU*C3*QIJK*DS9*ISYM(K)
   24 CONTINUE
      M4 = M2 + (K-1) * NSEG
      G(N,L) = G(N,L) + DD*TCON(M4) - DS*UCON(M4)
   25 CONTINUE
   20 CONTINUE
      RETURN
      END
```

```
      SUBROUTINE BDYSTR (C)
      COMMON / ARRAY1 / XYZ(160,2,2), UCON(200), TCON(200), LOC(200)
      COMMON / ARRAY4 / NBDY(50,3)
      COMMON / MATCON / FMU, POISN, PI, P1, P2, P3, P4, P5
      COMMON / CONTR1 / NSEG, NSYM, NTOTAL, NSIZE, NPT, NBDYP
      COMMON / CONTR2 / TITL(16), IPUNCH, ISTRS, IBDY
      COMMON / TIMERS / TIM(10)
      DIMENSION A(2), E1(2), E2(2), P(3,2), R(2), DU(2), T(2), C(50,4)
      IF (NBDYP.EQ.0) RETURN
      CALL TIME ( TIM(9) )
      C1 = 1.-2.*POISN
      C2 = 1.-POISN
      WRITE (6,2000) TITL
      WRITE (6,2100) ((NBDY(I,J),J=1,3),I=1,NBDYP)
      WRITE (6,2000) TITL
      IF (ISTRS.EQ.0) WRITE (6,2050)
      IF (ISTRS.EQ.1) WRITE (6,2060)
      WRITE (6,2200)
C
C  I0 = BASE SEGMENT NUMBER
C  I1 = REAR DIFFERENCE SEGMENT NUMBER
C  I2 = FORWARD DIFFERENCE SEGMENT NUMBER
C
      DO 15 N = 1,NBDYP
      I0 = NBDY (N,1)
      I1 = NBDY (N,2)
      I2 = NBDY (N,3)
      DO 20 M = 1,2
      P(1,M) = (XYZ(I0,1,M) + XYZ(I0,2,M))/2.
      P(2,M) = (XYZ(I1,1,M) + XYZ(I1,2,M))/2.
      P(3,M) = (XYZ(I2,1,M) + XYZ(I2,2,M))/2.
      R(M) = P(3,M) - P(2,M)
   20 A(M) = XYZ(I0,2,M) - XYZ(I0,1,M)
      SMAG = SQRT(R(1)**2 + R(2)**2)
      AMAG = SQRT(A(1)**2 + A(2)**2)
      DO 25 M = 1,2
      E2(M) = A(M)/ AMAG
      K = 3 - M
      E1(K) = E2(M) * (-1)**(K+1)
      I3 = I1 + (M-1)*NSEG
      I4 = I2 + (M-1)*NSEG
      I5 = I0 + (M-1)*NSEG
      DU(M) = (UCON(I4) - UCON(I3))/SMAG
   25 T(M) = TCON(I5)
      M = 0
      DO 30 I = 1,2
      DO 30 J = I,2
      M = M + 1
      DIJ = 0.
      IF (I.EQ.J) DIJ = 1.
      C(N,M) = (C1/(2.*C2))*(T(I)*E1(J) + T(J)*E1(I)) - (FMU/C2)*POISN*
     1          (E2(J)*DU(I) + E2(I)*DU(J))
      DO 30 K = 1,2
      A1 = E1(I)*E1(J)*E1(K) + E1(I)*E2(J)*E2(K) +
     1     E2(I)*E1(J)*E2(K) + E2(I)*E2(J)*E1(K)
      A2 = E1(I)*E1(J)*E2(K) - E1(I)*E2(J)*E1(K) - E2(I)*E1(J)*E1(K)
      A3 = E1(I)*E2(J)*E1(K) + E2(I)*E1(J)*E1(K)
```

```
      A4 = E2(I)*F2(J)*E2(K)
      C(N,M) = C(N,M) - (C1/(2.*C2))*DIJ*E1(K)*T(K) + (1./(2.*C2))*(A1*
     1         T(K)) + (FMU/C2)*(C1*A2 + C2*A3 + 3.*A4)*DU(K) -
     2         (FMU/C2)*C1*DIJ*E2(K)*DU(K)
   30 CONTINUE
      IF (ISTRS.EQ.1) GO TO 35
      C(N,4) = POISN * (C(N,1) + C(N,3))
   35 THETA = (C(N,1) + C(N,3) + C(N,4))/3.
      TAUOCT = SQRT(2.*(C(N,1)**2+C(N,3)**2+C(N,4)**2-C(N,1)*C(N,3)-
     1     C(N,3)*C(N,4)-C(N,1)*C(N,4)+3.*C(N,2)**2))/3.
   15 WRITE (6,2300) IO,(C(N,M),M=1,4),THETA,TAUOCT,P(1,1),P(1,2)
      CALL TIME ( TIM(10) )
      RETURN
 1000 FORMAT (24I3)
 2000 FORMAT (1H1, 10X, 16A5)
 2050 FORMAT ( / 4( 18H PLANE STRAIN **** ) )
 2060 FORMAT ( / 4( 18H PLANE STRESS **** ) )
 2100 FORMAT (/ 5X 11HBASE NUMBER 2X 11HREAR NUMBER 3X 10HFWD NUMBER //
     1        ( 3I12 /) )
 2200 FORMAT (7H0SEGMENT 2X 10H SIGMA(XX) 2X 10H SIGMA(XY) 2X
     1     10H SIGMA(YY) 2X 10H SIGMA(ZZ) 4X 6H THETA 6X 7H TAUOCT
     2     5X 2H X 6X 2H Y)
 2300 FORMAT (2X I3, 2X 6F12.2, 2F8.4)
      END
```

```
SUBROUTINE DOTPRD (A, B, C)
DIMENSION A(2), B(2)
C = A(1)*B(1) + A(2)*B(2)
RETURN
END
```

```
      SUBROUTINE SOLVER (N, X, F, A)
      DIMENSION A(N,N), X(N), F(N), XX(160)
      DOUBLE PRECISION X
      DO 10 I = 1, N
      F(I) = 0.0
   10 CONTINUE
      N1 = N - 1
      DO 60 I = 2, N
      DO 55 J = I, N
      IF (ABS(A(I-1,I-1)) .GT. 0.) GO TO 45
      I1 = I - 1
      WRITE (6,510) I1
      RETURN
   45 CONTINUE
      CX = A(J,I-1) / A(I-1,I-1)
      K2 = I
      DO 50 K = I, N
      A(J,K2) = A(J,K2) - CX * A(I-1,K2)
      K2 = K2 + 1
   50 CONTINUE
      A(J,I-1) = CX
   55 CONTINUE
   60 CONTINUE
C     FORWARD PASS - OPERATE ON RIGHT HAND SIDE AS
C     ON MATRIX
   62 CONTINUE
      DO 70 I = 2, N
      DO 65 J = I, N
      X(J) = X(J) - X(I-1) * A(J,I-1)
   65 CONTINUE
   70 CONTINUE
C
C     BACKWARD PASS - SOLVE FOR AX = B
      XX(N) = X(N) / A(N,N)
      DO 80 I = 1, N1
      SUM = 0.0
      I2 = N - I + 1
      DO 75 J = I2, N
      SUM = SUM + A(I2-1,J) * XX(J)
   75 CONTINUE
      XX(I2-1) = (X(I2-1)-SUM) / A(I2-1,I2-1)
   80 CONTINUE
      DO 90 I = 1, N
      F(I) = F(I) + XX(I)
   90 CONTINUE
      RETURN
  510 FORMAT(/1X 25HERROR RETURN FROM SEQSOV    I10,
     1 35HDIAGONAL TERM REDUCED TO ZERO     / )
      END
```

5.2 TWO DIMENSIONAL ANISOTROPIC BOUNDARY-INTEGRAL EQUATION METHOD

5.2.1 Formulation of the Field Equations

The present note concerns the application of the Boundary-Integral Method to the solution of two dimensional, plane stress problems for fully anisotropic, elastic materials. The nature of the equations is such that engineering notation for all field variables is convenient. The notation and theoretical development of the field equations follows from Lekhnitskii [1][1]. The development of the boundary-integral equations follows the usual method outlined by Cruse [2]. The solution of the problem of unit loads in the x- and y-directions, called the fundamental solution will be first be obtained. Next, the Betti reciprocal work theorem will be used to obtain Somigliana's identities for internal displacements and stresses. Finally, the Boundary-Integral Equation will be obtained from the Somigliana displacement identity.

In the plane stress equations presented in this note, the non-zero stress components are $\{\sigma_x, \sigma_y, \tau_{xy}\}$ and the corresponding strain components are $\{\epsilon_x, \epsilon_y, \gamma_{xy}\}$. The equilibrium equations for the stresses are

$$\begin{aligned} \frac{\partial \sigma_x}{\partial x} + \frac{\partial \tau_{xy}}{\partial y} &= 0 \\ \frac{\partial \tau_{xy}}{\partial x} + \frac{\partial \sigma_y}{\partial y} &= 0 \end{aligned} \tag{1}$$

The strain components are subject to the single compatibility equation

[1]Brackets refer to references at the end of this note.

$$\frac{\partial^2\epsilon_x}{\partial y^2} + \frac{\partial^2\epsilon_y}{\partial x^2} = \frac{\partial^2\gamma_{xy}}{\partial x\partial y} \qquad (2)$$

which guarantees the existence of single-valued displacements, u_x, u_y which are related to the strains by

$$\frac{\partial u_x}{\partial x} = \epsilon_x \,, \quad \frac{\partial u_y}{\partial y} = \epsilon_y$$
$$\frac{\partial u_x}{\partial y} + \frac{\partial u_y}{\partial x} = \gamma_{xy} \qquad (3)$$

The constitutive law for the fully-anisotropic elastic material in plane stress can be given in matrix form as

$$\begin{Bmatrix} \epsilon_x \\ \epsilon_y \\ \gamma_{xy} \end{Bmatrix} = \begin{bmatrix} \beta_{11} & \beta_{12} & \beta_{16} \\ \beta_{12} & \beta_{22} & \beta_{26} \\ \beta_{16} & \beta_{26} & \beta_{66} \end{bmatrix} \begin{Bmatrix} \sigma_x \\ \sigma_y \\ \tau_{xy} \end{Bmatrix} \qquad (4)$$

The β_{ij}'s are the material compliances and are known to be the components of a fourth-order tensor, as the strains[2] and stresses are components of second order tensors. The tensor character of the compliances is basic for the application of the current results to composite materials, as discussed by Ashton et. al. [3].

The compliances may be given in terms of engineering material constants

$$\begin{aligned} \beta_{11} &= 1/E_x \,, & \beta_{12} &= -\nu_{xy}/E_x \\ \beta_{22} &= 1/E_y \,, & \beta_{16} &= \eta_{xy,x}/E_x \\ \beta_{26} &= \eta_{xy,y}/E_y \,, & \beta_{66} &= 1/G_{xy} \end{aligned} \qquad (5)$$

[2] Using $\gamma_{xy}/2$ as the tensorial shear component.

For orthotropic materials $\beta_{16} = \alpha_{26} = 0$. For later reference the stiffness coefficients are now introduced but not put in engineering terms

$$\begin{Bmatrix} \sigma_x \\ \sigma_y \\ \tau_{xy} \end{Bmatrix} = \begin{bmatrix} \alpha_{11} & \alpha_{12} & \alpha_{16} \\ \alpha_{12} & \alpha_{22} & \alpha_{26} \\ \alpha_{16} & \alpha_{26} & \alpha_{66} \end{bmatrix} \begin{Bmatrix} \epsilon_x \\ \epsilon_y \\ \gamma_{xy} \end{Bmatrix} \tag{6}$$

The Airy Stress Function is now introduced such that its existence guarantees satisfaction of equilibrium, Eq (1)

$$\sigma_x = \frac{\partial^2 F}{\partial y^2}\ , \quad \sigma_y = \frac{\partial^2 F}{\partial x^2}\ , \quad \tau_{xy} = -\frac{\partial^2 F}{\partial x \partial y} \tag{7}$$

Substitution of Eq (7) into Eq (4) and Eq (2) results in the following governing differential equation for F(x,y)

$$\begin{aligned} \beta_{11} \frac{\partial^4 F}{\partial y^4} - 2\beta_{16} \frac{\partial^4 F}{\partial x \partial y^3} + (2\beta_{12} + \beta_{66}) \frac{\partial^4 F}{\partial x^2 \partial y^2} \\ - 2\beta_{26} \frac{\partial^4 F}{\partial x^3 \partial y} + \beta_{22} \frac{\partial^4 F}{\partial x^4} = 0 \end{aligned} \tag{8}$$

Characteristic surfaces along which F(x,y) can be integrated may be found by introducing the notation

$$z = x + \mu y \ ; \qquad \mu = a + ib \quad , \qquad i = \sqrt{-1} \tag{9}$$

Substitution of Eq (9) into Eq (8) reduces Eq (8) to

$$\frac{d^4 F}{dz^4} [\beta_{11}\mu^4 - 2\beta_{16}\mu^3 + (2\beta_{12} + \beta_{66})\mu^2 - 2\beta_{26}\mu + \beta_{22}] = 0 \tag{10}$$

If we are to obtain non-trivial results to Eq (10) $d^4F / dz^4 \neq 0$ which requires

$$\beta_{11}\mu^4 - 2\beta_{16}\mu^3 + (2\beta_{12} + \beta_{66})\mu^2 - 2\beta_{26}\mu + \beta_{22} = 0 \qquad (11)$$

Eq (11) is the characteristic equation for the material; Lekhnitskii shows that the four roots of Eq (11) are never real and are distinct so long as the material is not isotropic. We denote the roots $\mu_j = a_j + ib_j$ $(j=1,2)$ and $\bar{\mu}_j = a_j - ib_j$. Lekhnitskii also shows that $b_j > 0$, from thermodynamic considerations. Thus the characteristic directions become

$$z_k = x + \mu_k y, \quad k = 1,2 \qquad (12)$$

and their conjugates.

The general form of the stress function can be given by the relation

$$F(x,y) = 2R \{ F_1(z_1) + F_2(z_2) \} \qquad (13)$$

Introducing the notation dF_k/dz_k (no summation on k) $= \Phi_k(z_k)$ the stresses become

$$\begin{aligned} \sigma_x &= 2R \{\mu_1^2 \Phi_1'(z_1) + \mu_2^2 \Phi_2'(z_2)\} \\ \sigma_y &= 2R \{\Phi_1'(z_1) + \Phi_2'(z_2)\} \\ \tau_{xy} &= -2R \{\mu_1\Phi_1'(z_1) + \mu_2\Phi_2'(z_2)\} \end{aligned} \qquad (14)$$

where the prime denotes ordinary differentiation. The strains may be obtained from Eq (14) and integrated to obtain the displacements

$$u_x = 2R\{ p_1 \Phi_1 (z_1) + p_2 \Phi_2(z_2) \}$$
$$u_y = 2R\{ q_1 \Phi_1 (z_1) + q_2 \Phi_2(z_2) \} \tag{15}$$

where

$$p_k = \beta_{11}\mu_k^2 + \beta_{12} - \beta_{16}\mu_k$$

$$q_k = \beta_{12}\mu_k + \beta_{22}/\mu_k - \beta_{26} \tag{16}$$

Equations (14) and (15) together with traction boundary conditions

$$t_x = \sigma_x n_x + \tau_{xy} n_y = g_1$$

$$t_y = \tau_{xy} n_x + \sigma_y n_y = g_2 \tag{17}$$

or displacement boundary conditions

$$u_x = h_1 \; ; \; u_y = h_2 \tag{18}$$

constitute the mathematical problem to be solved.

5.2.2 *Fundamental Solution: Point Force Problem*

The basic relation for the development of integral equations for the solution of the anisotropic problem is the solution for a point force in the infinite anisotropic plane. Two such solutions will be required: A unit force in the x-direction, and a unit force in the y-direction. Utilizing the traction formulae (17) it is easily shown that on an arbitrary closed surface

$$\begin{aligned} \oint_S t_x dS &= 2R [\![\mu_1\Phi_1 + \mu_2\Phi_2]\!] \\ \oint_S t_y dS &= -2R [\![\Phi_1 + \Phi_2]\!] \end{aligned} \tag{19}$$

where $[\![\quad]\!]$ denotes the jump in the enclosed quantities for a full cycle of S. If the path S encloses the point of load application, $z_o = x_o + i\, y_o$, then the results of (19) will be non-zero.

Let Φ_{jk} represent the stress function for a point load in the x_j[3] direction. The path integrals in (19) are seen to be of the opposite sign to the applied loads;

$$\begin{aligned} 2R [\![\Phi_{j1} + \Phi_{j2}]\!] &= \delta_{j2} \\ 2R [\![\mu_1\Phi_{j1} + \mu_2\Phi_{j2}]\!] &= -\delta_{j1} \end{aligned} \tag{20}$$

---

[3] We will now use indicial notation $(x,y) = (x_1, x_2)$ and its associated conventions. The index k will never be summed.

for the point load solutions. Functions which satisfy (20) for *any* closed path around z_o are

$$\Phi_{jk} = A_{jk} \log (z_k - z_{k_o}) \tag{21}$$

where $z_{k_o} = x_o + \mu_k y_o$. In what follows z_{k_o} will, for convenience only, be taken as the origin, $z_{k_o} = 0$. It may be shown by suitable investigation near $z_k = 0$ that (21) satisfies the requirements of a point force [4]. Since it is easily shown that

$$[\![\log z_k]\!] = 2\pi i \quad , \quad i = \sqrt{-1} \tag{22}$$

(20) leads to the result

$$\begin{aligned} A_{j1} - \bar{A}_{j1} + A_{j2} - \bar{A}_{j2} &= \delta_{j2}/2\pi i \\ \mu_1 A_{j1} - \bar{\mu}_1 \bar{A}_{j1} + \mu_2 A_{j2} - \bar{\mu}_2 \bar{A}_{j2} &= -\delta_{j1}/2\pi i \end{aligned} \tag{23}$$

It is also required that the displacement field surrounding the applied be single-valued. That is

$$[\![u_j]\!] = 0 \qquad j = 1, 2 \tag{24}$$

Substitution of (21) into (15) and taking the jump around a closed path we find in addition to (23)

$$\begin{aligned} p_1 A_{ji} - \bar{p}_1 \bar{A}_{ji} + p_2 A_{j2} - \bar{p}_2 \bar{A}_{j2} &= 0 \\ q_1 A_{ji} - \bar{q}_1 \bar{A}_{ji} + q_2 A_{j2} - \bar{q}_2 \bar{A}_{j2} &= 0 \end{aligned} \tag{25}$$

Together, (23) and (25) are sufficient to find A_{jk}. Taking the notation

$$\mu_k = \alpha_k + i\gamma_k \qquad i = \sqrt{-1} \qquad (26)$$

$$A_{jk} = C_{jk} + i\,D_{jk}$$

it is easily shown that (23) and (25) together with (16) reduce in real form to

$$\begin{bmatrix} (2\beta_{11}\alpha_1\gamma_1 - \beta_{13}\gamma_1) & [\beta_{11}(\alpha^2{}_1 - \gamma^2{}_1) + \beta_{12} - \beta_{13}\alpha_1] & (2\beta_{11}\alpha_2\gamma_2 - \beta_{13}\gamma_2) & [\beta_{11}(\alpha^2{}_2 - \gamma^2{}_2) + \beta_{12} - \beta_{13}\alpha_2] \\ [\beta_{12}\gamma_1 - \beta_{22}\gamma_1/(\alpha^2{}_1 + \gamma^2{}_1)] & [\beta_{12}\alpha_1 + \beta_{22}\,\alpha_1/(\alpha^2{}_1 + \gamma^2{}_1) - \beta_{23}] & [\beta_{12}\gamma_2 - \beta_{22}\gamma_2/(\alpha^2{}_2 + \gamma^2{}_2)] & [\beta_{12}\alpha_2 + \beta_{22}\alpha_2/(\alpha^2{}_2 + \gamma^2{}_2) - \beta_{23}] \\ 0 & 1 & 0 & 1 \\ \gamma_1 & \alpha_1 & \gamma_2 & \alpha_2 \end{bmatrix} \begin{Bmatrix} C_{j1} \\ D_{j1} \\ C_{j2} \\ D_{j2} \end{Bmatrix} = \begin{Bmatrix} 0 \\ 0 \\ -\delta_{j2}/4\pi \\ \delta_{j1}/4\pi \end{Bmatrix} \qquad (27)$$

Equation (27) becomes singular when $\mu_1 = \mu_2 = i$, but it will be shown that A_{jk} may be found for very nearly isotropic materials.

We now define two tensor fields: The first is U_{jk} and corresponds to the displacements for the stress function (21) according to (15)

$$U_{ji} = 2R\,\{P_{i1}A_{j1}\log z_1 + P_{i2}A_{j2}\log z_2\} \tag{28}$$

where $P_{1k} = p_k$, $P_{2k} = q_k$. Taking the derivatives of (21) at z_k according to (14) and substituting into (17), tractions on an arbitrary surface are found

$$T_{ji} = 2R\,\{Q_{i1}(\mu_1 n_1 - n_2)\,A_{j1}/z_1 + Q_{i2}\,(\mu_2 n_1 - n_2)\,A_{j2}/z_2\} \tag{29}$$

where

$$[\,Q_{ik}\,] = \begin{bmatrix} \mu_1 & \mu_2 \\ -1 & -1 \end{bmatrix} \tag{30}$$

5.2.3 *Boundary-Integral Equation*

Since the governing partial differential equation (10) admits no real characteristic surface the problem is elliptic and the stresses and displacements are continuous. Under such circumstances it is easily verified that Betti's reciprocal work theorem at the surface must be valid

$$\int_{S+\Gamma} T_{ji} u_i \, dS = \int_{S+\Gamma} U_{ji} t_i \, dS \tag{31}$$

The surface Γ is a circle of vanishing radius ε surrounding the point load; it is added to exclude the singularity from the volume. The second integral in (31) is convergent as $\varepsilon \to 0$. For continuous u_i it is sufficient to investigate the behavior of the integral

$$\lim_{\varepsilon \to 0} \int_{\Gamma} T_{ji} \, dS \tag{32}$$

At a circle centered at the applied load it is seen that

$$\mu_k n_1 - n_2 = -(\mu_k \cos\theta - \sin\theta) \tag{33}$$

and $dS = \varepsilon d\theta$, $0 \le \theta < 2\pi$. Extracting from (32) the variable part it is sufficient to find

$$\int_0^{2\pi} \frac{\mu_k n_1 - n_2}{z_k} \, dS = -\int_0^{2\pi} \frac{\mu_k \cos\theta - \sin\theta}{\mu_k \sin\theta + \cos\theta} \, d\theta \tag{34}$$

which, upon rearrangement becomes

$$\int_0^{2\pi} \frac{\mu_k n_1 - n_2}{z_k}\, dS = \mu_k \int \frac{d(\tan\theta)}{1-\mu_k^2\tan^2\theta} - (1+\mu_k^2) \int \frac{\cos\theta\, d(\cos\theta)}{(1+\mu_k^2)\cos^2\theta - \mu_k^2} \tag{35}$$

Equation (35) can then be integrated directly to obtain

$$\int_0^{2\pi} \frac{\mu_k n_1 - n_2}{z_k}\, dS = -\log\left[\cos\theta - \mu_k \sin\theta\right] \Big|_0^{2\pi} \tag{36}$$

Taking the real part of the argument of the log

$$\rho_k^2 = (\cos\theta - a_k \sin\theta)^2 + (b_k \sin\theta)^2 \tag{37}$$

and the imaginary part

$$\phi_k = -\tan^{-1}\left[\frac{b_k \sin\theta}{\cos\theta - a_k \sin\theta}\right] \tag{38}$$

the result to (36) is found to be

$$\int_0^{2\pi} \frac{\mu_k n_1 - n_2}{z_k}\, dS = 2\pi i \tag{39}$$

Substitution of (39) into (32) and using (23) leads to the usual Somigliana identity for the interior displacement

$$u_j(z_\circ) = -\int_S T_{ji}(z_k, z_\circ)\, u_i(z_k) dS(z_k) + \int_S U_{ji}(z_k, z_\circ)\, t_i(z_k) dS(z_k) \tag{40}$$

The Boundary-Integral Equation is found in the usual way [2] by allowing $z_\circ$ to approach the boundary from the inside and evaluating the jumps in the singular integrals in (40). A simple means for evaluating the jump is to place $z_\circ$ at the surface, augment the surface as shown in the figure and integrate (40).

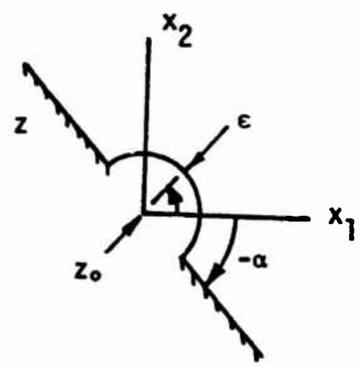

In this case $\mu_k n_1 - n_2 = \mu_k \cos\theta + \sin\theta$ since the normal (n_1, n_2) points *outward* from $z_\circ$. The range on θ is $-\alpha \le \theta < \pi - \alpha$. Again the only significant integral is in the first integral in (40)

$$\int_{-\alpha}^{\pi-\alpha} \frac{\mu_k n_1 - n_2}{z_k} \varepsilon d\theta = \int_{-\alpha}^{\pi-\alpha} \frac{\mu_k \cos\theta - \sin\theta}{\mu_k \sin\theta - \cos\theta} d\theta \tag{41}$$

which, by the same steps as above, becomes

$$\int_{-\alpha}^{\pi-\alpha} \frac{\mu_k n_1 - n_2}{z_k} \varepsilon d\theta = -i \left[\tan^{-1}\left(\frac{b_k \sin\theta}{\cos\theta - a_k \sin\theta} \right) \right]_{-\alpha}^{\pi-\alpha} \tag{42}$$

Substitution of the limits in (42) yields

$$\int_{-\alpha}^{\pi-\alpha} \frac{\mu_k n_1 - n_2}{z_k} \varepsilon d\theta = -i\pi \tag{43}$$

Again using the relations (23), (40) becomes

$$u_j/2 + \int_S T_{ji} u_i dS = \int_S U_{ji} t_i dS \tag{44}$$

Equation (44) is the Boundary-Integral Equation which relates unknown boundary data to known boundary data. Once (44) has been solved numerically (§V), (40) can be used to obtain interior displacements and stresses.

5.2.4 Somigliana's Identity for Interior Strains, Stresses

The displacement gradient tensor $u_{j,\ell}$ can be calculated from (40) by differentiation at z_o. Since $\partial/\partial x_\ell[\log(z_k-z_o)] = -\partial/\partial x_{\ell_o}[\log(z_k-z_o)]$ the differentiation may be written in terms of derivatives at z_k by a change in sign. Then

$$\frac{\partial u_j}{\partial x_\ell} = \int_S \frac{\partial T_{ji}}{\partial x_\ell} u_i dS - \int_S \frac{\partial U_{ji}}{\partial x_\ell} t_i dS \tag{45}$$

The tensorial strain at z_o is given by the symmetric part of (45)

$$\epsilon_{j\ell} = \frac{1}{2}(u_{j,\ell} + u_{\ell,j}) \tag{46}$$

such that

$$2\epsilon_{j\ell} = \int_S \left[\frac{\partial T_{ji}}{\partial x_\ell} + \frac{\partial T_{\ell i}}{\partial x_j}\right] u_i dS - \int_S \left[\frac{\partial U_{ji}}{\partial x_\ell} + \frac{\partial U_{\ell i}}{\partial x_j}\right] t_i dS \tag{47}$$

The kernels, $S_{j\ell i}$, $D_{j\ell i}$ respectively are given by

$$\begin{aligned} S_{j\ell i} &= -2R\,\{R_{\ell 1}Q_{i1}(\mu_1 n_1 - n_2)\,A_{j1}/z_1^2 + R_{\ell 2}Q_{i2}\,(\mu_2 n_1 - n_2)\,A_{j2}/z_2^2\} \\ &\quad -2R\,\{R_{j1}Q_{i1}(\mu_1 n_1 - n_2)\,A_{\ell 1}/z_1^2 + R_{j2}Q_{i2}\,(\mu_2 n_1 - n_2)\,A_{\ell 2}/z_2^2\} \\ D_{j\ell 1} &= 2R\,\{R_{\ell 1}P_{i1}A_{j1}\,/\,z_1 + R_{\ell z}P_{iz}A_{j2}/z_2\} \\ &\quad +2R\,\{R_{j1}P_{i1}A_{\ell 1}\,/\,z_1 + R_{j2}P_{i2}A_{\ell 2}/z_2\} \end{aligned} \tag{48}$$

where $R_{1k} = 1$, $R_{2k} = \mu_k$. It is assumed that the boundary is piecewise flat. Then (47) becomes

$$2\varepsilon_{j\ell} = \int_S S_{j\ell i}\, u_i dS - \int_S D_{j\ell i} t_i dS \tag{49}$$

The stresses can be determined by substitution of (49), with $\gamma_{xy} = 2\varepsilon_{12}$, $\varepsilon_x = \varepsilon_{11}$, $\varepsilon_y = \varepsilon_{22}$, into (6).

5.2.5 *Numerical Solution*

Following the procedure used in the isotropic theory, the boundary displacements and boundary tractions are assumed to be piecewise constant. When this is assumed over the M boundary segments (again taken as straight line segments), (44) becomes

$$u_j(n)/2 + \sum_{m=1}^{M} u_i(m) \int_{\Delta S_m} T_{ji}(n,m)dS = \sum_{m=1}^{M} t_i(m) \int_{\Delta S_m} U_{ji}(n,m)dS \quad (50)$$

Similarly the internal strains (49) become

$$2\varepsilon_{j\ell}(z_o) = \sum_{m=1}^{M} u_i(m) \int_{\Delta S_m} S_{j\ell i}(z_o,m)dS - \sum_{m=1}^{M} t_i(m) \int_{\Delta S_m} D_{j\ell i}(z_o,m)dS \quad (51)$$

By specifying the orientation of each line segment, ΔS_m, with its normal (n_1, n_2) the integrals in (50) and (51) may be solved for explicitly. The notation is defined in the figure below

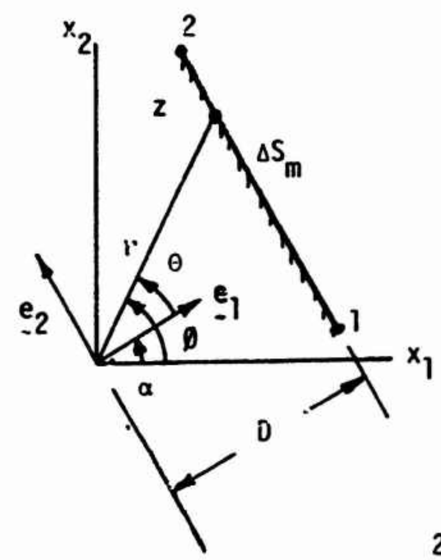

$$z_k = r(\cos\phi + \mu_k \sin\phi)$$
$$D = \underset{\sim}{r} \cdot \underset{\sim}{e}_1 \quad (52)$$
$$dS = Dd(\tan\theta)$$

The coordinate system $(\underset{\sim}{e}_1, \underset{\sim}{e}_2)$ is taken such that $\underset{\sim}{e}_1$ is in the direction of the *outward* normal and $\underset{\sim}{e}_2$ is tangent to ΔS_m, going from "1" to "2" keeping the material on the left. Since $\phi = \theta + \alpha$, where $\alpha = \cos^{-1}(n_1)$, (52) can be written

$$z_k = r\cos\theta(\cos\alpha - \sin\alpha\tan\theta + \mu_k\cos\alpha\tan\theta + \mu_k\sin\alpha) \tag{53}$$

so that

$$z_k = D\,[(\cos\alpha + \mu_k\sin\alpha) + (\mu_k\cos\alpha - \sin\alpha)\tan\theta] \tag{54}$$

The closed-form integrals for (50), (51) are now easily obtained, as the only variable is $\tan\theta$. Two special cases, $D = 0$ and the multivaluedness of $\log z_k$ will be discussed below. Defining integrals of the variables in the kernels with ΔI's we obtain

$$\begin{aligned}
\Delta U_{ji} &= \int_{\Delta S} U_{ji}\,dS = 2R\,\{P_{i1}A_{j1}\Delta I_{11} + P_{i2}A_{j2}\Delta I_{12}\} \\
\Delta T_{ji} &= \int_{\Delta S} T_{ji}\,dS = 2R\,\{Q_{i1}(\mu_1 n_1 - n_2)A_{j1}\Delta I_{21} \\
&\qquad + Q_{i2}(\mu_1 n_1 - n_2)\,A_{j2}\Delta I_{22}\}
\end{aligned} \tag{55}$$

and for the strains

$$\Delta D_{j\ell i} = 2\mathcal{R}\{R_{\ell 1}P_{i1}A_{j1}\Delta I_{31} + R_{\ell 2}P_{i2}A_{j2}\Delta I_{32}\}$$
$$+ 2\mathcal{R}\{R_{ji}P_{i1}A_{\ell 1}\Delta I_{31} + R_{j2}P_{i2}A_{\ell 2}\Delta I_{32}\}$$

(56)

$$\Delta S_{j\ell i} = -2\mathcal{R}\{R_{\ell 1}Q_{i1}(\mu_1 n_1 - n_2)A_{j1}\Delta I_{41} + R_{\ell 2}Q_{i2}(\mu_2 n_1 - n_2)A_{j2}\Delta I_{42}\}$$
$$-2\mathcal{R}\{R_{j1}Q_{i1}(\mu_1 n_1 - n_2)A_{\ell 1}\Delta I_{41} + R_{j2}Q_{i2}(\mu_2 n_1 - n_2)A_{\ell 2}\Delta I_{42}\}$$

The integrals are easily calculated for $D \neq 0$

$$\Delta I_1 = \int_1^2 \log z_k dS = \frac{1}{\mu_k \cos\alpha - \sin\alpha} \left[z_k(\log z_k - 1)\right]\Big|_1^2$$

$$\Delta I_2 = \Delta I_3 \int_1^2 \frac{dS}{z_k} = \frac{1}{\mu_k \cos\alpha - \sin\alpha} (\log z_k)\Big|_1^2$$

$$\Delta I_4 = \int_1^2 \frac{dS}{z_k^2} = \frac{1}{\mu_k \cos\alpha - \sin\alpha} \left(-\frac{1}{z_k}\right)\Big|_1^2$$

The case for $D = 0$ may be deduced as a special result of (57) or by integrating again, with proper substitutions for z_k and dS. Using "±" to denote the cases where $dS = +dr$ and $dS = -dr$ we note $\theta = \pm\pi/2$ and

$$z_k = \pm r\,(\mu_k \cos\alpha - \sin\alpha) \qquad (58)$$

Substitution of (58) into the integrals in (55), (56) we obtain

$$\Delta I_1 = \int_1^2 \log[\pm r(\mu_k \cos\alpha - \sin\alpha)]\ (\pm dr) = \frac{1}{\mu_k \cos\alpha - \sin\alpha}\ [z_k(\log z_k - 1)]\Big|_1^2$$

$$\Delta I_2 = \Delta I_3 = \int_1^2 \frac{dS}{z_k} = \frac{1}{\mu_k \cos\alpha - \sin\alpha}\ (\log z_k)\Big|_1^2 \qquad (59)$$

$$\Delta I_4 = \int_1^2 \frac{dS}{z_k^2} = -\frac{1}{(\mu_k \cos\alpha - \sin\alpha)^2}\ \left(\pm\frac{1}{r}\right)\Big|_1^2$$

The first two results in equation (57) contain the term log z_k. The log is multivalued, and has a jump of $+2\pi$ on the digital computer as θ passes from $\pi-\varepsilon$ to $\pi-\varepsilon$. To account for this on the computer the change in the imaginary part of log z_k is tested. If a change of more than π in the imaginary part is found then the result is corrected by adding $(\pm 2\pi)$ to the imaginary part of the log z_k.

5.2.6 Usage Guide for ANISOT

The computer program is divided into three major sections, along the same lines as the solution just detailed. The first section solves the boundary-integral equations (44), producing a fully known set of boundary tractions and displacements. The next section utilizes Somigliana's identity (51) to obtain stresses at specified interior points. The final section determines stresses at the surface of the body, using the tractions obtained in section one, and the tangential derivatives of the displacements.

The boundary solution may be output on punched cards if desired. This option allows the user to input the boundary solution directly, and the program will begin execution of sections two and three.

5.2.6.1 Problem Size Specifications

The program allows up to two degrees of symmetry of geometry and boundary conditions. Present array dimensions limit the number of boundary segments to 80 (320 with symmetry), but capacity may be increased by changing the common statements labeled ARRAY1 and ARRAY2. A number of other cards should also be modified, and are listed below, by card number:

ANI10065	ANI15235
ANI10070	ANI20035
ANI10100	ANI5005
ANI15050	

The number of interior points which may be specified is limited to 200, while the limit on surface stress points is 50. These limits may be increased by changing ARRAY3 and ARRAY4, respectively.

The time required for execution of each subroutine is calculated through an assembly language subroutine, TIME. Users of computers other than the Univac 1108 should provide their own routine for this purpose, or insert a dummy routine, TIME(T).

5.2.6.2 Specification of Material Constants

Material constants are specified through four matrices, listed below:

STIFF, stiffness matrix (6)

FLEX, compliance matrix (4)

MU, solutions to the characteristic equation (11)

AX, coefficients of the net load terms in Lekhnitskii's stress function (see §II)

The coefficients AX are calculated in a program called AXCALC, which serves as an auxiliary program. All the matrices described above may be obtained as punched output from AXCALC, and inserted directly into the data deck.

5.2.6.3 *Use of AXCALC*

This program makes use of a capability previously detailed [5] to solve the characteristic equation for a generally anisotropic material, symmetric about its mid-plane. The algorithm is specifically designed for a layered material, since major use will be found in the area of advanced fiber composites. AXCALC requires as input only the stacking sequence of the laminate, and the material properties of the individual laminae, in their principal material directions.

Input data required by AXCALC is summarized in the table below. Items which appear on the same card are bracketed, and the format for each card appears opposite the first item on that card.

INPUT FOR AXCALC		
ITEM	DESCRIPTION	FORMAT
NC	Number of laminates to be analyzed	I3
TITL	Title card - any 80 characters	16A5
NANG	Number of individual laminae	I3
[E11	Major Young's modulus (single lamina)	(3E15.10, F10.4)
E22	Minor Young's modulus	
G12	In-plane shear modulus	
V12]	Principal Poisson's ratio	
THETA(I)	Orientation angles of the individual laminae (angles measured from the x axis to the major axis of the layer)	10F8.3
THICK(I)	Thicknesses of individual laminae	8F10.8

5.2.6.4 *Identification of Parameters in ANISOT*

All parameters necessary for use of the integral equation program are defined below. For easy reference, the more important ones are defined on cards numbered ANI5065 - ANI15120 in subroutine SETUP. All the descriptions below are summarized in Table 2, and parameters which may be described concisely appear only in Table 2.

NODE (I,J) - a temporary array which stores the two node numbers associated with each segment number ('rear' number, then 'forward' number)

XYZM (I,J) - a temporary array containing the x_1 and x_2 coordinates of each node, in that order.

PTIN (I,J) - coordinates of the interior stress solution points (x_1,x_2). These are read only if NPT $\neq 0$.

NBDY (I,J) - three segment numbers necessary for the surface stress solution, read only if NBDYP $\neq 0$. For each segment on which a stress solution is desired, three segment numbers are read, in the following order: segment number on which stress solution is desired; segment number for the "rear" difference value of $\Delta u/\Delta s$; segment number for the "forward" difference value of $\Delta u/\Delta s$. The 'forward' direction is taken as the positive "s" direction, always directed along the boundary of the body with the material on the left.

5.2.6.5 *Boundary Conditions*

Both traction and displacement boundary conditions are possible, and are input by means of a NAMELIST read statement. The boundary data is preceded and followed by control cards, as shown below:

```
_$ BDYCON
  {DATA
_$ END
```

All boundary conditions are initialized to zero and the boundary condition key, LDC(I), is initialized to 1, meaning a traction boundary condition is assumed for each segment. Setting LDC = 2 means a displacement boundary condition will be specified for the given segment and direction. Traction conditions are specified by a parameter TCON(I), while displacement conditions are specified by UCON(I).

All x_1-direction boundary data is stored, followed by x_2-direction data. The value of the subscript I for the boundary parameters (UCON, TCON, LDC) is determined in the following manner. For data specified in the x_1 direction,

I = the segment number (N), *but* for the x_2 direction

I = N + NSEG, where NSEG is the total number of boundary segments.

For example consider a body which has been represented by 24 segments.

Tractions specified on segment 6:

_TCON(6) = .100E04, (x_1 traction)

_TCON(30) = .325E04, (x_2 traction)

Displacements specified on segment 9:

_LDC(9) = 2, LDC(33) = 2,

_UCON(9) = 0.001, (x_1 displacement)

_UCON(33) = 0.004, (x_2 displacement)

Displacements set at zero on segment 1:

_LDC(1) = 2, (x_1)

_LDC(25) = 2, (x_2)

5.2.6.6 Input Data for ANISOT

ITEM	DESCRIPTION	FORMAT
NC	Number of problems to be solved	I3
TITL	Title card -any 80 characters	16A5
NSEG	Number of segments on the boundary	10I5
NSYM	Degrees of symmetry (y, then x)	
NNOD	Number of boundary nodes connecting segments	
IPUNCH	= 0, the boundary solution will not be punched	
ISTRS	= 0, plane strain ; = 1 plane stress	
IBDY	≠ 0, boundary data read from cards	
NPT	Number of interior points for stress solution	
NBDYP	Number of points for boundary stresses	
NODE(I,J)	Nodes associated with each segment number	24I3
XYZM(I,J)	(x_1, x_2) coordinates of each node	16F5.3
STIFF*	Stiffness matrix (6)	6E13.7
FLEX*	Compliance matrix (4)	6E13.7
MU*	Solutions of the characteristic equation (11)	4E20.10
AX(I,J)*	Coefficients of stress function (see §II)	4E20.10
Boundary Conditions	a NAMELIST read statement (See standard references for format)	
PTIN(I,J)	Interior Stress Solution points (x_1, x_2)	16F5.3
NBDY(I,J)	Segment numbers associated with surface stress solutions.	24I3

*Cards available as direct output of AXCALC

5.2.7 References

[1] S. G. Lekhnitskii, *Theory of Elasticity of an Elastic Body*, Holden-Day (1963).

[2] T. A. Cruse, *Application of the Boundary-Integral Equation Method to Problems of Solid Mechanics* (In preparation).

[3] J. E. Ashton, J. C. Halpin, P. H. Petit, *Primer on Composite Materials: Analysis*, Technomic (1969).

[4] E. Sternberg, R. A. Eubanks, "On the Concept of Concentrated Loads and an Extension of the Uniqueness Theorem in the Linear Theory of Elasticity", *Journal of Rational Mechanics and Analysis*, 4 (1955).

[5] H. J. Konish, Jr., "Numerical Calculation of the Characteristic Parameters for a Generally Anisotropic Plate - MULTMU Usage Guide", Report SM-65, Carnegie-Mellon University, (June 1971).

5.2.8 *Listing for AXCALC Computer Program*

```
C   DETERMINES COEFFICIENTS OF NET LOAD TERMS FOR ANISOTROPIC STRESS FTN
       COMMON / MATCON / E11, E22, G12, V12, E(3,3), BETA(3,3)
       COMMON / GEOMTY / THETA(10), THICK(10), NANG, PI
       COMMON / ROOTS1 / LAMDA(20)
       DIMENSION STIF(6), FLEX(6), DELTA(2,2)
       DIMENSION TITL(16), C(4,4), B(4,4), RHS(4), X(4), R(4), XI(4,4)
       COMPLEX LAMDA
C
C      NC = NUMBER OF CASES TO BE SOLVED SEQUENTIALLY
C      N = ORDER OF CHARACTERISTIC EQUATION.
C      THETA = ANGLE FROM THE X-AXIS TO THE 1-AXIS, IN DEGREES.
C      E11, E22, V12, AND G12 ARE THE MATERIAL PROPERTIES OF THE
C           INDIVIDUAL LAMINAE.
C      K = NUMBER OF LAMINAE IN THE LAMINATE.
C      THICK = THICKNESS OF EACH LAMINA IN THE LAMINATE.
C
       PI = 3.1415926536
       DO 15 I = 1,2
       DO 15 J = 1,2
       DELTA(I,J) = 0.0
    15 IF (I.EQ.J) DELTA(I,J) = 1.0
       READ(5,100) NC
    45 WRITE(6,105) NC
       NC = NC - 1
       IF (NC.LT.0) STOP
       READ(5,110) TITL
       READ(5,120) NANG
       READ(5,125) E11,E22,G12,V12
       READ(5,130) (THETA(I), I = 1,NANG)
       READ(5,135) (THICK(I), I = 1,NANG)
       CALL MULTMU
       K = 0
       DO 25 I = 1,3
       DO 25 J = I,3
       K = K + 1
       STIF(K) = E(I,J)
    25 FLEX(K) = BETA(I,J)
       WRITE (7,1000) STIF
       WRITE (7,1000) FLEX
       WRITE(6,115) TITL
       WRITE(6,140)
       WRITE(6,145) E11, E22, G12, V12
       WRITE(6,150)
       WRITE(6,155) (THETA(L), L = 1,NANG)
       WRITE(6,160)
       WRITE(6,165) (THICK(L), L = 1,NANG)
       WRITE(6,180)
       WRITE(6,175) ((E(I,J),J = 1,3), I = 1,3)
       WRITE(6,190)
       WRITE(6,175) ((BETA(I,J), J = 1,3), I = 1,3)
       WRITE(6,195)
       WRITE(6,200) (LAMDA(I), I = 1,4)
       ALPH1 = REAL ( LAMDA(1) )
       GAM1 = ABS( AIMAG( LAMDA(1) ) )
       ALPH2 = REAL( LAMDA(3) )
       GAM2 = ABS( AIMAG( LAMDA(3) ) )
       WRITE(7,280) ALPH1, GAM1, ALPH2, GAM2
```

```
      C(1,1) = 2.*BETA(1,1)*ALPH1*GAM1 - BETA(1,3)*GAM1
      C(1,3) = 2.*BETA(1,1)*ALPH2*GAM2 - BETA(1,3)*GAM2
      C(1,2) = BETA(1,1)*(ALPH1**2-GAM1**2) + BETA(1,2) -BETA(1,3)*ALPH1
      C(1,4) = BETA(1,1)*(ALPH2**2-GAM2**2) + BETA(1,2) -BETA(1,3)*ALPH2
      C(2,1) = BETA(1,2)*GAM1-BETA(2,2)*GAM1/(ALPH1**2+GAM1**2)
      C(2,2) = BETA(1,2)*ALPH1 + BETA(2,2)*ALPH1/(ALPH1**2+GAM1**2)
     1 - BETA(2,3)
      C(2,3) = BETA(1,2)*GAM2-BETA(2,2)*GAM2/(ALPH2**2+GAM2**2)
      C(2,4) = BETA(1,2)*ALPH2 + BETA(2,2)*ALPH2/(ALPH2**2+GAM2**2)
     1 - BETA(2,3)
      C(3,1) = 0.0
      C(3,3) = 0.0
      C(3,2) = 1.0
      C(3,4) = 1.0
      C(4,1) = GAM1
      C(4,3) = GAM2
      C(4,2) = ALPH1
      C(4,4) = ALPH2
      DO 35 I = 1,2
      DO 35 J = 1,4
   35 C(I,J) = C(I,J) * E22
      DO 05 I=1,4
      DO 05 J=1,4
   05 B(I,J) = C(I,J)
      CALL INVR (C, 4, DUMMY, 0, DET, 4, 4)
      DO 10 I = 1,4
      DO 10 J = 1,4
      XI(I,J) = 0.0
      DO 10 K = 1,4
   10 XI(I,J) = XI(I,J) + C(I,K) * B(K,J)
      WRITE(6,250)
      WRITE(6,210) ((XI(I,J),J=1,4),I=1,4)
      DO 40 K = 1,2
      RHS(1) = 0.0
      RHS(2) = 0.0
      RHS(3) = -DELTA(K,2)/(4.*PI)
      RHS(4) =  DELTA(K,1)/(4.*PI)
      WRITE(6,260)
      WRITE(6,210) (RHS(I) , I = 1,4)
      DO 20 I = 1,4
      X(I) = 0.0
      DO 20 J = 1,4
   20 X(I) = X(I) + C(I,J) * RHS(J)
      WRITE(6,270) (X(I),I=1,4)
      WRITE(7,280) (X(I),I=1,4)
      DO 30 I = 1,4
      R(I) = 0.0
      DO 30 J = 1,4
   30 R(I) = R(I) + B(I,J) * X(J)
      WRITE(6,260)
      WRITE(6,210) (R(I),I=1,4)
   40 CONTINUE
      GO TO 45
  100 FORMAT(I3)
  105 FORMAT(1H1,I3)
  110 FORMAT(16A5)
  115 FORMAT(1H1,16A5)
  120 FORMAT(2I3)
```

```
125 FORMAT(3F15.10,F10.4)
130 FORMAT(10F8.3)
135 FORMAT(8F10.8)
140 FORMAT(1H0,36X,'E11',7X,'E22',7X,'G12',7X,'V12',7X,'V21')
145 FORMAT(1H ,30X,5E10.4)
150 FORMAT(1H0,30X,'ORIENTATION, TOP TO BOTTOM, IN DEGREES')
155 FORMAT(48X,F10.5)
160 FORMAT(1H0,30X,'LAMINA THICKNESS, TOP TO BOTTOM, IN INCHES')
165 FORMAT(48X,F10.7)
170 FORMAT(1H0,30X,'THE A-MATRIX FOR THIS LAMINATE IS')
175 FORMAT(     (30X,3(E14.5,5X)),/)
180 FORMAT(1H0,30X,'THE E-MATRIX FOR THIS LAMINATE IS')
190 FORMAT(1H0,30X,'THE PLANE-STRESS BETA MATRIX IS')
195 FORMAT(1H0,20X,'THE MU-VALUES FOR THIS LAMINATE ARE')
200 FORMAT(     2(5X,F20.12),'J')
210 FORMAT((/4E14.8) )
250 FORMAT ( //////, 10X, ' THE IDENDITY MATRIX IS    ', // )
260 FORMAT( ////// , 10X , 'THE RHS VECTOR ' , ////  )
270 FORMAT ( ////// , 10X ,  'A1 = ',2E14.7,'J',/ 10X,'A2 = ',2E14.7,
   1 'J', //// )
280 FORMAT (4F20.10)
1000 FORMAT (6E13.7)
     END
```

```
      SUBROUTINE MULTMU
      COMMON / MATCON / E11, E22, G12, V12, E(3,3), BETA(3,3)
      COMMON / GEOMTY / THETA(10), THICK(10), NANG, PI
      COMMON / ROOTS1 / LAMDA(20)
      DIMENSION QB(10,3,3), A(3,3), COFAC(3,3), TRANS(3,3)
      DIMENSION D(11)
      COMPLEX LAMDA
      K = NANG
      V21 = E22*V12/E11
      Q11 = E11/(1.0 - V12*V21)
      Q22 = E22/(1.0 - V12*V21)
      Q12 = V21*Q11
      Q66 = G12
      H = 0.0
      DO 10 L = 1,K
      H = H + THICK(L)
   10 CONTINUE
      DO 15 L = 1,K
      THRAD = PI*THETA(L)/180.0
      T = COS(THRAD)
      S = SIN(THRAD)
      QB(L,1,1) = Q11*(T**4) + 2.*(Q12 + 2.*Q66)*((S*T)**2) + Q22*(S**4)
      QB(L,2,2) = Q11*(S**4) + 2.*(Q12 + 2.*Q66)*((S*T)**2) + Q22*(T**4)
      QB(L,1,2) = (Q11 +Q22 - 4.*Q66)*((S*T)**2) + Q12*((S**4) +(T**4))
      QB(L,1,3) = (Q11 -Q12 -2.*Q66)*S*(T**3) + (Q12 - Q22 + 2.*Q66)*T*
     1            (S**3)
      QB(L,2,3) = (Q11 -Q12 -2.*Q66)*T*(S**3) + (Q12 - Q22 + 2.*Q66)*S*
     1            (T**3)
      QB(L,3,3) = (Q11 + Q22 - 2.*(Q12 + Q66))*((S*T)**2) + Q66*((S**4)
     1            + (T**4))
      QB(L,2,1) = QB(L,1,2)
      QB(L,3,2) = QB(L,2,3)
      QB(L,3,1) = QB(L,1,3)
   15 CONTINUE
      DO 20 I = 1,3
      DO 25 J= 1,3
      A(I,J) = 0.0
      DO 30 L = 1,K
      ASUM = QB(L,I,J)*THICK(L)
      A(I,J) = A(I,J) + ASUM
   30 CONTINUE
      E(I,J) = A(I,J)/H
   25 CONTINUE
   20 CONTINUE
      DET = (E(1,1)*E(2,2)*E(3,3)) + (E(1,2)*E(2,3)*E(3,1)) +
     1      (E(1,3)*E(2,1)*E(3,2)) - (E(3,1)*E(2,2)*E(1,3)) -
     2      (E(3,2)*E(2,3)*E(1,1)) - (E(3,3)*E(2,1)*E(1,2))
      COFAC(1,1) =          (E(2,2)*E(3,3)) - (E(3,2)*E(2,3))
      COFAC(1,2) = -1.0*((E(2,1)*E(3,3)) - (E(3,1)*E(2,3)))
      COFAC(1,3) =          (E(2,1)*E(3,2)) - (E(3,1)*E(2,2))
      COFAC(2,1) = -1.0*((E(1,2)*E(3,3)) -(E(3,2)*E(1,3)))
      COFAC(2,2) =          (E(1,1)*E(3,3)) - (E(3,1)*E(1,3))
      COFAC(2,3) = -1.0*((E(1,1)*E(3,2)) - (E(3,1)*E(1,2)))
      COFAC(3,1) =          (E(1,2)*E(2,3)) - (E(2,2)*E(1,3))
      COFAC(3,2) = -1.0*((E(1,1)*E(2,3)) - (E(2,1)*E(1,3)))
      COFAC(3,3) =          (E(1,1)*E(2,2)) - (E(2,1)*E(1,2))
      DO 35 I = 1,3
```

```
      DO 40 J = 1,3                                                     AXC15285
      TRANS(I,J) = COFAC(J,I)                                           AXC15290
      BETA(I,J) = (TRANS(I,J))/DET                                      AXC15295
   40 CONTINUE                                                          AXC15300
   35 CONTINUE                                                          AXC15305
      D(1) = BETA(1,1)                                                  AXC15310
      D(2) = -2.0*BETA(1,3)                                             AXC15315
      D(3) = 2.0*BETA(1,2) + BETA(3,3)                                  AXC15320
      D(4) = -2.0*BETA(2,3)                                             AXC15325
      D(5) = BETA(2,2)                                                  AXC15330
      CALL ROOTS(D,4,LAMDA)*                                            AXC15335
      RETURN                                                            AXC15340
      END                                                               AXC15345
```

*Standard root solving routine called here. User must supply such a routine.

```
      SUBROUTINE INVR    (A, N, B, M, D, IS, JS)
C
C   A = MATRIX, DIMENSIONS SHOWN, IN WHICH A SUBMATRIX IN UPPER LEFT-
C         HAND CORNER IS TO BE INVERTED
C   N = ORDER OF SUBMATRIX
C   D = DETERMINANT
C   M = 0, THEN
C         B = B(1,1) IN CALLING ROUTINE, AND INVERSE STORED IN A
C   M = 1, THEN
C         B = B(N,1) IN CALLING ROUTINE, AND A-INVERSE * B RETURNED IN B
C   M = M (.GT. 1), THEN
C         B = B(N,M) IN CALLING ROUTINE, AND A-INVERSE * B RETURNED IN B
C   A-INVERSE IS NOT DESTROYED IN LAST TWO CASES
C
      DIMENSION A(IS,JS), B( 1,1), IN(100,2), IP(100), P(100)
      D = 1.0
      DO 03  J = 1,N
   03 IP(J) = 0
      DO 60  I = 1,N
      AMAX = 0.0
      DO 18  J = 1,N
      IF (IP(J) - 1) 06, 18, 06
   06 DO 15  K = 1,N
      IF (IP(K) - 1) 09, 15, 72
   09 IF (ABS(AMAX) - ABS(A(J,K))) 12, 15, 15
   12 IR = J
      IC = K
      AMAX = A(J,K)
   15 CONTINUE
   18 CONTINUE
      IP(IC) = IP(IC) + 1
      IF (IR - IC) 21, 33, 21
   21 D = -D
      DO 24  L = 1,N
      SWAP = A(IR,L)
      A(IR,L) = A(IC,L)
   24 A(IC,L) = SWAP
      IF (M) 33, 33, 27
   27 DO 30  L = 1,M
      SWAP = B(IR,L)
      B(IR,L) = B(IC,L)
   30 B(IC,L) = SWAP
   33 IN(I,1) = IR
      IN(I,2) = IC
      P(I) = A(IC,IC)
      D = D * P(I)
      A(IC,IC) = 1.0
      DO 36  L = 1,N
   36 A(IC,L) = A(IC,L) / P(I)
      IF (M) 45, 45, 39
   39 DO 42  L = 1,M
   42 B(IC,L) = B(IC,L) / P(I)
   45 DO 60  L1 = 1,N
      IF (L1 - IC) 48, 60, 48
   48 T = A(L1,IC)
      A(L1,IC) = 0.0
      DO 51  L = 1,N
```

```
 51 A(L1,L) = A(L1,L) - A(IC,L) * T
    IF (M) 60, 60, 54
 54 DO 57  L = 1,M
 57 B(L1,L) = B(L1,L) - B(IC,L) * T
 60 CONTINUE
    DO 69  I = 1,N
    L = N + 1 - I
    IF (IN(L,1) - IN(L,2)) 63, 69, 63
 63 JR = IN(L,1)
    JC = IN(L,2)
    DO 66  K = 1,N
    IF (N.EQ.0)  JR=K
    SWAP = A(K,JR)
    A(K,JR) = A(K,JC)
 66 A(K,JC) = SWAP
 69 CONTINUE
 72 RETURN
100 FORMAT (//10F13.5)
300 FORMAT (1H1)
     END
```

5.2.9 *Listing for ANISOT Computer Program*

```
C
C  MAIN PROGRAM -- INITIALIZES DATA - CALLS SUBROUTINES
C
      COMMON / ARRAY1 / XYZ(100,2,2), UCON(200), TCON(200), LOC(200)
      COMMON / ARRAY2 / BVAL(200)
      COMMON / MATCON / PI,FMU,PQ(2,2),MU(2),FLEX(6),STIF(6),AX(2,2)
      COMMON / CONTR1 / NSEG, NSYM, NTOTAL, NSIZE, NPT, NBDYP
      COMMON / CONTR2 / TITL(16), IPUNCH, ISTRS, IBDY
      COMMON / TIMERS / T (10)
      COMPLEX PQ, MU, AX
C
C  THE DIMENSIONS OF THE FOLLOWING ARRAYS ARE PROBLEM DEPENDENT
C
      DIMENSION C(160,160)
      DOUBLE PRECISION RHS(160)
      READ (5,100) NC
    5 WRITE (6,200) NC
      NC = NC - 1
      IF (NC .LT. 0) STOP
      PI = 3.14159265
      DO 10 I = 1,200
      UCON(I) = 0.
      TCON(I) = 0.
   10 BVAL(I) = 0.
      CALL TIME ( T(1) )
      DO 20 I = 2,10
   20 T(I) = 0.
      CALL SETUP
      IF (IBDY.NE.0) GO TO 30
      CALL BVSOLU (C, RHS)
   30 CALL INSOLU (C)
      CALL BDYSTR (C)
C
C  CALCULATE TIME CHART
C
      T(2) = (T(2)-T(1))*10**(-3)
      T(4) = (T(4)-T(3))*10**(-3)
      T(6) = (T(6)-T(5))*10**(-3)
      T(8) = (T(8)-T(7))*10**(-3)
      T(10) = (T(10)-T(9))*10**(-3)
      WRITE (6,2000)  TITL
      WRITE (6,2100)
      WRITE (6,2200) T(2), T(4), T(6), T(8), T(10)
      GO TO 5
  100 FORMAT ( I3 )
  200 FORMAT ( 1H1, 5X I3)
 1000 FORMAT ( 16A5)
 2000 FORMAT (1H1, 16A5)
 2100 FORMAT ( 21H TIME BREAKDOWN CHART //)
 2200 FORMAT ( 5X 15HTIME FOR SETUP    F12.7, 2X 7HSECONDS //
     1         5X 15HTIME FOR DELINT   F12.7, 2X 7HSECONDS //
     2         5X 15HTIME FOR SOLVER   F12.7, 2X 7HSECONDS //
     3         5X 15HTIME FOR INSOLU   F12.7, 2X 7HSECONDS //
     4         5X 15HTIME FOR BDYSOL   F12.7, 2X 7HSECONDS)
      END
```

```
      SUBROUTINE SETUP                                                  ANI15000
      COMMON / ARRAY1 / XYZ(100,2,2), UCON(200), ICON(200), LOC(200)    ANI15005
      COMMON / ARRAY2 / BVAL(200)                                       ANI15010
      COMMON / ARRAY3 / PTIN(100,2)                                     ANI15015
      COMMON / ARRAY4 / NBDY(50,3)                                      ANI15020
      COMMON / MATCON / PI,FMU,PQ(2,2),MU(2),FLEX(6),STIF(6),AX(2,2)    ANI15025
      COMMON / TIMERS / TIM(10)                                         ANI15030
      COMMON / CONTR1 / NSEG, NSYM, NTOTAL, NSIZE, NPT, NBDYP           ANI15035
      COMMON / CONTR2 / TITL(16), IPUNCH, ISTRS, IBDY                   ANI15040
      NAMELIST / BDYCON / UCON, ICON, LOC                               ANI15045
      DIMENSION NODE(100,2), XYZM(100,2)                                ANI15050
      COMPLEX PQ, MU, AX                                                ANI15055
      EQUIVALENCE (NODE, LOC), (XYZM, UCON)                             ANI15060
C                                                                       ANI15065
C  NSEG = NUMBER OF SEGMENTS ON THE BOUNDARY                            ANI15070
C  NSYM = NUMBER OF DEGREES OF SYMMETRY STARTING WITH Y, THEN X         ANI15075
C  NNOD = NUMBER OF BOUNDARY NODES CONNECTING BOUNDARY SEGMENTS         ANI15080
C  IPUNCH = 1 -- THE BOUNDARY SOLUTION WILL BE PUNCHED OUT              ANI15085
C  ISTRS = 0, PLSTRN -- ISTRS = 1, PLSTRS                               ANI15090
C  IF IBDY.EQ.0  ---  BOUNDARY DATA STORED IN COMMON                    ANI15095
C  IF IBDY.NE.0  ---  BOUNDARY DATA READ IN FROM CARDS ADDED TO END     ANI15100
C                     OF THE DATA DECK                                  ANI15105
C  NPT = NUMBER OF INTERIOR SOLUTION POINTS FOR STRESS SOLUTION         ANI15110
C  NBDYP = NUMBER OF BOUNDARY POINTS FOR STRESS SOLUTION                ANI15115
C                                                                       ANI15120
      READ (5,1000) TITL                                                ANI15125
      READ (5,1100) NSEG, NSYM, NNOD, IPUNCH, ISTRS, IBDY, NPT, NBDYP   ANI15130
      READ (5,1200) ((NODE(I,J),J=1,2),I=1,NSEG)                        ANI15135
      READ (5,1300) ((XYZM(I,J),J=1,2),I=1,NNOD)                        ANI15140
      READ (5,1400) STIF                                                ANI15145
      READ (5,1400) FLEX                                                ANI15150
      READ (5,1700) MU                                                  ANI15155
      READ (5,1700) ((AX(I,J),J=1,2),I=1,2)                             ANI15160
      WRITE (6,2000) TITL                                               ANI15165
      WRITE (6,2100) NSEG, NSYM, NNOD, IPUNCH, ISTRS, IBDY, NPT, NBDYP  ANI15170
      WRITE (6,2200) ((NODE(I,J),J=1,2),I=1,NSEG)                       ANI15175
      WRITE (6,2300) ((XYZM(I,J),J=1,2),I=1,NNOD)                       ANI15180
      WRITE (6,2400) STIF                                               ANI15185
      WRITE (6,2400) FLEX                                               ANI15190
      WRITE (6,2700) MU                                                 ANI15195
      WRITE (6,2700) ((AX(I,J),J=1,2),I=1,2)                            ANI15200
      NSIZE = 2 * NSEG                                                  ANI15205
      DO 10 I = 1,NSEG                                                  ANI15210
      DO 10 J = 1,2                                                     ANI15215
      DO 10 K = 1,2                                                     ANI15220
      N = NODE(I,J)                                                     ANI15225
   10 XYZ(I,J,K) = XYZM(N,K)                                            ANI15230
      DO 20 I = 1,200                                                   ANI15235
      UCON(I) = 0.                                                      ANI15240
   20 LOC(I) = 1                                                        ANI15245
      READ (5,BDYCON)                                                   ANI15250
      IF (NPT.EQ.0) GO TO 30                                            ANI15255
      READ  (5,1500) ((PTIN(I,J),J=1,2),I=1,NPT)                        ANI15260
      WRITE (6,2500) ((PTIN(I,J),J=1,2),I=1,NPT)                        ANI15265
   30 IF (NBDYP.EQ.0) GO TO 40                                          ANI15270
      READ  (5,1600) ((NBDY(I,J),J=1,3),I=1,NBDYP)                      ANI15275
      WRITE (6,2600) ((NBDY(I,J),J=1,3),I=1,NBDYP)                      ANI15280
```

```
   40 CONTINUE
      NFAC = 2**NSYM
      IF (NSYM.EQ.0) NFAC = 1
      NTOTAL = NSEG * NFAC
C
C  CALCULATE NEEDED MATERIAL CONSTANTS
C
      DO 50 K = 1,2
      PQ(1,K) = FLEX(1)*MU(K)**2 + FLEX(2) - FLEX(3)*MU(K)
   50 PQ(2,K) = FLEX(2)*MU(K) + FLEX(4)/MU(K) - FLEX(5)
      FMU = STIF(1)
      CALL TIME ( TIM(2) )
      RETURN
 1000 FORMAT (16A5)
 1100 FORMAT (10I5)
C
C  ****** CAUTION*****  FORMATS PROBLEM DEPENDENT  ***** CAUTION ******
C
 1200 FORMAT (24I3)
 1300 FORMAT (16F5.3)
 1400 FORMAT ( 6E13.7 )
 1500 FORMAT (16F5.3)
 1600 FORMAT (24I3)
 1700 FORMAT(4E20.10)
 2000 FORMAT (1H1, 10X, 16A5)
 2100 FORMAT (// 10I5)
 2200 FORMAT (// 8(3X 2I3))
 2300 FORMAT (// 4(3X 2F10.6))
 2400 FORMAT ( 10X 3E12.7 /, 22X 2E12.7 /, 34X E12.7 )
 2500 FORMAT (// 4(3X 2F10.6))
 2600 FORMAT (// 6(3X 3I3))
 2700 FORMAT ( 2( 2F10.6,8X ) )
 2800 FORMAT ( 5X, 8E12.6 )
      END
```

```
      SUBROUTINE HVSOLU (C, RHS)
      COMMON / ARRAY1 / XYZ(100,2,2), UCON(200), TCON(200), LOC(200)
      COMMON / ARRAY2 / BVAL(200)
      COMMON / MATCON / PI,FMU,PQ(2,2),MU(2),FLEX(6),STIF(6),AX(2,2)
      COMMON / CONTR1 / NSEG, NSYM, NTOTAL, NSIZE, NPT, NBDYP
      COMMON / CONTR2 / TITL(16), IPUNCH, ISTRS, IBUY
      COMMON / TIMERS / TIM (10)
      DIMENSION A(200), PXYZ(2), C(NSIZE,NSIZE)
      EQUIVALENCE (A, UCON)
      DOUBLE PRECISION RHS(NSIZE)
      COMPLEX PQ, MU, AX
      NMAX = 2 * NSEG
      WRITE (6,2000) TITL
      IF (ISTRS.EQ.0) WRITE (6,2050)
      IF (ISTRS.EQ.1) WRITE (6,2060)
      WRITE (6,2100)
C
C  WRITE THE STARTING BOUNDARY CONDITIONS
C
      DO 10 I = 1,NSEG
      J = I + NSEG
      DO 15 N = 1,2
   15 PXYZ(N) = (XYZ(I,1,N) + XYZ(I,2,N))/2.
   10 WRITE (6,2200) I, UCON(I), UCON(J), TCON(I), TCON(J),
     1                 LOC(I), LOC(J), PXYZ(1), PXYZ(2)
      DO 20 I = 1,NMAX
      RHS(I) = 0.0D0
      IF (LOC(I).EQ.1) GO TO 30
      BVAL(I) = FMU * UCON(I)
      GO TO 20
   30 BVAL(I) = TCON(I)
   20 CONTINUE
C
C  CALCULATE DELU, DELT, RHS
C
      CALL TIME ( TIM(3) )
      CALL DELINT (C, RHS)
      CALL TIME ( TIM(4) )
C
C  WRITE RIGHT HAND SIDE VECTOR
C
      WRITE (6,2300) TITL
      DO 40 I = 1,NSEG
      J = I + NSEG
   40 WRITE (6,2400) I, RHS(I), RHS(J)
C
C  SOLVE SYSTEM OF EQUATIONS
C
      CALL TIME ( TIM(5) )
      CALL SOLVER (NMAX, RHS, A, C)
      CALL TIME ( TIM(6) )
C
C  FILL IN UCON, TCON  --- PRINT RESULTS
C
      DO 50 I = 1,NMAX
      IF (LOC(I).EQ.1) GO TO 60
      TCON(I) = FMU * A(I)
```

```
      UCON(I) = (1./FMU) * BVAL(I)
      GO TO 50
   60 TCON(I) = BVAL(I)
      UCON(I) = A(I)
   50 CONTINUE
      WRITE (6,2000) TITL
      IF (ISTRS.EQ.0) WRITE (6,2050)
      IF (ISTRS.EQ.1) WRITE (6,2060)
      WRITE (6,2100)
      DO 70 I = 1,NSEG
      J = I + NSEG
      DO 80 N = 1,2
   80 PXYZ(N) = (XYZ(I,1,N) + XYZ(I,2,N))/2.
   70 WRITE (6,2200) I, UCON(I), UCON(J), TCON(I), TCON(J),
     1                          LOC(I), LOC(J), PXYZ(1), PXYZ(2)
      IF (IPUNCH.EQ.0) RETURN
      DO 120 I = 1,NSEG
      J = I + NSEG
  120 WRITE (7,2500) I, UCON(I), UCON(J)
      DO 130 I = 1,NSEG
      J = I + NSEG
  130 WRITE (7,2500) I , TCON(I), TCON(J)
      RETURN
 2000 FORMAT (1H1, 16A5 // 10X 19HBOUNDARY CONDITIONS)
 2050 FORMAT ( / 4( 18H PLANE STRAIN **** ) )
 2060 FORMAT ( / 4( 18H PLANE STRESS **** ) )
 2100 FORMAT (// 4X 4H SEG 7X 2HU1 10X 2HU2 10X 2HT1 10X 2HT2 8X 4HLOC1
     1  6X 4HLOC2 8X 2HX1 10X 2HX2 //)
 2200 FORMAT (2X I5, 2F12.8, 2F12.0, 6X I1, 11X I1, 2F12.6)
 2300 FORMAT (1H1, 16A5 // 10X 22HRIGHT HAND SIDE VECTOR //)
 2400 FORMAT (5X, I5, 2E15.8)
 2500 FORMAT ( I10, 2E30.10)
 3000 FORMAT (/// ( 2(8F12.6 /) //) )
      END
```

```
      SUBROUTINE DELINT (G, RHS)
      COMMON / ARRAY1 / XYZ(100,2,2), UCON(200), ICON(200), LOC(200)
      COMMON / ARRAY2 / BVAL(200)
      COMMON / MATCON / PI,FMU,PQ(2,2),MU(2),FLEX(6),STIF(6),AY(2,2)
      COMMON / CONTR1 / NSEG, NSYM, NTOTAL, NSIZE, NPT, NBDYP
      COMMON / CONTR2 / TITL(16), IPUNCH, ISTRS, IBUY
      DIMENSION A(2), E1(2), E2(2), P(2), X(2,2), R1(2) [illegible]2)
      DIMENSION ISYM(2), G(NSIZE,NSIZE)
      DIMENSION XX1(50), XX2(50), XX3(50), XX4(50)
      DOUBLE PRECISION RHS(NSIZE)
      COMPLEX PQ, MU, AX
      COMPLEX AK(2), BK(2), ZK1(2), ZK2(2), DI1(2), DI2(2)
      COMPLEX U(2,2), T(2,2), TRANS, LOG1(2), LOG2(2)
      COMPLEX MUKPOW
      INTEGER SGNI
      SPHT = 1.
      DO 63 I = 1,50
      XX1(I) = 0.
      XX2(I) = 0.
      XX3(I) = 0.
      XX4(I) = 0.
   63 CONTINUE
      DO 10 I = 1,NSIZE
      DO 10 J = 1,NSIZE
   10 G(I,J) = 0.
      DO 20 M = 1,NTOTAL
      M1 = (M-1)/NSEG
      M2 = M - M1*NSEG
      M3 = M2 + NSEG
C
C     COMPUTE SYMMETRY COEFFICIENTS USING Y, THEN X
C
      IFLAG = 1
      DO 16 K = 1,2
      J = 3 - K
      I = (M-1)/(NSEG*((2**J)/2))
      ISYM(K) = (-1)**I
      IF (I.EQ.0) ISYM(K) = 1
   16 IFLAG = IFLAG * ISYM(K)
      DO 30 J = 1,2
      IF (IFLAG.GT.0) GO TO 25
      X(1,J) = XYZ(M2,2,J) * ISYM(J)
      X(2,J) = XYZ(M2,1,J) * ISYM(J)
      GO TO 35
   25 X(1,J) = XYZ(M2,1,J) * ISYM(J)
      X(2,J) = XYZ(M2,2,J) * ISYM(J)
   35 CONTINUE
C
C     DEFINE DIRECTION OF THE LINE SEGMENT   E2 = A(J) / AMAG
C
   30 A(J) = X(2,J) - X(1,J)
      AMAG = SQRT (A(1)**2 + A(2)**2)
      DO 33 I = 1,2
      E2(I) = A(I)/AMAG
      J = 3 - I
   33 E1(J) = E2(I) * (-1)**(J+1)
```

```
C   CALCULATE THE ANGLES T1 AND T2 AND THE DISTANCE D
C
      DO 20 N = 1,NSEG
      DO 15 J = 1,2
      P(J) = (XYZ(N,1,J) + XYZ(N,2,J))/2.
      R1(J) = X(1,J) - P(J)
      R2(J) = X(2,J) - P(J)
   15 CONTINUE
      CALL DOTPRD (R1, E1, D)
      CALL DOTPRD (R1, E2, R12)
      CALL DOTPRD (R2, E2, R22)
      CALL DOTPRD (R1, R1, R1MAG)
      CALL DOTPRD (R2, R2, R2MAG)
      R1MAG = SQRT (R1MAG)
      R2MAG = SQRT (R2MAG)
      RA = ABS(R12)
      RB = ABS(R22)
      RMAG = AMAX1 (RA, RB)
      IF (ABS(D /RMAG).LT.1.0E-03) GO TO 40
C
C CALCULATE DI1, DI2 FOR D.NE.0
C
      TN1 = R12 / D
      TN2 = R22 / D
      DO 50 I = 1,2
      AK(I) = E1(2)*MU(I) + E1(1)
      BK(I) = E1(1)*MU(I) - E1(2)
      ZK1(I) = D * (AK(I) + BK(I) * TN1)
      ZK2(I) = D * (AK(I) + BK(I) * TN2)
      LOG1(I) = CLOG( ZK1(I) )
      LOG2(I) = CLOG( ZK2(I) )
      DPHI = AIMAG (LOG2(I) - LOG1(I))
      SPHI = SIGN (SPHI, DPHI)
      IF (ABS(DPHI).GT.PI) LOG2(I) = LOG2(I) - SPHI * CMPLX(0.0, 2.*PI)
      DI1(I) = ZK2(I) * (LOG2(I) - 1.) / BK(I)
     1         - ZK1(I) * (LOG1(I) - 1.) / BK(I)
      DI2(I) = (LOG2(I) - LOG1(I)) / BK(I)
   50 CONTINUE
      GO TO 60
   40 CONTINUE
C
C CALCULATE DI1, DI2 FOR D.EQ.0
C
      DO 55 I = 1,2
      BK(I) = E1(1)*MU(I) - E1(2)
      DI1(I) = R22 * (CLOG(BK(I)*R22) - 1.)
     1         - R12 * (CLOG(BK(I) * R12) - 1.)
      DI2(I) =      (ALOG(RB) - ALOG(RA)) / BK(I)
   55 CONTINUE
   60 CONTINUE
C
C CALCULATE DELU, DELT INTEGRALS
C
      DO 64 I = 1,2
      DO 64 J = I,2
      T(J,I) = CMPLX(0.0,0.0)
      U(J,I) = CMPLX(0.0,0.0)
   64 CONTINUE
```

```
      DO 65 I = 1,2                                                     ANT25575
      DO 65 J = 1,2                                                     ANT25580
      DO 65 K = 1,2                                                     ANT25585
      SGNT = (-1)**(3-I)                                                ANT25590
      MUKPOW = MU(K)**(2-I)                                             ANT25595
      U(J,I) = U(J,I) + PQ(I,K)*AX(J,K)*DI1(K)                          ANT25600
      T(J,I) = T(J,I) + (MU(K)*E1(1)-E1(2))*MUKPOW*SGNT                 ANT25605
     1                    *AX(J,K)*UI2(K)                               ANT25610
   65 CONTINUE                                                          ANT25615
      XX1(N) = XX1(N) + 2.*REAL(T(1,1))                                 ANT25620
      XX2(N) = XX2(N) + 2.*REAL(T(1,2))                                 ANT25625
      XX3(N) = XX3(N) + 2.*REAL(T(2,1))                                 ANT25630
      XX4(N) = XX4(N) + 2.*REAL(T(2,2))                                 ANT25635
   75 DO 85 IX = 1,2                                                    ANT25640
      DO 85 JX = 1,2                                                    ANT25645
      N4 = N  + (IX-1)*NSEG                                             ANT25650
      M4 = M2 + (JX-1)*NSEG                                             ANT25655
      IF (IX.EQ.JX.AND.M.EQ.N) T(IX,JX) = CMPLX(0.25,0.0)               ANT25660
      IF (LOC(M4).EQ.1) GO TO 90                                        ANT25665
      TRANS = U(IX,JX)                                                  ANT25670
      U(IX,JX) = -(1./FMU) * T(IX,JX)                                   ANT25675
      T(IX,JX) = -FMU * TRANS                                           ANT25680
   90 RHS(N4) = RHS(N4) + 2.*REAL(U(IX,JX)) * RVAL(M4) * ISYM(JX)       ANT25685
      G(N4,M4) = G(N4,M4) + 2.*REAL(T(IX,JX)) * ISYM(JX)                ANT25690
   85 CONTINUE                                                          ANT25695
   20 CONTINUE                                                          ANT25700
      WRITE(6,2600) TITL                                                ANT25705
 2600 FORMAT(1H1,16A5//10X,17HCOLUMN SUM CHECKS//)                      ANT25710
      DO 95 I = 1,NSEG                                                  ANT25715
   95 WRITE (6,2500) I, XX1(I), XX2(I), XX3(I), XX4(I)                  ANT25720
      RETURN                                                            ANT25725
 2000 FORMAT(1X,3I4,3F8.5,10F9.5  )                                     ANT25730
 2100 FORMAT ( 5X I4, 2F20.10, I4)                                      ANT25735
 2200 FORMAT(1X,3I4,12E9.4 )                                            ANT25740
 2300 FORMAT (10X, 4E15.7)                                              ANT25745
 2400 FORMAT (10X, 6I4, 6E15.7)                                         ANT25750
 2500 FORMAT (3X, I4, 4F20.15)                                          ANT25755
      END                                                               ANT25760
```

```
      SUBROUTINE INSOLU( C )
      COMMON / ARRAY1 / XYZ(100,2,2), UCON(200), TCON(200), LOC(200)
      COMMON / ARRAY3 / PTIN(100,2)
      COMMON / MATCON / PI,FMU,PQ(2,2),MU(2),FLEX(6),STIF(6),AX(2,2)
      COMMON / TIMERS / TIM (10)
      COMMON / CONTR1 / NSEG, NSYM, NTOTAL, NSIZE, NPT, NBDYP
      COMMON / CONTR2 / TITL(16), IPUNCH, ISTRS, IBDY
      DIMENSION C(100,6), A(4), PXYZ(3)
      COMPLEX PQ, MU, AX
      IF (IBDY.NE.0) GO TO 100
  110 IF (NPT.EQ.0) RETURN
      CALL TIME ( TIM(7) )
      WRITE (6,2000) TITL
      IF (ISTRS.EQ.0) WRITE (6,2050)
      IF (ISTRS.EQ.1) WRITE (6,2060)
C
C  CALL FOR CALCULATION OF DELD AND DELS
C
      WRITE (6,2100)
      A(4) = 0.
      CALL DELSD (C)
      DO 10 NP = 1,NPT
      C(NP,5) = C(NP,5) * 2.
      A(1) = STIF(1)*C(NP,4) + STIF(3)*C(NP,5) + STIF(2)*C(NP,6)
      A(2) = STIF(3)*C(NP,4) + STIF(6)*C(NP,5) + STIF(5)*C(NP,6)
      A(3) = STIF(2)*C(NP,4) + STIF(5)*C(NP,5) + STIF(4)*C(NP,6)
      WRITE (6,2200) NP, (A(K),K=1,4), PTIN(NP,1), PTIN(NP,2)
   10 CONTINUE
      CALL TIME ( TIM(8) )
      RETURN
  100 WRITE (6,2000) TITL
      DO 120 I = 1,NSEG
      J = I + NSEG
  120 READ (5,1100) N, UCON(I), UCON(J)
      DO 130 I = 1,NSEG
      J = I + NSEG
  130 READ (5,1100) N, TCON(I), TCON(J)
      WRITE (6,2300)
      DO 140 I = 1,NSEG
      J = I + NSEG
      DO 150 N = 1,2
  150 PXYZ(N) = (XYZ(I,1,N) + XYZ(I,2,N))/2.
  140 WRITE (6,2400) I, UCON(I), UCON(J), TCON(I), TCON(J),
     1                    LOC(I), LOC(J), PXYZ(1), PXYZ(2)
      GO TO 110
 1100 FORMAT (I10, 2E30.10)
 2000 FORMAT (1H1, 10X, 16A5)
 2050 FORMAT ( / 4( 18H PLANE STRAIN **** ) )
 2060 FORMAT ( / 4( 18H PLANE STRESS **** ) )
 2100 FORMAT (6H0POINT, 2X 10H SIGMA(XX) 2X 10H SIGMA(YY) 2X
     1       10H SIGMA(XY) 2X 10H SIGMA(ZZ) 5X 2H X 6X 2H Y)
 2200 FORMAT (2X I3, 2X 4F12.2, 2F8.4)
 2300 FORMAT (// 4X 4H SEG 7X 2HU1 10X 2HU2 10X 2HT1 10X 2HT2 8X 4HLOC1
     1  6X 4HLOC2 8X 2HX1 10X 2HX2 //)
 2400 FORMAT (2X I5, 2F12.8, 2F12.0, 6X I1, 11X I1, 2F12.6)
      END
```

```
      SUBROUTINE DELSU (G)
      COMMON / ARRAY1 / XYZ(100,2,2), UCON(200), ICON(200), LOC(200)
      COMMON / ARRAY3 / PTIN(100,2)
      COMMON / MATCON / PI,FMU,PQ(2,2),MU(2),FLEX(6),STIF(6),AX(2,2)
      COMMON / CONTR1 / NSEG, NSYM, NTOTAL, NSIZE, NPT, NHDYP
      COMMON / CONTR2 / TITL(16), IPUNCH, ISTRS, IBDY
      DIMENSION A(2), E1(2), E2(2), P(2), X(2,2), R1(2), R2(2)
      DIMENSION ISYM(2), G(100,6)
      COMPLEX PQ, MU, AX
      COMPLEX AK(2), BK(2), ZK1(2), ZK2(2), DI3(2), DI4(2), DU, DS
      COMPLEX LOG1(2), LOG2(2)
      SPHT = 1.
      DO 10 I = 1,100
      DO 10 J = 1,6
   10 G(I,J) = 0.
      DO 20 M = 1,NTOTAL
      M1 = (M-1)/NSEG
      M2 = M - M1*NSEG
C
C  COMPUTE SYMMETRY COEFFICIENTS USING Y, THEN X
      IFLAG = 1
      DO 16 K = 1,2
      J = 3 - K
      I = (M-1)/(NSEG*((2**J)/2))
      ISYM(K) = (-1)**I
      IF (I.EQ.0) ISYM(K) = 1
   16 IFLAG = IFLAG * ISYM(K)
      DO 32 J = 1,2
      IF (IFLAG.GT.0) GO TO 23
      X(1,J) = XYZ(M2,2,J) * ISYM(J)
      X(2,J) = XYZ(M2,1,J) * ISYM(J)
      GO TO 35
   23 X(1,J) = XYZ(M2,1,J) * ISYM(J)
      X(2,J) = XYZ(M2,2,J) * ISYM(J)
   35 CONTINUE
C
C  DEFINE DIRECTION OF THE LINE SEGMENT E2 = A(J)/AMAG
C
   32 A(J) = X(2,J) - X(1,J)
      AMAG = SQRT (A(1)**2 + A(2)**2)
      DO 33 I = 1,2
      E2(I) = A(I)/AMAG
      J = 3 - I
   33 E1(J) = E2(I) * (-1)**(J+1)
C
C  CALCULATE THE ANGLES T1 AND T2 AND THE DISTANCE D
C
      DO 20 N = 1,NPT
      DO 15 J = 1,2
      P(J) = PTIN(N,J)
      R2(J) = X(2,J) - P(J)
      R1(J) = X(1,J) - P(J)
   15 CONTINUE
      D1 = 0.
      D2 = 0.
      DO 17 J=1,2
      D1 = D1 + R1(J)*R1(J)
```

```
17 D2 = D2 + R2(J)*R2(J)
   D1 = SQRT(D1)
   D2 = SQRT(D2)
   CALL DOTPRD (R1, E1, D)
   CALL DOTPRD (R1, E2, R12)
   CALL DOTPRD (R2, E2, R22)
   CALL DOTPRD (R1, R1, R1MAG)
   CALL DOTPRD (R2, R2, R2MAG)
   R1MAG = SQRT (R1MAG)
   R2MAG = SQRT (R2MAG)
   RA = ABS(R12)
   RB = ABS(R22)
   RMAG = AMAX1(RA,RB)
   IF (ABS(D /RMAG).LT.1.0E-03) GO TO 40
   TN1 = R12 / D
   TN2 = R22 / D
C
C  CALCULATE DI3, DI4 FOR D.NE.0
C
   DO 45 I = 1,2
   AK(I) = E1(2)*MU(I) + E1(1)
   BK(I) = E1(1)*MU(I) - E1(2)
   ZK1(I) = D * (AK(I) + BK(I) * TN1)
   ZK2(I) = D * (AK(I) + BK(I) * TN2)
   LOG1(I) = CLOG( ZK1(I) )
   LOG2(I) = CLOG( ZK2(I) )
   DPHI = AIMAG (LOG2(I) - LOG1(I))
   SPHI = SIGN (SPHI, DPHI)
   IF (ABS(DPHI).GT.PI) LOG2(I) = LOG2(I) - SPHI * CMPLX(0.0, 2.*PI)
   DI3(I) = (LOG2(I) - LOG1(I)) / BK(I)
   DI4(I) = -(1./ZK2(I) - 1./ZK1(I) ) /  BK(I)
45 CONTINUE
   GO TO 50
C
C  CALCULATE DI3, DI4 FOR D.EQ.0
C
40 CONTINUE
   DO 55 I = 1,2
   BK(I) = E1(1)*MU(I) - E1(2)
   DI3(I) =     (ALOG(RB) - ALOG(RA)) / BK(I)
   DI4(I) = -(1./R22 - 1./R12) / BK(I)**2
55 CONTINUE
50 CONTINUE
C
C  CALCULATE DD, DS, STRAINS AND STRESSES
C
   L1 = 3
   DO 25 I = 1,2
   DO 25 L = I,2
   L1 = L1 + 1
   DO 25 J = 1,2
   DD = CMPLX(0.0,0.0)
   DS = CMPLX(0.0,0.0)
   DO 30 K = 1,2
   DD =((PO(J,K)*AX(I,K)*DI3(K)*(MU(K)**(L-1))
  1      +PO(J,K)*AX(L,K)*DI3(K)*(MU(K)**(I-1))))/2.+ DD
   DS =(-(MU(K)*E1(1)-E1(2))*MU(K)**(2-J)*AX(I,K)*MU(K)**(L-1)*DI4(K)
  1      *((-1)**(3-J))
```

```
2       -(MU(K)*E1(1)-F1(2))*MU(K)**(2-J)*AX(L,K)*MU(K)**(I-1)*DI4(K)ANI35575
3       *((-1)**(3-J)))/2.   + DS                                       ANI35580
30 CONTINUE                                                             ANI35585
   M4 = M2 + (J-1)*NSEG                                                 ANI35590
   G(N,L1)= G(N,L1)- 2.*REAL(DD)*TCON(M4)*ISYM(J)                       ANI35595
1                   + 2.*REAL(DS)*UCON(M4)*ISYM(J)                      ANI35600
25 CONTINUE                                                             ANI35605
20 CONTINUE                                                             ANI35610
   RETURN                                                               ANI35615
   END                                                                  ANI35620
```

```
      SUBROUTINE BDYSTR (G)
      COMMON / ARRAY1 / XYZ(100,2,2), UCON(200), TCON(200), LOC(200)
      COMMON / ARRAY4 / NBDY(50,3)
      COMMON / MATCON / PI,FMU,PQ(2,2),MU(2),FLEX(6),STIF(6),AX(2,2)
      COMMON / CONTR1 / NSEG, NSYM, NTOTAL, NSIZE, NPT, NBDYP
      COMMON / CONTR2 / TITL(16), IPUNCH, ISTRS, IBDY
      COMMON / TIMERS / TIM(10)
      DIMENSION A(2), E1(2), E2(2), P(3,2), R(2), DU(2), G(50,6)
      DIMENSION Q(3,3), E(3,3), COFAC(3,3), T(3,3), T1(3,3)
      DIMENSION RHS(3), TRAC(2), TCN(2), TEMP(3,3), ANS(3)
      COMPLEX PQ, MU, AX
      IF (NBDYP.EQ.0) RETURN
      CALL TIME ( TIM(9) )
      WRITE (6,2000) TITL
      WRITE (6,2100) ((NBDY(I,J),J=1,3),I=1,NBDYP)
      WRITE (6,2000) TITL
      IF (ISTRS.EQ.0) WRITE (6,2050)
      IF (ISTRS.EQ.1) WRITE (6,2060)
      WRITE (6,2200)
C
C  I0 = BASE SEGMENT NUMBER
C  I1 = REAR DIFFERENCE SEGMENT NUMBER
C  I2 = FORWARD DIFFERENCE SEGMENT NUMBER
C
      DO 15 N = 1,NBDYP
      I0 = NBDY (N,1)
      I1 = NBDY (N,2)
      I2 = NBDY (N,3)
      DO 20 M = 1,2
      P(1,M) = (XYZ(I0,1,M) + XYZ(I0,2,M))/2.
      P(2,M) = (XYZ(I1,1,M) + XYZ(I1,2,M))/2.
      P(3,M) = (XYZ(I2,1,M) + XYZ(I2,2,M))/2.
      R(M) = P(3,M) - P(2,M)
   20 A(M) = XYZ(I0,2,M) - XYZ(I0,1,M)
      SMAG = SQRT(R(1)**2 + R(2)**2)
      AMAG = SQRT(A(1)**2 + A(2)**2)
C
C  CALCULATE DU/DS, TRAC FOR GLOBAL CORRDINATE SYSTEM
C
      DO 25 M = 1,2
      E2(M) = A(M)/ AMAG
      K = 3 - M
      E1(K) = E2(M) * (-1)**(K+1)
      I3 = I1 + (M-1)*NSEG
      I4 = I2 + (M-1)*NSEG
      I5 = I0 + (M-1)*NSEG
      DU(M) = (UCON(I4) - UCON(I3))/SMAG
   25 TRAC(M) = TCON(I5)
C
C  TRANSFORM DU/DS INTO EPS --- TRAC INTO TCN, IN LOCAL COORDINATES
C
      CALL DOTPRD (DU, E2, EPS)
      DO 40 I = 1,2
   40 TCN(I) = 0.
      DO 45 I = 1,2
      TCN(1) = TCN(1) + E1(I)*TRAC(I)
   45 TCN(2) = TCN(2) + E2(I)*TRAC(I)
```

```
C
C   CALCULATE TRANSFORMATION MATRIX T(I,J) AND ITS INVERSE TI(I,J)
C
      C = E1(1)
      S = E1(2)
      T(1,1) = C*C
      T(1,2) = S*S
      T(1,3) = S*C*2.
      T(2,1) = S*S
      T(2,2) = C*C
      T(2,3) =-S*C*2.
      T(3,1) =-S*C
      T(3,2) = S*C
      T(3,3) = C*C - S*S
C
C ************            ************
C
      TI(1,1) = T(1,1)
      TI(1,2) = T(1,2)
      TI(1,3) =-T(1,3)
      TI(2,1) = T(2,1)
      TI(2,2) = T(2,2)
      TI(2,3) =-T(2,3)
      TI(3,1) =-T(3,1)
      TI(3,2) =-T(3,2)
      TI(3,3) = T(3,3)
C
C   CALCULATE MATERIAL STIFFNESSES IN LOCAL COORDINATE SYSTEM
C
      K = 0
      DO 50 I = 1,3
      DO 50 J = I,3
      K = K + 1
      Q(I,J) = STIF(K) * (2.**(J/3))
      IF (I.EQ.J) GO TO 50
      Q(J,I) = STIF(K)
   50 CONTINUE
      DO 55 I = 1,3
      DO 55 J = 1,3
      TEMP(I,J) = 0.
      DO 55 K = 1,3
   55 TEMP(I,J) = TEMP(I,J) + Q(I,K)*TI(K,J)
      DO 60 I = 1,3
      DO 60 J = 1,3
      Q(I,J) = 0.
      DO 60 K = 1,3
   60 Q(I,J) = Q(I,J) + T(I,K)*TEMP(K,J)
                                            Q(1,3) = Q(1,3) /2.
                                            Q(2,3) = Q(2,3) /2.
                                            Q(3,3) = Q(3,3) /2.
C
C   CALCULATE COEFFICIENTS OF REARRANGED EQUATIONS
C
      E(1,1) = Q(1,1) - Q(1,2)*Q(1,2)/Q(2,2)
      E(1,2) = Q(1,2)
      E(1,3) = Q(1,3) - Q(1,2)*Q(2,3)/Q(2,2)
      E(2,1) =-Q(1,2)
      E(2,2) = Q(2,2)
      E(2,3) =-Q(2,3)
      E(3,1) = Q(1,3) - Q(1,2)*Q(2,3)/Q(2,2)
      E(3,2) = Q(2,3)
```

```
      E(3,3) = Q(3,3) - Q(2,3)*Q(2,3)/Q(2,2)
      DET = (E(1,1)*E(2,2)*E(3,3)) + (E(1,2)*E(2,3)*E(3,1)) +
     1      (E(1,3)*E(2,1)*E(3,2)) - (E(3,1)*E(2,2)*E(1,3)) -
     2      (E(3,2)*E(2,3)*E(1,1)) - (E(3,3)*E(2,1)*E(1,2))
      COFAC(1,1) =          (E(2,2)*E(3,3)) - (E(3,2)*E(2,3))
      COFAC(1,2) = -1.0*((E(2,1)*E(3,3)) - (E(3,1)*E(2,3)))
      COFAC(1,3) =          (E(2,1)*E(3,2)) - (E(3,1)*E(2,2))
      COFAC(2,1) = -1.0*((E(1,2)*E(3,3)) -(E(3,2)*E(1,3)))
      COFAC(2,2) =          (E(1,1)*E(3,3)) - (E(3,1)*E(1,3))
      COFAC(2,3) = -1.0*((E(1,1)*E(3,2)) - (E(3,1)*E(1,2)))
      COFAC(3,1) =          (E(1,2)*E(2,3)) - (E(2,2)*E(1,3))
      COFAC(3,2) = -1.0*((E(1,1)*E(2,3)) - (E(2,1)*E(1,3)))
      COFAC(3,3) =          (E(1,1)*E(2,2)) - (E(2,1)*E(1,2))
      DO 65 I = 1,3
      DO 65 J = 1,3
   65 TEMP(I,J) = COFAC(J,I)/DET
      RHS(1) = TCN(1)
      RHS(2) = EPS*Q(2,2)
      RHS(3) = TCN(2)
C
C  CALCULATE UNKNOWN HOOP STRESS
C
      DO 70 I = 1,3
      ANS(I) = 0.
      DO 70 J = 1,3
   70 ANS(I) = ANS(I) + TEMP(I,J)*RHS(J)
      G(N,1) = TCN(1)
      G(N,2) = TCN(2)
      G(N,3) = ANS(2) * Q(2,2)
      G(N,4) = EPS
      G(N,5) = ANS(1)
      G(N,6) = ANS(3)
      WRITE (6,100) STIF , Q, T, TI, RHS, ANS
  100 FORMAT ( // (3(3E12.7 /)//))
   15 WRITE (6,2300) IO, (G(N,M),M=1,4),P(1,1),P(1,2)
      CALL TIME ( TIM(10) )
      RETURN
 1000 FORMAT (24I3)
 2000 FORMAT (1H1, 10X, 16A5)
 2050 FORMAT ( / 4( 18H PLANE STRAIN **** ) )
 2060 FORMAT ( / 4( 18H PLANE STRESS **** ) )
 2100 FORMAT (/ 5X 11HBASE NUMBER 2X 11HREAR NUMBER 3X 10HFWD NUMBER //
     1       ( 3I12 /) )
 2200 FORMAT (7HOSGMENT 2X 10H NORMAL ST 2X 10H SHEAR STR 2X
     1      10H HOOP STRS 2X 10H HOOP STRN 5X 2H X 6X 2H Y)
 2300 FORMAT (2X I3, 2X 3F12.2, F12.9, 2F8.4)
      END
```

```
SUBROUTINE DOTPRD (A, B, C)                                        ANT45000
DIMENSION A(2), B(2)                                               ANT45005
C = A(1)*B(1) + A(2)*B(2)                                          ANT45010
RETURN                                                             ANT45015
END                                                                ANT45020
```

```
      SUBROUTINE SOLVER (N, X, F, A)
      DIMENSION A(N,N), X(N), F(N), XX(160)
      DOUBLE PRECISION X
      DO 10 I = 1, N
      F(I) = 0.0
   10 CONTINUE
      N1 = N - 1
      DO 60 I = 2, N
      DO 55 J = I, N
      IF (ABS(A(I-1,I-1)) .GT. 0.) GO TO 45
      I1 = I - 1
      WRITE (6,510) I1
      RETURN
   45 CONTINUE
      CX = A(J,I-1) / A(I-1,I-1)
      K2 = I
      DO 50 K = I, N
      A(J,K2) = A(J,K2) - CX * A(I-1,K2)
      K2 = K2 + 1
   50 CONTINUE
      A(J,I-1) = CX
   55 CONTINUE
   60 CONTINUE
C     FORWARD PASS - OPERATE ON RIGHT HAND SIDE AS
C     ON MATRIX
   62 CONTINUE
      DO 70 I = 2, N
      DO 65 J = I, N
      X(J) = X(J) - X(I-1) * A(J,I-1)
   65 CONTINUE
   70 CONTINUE
C
C     BACKWARD PASS - SOLVE FOR AX = B
      XX(N) = X(N) / A(N,N)
      DO 80 I = 1, N1
      SUM = 0.0
      I2 = N - I + 1
      DO 75 J = I2, N
      SUM = SUM + A(I2-1,J) * XX(J)
   75 CONTINUE
      XX(I2-1) = (X(I2-1)-SUM) / A(I2-1,I2-1)
   80 CONTINUE
      DO 90 I = 1, N
      F(I) = F(I) + XX(I)
   90 CONTINUE
      RETURN
  510 FORMAT(/1X 25HERROR RETURN FROM SEQSOV    I10,
     1 35HDIAGONAL TERM REDUCED TO ZERO     / )
       END
```

5.3 EXAMPLE SOLUTIONS FOR ISOTROPIC AND ANISOTROPIC BOUNDARY-INTEGRAL EQUATION METHOD

5.3.1 *Tension of an Isotropic Plate*

The group of problems discussed herein are provided for two major purposes, the first to determine solution accuracy, and the second to provide guidelines in the use of the program, called DIPOME.

Since both tractions and displacements are assumed constant along each segment, it is logical to theorize that the solution will be more accurate for shorter segment lengths. If then two questions remain: What accuracy is obtainable, and how is this accuracy related to the segment length used in the model.

5.3.1.1 *Circular Cutout*

A circular cutout, of unit radius, was modeled by segments of equal length. Ten problems were solved, with the only variable being the number of segments employed. In each problem the stress distribution along the x and y axes interior to the plate was obtained. Stresses were computed at points ranging from 0.001 inches to over 5.0 inches from the surface of the cutout. Table 1 shows a comparison of the solutions obtained in three of these problems to the theoretical results of Timoshenko. These solutions follow the theoretical curve closely in all cases, except in the immediate vicinity of the cutout.

This behavior is due largely to the presence of a sharp corner at the intersection of each axis with the cutout, as shown in Figure 1. This is a consequence of the approximation of the surface by straight line segments. Use of shorter segment lengths reduces the sharpness of this corner and produces less distortion, as seen in the table. Further deviation from the theoretical solution is a result of the surface approximations inherent in averaging tractions and displacements over each segment.

Stresses at the surface of the cutout are computed by a finite difference technique, using the displacements of the two segments adjacent to each of the intersections, as shown in Figure 1. Once the strain is computed by the equation below, Hooke's law is used to obtain the stress. Surface stresses are computed at nodes around the entire cutout, with an average error of about two per cent. For brevity only the stress at the intersection of the cutout and y-axis is shown here (Table 1).

$$\varepsilon_x = \frac{U_{x(2)} - U_{x(1)}}{\ell}$$

The influence of segment length on solution accuracy is summarized in Figure 3. The graph results from comparisons of interior stresses, where γ^* represents the last data point obtained before the data diverges from theoretical curve of Timoshenko.

5.3.1.2 Elliptical Cutout

The problem of an elliptical cutout in an infinite plate under tension was solved by Inglis in 1913. He found that the maximum stresses in the plate occur at the surface of the cutout, at the point where the radius of curvature is smallest. The stress concentration here is given by:

$$SCF = 1 + 2\ a/b$$

where a/b is the aspect ratio of the ellipse.

Prediction capability for a range of stress concentrations was investigated, and results are reported here for concentrations of 5, 10, and 40. By the equation above, aspect ratios of the resulting ellipses were 2.0, 4.5, and 19.5.

For each aspect ratio a number of problems was solved, using varying numbers of segments to model the elliptical surface. Elliptic coordinates were used to divide the surface, so that a constant value of segment length/radius of curvature was obtained. It may be shown that this will be accomplished by using equal increments of the coordinate η. It was hoped that accuracy of the internal solution might be related to this ratio.

The stress distribution along the x and y axes interior to the plate was obtained, at points ranging from 0.001 inch to 5.0 inches from the cutout surface. Tables 2 through 7 show a comparison of the results with the theoretical results of Inglis. Again it must be noted that the computed results are inaccurate for points very near the cutout surface, due to the sharp corner produced by the model (See Figure 2).

Stresses at the surface of the cutout are computed by a finite difference technique, as previously described. Results of this calculation are shown only at the intersection of the x and y axes with the cutout, and appear in Tables 2 through 7.

The relationship between interior solution accuracy and the value of segment length/radius of curvature employed in a given problem is shown in Figure 4. Results were obtained for four aspect ratios, and the plots are nearly straight lines for each aspect ratio, for values of length parameter down to 0.052. It may be seen that solution accuracy is functionally related to the ratio of segment length to radius of curvature, but this parameter alone does not characterize accuracy.

We see that the Boundary-Integral Equation method is a reliable numerical technique for the prediction of stress concentrations in two dimensional isotropic problems. Results indicate that the method is consistent as well as accurate in calculating stress concentrations as high as 40. Solution accuracy is dependent both on the stress concentration gradients present and on the length of segment used to model the surface.

In employing this program, it should be noted that solution time required for interior points is approximately ten times that required for boundary solution points.

5.3.2 Tension of an Anisotropic Plate with a Circular Cutout

The program used for the solution of the following problems is called ANISOT, and provides a solution capability for two dimensional generally anisotropic materials. The use of the program is restricted only by the requirement that the material employed be mid-plane symmetric. It is expected that the program will be especially useful in analysis of advanced fiber composites, so the problems solved here considered plates of boron-epoxy.

5.3.2.1 Orthotropic Material

A series of problems was solved, with the cutout surface represented by varying numbers of segments. In each case segments of equal length were used, and the number of segments ranged from 20 to 180. Identical series of problems were solved for plates of unidirectional boron-epoxy, of zero degree and ninety degree orientations.

Again the stress distribution along the x and y axes interior to the body was obtained, as well as surface stresses around the entire cutout.

The hoop stresses around the cutout at the surface were compared to the theoretical results of Lekhnitskii, and results appear in Tables 8 and 9. These stresses are computed directly from displacements and tractions, and thus provide a means of evaluating the boundary solution capability of the program. Results compared extremely well with the theoretical calculations, even for the higher stress concentrations.

The accuracy of the solutions obtained are dependent on both the stress concentration gradients present and length of segment used in the model. This behavior is expected, since the basic algorithms employed are similar to those of the isotropic program, DIPOME. Time required for interior solution points was again about ten times that for boundary points.

5.3.3.2 Anisotropic Material

The problem of a circular cutout in an infinite plate was next solved for a completely anisotropic material, unidirectional boron-epoxy at an orientation of 45 degrees. There was no symmetry about either the x or y axis, as had been present before, so the entire cutout surface was modeled.

As before, the hoop stresses at the surface of the cutout were obtained and are compared with the results of Lekhnitskii in Tables 10 and 11. Two problems were solved, one employing 20 segments, and the other 90 segments, to represent the surface. Here again agreement with theoretical results was excellent along the entire surface.

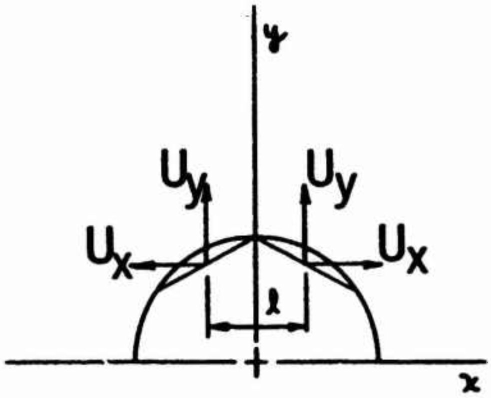

Figure 1: Dipome Model – Circle

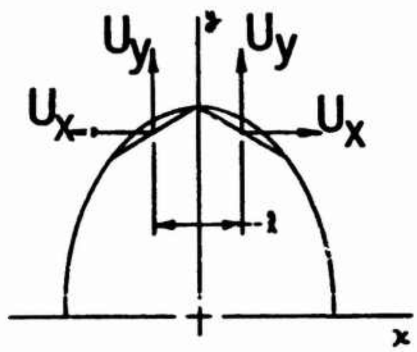

Figure 2: – Dipome Model – Ellipse

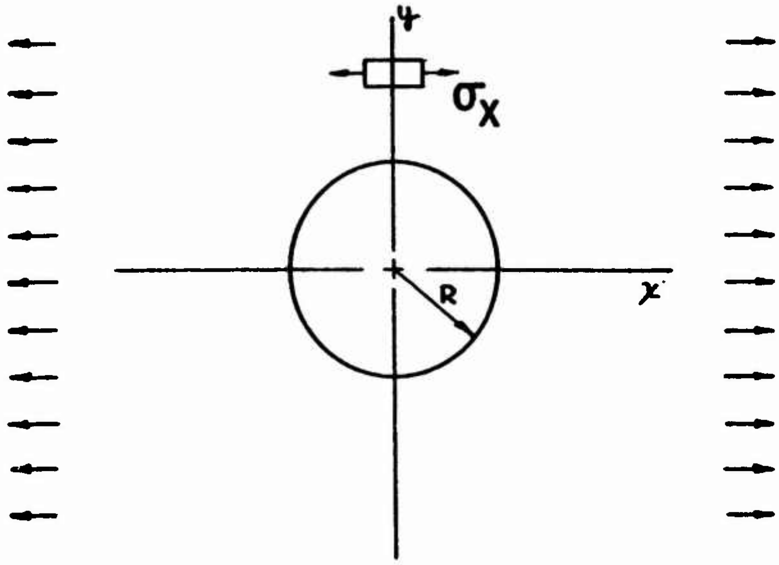

TABLE 1 — INTERIOR STRESS SOLUTIONS — DIPOME

Y – R	Timoshenko	40 Segments	120 Segments	200 Segments
0.00	3.00	3.02	3.02	3.09
.001	2.99	27.12	10.36	7.05
.005	2.96	7.03	3.78	3.21
.010	2.93	4.53	3.05	2.88
.020	2.87	3.31	2.80	2.83
.030	2.80	2.92	2.76	2.79
.040	2.74	2.74	2.72	2.74
.050	2.69	2.64	2.68	2.69
.070	2.58	2.52	2.58	2.58
.100	2.44	2.40	2.44	2.44
.200	2.07	2.07	2.07	2.07
.400	1.65	1.65	1.65	1.65
.600	1.42	1.42	1.42	1.42
.900	1.25	1.25	1.25	1.25
1.50	1.12	1.12	1.12	1.12
2.00	1.07	1.08	1.07	1.07
3.00	1.04	1.04	1.04	1.04

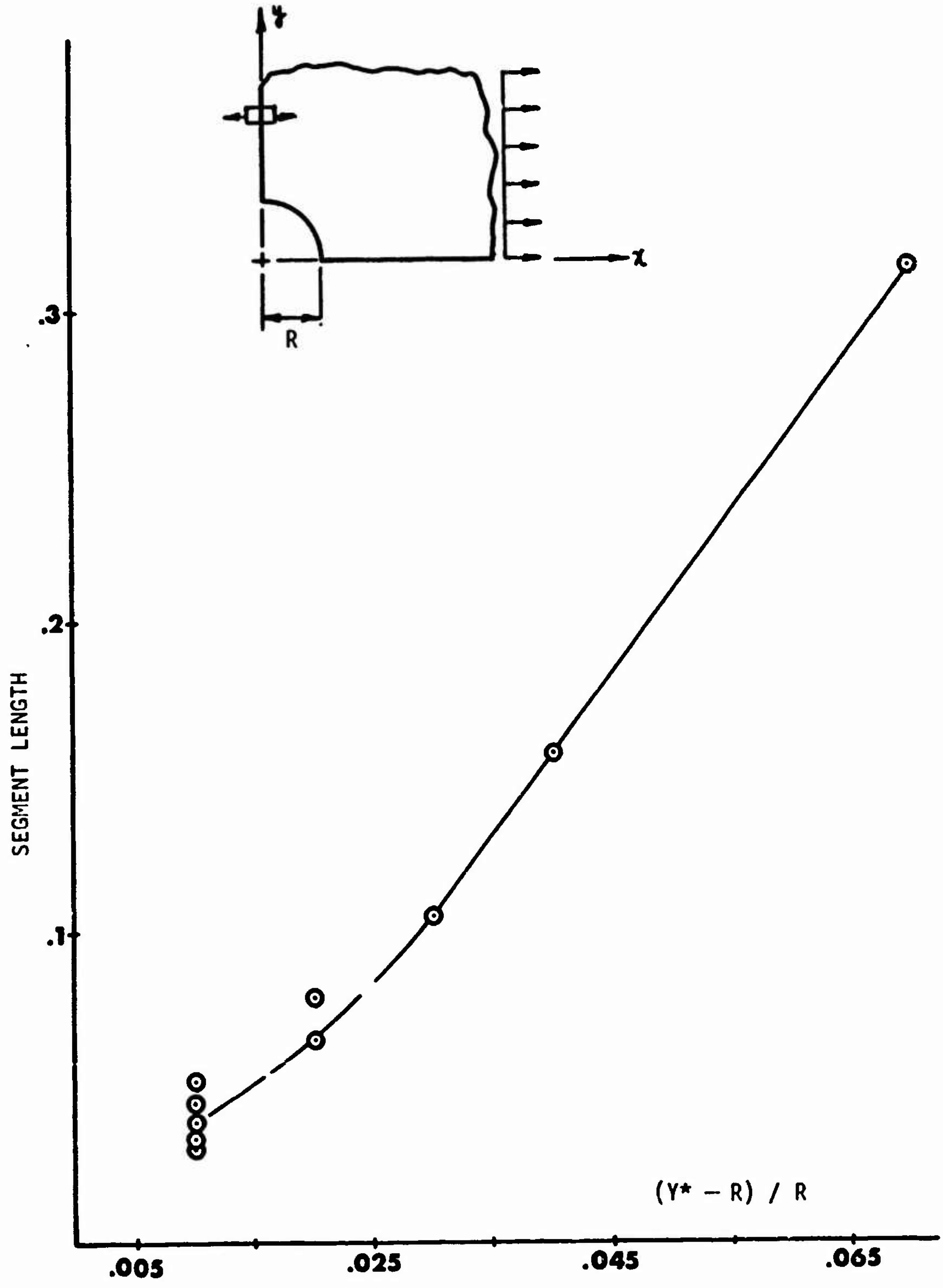

Figure 3: Accuracy of DIPOME – Circular Cutout

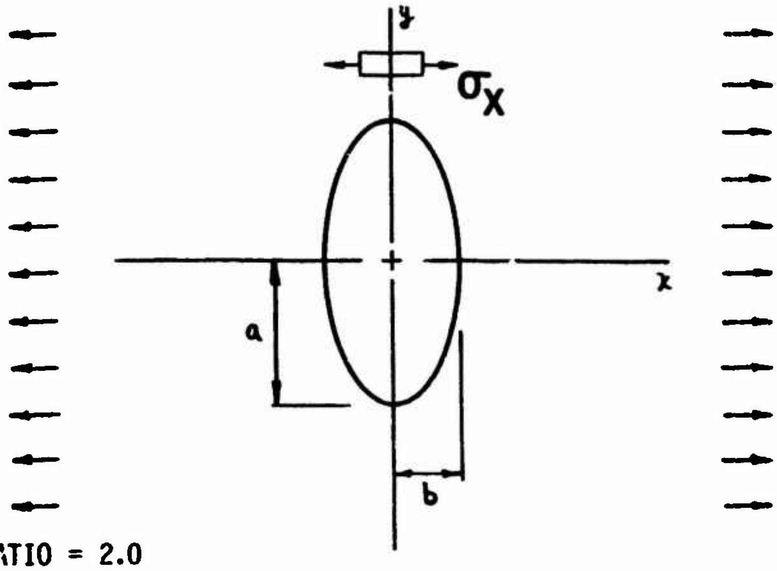

ASPECT RATIO = 2.0

TABLE 2 — INTERIOR STRESS SOLUTIONS — DIPOME

$\frac{y-a}{c}$	Inglis	40 Segments	120 Segments	200 Segments
0.00	5.00	5.116	5.01	5.002
.001	4.96	101.9	35.2	22.3
.005	4.82	9.81	5.52	4.89
.010	4.65	6.13	4.59	4.56
.020	4.34	4.54	4.29	4.35
.030	4.03	4.04	4.08	4.09
.040	3.85	3.78	3.86	3.86
.050	3.65	3.59	3.66	3.66
.070	3.31	3.29	3.32	3.32
.100	2.92	2.92	2.93	2.93
.200	2.18	2.19	2.19	2.19
.400	1.61	1.62	1.62	1.62
.600	1.40	1.40	1.40	1.40
.900	1.24	1.24	1.24	1.24

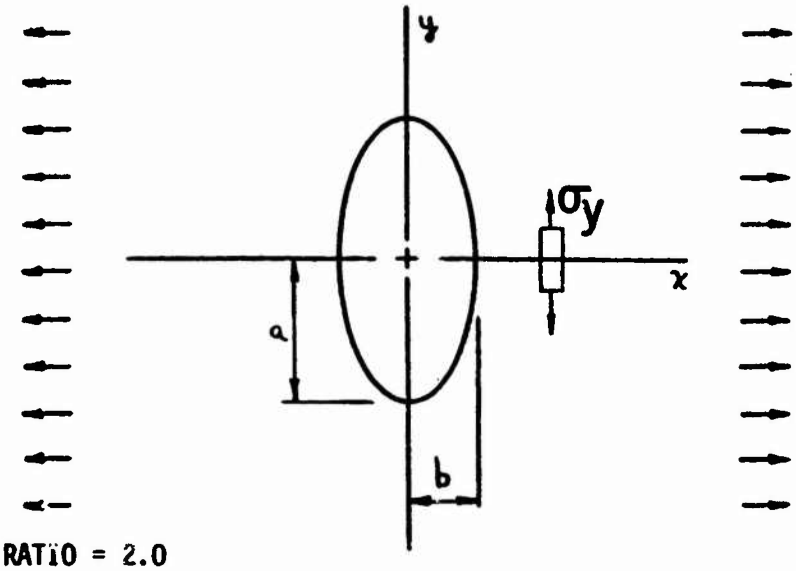

ASPECT RATIO = 2.0

TABLE 3 — INTERIOR STRESS SOLUTIONS — DIPOME

$\frac{x-b}{c}$	Inglis	40 Segments	120 Segments	200 Segments
0.00	-1.00	-0.983	-0.994	-0.996
.001	-0.997	-13.0	-4.90	-3.24
.005	-0.985	-2.42	-1.32	-1.11
.010	-0.970	-1.52	-1.03	-0.965
.020	-0.941	-1.09	-0.925	-0.926
.030	-0.912	-0.959	-0.895	-0.906
.040	-0.884	-0.888	-0.873	-0.882
.050	-0.857	-0.843	-0.850	-0.856
.070	-0.805	-0.782	-0.802	-0.804
.100	-0.805	-0.713	-0.729	-0.731
.200	-0.525	-0.518	-0.523	-0.524
.400	-0.251	-0.247	-0.250	-0.250
.600	-0.099	-0.097	-0.099	-0.099
.900	+0.006	+0.008	+0.007	+0.007

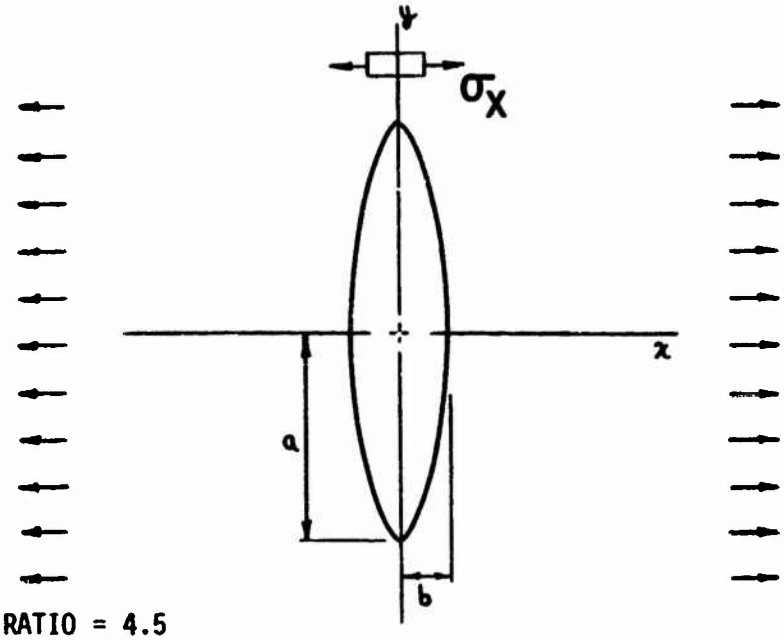

ASPECT RATIO = 4.5

TABLE 4 — INTERIOR STRESS SOLUTIONS — DIPOME

$\frac{y-a}{c}$	Inglis	40 Segments	120 Segments	200 Segments
0.00	10.0	11.33	10.14	10.04
.001	9.60	87.5	29.8	20.2
.005	8.31	11.37	8.30	8.32
.010	7.15	7.69	7.21	7.27
.020	5.67	5.75	5.75	5.75
.030	4.77	4.85	4.82	4.82
.040	4.16	4.24	4.20	4.20
.050	3.73	3.80	3.75	3.75
.070	3.14	3.19	3.16	3.16
.100	2.63	2.66	2.63	2.63
.200	1.90	1.91	1.90	1.90
.400	1.46	1.46	1.46	1.46
.600	1.30	1.30	1.30	1.30
.900	1.19	1.18	1.19	1.19

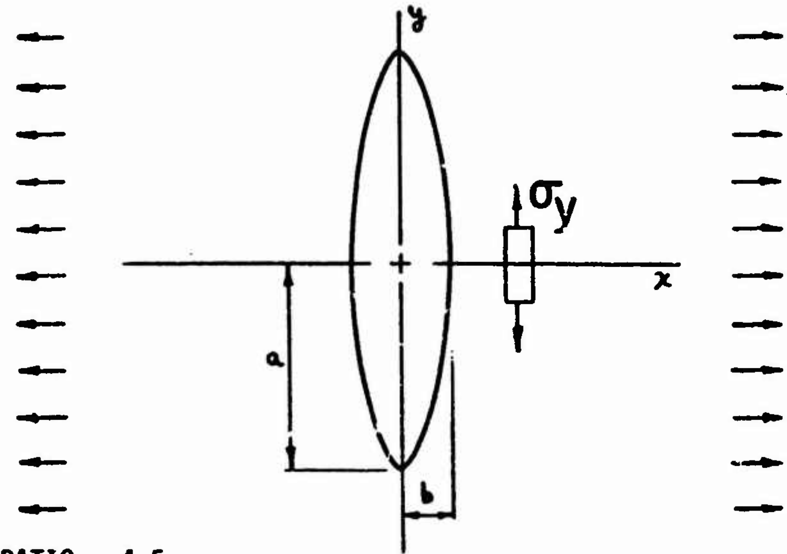

ASPECT RATIO = 4.5

TABLE 5 — INTERIOR STRESS SOLUTIONS — DIPOME

$\frac{x-b}{c}$	Inglis	40 Segments	120 Segments	200 Segments
0.00	-1.00	-0.984	-0.994	-0.997
.001	-0.997	-90.7	-21.4	-19.2
.005	-0.987	-2.43	-1.32	-1.11
.010	-0.974	-1.48	-1.03	-0.966
.020	-0.949	-1.08	-0.931	-0.937
.030	-0.923	-0.952	-0.908	-0.920
.040	-0.898	-0.893	-0.890	-0.893
.050	-0.874	-0.855	-0.870	-0.874
.070	-0.826	-0.804	-0.825	-0.826
.100	-0.758	-0.743	-0.756	-0.758
.200	-0.553	-0.549	-0.552	-0.553
.400	-0.258	-0.258	-0.258	-0.259
.600	-0.087	-0.088	-0.087	-0.087
.900	+0.029	+0.028	+0.029	+0.029

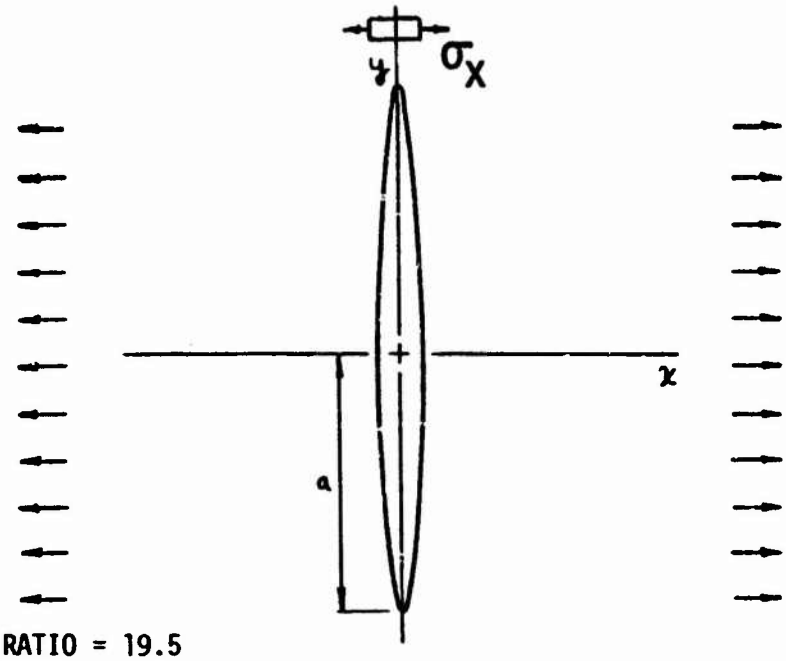

ASPECT RATIO = 19.5

TABLE 6 — INTERIOR STRESS SOLUTIONS — DIPOME

$\frac{y-a}{c}$	Inglis	40 Segments	120 Segments	200 Segments
0.00	40.0	88.7	50.9	44.5
.001	23.5	88.2	31.0	27.0
.005	10.9	16.9	11.7	11.4
.010	7.50	10.0	7.80	7.67
.020	5.22	6.28	5.32	5.27
.030	4.26	4.88	4.30	4.28
.040	3.70	4.12	3.72	3.71
.050	3.32	3.63	3.33	3.32
.070	2.83	3.03	2.84	2.83
.100	2.41	2.53	2.41	2.41
.200	1.81	1.85	1.81	1.81
.400	1.43	1.44	1.43	1.42
.600	1.28	1.29	1.28	1.28
.900	1.18	1.18	1.18	1.18

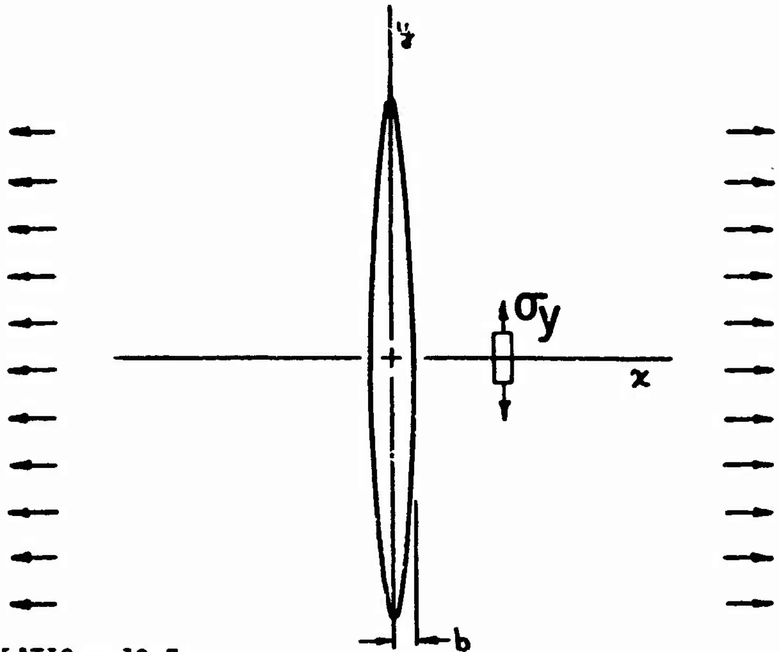

ASPECT RATIO = 19.5

TABLE 7 — INTERIOR STRESS SOLUTIONS — DIPOME

$\frac{x-b}{c}$	Inglis	40 Segments	120 Segments	200 Segments
0.00	-1.00	-.966	-.985	-.994
.001	-0.997	-10.9	-4.26	-2.89
.005	-0.989	-2.11	-1.22	-1.06
.010	-0.979	-1.37	-0.996	-0.959
.020	-0.957	-1.035	-0.921	-0.939
.030	-0.936	-0.928	-0.904	-0.926
.040	-0.915	-0.876	-0.890	-0.907
.050	-0.894	-0.845	-0.873	-0.887
.070	-0.852	-0.803	-0.834	-0.845
.100	-0.790	-0.752	-0.775	-0.784
.200	-0.598	-0.581	-0.587	-0.594
.400	-0.293	-0.294	-0.289	-0.291
.600	-0.099	-0.107	-0.099	-0.099
.900	+0.037	+0.030	+0.035	+0.037

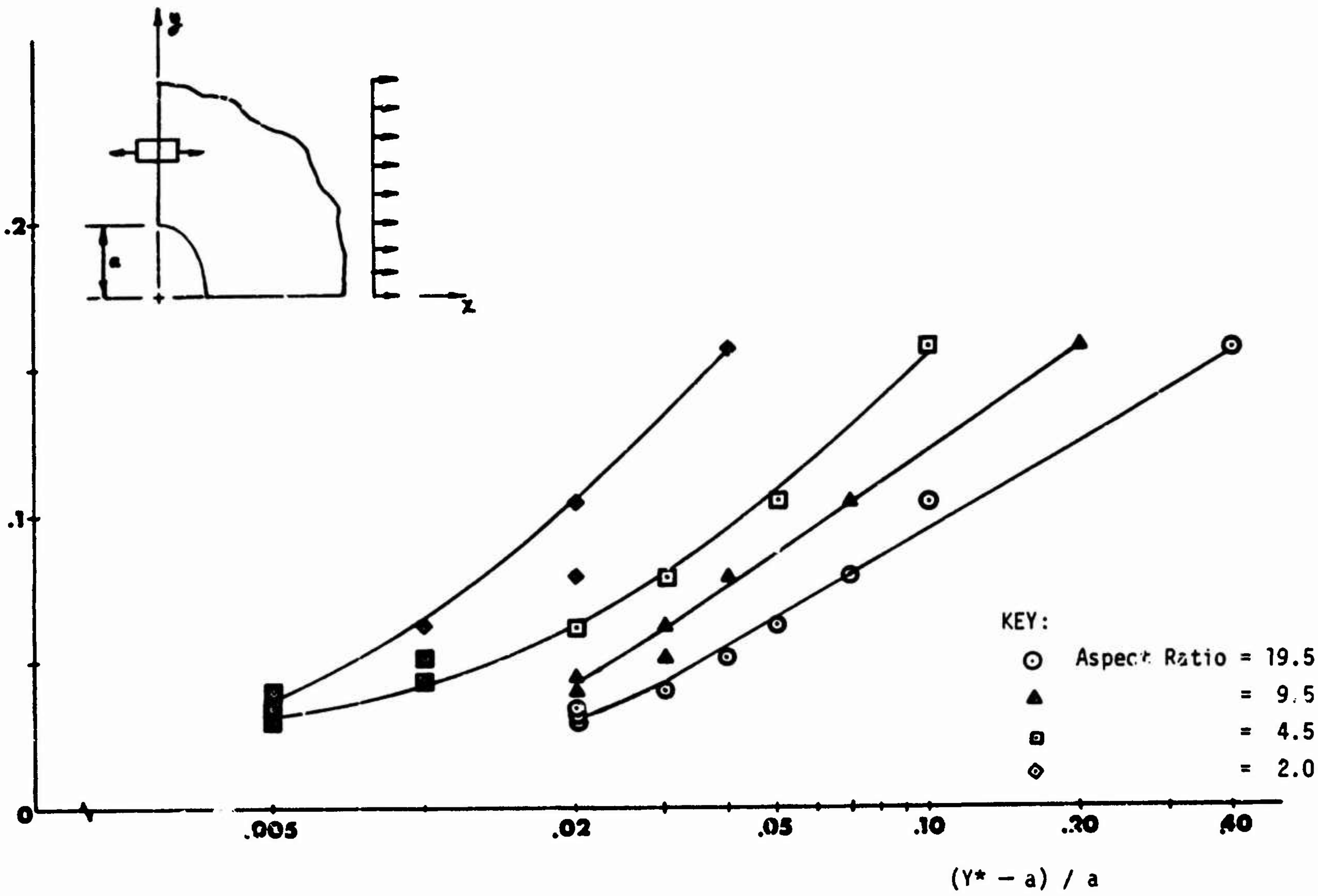

Figure 4: Accuracy of DIPOME — Elliptical Cutout

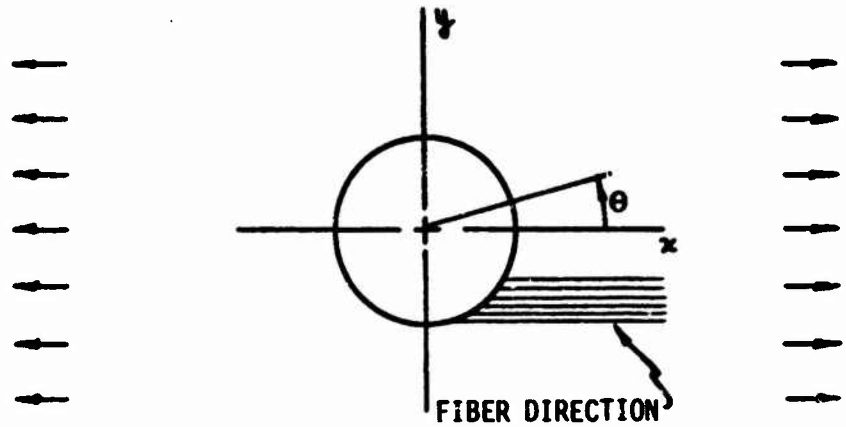

TABLE 8 — SURFACE HOOP STRESS COMPARISONS, $\alpha = 0°$			
θ(DEG)	20 Segments	180 Segments	EXACT*
1.0		-0.296	-0.299
5.0		-0.284	-0.287
9.0	-0.215	-0.258	-0.261
13.0		-0.222	-0.225
17.0		-0.180	-0.182
21.0		-0.133	-0.136
27.0	-0.054	-0.063	-0.065
29.0		-0.040	-0.041
33.0		0.008	0.006
37.0		0.058	0.056
41.0		0.111	0.110
45.0	0.164	0.170	0.170
49.0		0.240	0.240
53.0		0.326	0.326
57.0		0.435	0.436
63.0	0.642	0.681	0.682
65.0		0.799	0.798
69.0		1.111	1.114
73.0		1.609	1.614
77.0		2.441	2.447
81.0	3.532	3.889	3.880
65.0		6.130	6.127
89.0		8.160	8.127

*Due to Lekhnitskii

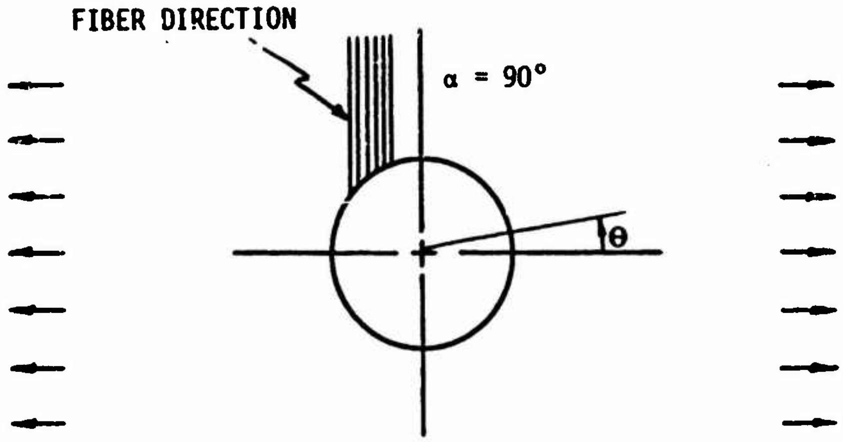

TABLE 9 — SURFACE HOOP STRESS COMPARISONS, α = 90°			
θ(DEG)	20 Segments	180 Segments	EXACT*
1.0		-3.19	-3.28
5.0		-2.22	-2.29
9.0	-0.367	-1.12	-1.165
13.0		-0.419	-0.442
17.0		+0.012	-0.008
21.0		0.281	+0.267
27.0	+0.625	0.546	0.538
29.0		0.616	0.608
33.0		0.741	0.736
37.0		0.859	0.856
41.0		0.979	0.976
45.0	+1.126	1.105	1.103
49.0		1.243	1.242
53.0		1.398	1.398
57.0		1.573	1.573
63.0	+1.892	1.877	1.878
65.0		1.990	1.991
69.0		2.229	2.230
73.0		2.478	2.481
77.0		2.723	2.725
81.0	+2.883	2.937	2.940
85.0		3.093	3.096
89.0		3.165	3.169

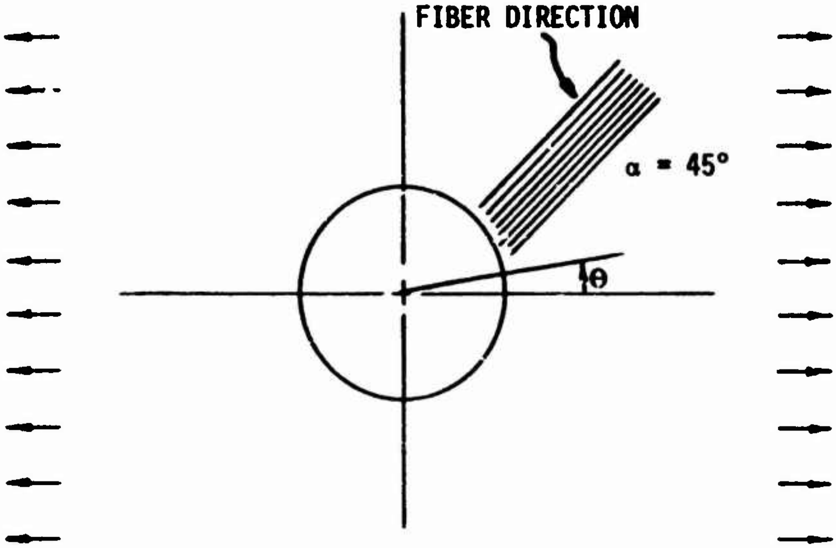

TABLE 10 — SURFACE HOOP STRESS COMPARISONS, α = 45°					
THETA	EXACT	90 Segments	THETA	EXACT	90 Segments
0	-0.812	-0.808	96	2.168	2.169
4	-0.706	-0.703	104	2.396	2.400
8	-0.596	-0.593	112	2.840	2.848
16	-0.337	-0.335	120	3.559	3.681
24	+0.015	+0.016	128	4.701	4.791
32	.499	.500	136	1.703	1.823
40	1.082	1.084	144	-1.799	-1.773
48	1.620	1.623	152	-1.804	-1.787
56	1.955	1.957	160	-1.444	-1.434
68	2.081	2.082	168	-1.151	-1.144
72	2.073	2.073	176	-0.918	-0.913
80	2.051	2.052	184	-0.706	-0.703
88	2.069	2.070			

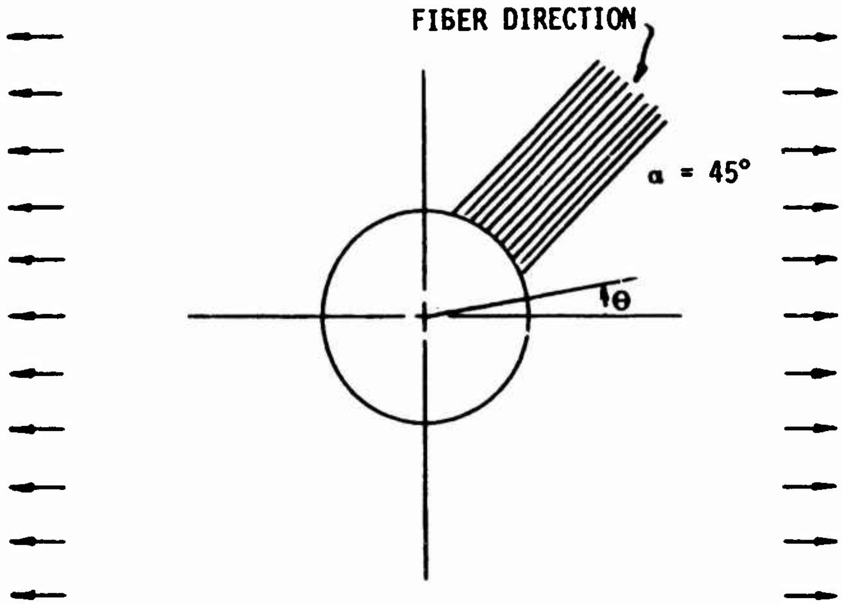

TABLE 11 — SURFACE HOOP STRESS COMPARISONS		
THETA	EXACT	20 Segments
9	-0.567	-0.565
27	0.180	0.186
45	1.436	1.477
63	2.067	2.107
81	2.050	2.065
99	2.235	2.246
117	3.296	3.473
135	2.453	3.189
153	-1.759	-1.747
171	-1.058	-1.043
189	-0.567	-0.565

5.4 *ADVANCED TOPICS IN ANISOTROPIC INTEGRAL EQUATION SOLUTION METHODS*

5.4.1 *Introduction*

The "integral equation method" referred to in this Section is basically a technique for obtaining accurate approximate solutions for a wide variety of physical problems governed by linear partial differential equations. As is clear from a number of papers e.g. [1,2,3,4,5] the method has reached a considerable stage of development and is emerging as an important tool comparable to and potentially, we think, better than finite element and finite difference techniques for certain problems. This appears to be particularly true for a variety of problems involving material composites.

A glance at the work cited above reveals that the method depends crucially on the existence and explicit definition of a fundamental singular solution to the appropriate governing partial differential equations. Therefore, in an attempt to open up the field of linear *three-dimensional anisotropic* elasticity to attack, via the integral equation method, considerable effort was directed toward investigating what is known of the necessary singular solution. As noted earlier, this solution is the field due to a concentrated force in an infinite anisotropic media. Two major works [6] and [7] were found on this topic, and examined with respect to the stated objective. Details primarily concerned with making representations of the singular solution available for practical purposes are given later in this Section.

The problem of interlaminar shear was investigated with a view toward attacking this problem (as defined by R. B. Pipes [8]) via the integral equation method. Under the appropriate assumptions, the relevant surface integrals reduce to path integrals around each of the layers. While the problem is not completely two-dimensional in nature, significant advantages still seem to be present with the integral equation method for both isotropic and anisotropic layers to warrant further investigation with test problems. Details of the formulation for isotropic layer assumptions and a discussion of the possibilities for anisotropic layers are included in this Section.

5.4.2 *Fundamental Three-Dimensional Anisotropic Singularity*

5.4.2.1 *Via John* [7]

The work by John [7] which is in essence "a somewhat heterogeneous collection of results on partial differential equations" contains, in Ch. III, a method for constructing the so-called *fundamental singular solution* for an elliptic system of linear partial differential equations with analytic coefficients. Since our main concern here is with homogeneous anisotropic elasticity theory, we will specialize John's development at the outset and explicitly deal with the system of equations

$$C_{ijkl}u_{k,lj} = 0 \tag{1}$$

Equations (1) are the equations of equilibrium in the absence of body forces for a linear elastic solid obeying the constitutive relation

$$\tau_{ij} = C_{ijkl}e_{kl} \tag{2}$$

in which C_{ijkl} are constants, and τ_{ij} , e_{ij} , u_i the stress, strain, and displacement components assuming the linearized theory. As usual we take

$$C_{ijkl} = C_{klij} \tag{3}$$

together with necessary symmetries in the first and second pair of indices such that C_{ijkl} implies at most twenty one independent constants.

We recognize that Eqs. (1) imply the existence of a set of differential operators L_{ij} such that Eqs. (1) may be written, for convenience in the symbolic form

$$L_{ik}[u_k] = 0 \tag{4}$$

where, specifically,

$$L_{ik} = C_{ijkl} \frac{\partial^2}{\partial x_l x_j} \tag{5}$$

A fundamental system of singular solutions U_{jk} of Eqs. (4) according to John [7] has property that the symbolic equations

$$L_{ik}[U_{jk}(x, y)] = 0 \qquad \text{for } x \neq y \tag{6}$$

are satisfied where x and y are two arbitrary points in space. Further, the functions U_{jk} have the additional property that

$$\int_{\partial R+\Gamma} [t_j(y) U_{jk}(x,y) - u_j(y) T_{jk}(x,y)] da(y) = 0 \tag{7}$$

where ∂R is the boundary of a regular region of space R, and Γ is the surface of a small sphere of radius ϵ surrounding the point x, n_k are the components of the "outer" normal at y(y on $\partial R + \Gamma$) to the region "enclosed by" $\partial R + \Gamma$, and T_{jk} represents a set of functions derivable from U_{jk}. The function u_i is an arbitrary solution to Eq. (4) and t_i, derivable from u_i, represents the surface traction on the anisotropic body which is assumed to occupy the region R. If we now take the limit in Eq. (7) as ϵ goes to zero, i.e., shrink Γ indefinitely about x, the orders of the singularities in U_{jk} and T_{jk} are such that Eq. (7) reduces to

$$u_k(x) = \int_{\partial R} [u_j(y) T_{jk}(x,y) - t_j(y) U_{jk}(x,y)] da(y) \tag{8}$$

A glance at the cited works [1,3,4,5] reveals that the above properties (6), (7), and (8) of the functions U_{jk} are precisely those needed to formulate the integral equation method for three-dimensional anisotropic elastic boundary value problems. Physically, U_{jk} represents a set of displacement or influence functions; i.e., $U_{jk}(\underset{\sim}{x},\underset{\sim}{y})$ is the displacement in the j coordinate direction at $\underset{\sim}{y}$ due to a concentrated force in the k coordinate direction at $\underset{\sim}{x}$. Further, T_{jk} represents traction components at $\underset{\sim}{y}$ across an arbitrary surface with orientation $\underset{\sim}{n}$. These are obtained from U_{jk} according to the familiar relation

$$T_{jk} = \frac{1}{2} C_{jplm}[U_{lk,m} + U_{mk,l}]\, n_p \tag{9}$$

just as the arbitrary traction t_j is related to u_j according to

$$t_j = \frac{1}{2} C_{jplm}\, [u_{l,m} + u_{m,l}]\, n_p \tag{10}$$

Thus since the relation (8) is the desired relation to accomplish the anisotropic formulation everything depends on the availability of an explicit relation for U_{jk}. To construct U_{jk} for Eqs. (4), with the properties (6) through (8) John [7], pg. 76, gives the formula

$$U_{jk}(\underset{\sim}{x},\underset{\sim}{y}) = \frac{-1}{16\pi^2} \Delta_{\underset{\sim}{y}} \int_{\Omega_{\underset{\sim}{\xi}}} P^{kj}(\underset{\sim}{\xi})[(\underset{\sim}{x}-\underset{\sim}{y})\cdot \underset{\sim}{\xi}]\operatorname{sgn}[(\underset{\sim}{x}-\underset{\sim}{y})\cdot\underset{\sim}{\xi}]\,d\Omega_{\underset{\sim}{\xi}} \tag{11}$$

In Eq. (11), Δ_y is the Laplacian with respect to the coordinates at $\underset{\sim}{y}$ of the integral over $\Omega_{\underset{\sim}{\xi}}$ which is a sphere of unit radius with origin at $\underset{\sim}{\xi} = \underset{\sim}{0}$. $P^{kj}(\underset{\sim}{\xi})$ is the inverse of the matrix $Q_{ik}(\underset{\sim}{\xi})$ which in turn is the characteristic form of the operator L_{ik}. This characteristic form is explicitly

$$Q_{ik}(\underset{\sim}{\xi}) = C_{ijkl}\xi_l\xi_j \tag{12}$$

in which ξ_i are components of the vector $\underset{\sim}{\xi}$.

Space does not permit nor would it be appropriate to discuss here the rather detailed, abstract, and frequently obscure arguments leading up to formula (11). Moreover, formula (11) as written above is an abridgement of the relations which appear in John [7] appropriate to anisotropic elasticity with the additional assumption of material homogeneity (C_{ijkl} constants). The actual treatment in John [7] deals with operators of more general order than two and in spaces of n dimension as well as allowing for the possibility of non-constant (but analytic) coefficients. This last feature could be of interest for problems involving inhomogeneous media. However, the remainder of the present discussion will be confined to U_{jk} as given by formula (11). Indeed, as will be explained, algebraic expressions for U_{jk} from Eq. (11) even under the present assumptions of *full* (21 constant) *anisotropy* will be difficult to obtain.

To best appreciate the last remark consider now formula (11) in more detail. Let $\underset{\sim}{x} - \underset{\sim}{y} \equiv \underset{\sim}{R}$ such that

$$\underset{\sim}{R} \cdot \underset{\sim}{\xi} \operatorname{sgn} \underset{\sim}{R} \cdot \underset{\sim}{\xi} = R \mid \cos \phi \mid \tag{13}$$

where R is the magnitude, i.e., $R \equiv \mid \underset{\sim}{R} \mid$, of $\underset{\sim}{R}$, $\xi = |\underset{\sim}{\xi}| = 1$, and ϕ is the angle between $\underset{\sim}{R}$ and $\underset{\sim}{\xi}$. Thus since R does not vary with $\underset{\sim}{\xi}$ Eq. (11) may be written

$$U_{jk}(\underset{\sim}{x},\underset{\sim}{y}) = \frac{-1}{16\pi^2} \Delta_{\underset{\sim}{y}} \{R \int_{\Omega_{\underset{\sim}{\xi}}} P^{kj}(\underset{\sim}{\xi}) \; |\cos \phi| d \; \Omega_{\underset{\sim}{\xi}}\} \tag{14}$$

Further, let

$$A_{jk} \equiv \int_{\Omega_{\underset{\sim}{\xi}}} P^{kj} \; (\underset{\sim}{\xi}) \; |\cos\phi| \; \; d\Omega_{\underset{\sim}{\xi}} \tag{15}$$

such that

$$U_{jk}(\underset{\sim}{x},\underset{\sim}{y}) = -\frac{1}{16\pi^2}\Delta_y\{RA_{jk}\} \tag{16}$$

Clearly A_{jk} is a tensor whose components depend only on C_{ijkl} and, of course, the choice of cartesian basis inasmuch as the components of U_{jk} itself depend on such a basis. Thus the ability to obtain explicit algebraic expressions for U_{jk} is dependent solely upon the ability to perform the integrations (15) for A_{jk}.

As mentioned earlier, $P^{kj}(\underset{\sim}{\xi})$ is the inverse of the quadratic form $Q_{ik}(\underset{\sim}{\xi})$ (Eq. 12). Explicitly,

$$P^{kj}(\underset{\sim}{\xi}) = \frac{\frac{1}{2}\varepsilon_{klm}\varepsilon_{jpq}Q_{lp}(\underset{\sim}{\xi})Q_{mq}(\underset{\sim}{\xi})}{\text{Det } Q} \tag{17}$$

in which ε_{ijk} is the alternating symbol and Det Q is the determinant of the matrix Q_{ik}. Now since Det Q is of sixth degree in ε_i and the numerator is (17) is of fourth degree, the ability to evaluate the elements A_{jk} analytically in closed form is largely dependent on the ability to factor the expressions implied by (17). Guided by the related investigations of Kroner [10] and Lie and Koehler [11] this is expected to be possible under the assumptions of special anisotropy, e.g., cubic or hexagonal symmetry. However, recognition of the tensor character of A_{jk} allows the following plan to be adopted in order to obtain explicit practical expressions for U_{jk} under more general conditions of anisotropy. Choose a convenient orthonormal basis and evaluate, *numerically* if need be, the integrals in (15) for a given set of C_{ijkl}. Having thus obtained a set of values for A_{jk} for that basis, A_{jk} for any other basis is obtainable by simple cartesian tensor transformation. Recognizing further that the direction cosines of $\underset{\sim}{R}$ referred to a given basis are of the form $[x_j(\underset{\sim}{x}) - x_j(\underset{\sim}{y})]/R$, allows the gradient and Laplacian with respect to $\underset{\sim}{y}$ to be evaluated as required in Eq. (16).

As an example of the above consider the special case of complete isotropy for which

$$C_{ijkl} = \lambda\, \delta_{ij}\delta_{kl} + \mu(\delta_{ij}\delta_{jl} + \delta_{il}\delta_{jk}) \tag{18}$$

where λ and μ are the Lame' elastic constants. Here it is easily shown through Eq. (17) that $P^{kj}(\underset{\sim}{\xi})$ has the form

$$P^{jk}(\underset{\sim}{\xi}) = \alpha(\delta_{ij} + \beta\xi_i\xi_j)$$

where α and β are constants obtainable from λ and μ alone. Thus the expressions for A_{jk} via Eq. (15) become

$$A_{jk} = \alpha\delta_{jk} \int_{\Omega_{\underset{\sim}{\xi}}} |\cos\phi|\, d\Omega_{\underset{\sim}{\xi}} + \alpha\beta \int_{\Omega_{\underset{\sim}{\xi}}} \xi_j\xi_k\, |\cos\phi|\, d\Omega_{\underset{\sim}{\xi}} \tag{19}$$

A little reflection on the integrals in Eq. (19) reveals that the first integral is twice the first moment of a unit hemispherical shell about the basal plane perpendicular to $\underset{\sim}{R}$. Similarly, the second integral represents the inertia components of a spherical shell referred to a given basis where the "mass density" ($|\cos\phi|$) of the shell varies linearly with respect to height above the same basal plane. Clearly, the calculations here would most conveniently be made taking one coordinate direction in the direction of $\underset{\sim}{R}$ and the other two in the mentioned basal plane. Subsequently, the desired A_{jk} for a more general orientation of basis with respect to $\underset{\sim}{R}$ could be easily obtained by cartesian tensor transformation. We note finally in passing that the result of the above calculations for material isotropy results in

$$U_{jk}(\underset{\sim}{x},\underset{\sim}{y}) = \frac{1}{16\pi\mu(1-\nu)R} \left[(3-4\nu)\delta_{jk} + \cos\psi_j \cos\psi_k\right] \tag{20}$$

in which $\nu=\lambda/2\ (\lambda+\mu)$ and ψ_j is the angle between the vector $\underset{\sim}{R}$ and the x_j axis. Expression (20) is the fundamental isotropic singular solution (see e.g. Cruse [3]).

The key feature of the above proposed method is the ability to perform, if need be, part of the calculation numerically and still obtain all dependence of U_{jk} on $\underset{\sim}{x},\underset{\sim}{y}$ and basis orientation with respect to $\underset{\sim}{x}-\underset{\sim}{y}$ analytically. This is important since gradients of U_{jk} at $\underset{\sim}{y}$ are required for the integral equation method and such gradients may therefore be taken analytically. Thus, in light of the goal of this portion of the research, i.e., obtaining an explicit, usable, algebraic form for U_{jk} for complete anisotropy, it appears, despite numerical evaluation of certain integrals in general, that the job can be done via the outlined method.

5.4.2.2 *Via Fredholm* [6]

The fundamental paper by Fredholm [6] displays an alternative method for constructing, in principle, the fundamental solution U_{jk} discussed above. Like John's [7], Fredholm's work leads to a formal implicit representation for the solution. However, unlike with John's procedure it is not clear to the writer that one would be able to effect as useful a reduction of the method except for special anisotropy, by any means numerical or otherwise

Fredholm motivates his work by attempting to extend the idea of the particular solution 1/r of Laplaces equation $\Delta u = 0$ to the equations of anisotropic elasticity (1). He first eliminates two components of u_k in Eqs. (4) and shows that the remaining component (and hence each component u_k) must satisfy a sixth-order differential equation of the form

$$f(u_k) = 0 \tag{21}$$

where f is a sixth-order linear homogeneous differential operator which is explicitly the determinant of L_{ik} (Eq. (5)). He then chooses as his fundamental solution

$$u_i = \int_c \frac{\psi_i(\xi,\eta)\ d\xi}{f_2(\xi,\eta)\ (\xi x_1 + \eta x_2 + x_3)} \tag{22}$$

where ψ_i are polynomials in ξ and η of the fifth order of lower and

$$f_2(\xi,\eta) \equiv \frac{\partial}{\partial\eta} f(\xi,\eta,\ 1), \tag{23}$$

with $f(\xi,\eta,\ 1)$ being the definite algebraic form obtained by replacing the operations $\partial/\partial x_i$, $(i = 1,2,3)$ by ξ,η, and 1, respectively. The integration is around a closed contour c in ξ space containing only those singular points which are roots of $f(\xi,\eta_c) = 0$ where η_0 is given by

$$\xi x_1 + \eta_0 x_2 + x_3 = 0 \tag{24}$$

The polynomials ψ_i above are complicated algebraic expressions (see [6] pg. 14) obtained from L_{ik}. Fredholm then goes on to show that each component of the required tensor field U_{jk} is of the form (22) and rigorously establishes all of the properties of the solution.

It seems clear from the work of Kroner [10] and Lie and Koehler [11] that any attempt to reduce Fredholm's method to something useful for other than hexagonal or cubic crystal symmetry assumptions would be most difficult indeed. Detailed information on the particulars of this can best be obtained by careful study of the references [10,11] plus Fredholm's original paper [6]. It should be clear; however, that if the previous discussion and reduction of John's [7] approach is valid as outlined, it must be possible to accomplish the same task via Fredholm also since the desired U_{jk} is unique. Nevertheless, the transformation of contour integral in space to one over the unit sphere, of functions which are necessarily related but not explicitly so, is bound to be an extremely difficult task. Further, for *practical* purposes and in light of the previous section the effort seems hardly worthwhile in the near future.

It is my judgement that to formulate the integral equation method for general anisotropic elasticity, the method of John as previously outlined is by far the most promising at this point. Indeed, the outlined reduction with the ability to obtain the necessary functional variational analytically is better than was hoped for at the start of the investigation. If a similar advantage plus others are present also in Fredholm's technique they are lost to me, although, to be fair, much more time was spent with [7] than [6] because of the positive indications of [7].

5.4.3 Investigation of the Interlaminar Shear Problem

Consider a laminated plate as shown in Fig. 1 loaded on its "x" faces in such a way (cf. Pipes [8]) that it may be assumed that the stress and strain fields are functions of y and z alone. Further it is assumed that displacement components are of the form

$$\begin{aligned} u_1 &= cx + U_1\ (y,z) \\ u_2 &= U_2\ (y,z) \\ u_3 &= U_3\ (y,z) \end{aligned} \tag{25}$$

where U_i, are arbitrary functions and c is a constant. Finally, under the assumption that each lamina is homogeneous and isotropic it is now desired to examine the possible simplifications which may arise with the integral equation method by the process of "integrating out" dependence on x.

Specifically, consider the boundary formula of Cruse ([3] Eq. (14)) written *for a typical lamina*

$$\frac{1}{2}\,u_j(P) + \int_S u_i(Q)T_{ji}(P,Q)dS(Q) = \int_S t_i(Q)U_{ji}(P,Q)dS(Q) \tag{26}$$

where explicity S is the union of surfaces S_x, S_y, S_z of the lamina perpendicular to the x, y, z directions, respectively, see Fig. 2. Clearly, each integral over S_x is an integral of functions of ($\pm\ell$, y, z) such that there is no explicit x dependence to be "removed" in those integrals. Further, since there is assumed to be no traction on the S_y surfaces we have

$$\int_{S_y} t_i(Q)U_{ji}(P,Q)dS\ (Q) \equiv 0 \tag{27}$$

Thus, it remains to consider the integrals

$$\int_{S_x+S_z} u_i(Q)T_{ji}(P,Q)dS(Q),\int_{S_z} t_i(Q)U_{ji}(P,Q)dS(Q) \tag{28}$$

insofar as integrating away the x dependence. More explicitly, integrals (28) may be written

$$\int_{-w}^{w} t_i(y,\pm t)\int_{-\ell}^{\ell} U_{ji}(x,y,\pm t;\xi,\eta,\zeta)dx\ dy \tag{29}$$

$$\int_{-w}^{w} u_i(y,\pm t)\int_{-\ell}^{\ell} T_{ji}(x,y,\pm t;\xi,\eta,\zeta)dx\ dy\ (i \neq 1) \tag{30}$$

$$\int_{-w}^{w} U_1(y,\pm t)\int_{\ell}^{\ell} T_{ji}(x,y,\pm t:\xi,\eta,\zeta)dx\ dy+ c\int_{-w}^{w}\int_{-\ell}^{\ell} xT_{ji}(x,y,\pm t;\xi,\eta,\zeta)\ dx\ dy \tag{31}$$

$$\int_{-t}^{t} u_i(\pm w,z)\int_{-\ell}^{\ell} T_{ji}(x,\pm w,\ z;\xi,\eta,\zeta)\ dx\ dz\ (i \neq 1) \tag{32}$$

$$\int_{-t}^{t} U_1(\pm w,z)\int_{-\ell}^{\ell} T_{ji}(x,\pm w,z;\xi,\eta,\zeta)dx\ dz+c\int_{-t}^{t}\int_{-\ell}^{\ell} xT_{ji}(x,\pm w,z;\xi,\eta,\zeta)dx\ dz \tag{33}$$

in which x, y, z are the coordinates of the point Q and ξ,η,ζ are the coordinates of the point P. Our task therefore is to examine the expressions for each component of the kernel functions U_{ij} and T_{ij} as given by Eqs. (5) and (7) in Cruse [3], and then perform the definite integrals with respect to x alone from $-\ell$ to ℓ as indicated in expressions (29) through (33) above. Note that performing the first integration with respect to x in expressions (31) and (33) will suffice since the second such integration is obtainable directly from the first by parts.

Careful consideration of the mentioned Eqs. (5) and (7) in [3] for the components of U_{ij} and T_{ij} and designating all parts of the integrands which are independent of x with the common symbol B leads, after some "bookkeeping", to the need to evaluate only integrals of the following type

$$\int_{-\ell}^{\ell} \frac{(x-\xi)^n \, dx}{[(x-\xi)^2 + B^2]^{m/2}} \tag{34}$$

where n takes on integer values from zero through 3 and m takes on integer values 1, 3 and 5. Such integrals for values of m and n indicated are standard entries in any short table of integrals and result in polynomial and/or logarithmic forms in the variable $(x - \xi)$.

Maintaining care with the mentioned bookkeeping problem, and recognizing that each of the $-\ell$ to ℓ integrations in expressions (29) through (33) result in new tensor functions $\hat{U}_{ji}$, $\hat{T}_{ji}$ independent of x, we may write the boundary formula (26) in the form

$$\begin{aligned} &\frac{1}{2} u_j(\xi,\eta,\zeta) + \int_{-t}^{t} U_i(\pm w,z)\hat{T}_{ji}(\pm\ell,\pm w,z,\xi,\eta,\zeta)\,dz \\ &+ \int_{-w}^{w} U_i(y,\pm t)\ \hat{T}_{ji}(\pm\ell,y,\pm t;\xi,\eta,\zeta)\,dy \\ &- \int_{-w}^{w} t_i(y,\pm t)\ \hat{U}_{ji}(\pm\ell,y,\pm t;\xi,\eta,\zeta)\ dy = \end{aligned} \tag{35}$$

$$\int_{S_x} [t_i(y,z)U_{ji}(\pm\ell,y,z;\xi,\eta,\zeta)\ U_i(y,z)T_{ji}(\pm\ell,y,z,\xi,\eta,\zeta)]\ dy\ dz$$

$$+ c\ f_j(\pm\ell,\pm w,\pm t;\xi,\eta,\zeta) \tag{35}$$

where f_j (ξ,η,ζ) is that function obtained by integrating *all*[1] terms T_{ji} with c as a constant multiplier.

The question now arises, to what extent may explicit dependence on the length ℓ of the lamina be eliminated and still retain sufficient information to obtain what is required in a given problem. Examination of the terms in equation (35) reveals that as ℓ goes to infinity, f_j is bounded, and all components of U_{ji} and T_{ji}, with the exception of U_{11}, are zero or finite. The U_{11} component, which alone contains logarithmic terms blows up with increasing ℓ. However, since it may be argued that the component of traction t_1 on the surfaces S_z must be zero for isotropic media under the present assumptions, no difficulty is, in fact, encountered with that term. Finally, it is clear that the integrals over S_x on the right side of Eq. (35) vanish with increasing ℓ, such that all "input" information on the faces S_x indefinitely far apart is contained in the limit of the term c f_j.

It is now evident that it suffices to consider the "mid-x" plane of a typical lamina and to allow point P to occupy positions only on the rectangular boundary of this plane (i.e., consider only $\xi = 0$). Thus, Eq. (35) in reduced, x-independent, form may be written

---

[1]Note that one term is contributed to f_j from each pair of surfaces of the lamina.

$$\frac{1}{2} U_j(\eta,\zeta) + \int_{-t}^{t} U_i(\pm w,z)\hat{T}'_{ji}(\pm w,z,\eta,\zeta)dz - \int_{-w}^{w} t_i(y,\pm t)\hat{U}'_{ji}(y,\pm t;\eta,\zeta)dy$$

$$+ \int_{-w}^{w} U_i(y,\pm t)\hat{T}'_{ji}(y,\pm t,\eta,\zeta)dy = C\, f'_j\ (\pm w,\pm t,\eta,\zeta) \tag{36}$$

where the primes indicate limiting forms of the functions as $\ell \to \infty$ and $\xi = 0$.

Application of Eq. (36) in the solution of the interlaminar shear problem is as follows. Specify the constant c and perform the necessary integrations to obtain the function f'_j ($\pm$w, $\pm$t, η, s) for each lamina mid-plane. Then, write Eq. (36) for each such plane using an appropriate approximation scheme as, perhaps, outlined by [1,4]. Recognize further that the two integrals in Eq. (36) from -w to w for a given lamina mid-plane are coupled with similar integrals for the remaining lamina. The boundary conditions between lamina are that U_i and t_i be continuous across the adjacent boundaries and that the top and bottom boundaries are free of traction t_i. Unknowns to be obtained therefore by numerical solution of the integral equations are discrete values of $U_i(y,z)$ and $t_i(y,z)$ at selected discrete points on the boundaries of the lamina mid-planes.

Note in the above that while the integrations in Eq. (36) are over the lamina mid-plane boundaries all indices have the range 1, 2, 3 such that as mentioned in the introduction the problem is not truly two-dimensional in nature. However, it appears that the method outlined above is most feasible with much promise for success in light of numerical work already accomplished for both two and three dimensional problems (e.g. [2,3,9,12]). Most important, coupling the above ideas with those set forth in the previous section, it is possible to attack the difficult interlaminar shear problem under the assumption of fully anisotropic or specially anisotropic lamina.

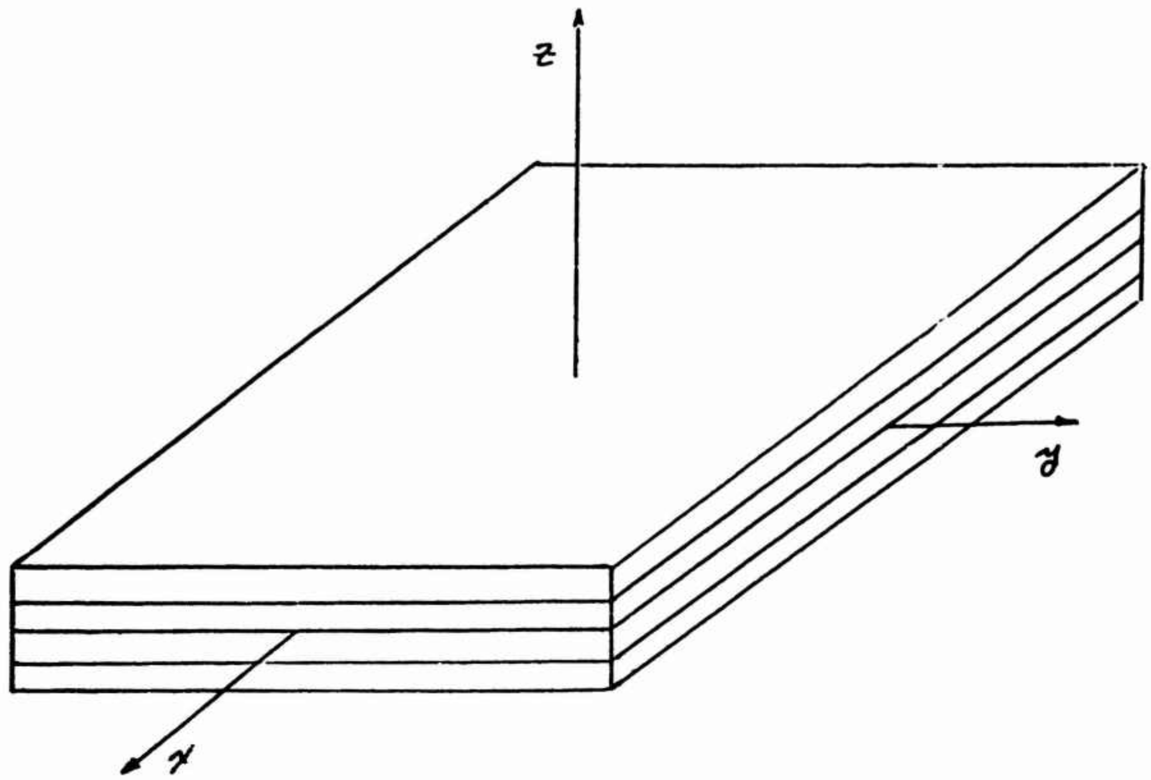

FIGURE 1: GEOMETRY FOR INTERLAMINAR SHEAR PROBLEM

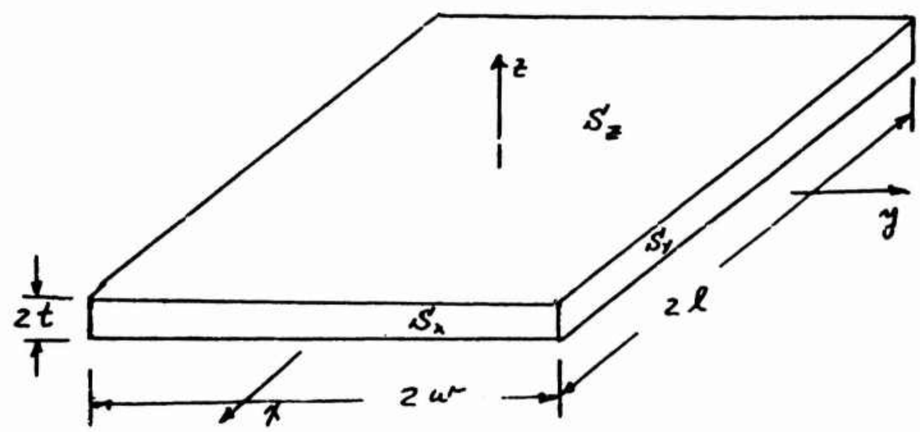

FIGURE 2: INDIVIDUAL LAMINA NOTATION

5.4.4 *References*

[1] F. J. Rizzo, "An Integral Equation Approach to Boundary Value Problems of Classical Elastostatics", *Quart. Appl. Math.*, 25, (1967) 83-95.

[2] T. A. Cruse, "A Direct Formulation and Numerical Solution of the General Transient Elastodynamic Problem II", *J. Math. Anal. Appl.*, 22, (1968) 341-355.

[3] T. A. Cruse, "Numerical Solutions in Three-Dimensional Elastostatics", *Int. J. Solids Structures*, 5, (1969) 1259-1274.

[4] F. J. Rizzo and D. J. Shippy, "A Formulation and Solution Procedure for the General Non-Homogeneous Elastic Inclusion Problem", *Int. J. Sol. Struc.*, 4, (1968) 1161-1179.

[5] F. J. Rizzo and D. J. Shippy, "A Method of Solution for Certain Problems of Transient Heat Conduction, *AIAA J.*, (to appear) (1970).

[6] I. Fredholm, "Sur les equations de l'equilibre d'un corps solide elastique", *Acta Math*, 23, (1900) 1-42.

[7] F. John, "Plane Waves and Spherical Means Applied to Partial Differential Equations", *Interscience, No. 2,* New York, London, (1955).

[8] B. Pipes, "Effects of Interlaminar Shear Stress Upon Laminate Membrane Performance", AFML/Industry Sponsored IRAD Status Report on Adv. Comp. Mat'ls., (1970).

[9] W. V. Lovitt, *Linear Integral Equations,* Dover, New York, (1950).

[10] E. Kroner, "Das Fundamentalintegral der anisotropen elastischen Differentialgleichungen", *Zeitschrift fur Physic, Bd. 136,* (1953) 402-410.

[11] K. H. C. Lie and J. S. Koehler, "The Elastic Stress Field Produced by a Point Force in a Cubic Crystal", *Adv. in Physics,* 17, No. 67, (1968) 421.

[12] F. J. Rizzo and D. J. Shippy, "A Method for Stress Determination in Plane Anisotropic Elastic Bodies", *J. Comp. Mat'ls.*, 4, (1970) 36-61.